Copyright Warning & Restrictions

The copyright law of the United States (Title 17, United States Code) governs the making of photocopies or other reproductions of copyrighted material.

Under certain conditions specified in the law, libraries and archives are authorized to furnish a photocopy or other reproduction. One of these specified conditions is that the photocopy or reproduction is not to be "used for any purpose other than private study, scholarship, or research." If a, user makes a request for, or later uses, a photocopy or reproduction for purposes in excess of "fair use" that user may be liable for copyright infringement,

This institution reserves the right to refuse to accept a copying order if, in its judgment, fulfillment of the order would involve violation of copyright law.

Please Note: The author retains the copyright while the New Jersey Institute of Technology reserves the right to distribute this thesis or dissertation

Printing note: If you do not wish to print this page, then select "Pages from: first page # to: last page #" on the print dialog screen

ABSTRACT

REMOVAL OF VOCs FROM AIR BY ABSORPTION AND STRIPPING IN HOLLOW FIBER DEVICES

by

Tarun K. Poddar

Large volumes of exhaust air streams contaminated with volatile organic compounds (VOCs) such as toluene, xylene, acetone etc. are discharged into the atmosphere by various industrial facilities. Common technologies for VOC emission abatement e.g., activated carbon adsorption, absorption in a liquid, incineration and catalytic oxidation, have many strengths as well as considerable limitations. In this study, a regenerative absorption-based removal of VOCs from N_2 in an inert, nonvolatile, organic liquid flowing in compact hollow fiber devices has been developed. The process eliminates flooding, loading and entrainment encountered in conventional absorption devices.

Contaminated air/N_2 stream was fed through the tube side of the hollow fiber module; a suitable inert absorbent liquid having a high solubility for the VOCs and extremely low vapor pressure was pumped countercurrently over the outside (shell side) of the fibers. The absorbent liquid was regenerated by vacuum in a separate hollow fiber membrane-based stripper. Two types of hollow fiber membranes were studied: one having microporous wall and the other having a nonporous VOC-permeable coating on the outer surface of a microporous hollow fiber. Criteria for nondispersive operation have been developed for each case. Experiments were conducted for the absorption of acetone, methylene chloride, toluene and methanol from the respective VOC-N_2 gas mixture using two different inert absorbent liquids, silicone oil and Paratherm™. Theoretical models have been developed from first principles to simulate the behavior of absorption as well as the combined absorption-stripping process.

Highest mass transfer coefficient was obtained for toluene absorption followed by methylene chloride, acetone and methanol absorption. Studies with multicomponent VOC-N_2 gas mixtures also showed that percent toluene removal was highest followed by methylene chloride, acetone and methanol. The behaviors of VOC mass transfer coefficients have been illustrated as a function of the gas and liquid flow rates. A comprehensive characterization of different resistances making up the overall resistance in VOC absorption has been carried out to develop a predictive capability and compare two types of fibers. Relative absorption performance between the two types of fiber for a given VOC was dependent on the diffusivity of the VOC in the absorbent liquid used. VOC absorption characteristics were determined and compared for the two absorbents used. The absorbent-filled porous membrane was found to contribute significantly to the total mass transfer resistance. Continuous absorption-stripping experiments employing recycling of the absorbent liquid via regeneration in a hollow fiber stripper were also accomplished. The overall performance of the combined process appears to be controlled by stripping due to the low temperature and lower membrane surface area in the stripper. The difference between only absorption and combined absorption-stripping results was more pronounced for VOC-absorbent system having higher Henry's law constant and diffusivity. Simulated results obtained from the mathematical models agree well with the experimental results for absorption as well as for combined absorption-stripping.

REMOVAL OF VOCs FROM AIR BY ABSORPTION AND STRIPPING IN HOLLOW FIBER DEVICES

by
Tarun K. Poddar

A Dissertation
Submitted to the Faculty of
New Jersey Institute of Technology
in Partial Fulfillment of the Requirements for the Degree of
Doctor of Philosophy

Department of Chemical Engineering,
Chemistry and Environmental Science

October 1995

APPROVAL PAGE

REMOVAL OF VOCs FROM AIR BY ABSORPTION AND STRIPPING IN HOLLOW FIBER DEVICES

Tarun K. Poddar

Dr. Kamalesh Sirkar, Dissertation Advisor — Date
Professor of Chemical Engineering and Sponsored
Chair in Membrane Separations and Biotechnology
New Jersey Institute of Technology

Dr. Henry Shaw, Committee Member — Date
Professor of Chemical Engineering
New Jersey Institute of Technology

Dr. Dana Knox, Committee Member — Date
Associate Professor of Chemical Engineering
New Jersey Institute of Technology

Dr. Demetri Petrides, Committee Member — Date
Assistant Professor of Chemical Engineering
New Jersey Institute of Technology

Dr. Namunu Meegoda, Committee Member — Date
Associate Professor of Civil and Environmental Engineering
New Jersey Institute of Technology

BIOGRAPHICAL SKETCH

Author: Tarun K. Poddar

Degree: Doctor of Philosophy in Chemical Engineering

Date: October 1995

Undergraduate and Graduate Education:

- Doctor of Philosophy in Chemical Engineering, New Jersey Institute of Technology, Newark, NJ, 1995
- Master of Science in Chemical Engineering, Indian Institute of Technology, Kanpur, India, 1986
- Bachelor of Science in Chemical Engineering, Jadavpur University, Calcutta, India, 1984

Major: Chemical Engineering

Presentations and Publications:

Tarun K. Poddar, R.P. Singh and P.K. Bhattacharya,"Ultrafiltration flux and rejection characteristics of black liquor and polyethyleneglycol", *Chem. Eng. Comm.*, **75**, 39 (1989).

Tarun K. Poddar, "Calibrating Storage Vessels", *Chemical Engineering*, November **11**, 177 (1992).

Tarun K. Poddar, "Optimum design of heat exchanger - a simplified method", *Hydrocarbon Processing* (to be published).

Tarun K. Poddar, Sudipto Majumdar and Kamalesh K. Sirkar, "Removal of VOCs from air by absorption and stripping in hollow fiber devices", Paper presented at the sixth annual meeting of *North American Membrane Society*, Denver, May 1994.

Tarun K. Poddar, Sudipto Majumdar and Kamalesh K. Sirkar, "Removal of VOCs from air by absorption and stripping in hollow fiber modules", Paper to be presented at the annual meeting of *American Institute of Chemical Engineers*, San Francisco, November, 1994.

This dissertation is dedicated to my parents
and
my wife

ACKNOWLEDGMENT

I like to express my deep gratitude to Professor K. K. Sirkar for his valuable suggestions at right moments, constructive guidance and help without which this work would not have been possible. I thank my committee members Dr. Henry Shaw, Dr. Dana Knox, Dr. Demetri Petrides and Dr. Namunu Meegoda for all the suggestions made.

Financial supports provided by Hazardous Substance Management Research Center at New Jersey Institute of Technology, Newark, NJ; Emission Reduction Center at New Jersey Institute of Technology, Newark, NJ and New Jersey Institute of Technology, Newark, NJ are highly appreciated.

I am also grateful to all of my colleagues and friends for their unconditional help, suggestions and their nice company which nourished me throughout this long journey. The names readily coming to my mind are Dr. Majumdar, Dr. Guha, Dr. Cha, Dr. Bhaumik, Dr. Mallick, Dr. Lee, Dr. Yang, Uttam, Sharma, Stephanie, Dilip, Malik, Shyamal and Gordona. Special thanks are due to Dr. Majumdar for his help in making me understand and starting off this work.

I specially thank Mrs. Judy Kapp for her prompt help in straightening out numerous administrative problems as and when developed. I am thankful to Mr. Yogi of Chemistry laboratory who has extended his generous helping hand at any odd situation by providing innumerable laboratory items. Thanks are also due to Mr. William Guzy and Mr. Clint Brockway for their help in various occasions.

I take this opportunity to thank sincerely my family members and specially my brothers for their encouragement and inspiration throughout my career.

Last but not the least, I express my heartfelt gratitude to my wife for her support, endurance and love which made this effort enjoyable and successful.

TABLE OF CONTENTS

TABLE OF CONTENTS
(Continued)

TABLE OF CONTENTS
(Continued)

TABLE OF CONTENTS
(Continued)

LIST OF TABLES

LIST OF FIGURES

LIST OF FIGURES
(Continued)

LIST OF FIGURES
(Continued)

LIST OF FIGURES
(Continued)

LIST OF FIGURES
(Continued)

LIST OF FIGURES
(Continued)

Figure **Page**

LIST OF SYMBOLS

A	:	Defined in equation 2.52
A_{Hi}	:	Constant in equation 2.100
A_m	:	Membrane area based on inside diameter in case of porous fiber and based on outside diameter in case of skinned fiber (cm^2)
A_m	:	Membrane area based on ioutside diameter (cm^2)
a	:	Defined in equation 2.48, specific surface area of mass transfer (cm^2/cm^3)
a'	:	Defined in equation 2.56
a_s	:	Defined in equation 2.81
B	:	Defined in equation 2.53
B_{Hi}	:	Constant in equation 2.100
b'	:	Defined in equation 2.57
C_{ig}	:	Local concentration of species i in gas phase (gmol/cc)
C_{il}	:	Local concentration of species i in liquid phase (gmol/cc)
$<C_{ig}>$	:	Average concentration of species i in gas phase (gmol/cc)
$<C_{il}>$	:	Average concentration of species i in liquid phase (gmol/cc)
c'	:	Defined in equation 2.58
$\overline{c}_i$	:	Mean speed of gas molecule of species i (cm/sec)
D	:	Defined in equation 2.54
D_{if}	:	Diffusivity of species i in imaginary fluid-filled membrane phase (cm^2/sec)
D_{ig}	:	Diffusivity of species i in gas phase (cm^2/sec)
D_{igp}	:	Diffusivity of species i in gas phase inside a straight pore (cm^2/sec)
D_{il}	:	Diffusivity of species i in liquid phase (cm^2/sec)
D_{im}	:	Diffusivity of species i in absorbent-filled membrane phase (cm^2/sec)

LIST OF SYMBOLS
(Continued)

d_i	:	Inside diameter of the hollow fiber (cm)
d'	:	Defined in equation 2.59
e'	:	Defined in equation 2.60
G	:	Gas flow rate through packed tower (gm/sec)
H_i	:	Dimensionless Henry's law constant of species i between gas and liquid phase
K_{OG}	:	Gas phase based overall mass transfer coefficient (cm/sec)
k	:	Mass transfer coefficient of an individual phase (cm/sec)
L	:	Effective length of the module (cm), liquid flow rate through packed tower (gm/sec)
M	:	Defined in equation 2.28
M_i	:	Molecular weight of gaseous species, i (gm/gmol)
N	:	Defined in equation 2.50
N_f	:	Number of hollow fibers in a module
N_s	:	Defined in equation 2.83
n	:	Number of segments in z direction
P	:	Defined in equation 2.15
p	:	Pressure
p_i	:	Partial pressure of VOC species i
Q	:	Defined in equation 2.47
q_c	:	Permeability of VOC through the silicone skin (cm^2/sec)
q_o	:	Overall permeability of VOC through composite membrane (cm^2/sec)
R	:	Universal gas constant
R_{OG}	:	Gas phase based overall resistance to mass transfer (sec/cm)

LIST OF SYMBOLS
(Continued)

R_m	:	Resistance of porous membrane (sec/cm)
R_c	:	Resistance of silicone skin (sec/cm)
r_i	:	Inside radius of the fiber (cm)
r_c	:	Outside radius of the coated fiber (cm)
r_e	:	Outside radius of hypothetical free surface defined in equation 2.1 (cm)
r_o	:	Outside radius of the porous substrate (cm)
r_s	:	Inside radius of the shell (cm)
$(r_s)_{ln}$	:	Logarithmic mean of r_o and r_i (cm)
$(r_c)_{ln}$	:	Logarithmic mean of r_c and r_o
S	:	Defined in equation 2.55
T	:	Temperature (K)
t	:	Temperature (°C)
$<V_t>$	:	Volumetric flow rate of gas inside the tube per fiber (cc/sec)
$<V_s>$	:	Volumetric flow rate of liquid in the shell side per fiber (ml/sec)
$<v_{zt}>$	:	Average velocity of gas inside the tube per fiber (cm/sec)
$<v_{zs}>$	:	Average velocity of liquid in the shell side per fiber (cm/sec)
w_i	:	Steady state permeation rate of species i through the composite membrane (mol/sec-cm^2)
X	:	Defined in equation 2.33
x_{io}	:	Feed outlet mole fraction of VOC
Y	:	Defined in equation 2.62
y	:	Defined in equation 2.51
y_{ii}	:	Permeate inlet mole fraction of VOC (at the closed end)
z	:	z coordinate

LIST OF SYMBOLS
(Continued)

Greek Symbols

α	:	Permeability ratio between VOC and nitrogen
γ	:	Ratio of permeate-side pressure to feed-side pressure
Δ_{ig}	:	Ratio of VOC diffusivity in N_2 at any pressure to that at atmospheric pressure
δ_c	:	Thickness of the silicone skin (cm)
δ_o	:	Overall thickness of the composite membrane (cm)
δ_s	:	Thickness of the porous substrate (cm)
ε	:	Surface porosity of porous membrane
μ	:	Viscosity of gas (cp)
ϕ_{ig}	:	Dimensionless concentration of species i in gas phase
$<\phi_{ig}>$	:	Average dimensionless concentration of species i in gas phase
ϕ_{il}	:	Dimensionless concentration of species i in liquid phase
$<\phi_{il}>$	:	Average dimensionless concentration of species i in liquid phase
ζ	:	Dimensionless distance, defined in equation 2.9
κ	:	Defined in equation 2.40
λ	:	Ratio of volumetric gas flow rate at any axial location inside the fiber to that at atmospheric pressure, equation 2.25
ξ	:	Dimensionless radius, equation 2.9
ρ_l	:	Absorbent liquid density (gm/ml)
Φ	:	Ratio of gas phase VOC concentration at the module exit to that at the module entrance
τ	:	Tortuosity of the porous membrane

Subscripts

i	:	VOC species
in	:	Inlet
fi	:	Feed inlet
fo	:	Feed outlet
g	:	Gas
l	:	Liquid
m	:	Porous membrane
c	:	Nonporous silicone skin
out	:	Outlet
ref	:	Ambient temperature and atmospheric pressure as reference condition
s	:	Shell side
sp	:	Sweep gas
t	:	Tube side

Superscripts

s	:	Stripping

CHAPTER 1

INTRODUCTION

Volatile organic compounds (VOCs) are any carbon-bearing compound, excluding oxides of carbon, carbonic acid, metallic carbides or carbonates and ammonium carbonate, which take part in various photochemical reactions in the atmosphere. Some organic compounds are not considered VOCs because of their negligible photochemical reactivity. Methane, ethane, methyl chloroform, 1,1,1-trifluoroethane etc. are typical examples of such compounds. However, the criterion defining negligible photochemical reactivity is rather ambiguous. According to the Environmental Protection Agency (EPA), VOCs are organic chemicals having vapor pressure more than 0.1 mm of Hg at a standard condition of 20°C temperature and 760 mm Hg pressure (Mukhopadhyay and Moretti, 1993). The name, formula and other pertinent data of various VOCs are available in literature (Shah and Singh, 1988). VOCs are primarily responsible for smog formation via photochemical reactions which in turn may cause haze, damage to plants and animal life and a number of health problems for humans. Exposure to some of the VOCs entails the risk of developing cancer too.

Large volumes of purge streams (generally nitrogen) and process exhaust air streams contaminated with numerous VOCs are being discharged into the atmosphere from various facilities. Petroleum and natural gas production and refinery, mineral processing, polymers and resins production, pharmaceutical production processes, agrochemical production units, production facilities for various organic chemicals, waste treatment disposal units, dry cleaning stores, surface coating process units are a few of the innumerable sources of emission of VOCs (Moretti and Mukhopadhyay, 1993). As pointed out earlier, emission of different VOCs from such facilities into the atmosphere is not only a potential health hazard and a threat to the environment but also a

tremendous financial loss. Clean Air Act Amendments of 1990 require control and elimination of VOCs from exhaust streams before they are discharged into the atmosphere.

There are a number of existing and emerging technologies for end-of-pipe VOC control: thermal oxidation or thermal incineration, catalytic oxidation or catalytic incineration, flares, condensation, absorption, adsorption, membrane separation or vapor permeation, biofiltration and UV oxidation. Selection of a technology for a particular application has to be made after satisfying various constraints that are technological, process-oriented, operational and economical in nature. Salient features of the different processes are discussed below.

Incineration is one of the three processes by which almost complete destruction of VOCs is possible. Flare and catalytic oxidation are the other two processes. Incineration differs from flaring since no visible flame is present and the combustion process is more directly controlled and monitored. The most important advantage of thermal incinerators is their high VOC destruction efficiency and their lack of dependence on the type of VOC present in the emission streams. Thermal incinerators burn hydrocarbons vapor and meet part of the system fuel requirement. The process becomes economically unattractive when VOC concentration is low due to the higher cost of the required supplemental fuel. Incinerators are also very costly to install because of support equipments, utilities including high pressure fuel supplies and substantial process control and monitoring equipment. At a higher level of operating temperature (near 1800°F) nitrogen oxides may be produced as secondary pollutant which would require further treatment such as catalytic reduction (Ruddy and Carroll, 1993). Halogenated compounds in the vent stream are converted to their acidic counterpart. There are also possibilities of formation of chlorinated compounds like dioxin (Armand et al., 1990).

Catalytic oxidation process destroys VOCs in a manner similar to thermal oxidation or incineration. The basic difference between the two processes is as follows:

catalytic oxidation operates at a lower temperatures (700°F - 900°F) compared to that in thermal oxidation (1300°F - 1800°F). This is possible because the presence of catalyst reduces the combustion energy requirements. Catalytic incinerators are very effective for low VOC concentrations (less than 1 percent by volume). Higher VOC concentration may overheat and deactivate the catalyst. In such cases, dilution air will be required to reduce the VOC concentration. Catalysts made out of precious metals are vulnerable to contamination and can easily be poisoned. Lead, zinc, mercury and other heavy metals, as well as halogenated compounds and hydrogen sulfide, are potential poisons to catalyst. Heavy hydrocarbons (even in small amounts) have a tendency to be deposited on fixed catalysts, which causes deactivation or masking. When catalyst becomes less active, the efficiency of the process cannot be restored just by raising the operating temperature; replacement of catalyst is essential and it is expensive. Catalytic systems, like thermal oxidizers, may produce secondary combustion wastes. Halogens and sulfur bearing compounds are converted to acidic species by catalytic combustion process. These need to be treated by acid-gas scrubbers. Nonrecyclable spent catalyst materials may require disposal as hazardous waste. However, unlike thermal oxidation, the lower operating temperature precludes the formation of nitrogen oxides.

Carbon adsorption is the most widely practiced process for control and recovery of VOCs from gaseous streams. It can achieve recovery efficiency as high as 99 % or more. However, achievable recovery efficiency depends on the chemical characteristics of the VOCs in the emission streams. Generally low molecular weight compounds such as methane, ethane, propane etc. cannot be removed effectively as they are adsorbed very weakly on the activated carbon. Carbon adsorption is very effective at low VOC concentrations. However, the process is quite expensive when organic concentration in the stream exceeds 0.1 - 0.5 % (Baker et al., 1989).

One of the significant drawbacks of carbon adsorption is its inability to treat compounds like aldehydes, ketones, etc. Those may result in temperature excursions or

development of hot spots in the bed because of the exothermic reaction on the carbon surface. Persistent operational problems and even fire in the activated charcoal plants have been reported (Armand et al., 1990). The exothermic adsorption process leads to high temperatures in carbon beds for higher organic concentrations. Relative humidity should be lower than 30-50% for carbon adsorption to be effective. For streams with VOC concentration less than 1 % by volume, a low moisture content is essential because water molecule competes with VOCs for adsorption sites on the activated carbon. Contamination of activated carbon and equipment corrosion are endemic. Although dry solvents are not particularly corrosive, corrosion occurs during steaming to recover the solvent from the carbon bed. Many solvents hydrolyze in the presence of water or steam at a high temperature and the activated carbon acts as a catalyst (Kohl and Riesenfeld, 1979). Therefore, expensive construction materials are often used.

Recovery of VOC by condensation is prevalent in chemical and pharmaceutical process industries. Condensation of VOC vapors is achieved by lowering the temperature of the stream; it may also involve raising the pressure of the stream. Condensation is most effective and efficient for VOCs having boiling points above 100°F at relatively high concentrations (more than 5000 ppmv). Low boiling VOCs need extreme cooling or pressurization which increases the operating cost. The primary advantage of refrigeration is that it produces a high-purity product that can be directly recycled into the product stream or sold without any further processing. Refrigeration can handle chemicals that prove troublesome to desorb from carbon or that cause temperature rise on activated carbon systems. Disadvantages of condensation are the high energy consumption and associated refrigeration cost required to cool the total gas stream. In order to achieve high recovery efficiency (90 - 95 %) it is necessary to attain temperatures as low as -100°F to -200°F. Generally such a low temperature range is achieved by cascade cooling using more than one coolant. Among various auxiliary equipments often a precooler is used to remove moisture before the stream enters the condenser. Recovered water from a

refrigeration unit is generally contaminated with organic solvents and needs further treatment prior to discharge.

Absorption is the selective transfer of one or more species from a gas mixture to a suitable liquid solvent. Difference between the actual gas phase concentration of the species and the gas phase concentration which is in equilibrium with the liquid phase concentration is the driving force for absorption. Packed tower, spray tower, plate column, venturi etc. are conventional absorption equipments which provide the necessary gas-liquid contact area for mass transfer to take place. The recovery efficiency in absorption is highly dependent on the solvent used (it must have high solubility for the specific VOC) and the equipment design. For a given system, absorption efficiency can be increased by increasing the gas-liquid contact area in the equipment, chilling the absorbent liquid, pressurizing the gas stream and increasing the flow rate of the absorbent. However, all such improvements add to the cost/or complexities of the process. Absorption system can be designed to handle a gas capacity of 2000 - 100,000 cfm and VOC concentration ranges from 500 - 5000 ppmv or higher. The process is more efficient at higher VOC concentrations. The applicability of absorption is limited by the availability of a suitable solvent for the VOCs in the gas stream. Moreover a single solvent may not be efficient for all VOCs present in the stream. The final recovery efficiency of the process is limited not only by the absorption capacity but also by the subsequent regeneration of VOCs from the spent solvent. Absorption system also requires various auxiliary units like chiller, heat exchanger, vacuum units, condenser and several pumps.

Another technique for VOC separation from air involves the use of a permselective membrane. Nonporous polymeric membranes are highly selective for VOCs (Peinemann et al., 1986). Gas streams containing 0.05 to 20 percent by volume VOCs can be effectively treated through membrane separation. Feed stream temperatures up to 140°F can be tolerated; higher temperature is detrimental for membrane materials. The vapor laden air at atmospheric or slightly above atmospheric pressure is passed through one side

of the membrane and vacuum is applied to the other side. Due to the difference in the partial pressure of VOC across the membrane, the VOC permeates through the latter. The permeate stream concentrated in the VOC is subjected to condensation for recovery of the organic solvent.

There are two types of membrane which can be used for VOC separation from air/nitrogen. One is a VOC-selective membrane which has a high VOC permeability. As the permeation takes place, the driving force for permeation decreases gradually along the length of the membrane separator as the feed VOC concentration drops due to permeation. It is not economically viable to reduce the feed VOC concentration to less than 200-100 ppmv. The second type of membrane, air/nitrogen selective membrane, has other deficiencies. Air/nitrogen has generally low permeability through most membranes. Though the driving force for permeation of air/nitrogen is high, the amount of air/nitrogen to be permeated through the membrane will be enormous. This will increase the membrane area requirement and capacity of the vacuum pump. Both types of membranes are considerably permeable to moisture which causes ice crystal formation in the subsequent condensation stage. However, operating cost of a membrane system is relatively low because fuel and electricity are required for only the compressor and vacuum pump. Operation and maintenance requirements are less demanding than in other technologies. The system is very compact in size and generates no secondary wastes.

One can also use biofilters for VOCs. However, the microorganisms, if available, cannot handle any arbitrary VOC mixture. Reduction of VOCs to 1-5 ppmv level in air by bugs, if successful, is going to require an enormous research and development effort. There is a need for a simple, cheap and reliable technique that can be easily developed and used at any scale.

In this study, a highly efficient and compact hollow fiber absorber has been employed to remove VOCs from nitrogen. Volatile solvents have been recovered for recycle in a hollow-fiber membrane stripper and subsequent condensation to prevent air

pollution. Hollow fiber membrane contactors can have different configurations. In this study contactors used are in parallel flow configuration. In general such hollow fiber gas-liquid contactors have the following merits over conventional contacting equipment.

1. High surface area per unit volume of the contactor.
2. Independent control of gas and liquid flow rates is possible without any hydrodynamical problems like flooding, loading, weeping etc.
3. Since the gas-liquid contacting is nondispersive in nature, there is no entrainment of liquids drops with the exiting gas stream. This eliminates the use of any demisting device which otherwise is essential in case of dispersive contacting devices.
4. Higher volumetric mass transfer coefficient than that in conventional contacting units.
5. Small and compact and can be installed in any angular location.
6. Calculation of gas-liquid interfacial area is straightforward.
7. Modular in nature and easy to scale up or down.

The first application of porous membrane as a gas-liquid contactor was for blood oxygenation (Esato and Eiseman, 1975): flat hydrophobic Teflon membrane known as Gore-Tex was used. Subsequently microporous polypropylene hydrophobic hollow fibers were used for blood oxygenation by Tsuji et al. (1981). There are a number of applications of hollow fiber contactors for acid gas cleanup. Absorption of different acid gases in various solvents and aqueous solutions using hydrophobic microporous hollow fiber devices was studied by Zhang and Cussler (1985a, 1985b). A ten fold increase in gas separation efficiency in hollow fiber devices over conventional packed columns was observed by Yang and Cussler (1986). Hollow fiber gas-liquid contactors were also used for flue gas desulfurization studies (Ogundiran et al., 1988). Karoor and Sirkar (1993) have studied absorption of pure CO_2, pure SO_2 and their individual mixtures in nitrogen using similar hollow fiber devices. Both physical absorption and absorption with chemical reactions were carried out. A much lower HTU for hollow fiber devices over conventional packed columns was reported. Absorption of CO_2 with mixtures of glycerol

and water in various proportions was conducted in microporous hollow fiber modules by Kreulen et al. (1993). A better performance compared to a bubble column was reported in terms of $k_L a$ values. Hollow fiber devices have also been used to strip volatile species from water (Zhang and Cussler, 1985a; Semmens et al., 1989).

A schematic diagram of a hollow fiber module is shown in Figure 1.1. A bundle of hollow fibers made out of hydrophobic polypropylene is inserted inside a metallic shell and both ends of the fibers are potted with epoxy. These hollow fiber devices resemble shell-and-tube heat exchangers. In the scheme studied, VOC contaminated nitrogen stream is passed through the inside (tube side) of the fibers and a nonvolatile, nontoxic, inert organic solvent is passed countercurrently through the shell side of the module (Figure 1.1). Hollow fibers provide the necessary gas-liquid contact area for mass transfer. VOCs are effectively removed from air to the desired level and concentrated in the absorbent. The VOCs are recovered and the absorbent liquid regenerated by applying vacuum (and/or by heating the spent absorbent). The solutes and the absorbent can be reused since the latter is nonvolatile. The stripping is carried out in a separate hollow fiber module. For ultimate destruction of VOCs, the present technique will make it much more efficient than direct incineration of VOCs in air. First, a much smaller volume of gas is to be incinerated. Secondly, the recovered VOCs will directly act as fuel requiring no supplemental fuel-firing.

The VOC absorption studied here employs two novel types of hollow fiber membrane absorption. In the first type, the fibers are microporous and hydrophobic and the absorbing organic solvent contacting the nitrogen/air spontaneously wets the pores. Whether the absorbent liquid will enter the pore or not will depend on the pore size, pressure differential across the membrane and interaction between membrane material and the absorbent liquid. The pressure differential at which the liquid breaks through the pores is described by the well known Laplace equation

$$\Delta p = 2(\gamma / r)\cos\theta \qquad (1.1)$$

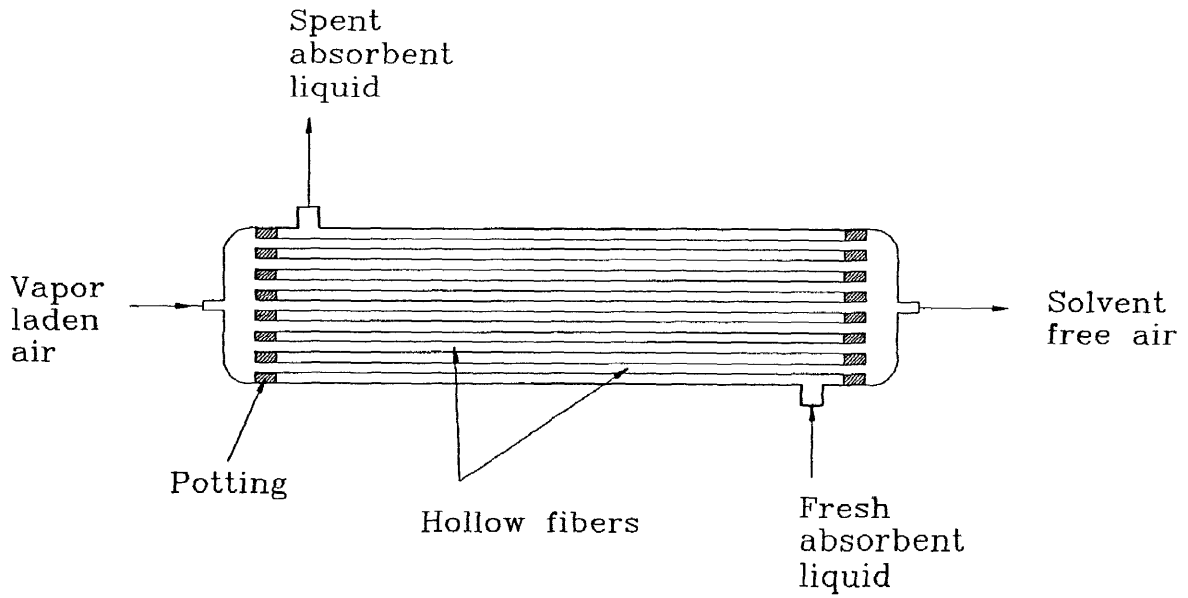

Figure 1.1 Schematic Diagram of a Parallel Flow Hollow Fiber Module

Here, Δp is the breakthrough pressure differential, γ is the surface tension, r is the pore radius, and θ is the contact angle. For a given membrane material - liquid system when contact angle is more than 90°, pores will not be wetted by the absorbent liquid; as the contact angle decreases below 90° the tendency of wetting the pores increases. Hence, in order to achieve nondispersive gas-liquid contacting using a wetting organic absorbent, the organic absorbent pressure has to be maintained lower than that of the gas stream in the fiber bore and the gas-liquid contacting interface at the pore mouth is on the gas side of the fiber.

Figure 1.2 illustrates the partial pressure profile of a VOC being absorbed in such a configuration. This is unlike conventional hollow fiber gas-liquid contactors where the pore is usually gas-filled, the absorbent does not wet the hydrophobic fibers, the absorbent is at a pressure higher than that of the gas and the gas-liquid contacting interface at the pore mouth is on the liquid side of the fiber (Zhang and Cussler, 1985a and 1985b; Karoor and Sirkar, 1993). Karoor and Sirkar (1993) also studied nondispersive gas absorption using an aqueous nonwetting absorbent in the pores of a microporous hydrophobic fiber and the gas phase at a higher pressure. Since the absorbent was nonwetting, it had to be introduced by a complicated exchange process (Bhave and Sirkar, 1986, 1987). No such exchange process is used or needed here due to spontaneous wetting of the pores by the organic absorbent. Jansen et al.(1993) have attempted VOC recovery from air in microporous membrane contactors using organic solvents which wet the membrane pores. For such a system, successful stabilization of gas-liquid interface at the pore mouth at the gas side of the membrane could not be achieved by them because of a lack of proper pressure differential conditions.

In the second type, the microporous hydrophobic hollow fiber has an ultrathin (~1 μm) but highly VOC-permeable plasma polymerized nonporous silicone skin on the outside surface of the hollow fiber. The trace contamination of the feed stream by the essentially nonvolatile absorbent is, however, reduced here by orders of magnitude since

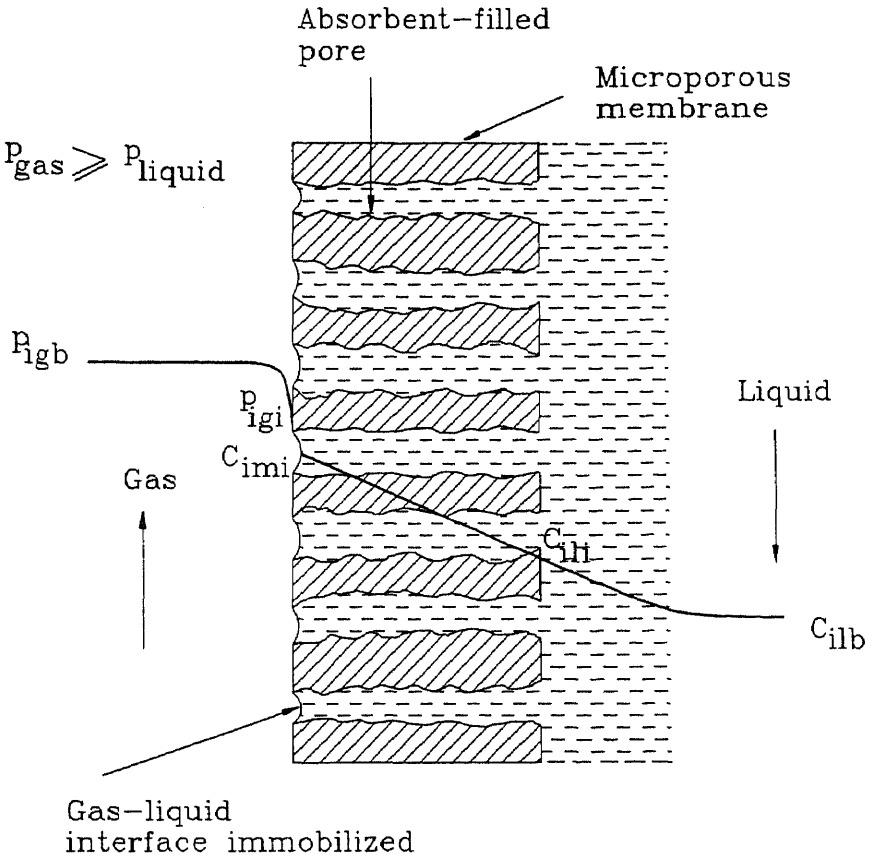

Figure 1.2 Local Partial Pressure and Concentration Profiles of VOC Being Absorbed in a Microporous/Porous Hollow Fiber Module

the thin nonporous skin is a significant barrier to permeation for the higher molecular weight absorbent molecules. The absorbent may flow through the tube-side or the shell-side. In this work, absorbent flow takes place primarily in the shell-side to eliminate the immobilized liquid phase mass transfer resistance in the pores of the microporous support beneath the nonporous skin. This flow configuration also avoids excessive pressure drop that the liquid stream may encounter while flowing through the fiber bore. Figure 1.3 illustrates the partial pressure profile of a VOC being absorbed through such a skinned membrane. The ultrathin plasma-polymerized nonporous silicone skin on the microporous hydrophobic fibers in the hollow fiber membrane absorber (HFMA) provides additional resistance to the transport of the desirable gaseous species. These hollow fiber membranes having an ultrathin skin can provide, however, a new dimension to selective absorption free of absorbent vapor contamination since direct gas-liquid contact is eliminated under appropriate phase pressure conditions.

For nondispersive VOC absorption to be effective in such a hollow fiber, the phase pressure conditions have to be different from that in fibers without a skin. For shell-side organic absorbent flow and tube-side gas flow, it is preferable to have the liquid and the gas pressures essentially equal or the liquid pressures should be higher for the skinned membrane (Figure 1.3). Otherwise, if the gas pressure is higher, gases like oxygen, nitrogen, etc. will permeate easily through the silicone skin and bubble through the flowing organic solvent. Such bubbling will increase as the gas pressure increases. This may or may not be beneficial to the VOC mass transfer process but it will certainly not be nondispersive. Further, these air or nitrogen bubbles will be saturated with VOCs and would need to be recycled back to the feed gas stream after disengagement from the organic solvent at the end of the module. That would reduce the gas scrubbing throughput substantially.

The skinned fibers being used are intrinsically different from conventional silicone rubber coating applied onto microporous fibers. The skin developed by plasma

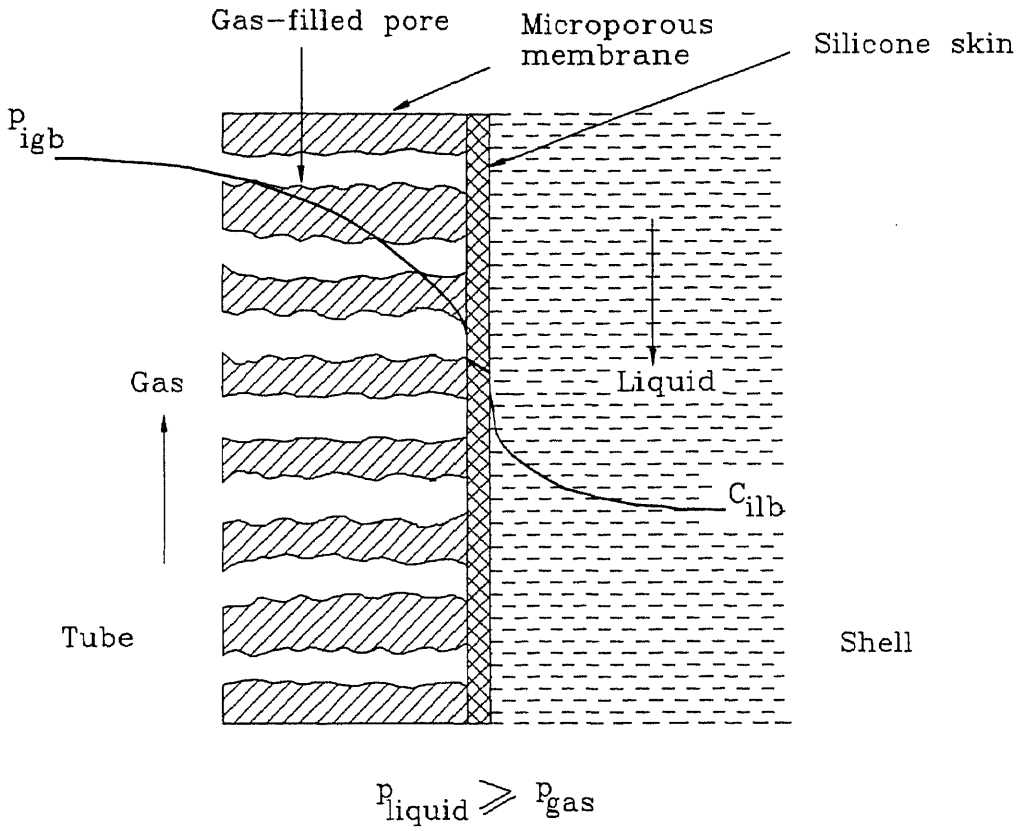

Figure 1.3 Local Partial Pressure and Concentration Profiles of VOC Being Absorbed in Microporous/Porous Hollow Fibers Having a Nonporous Silicone Skin on the Outer Surface

polymerization on the microporous hollow fiber substrate develops an integral bonding with the substrate which has a much greater resistance to solvent swelling. Conventional silicone rubber coating will swell in the presence of organic solvents and are likely to develop leaks and detachment from the substrate leading to performance instability and deterioration (Kvaerner Engineering, 1993).

A module made out of such fibers is also employed here for the VOC stripping process. VOC-contaminated absorbent liquid is passed through the shell side of the module and vacuum is applied on the tube side. Because of the difference in the partial pressure of VOC, the latter gets desorbed from the liquid phase and permeates through the highly VOC-permeable silicone skin and gets condensed in the condenser. Figure 1.4 depicts the concentration and partial pressure profile of a VOC being stripped from the absorbent liquid through the silicone skin.

Selection of the absorbent is a key element in absorption system design. Two different absorbents are used in this study; both of them are inert, nontoxic, essentially nonvolatile and water insoluble. One is silicone oil 50 cs and the other one is Paratherm™, a heat transfer oil. Different VOCs were employed in this study: one alcohol (methanol), one ketone (acetone), one chlorinated VOC (methylene chloride) and one highly nonpolar aromatic solvent (toluene). Broad classes of VOCs are therefore covered in this study.

The absorption process is often used for higher VOC concentrations in the gas stream and is accompanied by other polishing processes such as activated carbon adsorption or catalytic oxidation located downstream. Here the possibility of using absorption as a polishing technology for VOC removal has been explored. Studies were therefore conducted with low feed VOC concentrations (maximum of 1000 ppmv).

This thesis involves both experimental studies as well as development of mathematical models for the processes employed. Development of theoretical models for absorption as well as stripping have been presented in Chapter 2. A generalized

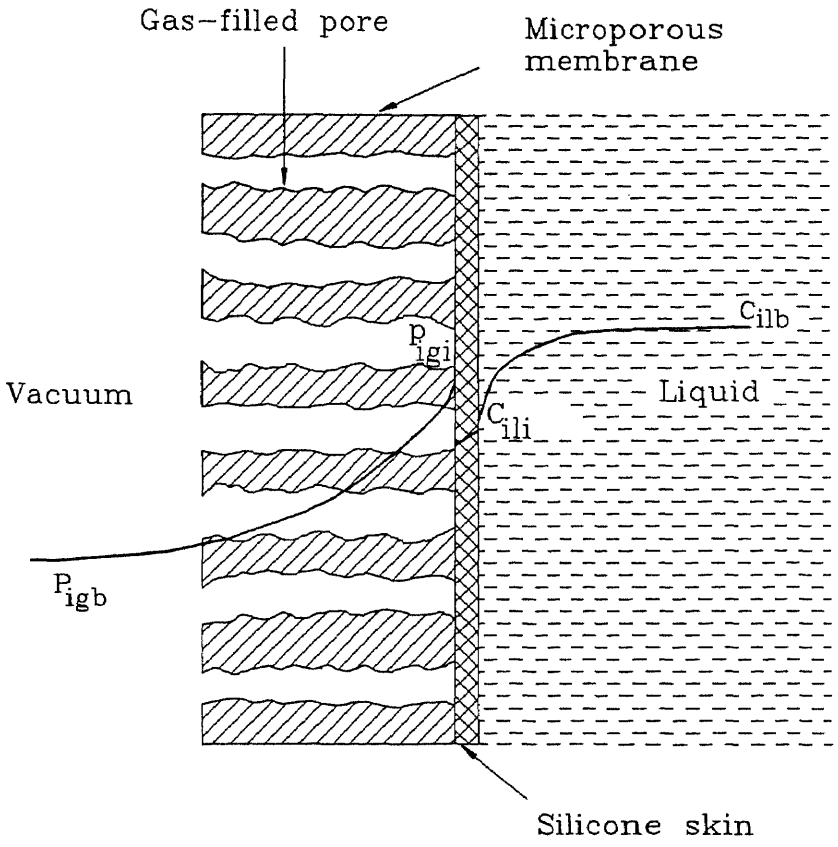

Figure 1.4 Local Partial Pressure and Concentration Profiles of VOC Being Stripped from Absorbent in Hollow Fiber Module

absorption model was developed from first principles. Solution was obtained in an analytical form which was ultimately employed in a numerical solution to obtain the simulated results. Solutions for absorptions in porous fiber and skinned fiber were obtained as special cases of a generalized solution by applying appropriate conditions. The overall performane of the combined absorption-stripping process was also simulated by combining the individual absorption and stripping model. This simulation has the capability of performance checking with respect to various parameters like stripping temperature, stripper area, applied vacuum, etc.

Experimental aspects of the work are discussed in detail in Chapter 3. Basic absorption studies were conducted using four different VOCs and two absorbents identified earlier for both types of hollow fibers. Closed loop simultaneous absorption and stripping experiments were also conducted with four different VOCs and two different absorbents. In such a simultaneous absorption-stripping process, the absorption was conducted using a module containing porous fibers while stripping was carried out in the module made out of the skinned fibers. No attempt was made to carry out experiments and analyses of the stripping process independently. The role of the stripping process in the overall performance of the combined absorption-stripping has been explored.

Different parameters are needed as input to the mathematical model to obtain simulated results. Three such important parameters are:

1. Henry's law constant for the different combinations of VOCs and absorbents.
2. Diffusivity of VOCs in the absorbents liquids.
3. Permeability of different VOCs through the nonporous silicone skin of skinned fibers.

None of these quantities are available in open literature. There is no adequate theoretical means to predict them either. These quantities were determined via independent experiments. Henry's law constants were measured by the variable volume headspace technique. Diffusivity of a VOC in the absorbent was measured indirectly by carrying out sweep gas-driven VOC permeation from nitrogen through an absorbent-filled

immobilized porous membrane. Permeability values of VOCs through the nonporous silicone skin were estimated by simple standalone permeation experiments for each individual VOC with the skinned fiber. Experimental techniques for each such measurement are discussed in detail in Chapter 3 while the theoretical basis for the estimation of each quantity is outlined in Chapter 2. The results of all experimental observations are presented and discussed in Chapter 4. This comprises results on Henry's law constant, diffusivity of different VOCs in absorbent liquids, permeability of each VOC through the silicone skin, absorption of different VOCs in two different absorbents using both types of fibers and combined absorption-stripping of VOCs. Model simulation results along with experimental results are also presented in this chapter. Experimental results in tabular form, a few sample calculations and computer programming codes are given in Appendix.

Finally two exploratory approaches were also investigated briefly. They require systematic study in future. Absorption/stripping phenomenon for VOC cleanup can be employed in a cyclic fashion. In such a case the process behavior in each cycle would be transient in nature. A preliminary unsteady-state absorption experiment was conducted to demonstrate the nature of the breakthrough curve of the transient absorption process. Few experiments were also conducted by appending the combined absorption-stripping process downstream of a membrane permeation (vapor permeation) process using higher VOC concentrations. The objective in these experiments was to demonstrate the possibility of using absorption-stripping process as an efficient polishing technology in combination with other processes for VOC cleanup. These experiments are discussed in detail in the recommendation part of Chapter 5.

CHAPTER 2

MODEL DEVELOPMENT AND THEORETICAL CONSIDERATIONS

This Chapter deals with the development of mathematical models for VOC absorption and VOC stripping in a hollow fiber module, numerical solution strategy and other theoretical considerations needed to interpret the experimental results. As described in Chapter 1, the hollow fiber module for absorption or stripping consists of a bundle of hollow polymeric porous fibers inserted in a metallic tube which forms the outer shell of the module (Figure 1.1). This device resembles a 1-1 shell-and-tube heat exchanger as far as the shell-and-tube configuration is concerned. The only difference is that the fibers are bundled in a random fashion in a hollow fiber module while tubes are arranged in a defined geometrical pitch in a shell-and-tube heat exchanger.

Two different types of fibers were used for absorption / stripping experiments. One type has a symmetric porous wall; the other one is a similar fiber having an ultrathin nonporous silicone skin on the outer surface. In the present study gas flows through the tube side (inside the fibers) and absorbent liquid flows through the shell side for both types of fibers. This flow arrangement is preferable to the other flow configuration, namely gas in the shell side and absorbent liquid in the tube side to avoid excessive pressure drop of the viscous absorbent liquid. There are other mass transfer considerations as well.

The nature of the fluid flow through the tube side is relatively well defined. In case of hollow fibers, the entry effects on mass transfer and momentum transfer are negligible due to the large length to diameter ratio and very low value of Schmidt numbers (Skelland, 1973) for gas a stream flowing through the tube side. Parabolic velocity distribution in the radial direction is assumed for laminar flow as the Reynolds number for gas stream through the tube side is below 300.

The nature of the liquid flow through the shell side is rather complicated, especially for a bundle of fibers not uniformly distributed. In an ideal contactor each and every fiber inside the module should be wetted and surrounded by the liquid passing through the shell side. Depending upon the packing density some of the fibers may be exposed to a lower velocity or higher velocity or almost stagnant liquid because of the so-called bypassing. However, the chances of poor contacting and bypassing would be rather low in the present system because the absorbent liquid has a natural tendency to wet the fiber surfaces and the shell-side flow rate is quite low so that nonuniformity in flow pattern is quite unlikely.

Shell-side flow situation in cylindrical assemblies has been analyzed by various authors. In the analysis of heat transfer in a flowing fluid outside a bundle of tubes, Happel (1959) assumed a coaxial annular flow envelope surrounding each tube. The effect of shell wall in the analysis had been considered by Schmid (1966). In their three dimensional analysis of heat transfer around a bundle of tubes arranged in a regular pitch, Sparrow et al. (1961) had concluded that the interaction between the tubes could be neglected if the space in between is not small. For a densely packed shell-and-tube heat exchanger, a maximum difference of 40 % in calculated Nusselt numbers was obtained by them while analyzing the problem using a 3 D model and a model assuming no interactions between the tubes.

In the present work, Happel's (1959) free surface model was used to analyze the flow situation on the shell side. This model has been successfully used in analyzing reverse osmosis in a hollow fiber module (Gill and Bansal, 1973) and SO_2 absorption from air into water in hollow fiber contactors (Karoor and Sirkar, 1993).

In Happel's model it was assumed that each and every fiber is surrounded by an equal volume of liquid envelope in the form of a coaxial annulus. The boundary of the annulus is known to be the free surface across which no mass, momentum or energy transfer takes place. The volume of the fluid associated with each fiber can simply be

obtained by dividing the shell-side void volume by the number of fibers present in the module. This model assumes no fiber-fiber interaction and is applicable to packing densities less than 0.5. The fibers are assumed to be distributed in a regular fashion. The analysis based on a single fiber can be extended to the whole device (Karoor and Sirkar, 1993). The longitudinal cross-section of a single fiber along with the associated fluid envelope and its free surface is shown in Figure 2.1 (Gill and Bansal, 1973). The outside radius of the free surface can be obtained from the following expression

$$r_e = \frac{r_s}{\sqrt{N_f}} \tag{2.1}$$

One can easily obtain the expression for shell side void volume fraction as

$$\varepsilon = 1 - N_f \left(\frac{r_o}{r_s} \right)^2 \tag{2.2}$$

where N_f is the number of fibers present in the module, r_s is the inside radius of the shell and r_o is the outside radius of the fiber.

2.1 Generalized Absorption Model

Development of a generalized model for predicting numerically the VOC concentration at the outlet of an absorption module made out of porous fibers as well as porous hollow fibers having an ultrathin nonporous silicone skin is presented next. The solutions for individual cases can be obtained by invoking the appropriate conditions.

2.1.1 General Solution Approach

To develop a generalized model it was assumed that the pores of the hollow fiber are filled with an imaginary fluid (Figure 2.2). At the beginning it could be assumed that this fluid is different from the gas stream flowing through the tube side and the absorbent

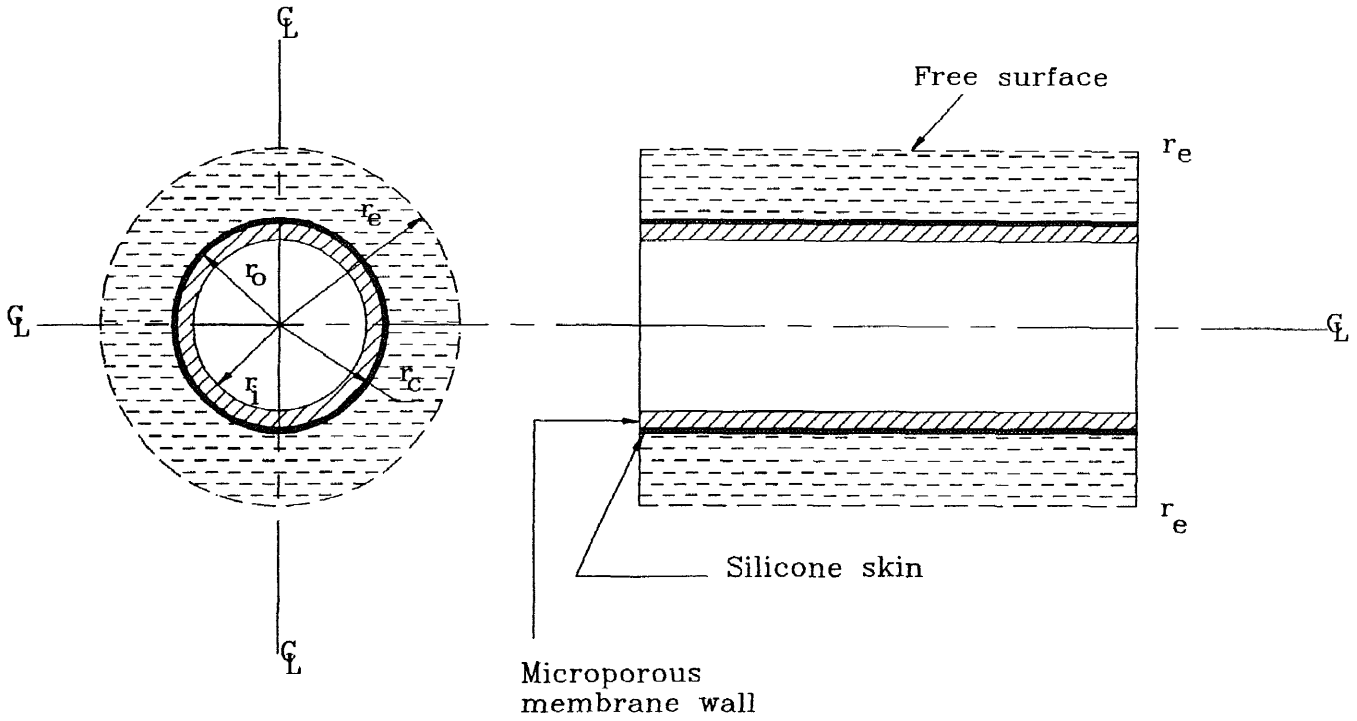

Figure 2.1 Absorbent-Filled Annular Space Associated with a Single Hollow Fiber

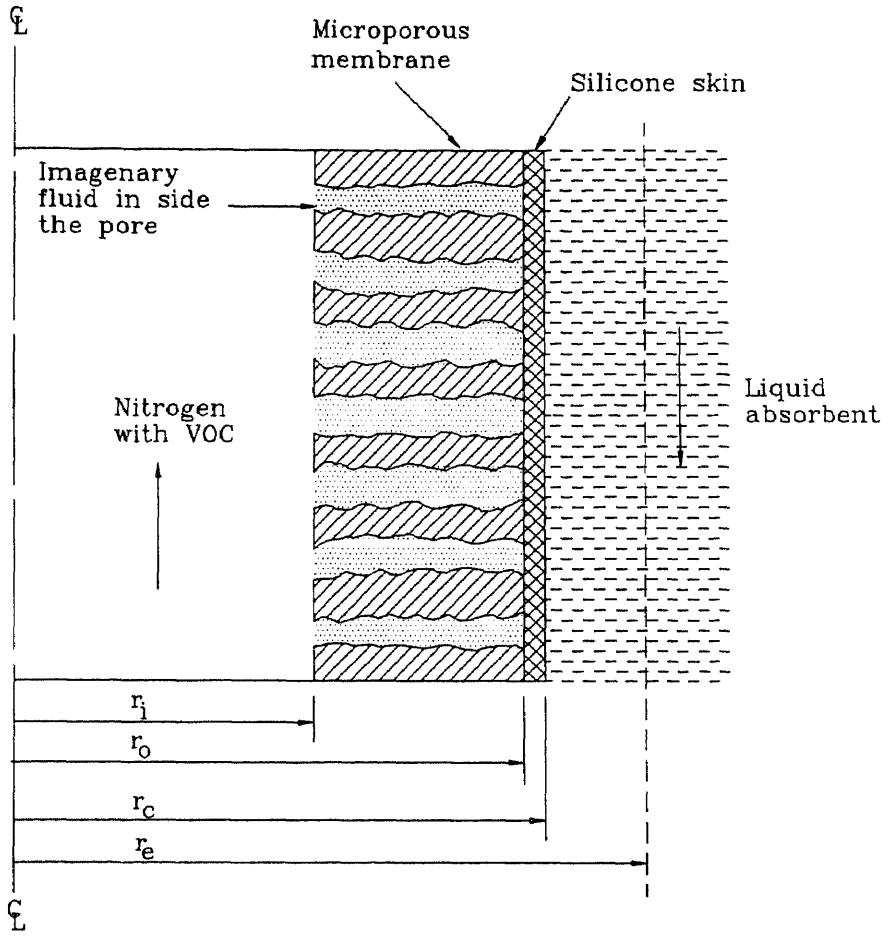

Figure 2.2 Cross Section of the Skinned Hollow Fiber Wall with Annular Space Filled with Absorbent, Pores are Assumed to be Filled with an Imaginary Fluid

liquid flowing through the shell side. The distribution coefficient of absorbing species i between gas phase and fluid phase inside the porous membrane is H_{i1} while the same between absorbent liquid phase and fluid phase inside the porous membrane is H_{i2}. For a direct contact between gas and absorbent liquid , the distribution coefficient of species i is H_i. The module is discretized along its length L into n small segments each having an equal length of $\Delta z = (L/n)$ (Figure 2.3). Conservation equations for the VOC were then solved to obtain the unknown radial concentration profiles for the first segment for both tube and shell side from known and assumed boundary conditions at one end of the first segment (here the gas outlet location). From the concentration profiles thus determined, expressions of average concentrations were obtained for the other end of the first segment; the latter became the known conditions for the next segment. This approach was continued till the last segment of the module was reached (i.e. z=L). The end condition (namely, the VOC concentration in N_2 at the inlet of the module) thus obtained was compared with the actual known inlet concentration. If these two did not match, then the assumed condition (i.e. VOC concentration in N_2 at the outlet of the module) was changed and the procedure was repeated till the two inlet concentrations matched.

The concentration profiles and the expressions for average concentration for the tube side as well as the shell side for the first segment were developed analytically. Two special cases were developed from the generalized solution. In case I (absorption in porous fiber) the imaginary fluid is nothing but the absorbent liquid in the shell side and there exists no silicone coating. In case II (absorption in skinned fiber) the imaginary fluid phase inside the porous membrane is same as the gas phase flowing through the tube side. Absorbent liquid in shell side cannot come in direct contact with gas flowing through the tube side because of the presence of the silicone skin on the outside surface of the fiber. The mathematical conditions for these two cases are discussed in section 2.1.5.3 and 2.1.5.4. These analytical solutions were used to develop the final numerical simulation for the absorption process in the module.

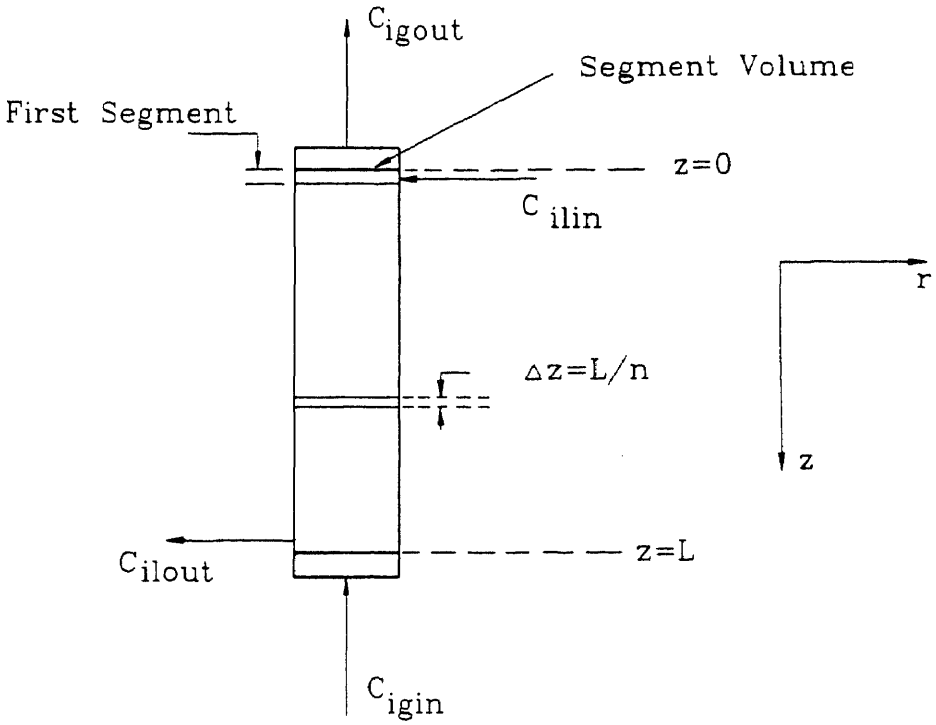

Figure 2.3 Schematic Diagram of Absorption Module for Numerical Simulation

2.1.2 Tube-Side Velocity Profile

For tube-side gas flow fully developed laminar flow is assumed. The resulting velocity profile is

$$v_{zt}(r) = 2\langle v_{zt}\rangle\left[1-\left(\frac{r}{r_i}\right)^2\right] \tag{2.3}$$

2.1.3 Shell-Side Velocity Profile

For fully developed laminar flow through the cylindrical annular space (Figure 2.1), the velocity profile in the positive z direction is given by (Happel, 1959)

$$v_{zs}(r) = 2\langle v_{zs}\rangle\left[1-\left(\frac{r_c}{r_e}\right)^2\right]\left[\frac{\left(\frac{r}{r_e}\right)^2-\left(\frac{r_c}{r_e}\right)^2+2\ln\left(\frac{r_c}{r}\right)}{3+\left(\frac{r_c}{r_e}\right)^4-4\left(\frac{r_c}{r_e}\right)^2+4\ln\left(\frac{r_c}{r_e}\right)}\right] \tag{2.4}$$

In deriving the above equation the following boundary conditions were assumed:

at $r = r_c$, $v_{zs} = 0$ (no slip condition);

at the free surface, $r = r_e$, $dv_{zs}/dr = 0$ (no momentum transfer).

2.1.4 Assumptions

The following assumptions are made to obtain the governing equations of VOC mass balance and their solutions.

1. Steady state and isothermal conditions.
2. Constant viscosity of the absorbent liquid.
3. Constant diffusivity of the VOC in the liquid absorbent.
4. Fully developed concentration profiles in both tube side and shell side.

5. No axial diffusion in both tube side and shell side.
6. No convective transport of VOC in the fluid-filled membrane phase.
7. No pressure drop for the absorbent liquid flowing through the shell side.
8. Negligible solubility of N_2 in absorbent.
9. Very low concentration of VOC in the gas phase. Hence, molar flow rate of gas through the fibers essentially remains constant.
10. Henry's law is applicable.

2.1.5 Model Development

Using assumption 1 the differential equation of mass balance for the VOC species i in the stagnant fluid inside the pores of the porous membrane phase can be written as

$$D_{im}\frac{1}{r}\frac{\partial}{\partial r}\left(r\frac{\partial C_{im}}{\partial r}\right) = 0 \qquad r_i \le r \le r_o \tag{2.5}$$

The above equation describes the diffusion of VOC through the fluid filled pores of the porous membrane. Although diffusion between the bulk fluid and the fluid inside the pores is generally two dimensional in nature, diffusional process is primarily one dimensional at high porosity (greater than 10%) (Keller and Stein, 1967). The effective diffusivity in the membrane phase D_{im} is defined by (Prasad and Sirkar, 1990)

$$D_{im} = \frac{D_{if}\varepsilon}{\tau} \tag{2.6}$$

Following boundary conditions are used to solve the membrane phase equation:

$$r = r_i, \qquad C_{im} = H_{il}C_{ig} \tag{2.7}$$

A flux continuity at the same boundary can also be assumed

$$r = r_i, \qquad D_{im}\left(\frac{\partial C_{im}}{\partial r}\right)_{r_i} = D_{ig}\left(\frac{\partial C_{ig}}{\partial r}\right)_{r_i} \tag{2.8}$$

A set of nondimensional variables are introduced now so that the solutions can be obtained in a nondimensional form

$$\phi_{im} = \frac{C_{im}}{C_{ig,in}};\ \phi_{ig} = \frac{C_{ig}}{C_{ig,in}};\ \phi_{il} = \frac{C_{il}}{C_{ig,in}};\ \xi = \frac{r}{r_i};\ \zeta = \frac{z}{L} \qquad (2.9)$$

The nondimensional forms of equation 2.5 and the boundary conditions are then:

$$\frac{1}{\xi}\frac{\partial}{\partial\xi}\left(\xi\frac{\partial\phi_{im}}{\partial\xi}\right) = 0 \qquad 1 \le \xi \le \xi_o \qquad (2.10)$$

$$\xi = 1,\ \phi_{im} = H_{il}\phi_{ig} \qquad (2.11)$$

$$\xi = 1, \qquad D_{im}\left(\frac{\partial\phi_{im}}{\partial\xi}\right)_{\xi=1} = D_{ig}\left(\frac{\partial\phi_{ig}}{\partial\xi}\right)_{\xi=1} \qquad (2.12)$$

The solution of equation 2.10 is

$$\phi_{im} = \frac{D_{ig}}{D_{im}}\left(\frac{\partial\phi_{ig}}{\partial\xi}\right)_{\xi=1}\ln\xi + H_{il}\phi_{ig}|_{\xi=1} \qquad (2.13)$$

At $\xi = \xi_o$, $\phi_{im} = \phi_{im}|_{\xi_o}$. Hence, the solution can be written as

$$\left(\frac{\partial\phi_{ig}}{\partial\xi}\right)_{\xi=1} = P(\phi_{im}|_{\xi_o} - H_{il}\phi_{ig}|_{\xi=1}) \qquad (2.14)$$

$$P = \frac{(D_{im}/D_{ig})}{\ln\xi_o} \qquad (2.15)$$

Using assumptions 1 and 5, the differential mass balance equation for VOC species i for the tube side is written as

$$D_{ig}\frac{1}{r}\frac{\partial}{\partial r}\left(r\frac{\partial C_{ig}}{\partial r}\right) = v_z(r)\frac{\partial C_{ig}}{\partial z} \qquad 0 \le r \le r_i \tag{2.16}$$

Different methods of obtaining the solution of the above type of equation (known as the Graetz problem in heat transfer) have been discussed in literature. Rigorous series solutions were obtained for constant wall heat flux and constant wall temperature in the analogous heat transfer problem for a parabolic velocity profile. A complete set of eigenvalues and eigenfunctions for the Graetz problem were presented and the solution was extended to arbitrary wall temperature and wall flux variation (Sellars et al., 1956). Solution was also obtained for assumed polynomial concentration profiles (Skelland, 1973). However, in the present problem, neither constant wall mass flux nor constant wall concentration could be assumed throughout the length of the module. The equation has been solved numerically by finite difference technique for constant average velocity (Karoor and Sirkar, 1993) to interpret the experimental results. Due to the pressure drop in the gas phase, a constant average gas velocity throughout the module length may not be a reasonable assumption unless the overall pressure drop across the module is insignificant compared to the inlet pressure. In the present work, an analytical approach has been taken via the assumption of similar concentration profiles throughout the length of the fiber to obtain the solution. As discussed in section 2.2.1, first the equation is solved for the first segment of length Δz using the following boundary conditions:

$$r = 0, \qquad \left(\frac{\partial C_{ig}}{\partial r}\right) = 0 \tag{2.17}$$

$$r = r_i, \qquad \left(\frac{\partial C_{ig}}{\partial r}\right) = finite \tag{2.18}$$

$$z = 0, \qquad C_{ig} = C_{ig,out} \tag{2.19}$$

Here, $C_{ig,out}$ is unknown. While solving the equations numerically a guess value for $C_{ig,out}$ will be assigned for iterative convergence to the concentration at the inlet of the module ($C_{ig,in}$). The conservation equation (equation 2.16) and boundary conditions (equations 2.17 through 2.19) can be rewritten in nondimensional form as

$$\frac{1}{\xi}\frac{\partial}{\partial\xi}\left(\xi\frac{\partial\phi_{ig}}{\partial\xi}\right) = \frac{v_{zi}(r)r_i^2}{D_{ig}L}\left(\frac{\partial\phi_{ig}}{\partial\zeta}\right) \qquad 0\le\xi\le1 \tag{2.20}$$

$$\xi = 0, \qquad \left(\frac{\partial\phi_{ig}}{\partial\xi}\right) = 0 \tag{2.21}$$

$$\xi = 1, \qquad \left(\frac{\partial\phi_{ig}}{\partial\xi}\right) = P(\phi_{im}|_{\xi_o} - H_{il}\phi_{ig}|_{\xi=1}) \tag{2.22}$$

$$\zeta = 0, \qquad \phi_{ig} = \phi_{ig,out} \tag{2.23}$$

The tube-side gas velocity profile is obtained from equation 2.3. Substitution of this with a negative sign (as the gas flows in the negative z direction) into equation 2.20 leads to the following equation:

$$\frac{1}{\xi}\frac{\partial}{\partial\xi}\left(\xi\frac{\partial\phi_{ig}}{\partial\xi}\right) = -\frac{\lambda}{\Delta_{ig}}\left(\frac{2<V_t>}{\pi D_{ig}L}\right)_{ref}(1-\xi^2)\left(\frac{\partial\phi_{ig}}{\partial\zeta}\right) \qquad 0\le\xi\le1 \tag{2.24}$$

Here 'ref' corresponds to the conditions at which gas flow rates are measured i.e. ambient temperature and atmospheric pressure at the module exit:

$$\lambda = \frac{<v_{zi}>}{<v_{zi}>_{ref}} = \frac{<V_t>}{<V_t>_{ref}} \tag{2.25}$$

$$\Delta_{ig} = \frac{D_{ig}}{(D_{ig})_{ref}} \tag{2.26}$$

For a fully developed concentration profile, $(\partial\phi_{ig}/\partial\zeta)_{\xi}$ is assumed not to be a function of ξ (Skelland, 1973). Hence, with the help of boundary conditions (equations 2.21 and 2.22), the solution of equation 2.24 can be obtained as

$$\phi_{ig} = -M\left(\frac{\xi^2}{4} - \frac{\xi^4}{16}\right) + c_2 \tag{2.27}$$

$$M = -4P(\phi_{im}|_{\xi_*} - H_{il}\phi_{ig}|_{\xi=1}) \tag{2.28}$$

Boundary condition 2.19 cannot be used directly to find out the integration constant c_2. It was obtained from the mass balance of species i for the segment Δz as follows (Bird et al., 1960):

$$-2\pi r_i \Delta z\left(D_{ig}\frac{\partial C_{ig}}{\partial r}|_{r_i}\right) = 4\pi\int_0^{r_i}(C_{ig} - C_{ig,out})\langle v_{zt}\rangle\left(1 - \frac{r^2}{r_i^2}\right)r\,dr \tag{2.29}$$

After nondimensionalizing the above equation and making necessary rearrangements, the expression for c_2 is obtained as (where $\Delta z = L/n$):

$$c_2 = \frac{7M}{96} + \frac{\pi M\Delta_{ig}}{2n\lambda}\left(\frac{D_{ig}L}{\langle V_t\rangle}\right)_{ref} + \phi_{ig,out} \tag{2.30}$$

Hence the concentration profile of component i in the tube side becomes

$$\phi_{ig} = -M\left(\frac{\xi^2}{4} - \frac{\xi^4}{16}\right) + \frac{7M}{96} + \frac{\pi M\Delta_{ig}}{2n\lambda}\left(\frac{D_{ig}L}{\langle V_t\rangle}\right)_{ref} + \phi_{ig,out} \tag{2.31}$$

Substituting the expression for M from equation 2.28 at $\xi = 1$, the above equation can be written as

$$(1 + 4PXH_{il})\phi_{ig}|_{\xi=1} - 4PX\phi_{im}|_{\xi_e} - \phi_{ig,out} = 0 \qquad (2.32)$$

where

$$X = \frac{11}{96} - \frac{\pi \Delta_{ig}}{2n\lambda}\left(\frac{D_{ig}L}{<V_t>}\right)_{ref} \qquad (2.33)$$

The species conservation equation for species i on the shell side is similar to that in the tube side:

$$D_{il}\frac{1}{r}\frac{\partial}{\partial r}\left(r\frac{\partial C_{il}}{\partial r}\right) = v_{zs}(r)\frac{\partial C_{il}}{\partial z} \qquad r_c \le r \le r_e \qquad (2.34)$$

The above equation has to be solved for the following boundary conditions:

$$r = r_c, \qquad \left(\frac{\partial C_{il}}{\partial r}\right) = finite \qquad (2.35)$$

$$r = r_e, \qquad \left(\frac{\partial C_{il}}{\partial r}\right) = 0 \qquad (2.36)$$

After substituting the expression for shell-side velocity profile from equation 2.4 into equation 2.34 and nondimensionalizing it, the following conservation equation and boundary conditions are obtained:

$$\frac{1}{\xi}\frac{\partial}{\partial \xi}\left(\xi\frac{\partial \phi_{il}}{\partial \xi}\right) = \frac{\kappa r_i^2}{D_{il}L}\left[\left(\frac{\xi}{\xi_e}\right)^2 - \left(\frac{\xi_c}{\xi_e}\right)^2 + 2\ln\left(\frac{\xi_c}{\xi}\right)\right]\left(\frac{\partial \phi_{il}}{\partial \zeta}\right) \qquad \xi_c \le \xi \le \xi_e \qquad (2.37)$$

$$\xi = \xi_c, \qquad \left(\frac{\partial \phi_{il}}{\partial \xi}\right) = finite \qquad (2.38)$$

$$\xi = \xi_e , \qquad \left(\frac{\partial \phi_{il}}{\partial \xi}\right) = 0 \tag{2.39}$$

where

$$\kappa = \frac{2\langle v_{zs}\rangle\left[1-\left(\frac{r_c}{r_e}\right)^2\right]}{3+\left(\frac{r_c}{r_e}\right)^4-4\left(\frac{r_c}{r_e}\right)^2+4\ln\left(\frac{r_c}{r_e}\right)} \tag{2.40}$$

The expression for the gradient in boundary condition 2.38 has to be found out from flux continuity relations at the interfaces. It is possible to write down two flux continuity equations at two different surfaces:

$$\xi = \xi_o, \qquad -D_{im}\left(\frac{\partial \phi_{im}}{\partial \xi}\right)_{\xi=1} \xi_o = \frac{q_c}{\delta_c}(\phi_{im}|_{\xi_o} - \phi^*_{im}|_{\xi_c})(r_c)_{\ln} \tag{2.41}$$

$$\xi = \xi_c, \qquad -D_{il}\left(\frac{\partial \phi_{il}}{\partial \xi}\right)_{\xi_c} \xi_c = \frac{q_c}{\delta_c}(\phi_{im}|_{\xi_o} - \phi^*_{im}|_{\xi_c})(r_c)_{\ln} \tag{2.42}$$

Here ϕ^*_{im} is the hypothetical concentration of VOC in the porous membrane phase in equilibrium with the VOC concentration in the absorbent liquid phase:

$$\phi^*_{im}|_{\xi_c} = \frac{\phi_{il}|_{\xi_c}}{H_{i2}} \tag{2.43}$$

$$(r_c)_{\ln} = \frac{r_c - r_o}{\ln(r_c/r_o)} \tag{2.44}$$

With the help of equations 2.41, 2.42, 2.12 and 2.14 the following relations can be obtained:

$$\left(\frac{\partial \phi_{il}}{\partial \xi}\right)_{\xi_c} \xi_c = Q(\phi_{im}|_{\xi_o} - H_{il}\phi_{ig}|_{\xi=1}) \tag{2.45}$$

$$H_{il}P\phi_{ig}|_{\xi=1} - (a+P)\phi_{im}|_{\xi_o} + \frac{a\phi_{il}|_{\xi_c}}{H_{i2}} = 0 \tag{2.46}$$

where

$$Q = \frac{(D_{im}/D_{il})}{\xi_c \ln \xi_o} \tag{2.47}$$

$$a = \frac{q_c(r_c)_{\ln}}{\delta_c D_{ig}} \tag{2.48}$$

Equation 2.37 can be solved in the manner by which the equation 2.24 was solved. The solution can be written at $\xi = \xi_c$ as

$$\phi_{il}|_{\xi_c} = Ny + \phi_{il,in} \tag{2.49}$$

where

$$N = -\frac{Q(\phi_{im}|_{\xi_o} - H_{il}\phi_{ig}|_{\xi=1})}{\left(\frac{A\xi_e}{\xi_c} - B\right)} \tag{2.50}$$

$$y = \frac{\xi_c^4}{16\xi_e^2} + \frac{D\xi_c^2}{2} - \frac{\xi_c^2}{2}\ln\xi_c - A\xi_e\ln\xi_c + \frac{LD_{il}}{\kappa n r_i^2} - \frac{S}{e'} \tag{2.51}$$

$$A = \frac{3\xi_e}{4} - \frac{\xi_c^2}{2\xi_e} + \xi_e \ln\left(\frac{\xi_c}{\xi_e}\right) \tag{2.52}$$

$$B = \frac{\xi_c}{2} - \frac{\xi_c^3}{4\xi_e^2} \tag{2.53}$$

$$D = 1 + \ln\xi_c - \frac{1}{2}\left(\frac{\xi_c}{\xi_e}\right)^2 \tag{2.54}$$

$$S = a' + b' + c' + d' \tag{2.55}$$

$$a' = \frac{\xi_e^8 - \xi_c^8}{128\xi_e^4} + \left(\frac{\ln\xi_c}{48\xi_e^2} - \frac{\xi_c^2}{96\xi_e^4}\right)(\xi_e^6 - \xi_c^6)$$

$$- \frac{1}{48\xi_e^2}\left[\xi_e^6\left(\ln\xi_e - \frac{1}{6}\right) - \xi_c^6\left(\ln\xi_c - \frac{1}{6}\right)\right] \tag{2.56}$$

$$b' = \frac{D}{4}\left(\frac{\xi_e^6 - \xi_c^6}{3\xi_e^2} + \left(\ln\xi_c - \frac{\xi_c^2}{2\xi_e^2}\right)(\xi_e^4 - \xi_c^4)\right)$$

$$- \frac{D}{4}\left[\xi_e^4\left(\ln\xi_e - \frac{1}{4}\right) - \xi_c^4\left(\ln\xi_c - \frac{1}{4}\right)\right] \tag{2.57}$$

$$c' = \frac{1}{12\xi_e^2}\left[\xi_c^6\left(\ln\xi_c - \frac{1}{6}\right) - \xi_e^6\left(\ln\xi_e - \frac{1}{6}\right)\right]$$

$$+\left(\frac{\xi_c^2}{8\xi_e^2} - \frac{\ln\xi_c}{4} - \frac{1}{8}\right)\left[\xi_e^4\left(\ln\xi_e - \frac{1}{4}\right) - \xi_c^4\left(\ln\xi_c - \frac{1}{4}\right)\right]$$

$$+ (\ln\xi_e)^2\frac{\xi_e^4}{4} - (\ln\xi_c)^2\frac{\xi_c^4}{4} \tag{2.58}$$

$$d' = -\frac{A}{4\xi_e}\left[\xi_e^4\left(\ln\xi_e - \frac{1}{4}\right) - \xi_c^4\left(\ln\xi_c - \frac{1}{4}\right)\right]$$

$$+ \left(\frac{A\xi_c^2}{2\xi_e} - A\xi_e\ln\xi_c - A\xi_e\right)\left[\xi_e^2\left(\ln\xi_e - \frac{1}{2}\right) - \xi_c^2\left(\ln\xi_c - \frac{1}{2}\right)\right]$$

$$+ A\xi_e[\xi_e^2(\ln\xi_e)^2 - \xi_c^2(\ln\xi_c)^2] \qquad (2.59)$$

$$e' = \frac{3}{4}\xi_e^2 + \frac{\xi_c^4}{4\xi_e^2} - \xi_c^2 + \xi_e^2\ln\left(\frac{\xi_c}{\xi_e}\right) \qquad (2.60)$$

Equation 2.49 can be further rearranged as follows:

$$QH_{i1}Y\phi_{ig}|_{\xi=1} - QY\,\phi_{im}|_{\xi_e} - \phi_{il}|_{\xi_e} + \phi_{il,in} = 0 \qquad (2.61)$$

where

$$Y = \frac{y}{\left(A\frac{\xi_e}{\xi_c} - B\right)} \qquad (2.62)$$

Concentrations of species i at three interfaces can be obtained by solving equations 2.32, 2.46 and 2.61:

$$\phi_{im}|_{\xi_e} = \frac{\phi_{ig,out}[H_{i1}QY + (H_{i1}H_{i2}P/a)] + \phi_{il,in}(1 + 4PXH_{i1})}{QY + H_{i2}(1 + P/a + 4PXH_{i1})} \qquad (2.63)$$

$$\phi_{ig}|_{\xi=1} = \frac{\phi_{ig,out}(QY + H_{i2} + H_{i2}P/a) + 4PX\phi_{il,in}}{QY + H_{i2}(1 + P/a + 4PXH_{i1})} \qquad (2.64)$$

$$\phi_{il}|_{\xi_c} = \frac{H_{i2}[H_{i1}QY\phi_{ig,out} + (1 + P/a + 4PXH_{i1})\phi_{il,in}]}{QY + H_{i2}(1 + P/a + 4PXH_{i1})} \tag{2.65}$$

2.1.5.1 Average Gas Phase Concentration at the Inlet of the First Segment The average concentration at the inlet of the first segment Δz can be easily obtained by simply equating the convective rate of transfer of i in the z direction with the diffusive rate of transfer of the same species in the radial direction at the boundaries of the segment volume:

$$-\frac{2}{n}\pi L D_{ig}\left(\frac{\partial \phi_{ig}}{\partial \xi}\right)_{\xi=1} = \langle V_t \rangle (\langle \phi_{ig} \rangle - \phi_{ig,out}) \tag{2.66}$$

Substituting the expression of $(\partial\phi_{ig}/\partial\xi)|_{\xi=1}$ from equations 2.22 and 2.28 into equation 2.66 and rearranging it with the help of equations 2.25 and 2.26 the expression for average gas phase concentration was obtained as

$$\langle \phi_{ig} \rangle = \frac{\pi L \Delta_{ig} M}{2n\lambda}\left(\frac{D_{ig}}{\langle V_t \rangle}\right)_{ref} + \phi_{ig,out} \tag{2.67}$$

2.1.5.2 Average Liquid Phase Concentration at the Outlet of the First Segment Average liquid phase concentration at the outlet of the first segment can be obtained in the way the average gas phase concentration at the inlet of the segment was obtained. Equating the convective transfer rate with diffusional transfer rate at the specific radial location over the boundaries of the segment volume the following relation was obtained:

$$-\frac{2}{n}\pi \xi_c L D_{il}\left(\frac{\partial \phi_{il}}{\partial \xi}\right)_{\xi_c} = \langle V_s \rangle (\langle \phi_{il} \rangle - \phi_{il,in}) \tag{2.68}$$

Substitution of equations 2.45, 2.50 and 2.60 into equation 2.68 and rearrangements yield:

$$\langle \phi_{il} \rangle = \frac{2\pi L D_{il} N e'}{n \langle V_s \rangle} + \phi_{il,in} \tag{2.69}$$

2.1.5.3 Case I - Absorption in Porous Fibers In case of a porous fiber there is no coating of silicone membrane; therefore, $\xi_c = \xi_0$, $\delta_c = 0$ and a = $\propto$ (equation 2.48). Absorbent liquid wets the fiber and pores are filled with the same (Figure 2.4). In other words, the fluid inside the pore is identical to that in the shell side. Hence, $H_{i2} = 1$. H_{i1} is dimensionless Henry's law constant of species i between the gas phase and the membrane phase (filled with the absorbent liquid) which in turn is simply H_i, the Henry's law constant between the gas and liquid phase. Further $D_{if} = D_{il}$ and equation 2.6 becomes

$$D_{im} = \frac{D_{il}\,\varepsilon}{\tau} \tag{2.70}$$

It is also possible to show that the interfacial concentrations at ξ_o and ξ_c are identical.

2.1.5.4 Case II- Absorption in Skinned Fibers In this case absorbent liquid cannot fill the pores due to the presence of the nonporous skin at the outer surface of the fiber and hence, the absorbent liquid cannot come in direct contact with the gas phase. Pores are filled with the gas phase (Figure 2.5). Hence, $H_{i1} = 1$. Further H_{i2} is the dimensionless Henry's law constant of VOC species between membrane phase (gas phase) and liquid absorbent phase , which is basically H_i . Further, D_{if} will be equal to D_{igp} and equation 2.6 becomes

$$D_{im} = \frac{D_{igp}\,\varepsilon}{\tau} \tag{2.71}$$

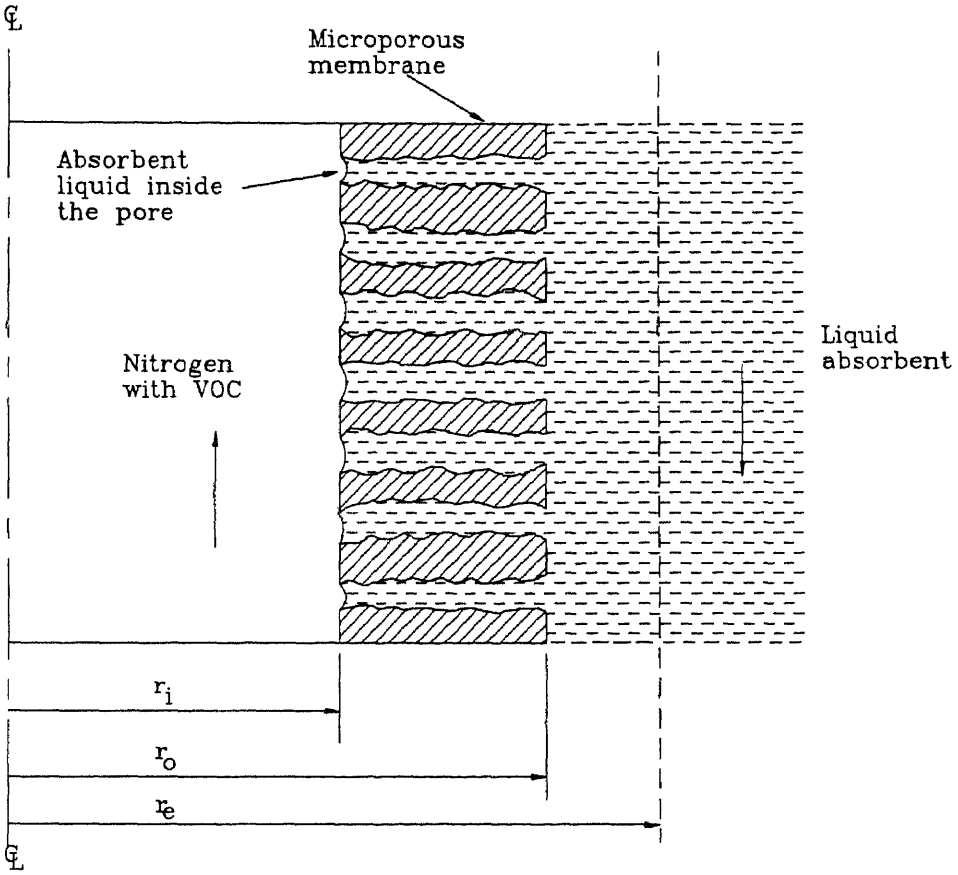

Figure 2.4 Case I, Cross Section of the Porous Hollow Fiber Wall with Absorbent-Filled Annular Space; Pores are also Filled with Absorbent Liquid

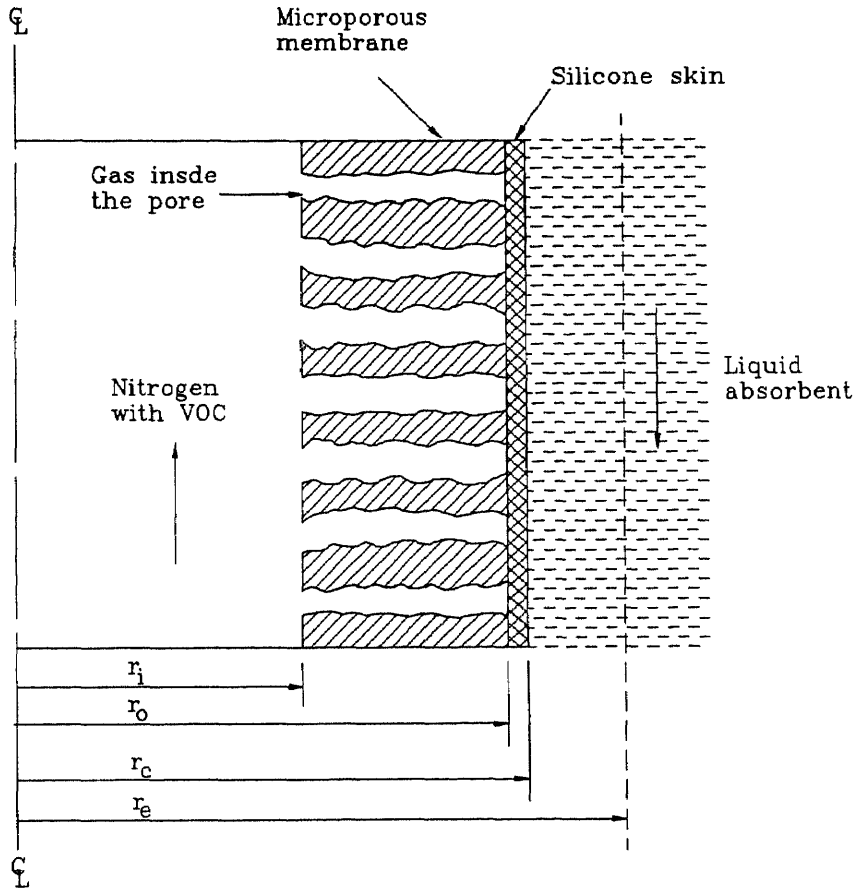

Figure 2.5 Case II, Cross Section of the Skinned Hollow Fiber Wall with Absorbent-Filled Annular Space; Pores are Filled with Gas

where D_{igp} is the diffusivity of gaseous species i inside a straight pore, the expression for which is given in section 2.3.5.

2.1.5.5 Pressure Drop in the Gas Phase When gas flows through the fibers, it encounters substantial pressure drop even at lower gas flow rates because of the extremely small diameter of the fibers. Due to this pressure drop, volumetric flow rate of gas stream per fiber ($<V_t>$) through the fiber is reduced along the length of the module. For laminar flow regime, pressure gradient in the negative z direction is given by Hagen-Poiseuille equation:

$$\frac{dp}{dz} = \frac{128\mu<V_t>}{\pi d_i^4} \tag{2.72}$$

Since the VOC concentration in the gas stream is extremely low, it is reasonable to assume that the molar flow rate of gas stream remains essentially constant. Applying ideal gas law (i.e. replacing $<V_t>$ with $p_{out}<V_{out}>/p$) and integrating equation 2.72, the pressure at the upstream of the segment Δz (where $\Delta z=L/n$) can be written as

$$p = \left[p_{out}^2 + \frac{256\mu L p_{out}<V_{t,out}>}{\pi d_i^4 n} \right]^{\frac{1}{2}} \tag{2.73}$$

2.1.5.6 Algorithm For Predicting the Gas Phase VOC Concentration at Module Exit The following algorithm is employed to calculate the outlet gas phase VOC concentration in ppmv as well as the ratio of outlet to inlet gas phase VOC concentration (both in ppmv) from the analytical expressions obtained in the section 2.1.5:

1. From the geometrical information of the module A, B, D, a′,b′,c′,d′,e′ and S were calculated. $(D_{ig})_{ref}$ was calculated for atmospheric condition. $<V_t>_{ref}$ was calculated by dividing measured volumetric gas flow rate by the number of fibers in th absorption module.

2. From the known value of p_{out}, p was calculated at the entrance of the module using equation 2.73 and n=1. Inlet gas phase VOC concentration in ppmv was then converted into gmol/cc .
3. A value of gas outlet concentration in ppmv was assumed and converted to gmol/cc.
4. $\phi_{ig,out}$ was obtained by dividing $c_{ig,out}$ (step 3) by $c_{ig,in}$ (step 2). $\phi_{il,in}$ was also calculated by dividing $c_{il,in}$ (gmol/ml) by $c_{ig,out}$ (step 3).
5. From known p_{out} and $<V_{out}>$, p was calculated at the inlet of the first segment of length Δz (Figure 2.3) from equation 2.73. Arithmetic average of p and p_{out} was then calculated for the segment.
6. The value of $\phi_{ig,out}$ was modified at the average gas pressure calculated in step 5.
7. D_{ig} was calculated from equation 2.104 for the segment at the average gas pressure in the tube side. $<V_t>$ value was also estimated at the average pressure of the segment. Once D_{ig} and $<V_t>$ values are known, λ and Δ_{ig} were calculated from equations 2.25 and 2.26 respectively.
8. X and Y were estimated from equations 2.33 and 2.62 respectively.
9. Appropriate values of a, P and Q were estimated from known parameters and the case under consideration (porous or skinned fiber).
10. Depending on the case, nondimensional interfacial concentrations were calculated from equations 2.63 through 2.65.
11. M and N were calculated for the required case from equations 2.28 and 2.50 respectively.
12. $<\phi_{ig}>$ and $<\phi_{il}>$ were estimated for the particular segment from equations 2.67 and 2.69 respectively.
13. $\phi_{ig,out}$ and $\phi_{il,in}$ were replaced by $<\phi_{ig}>$ and $<\phi_{il}>$ respectively for the next segment of equal length Δz.
14. Steps 5 to 13 were repeated till the module entrance was reached.

15. $\langle\phi_{ig}\rangle$ calculated for the last segment was compared with the known value of $\phi_{ig,in}$ If the two values matched within the given tolerance, then step 17 was executed, otherwise step 16 was executed.
16. Steps 3 through 15 are repeated with a different value of outlet gas phase concentration in ppmv.
17. The assumed value of outlet concentration is the predicted outlet concentration in ppmv. Φ will be the ratio of the predicted outlet concentration in ppmv to inlet concentration in ppmv.

2.2 Model For VOC Stripping

The VOC stripping operation was carried out in the skinned fiber module. VOC-contaminated absorbent liquid flows through the shell side of the module and vacuum was applied through the tube side of the module (Figure 2.6). A simpler approach has been taken in analyzing the stripping process. The flow configuration inside the tube under vacuum is not known for the present system. The VOC concentration in the tube side would be extremely low because of the extremely low absolute pressure. Hence, a constant average VOC concentration in the tube side could be reasonably assumed. The shell-side analysis is done via Happel's free surface model (1959).

2.2.1 Assumptions

The following assumptions are made in obtaining the governing equations of species balance and boundary conditions:

1. Steady state and isothermal conditions.
2. Constant viscosity of the absorbent liquid.
3. Constant diffusivity of VOC in liquid absorbent.
4. Fully developed concentration profiles in the shell side.
5. No axial diffusion in the shell side.

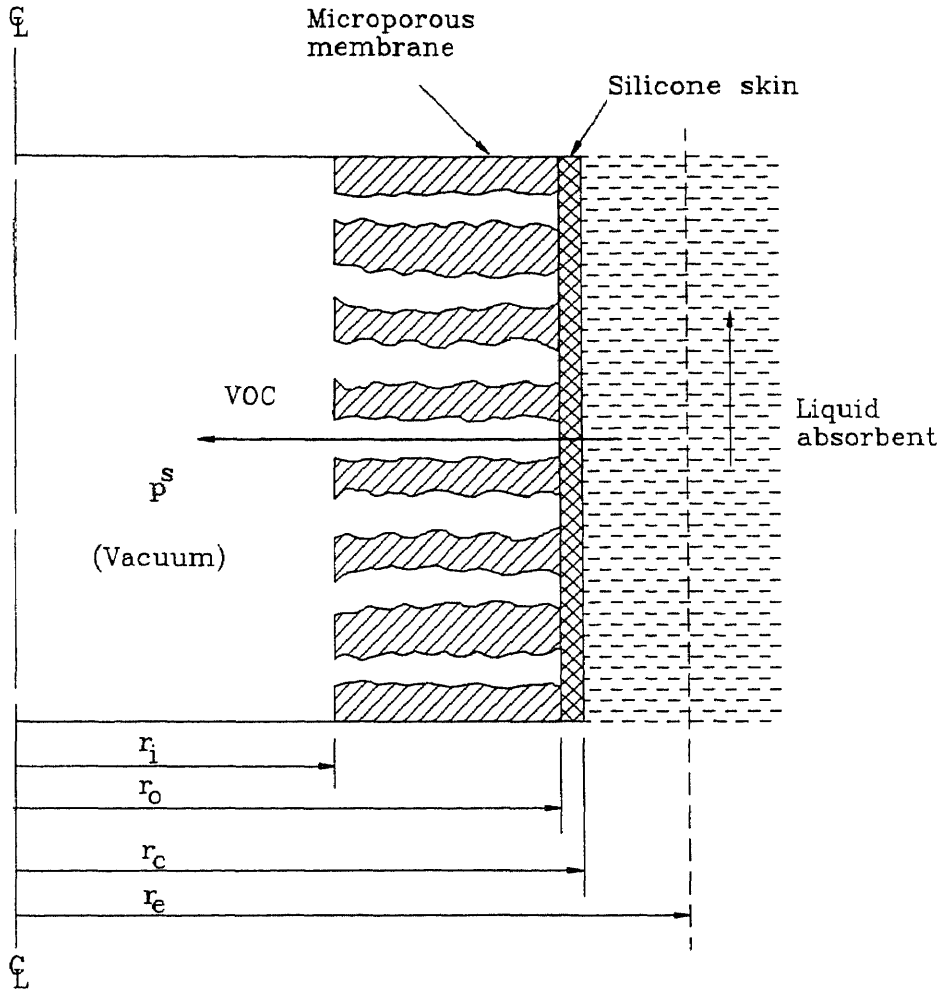

Figure 2.6 Cross Section of the Skinned Hollow Fiber Wall with Absorbent-Filled Annular Space; Vacuum in the Tube Side for Stripping

6. No convective transport of VOC in the gas filled membrane phase.
7. Negligible pressure drop for the absorbent liquid flowing through the shell side.
8. N_2 solubility in absorbent liquid is negligible.
9 Constant average concentration of VOC in the tube side for the whole module.
10. An overall q_o/δ_o for the composite membrane (porous membrane plus nonporous skin).
11. Henry's law is applicable.

2.2.2 Model Development

The mass conservation equation for species i in the shell side is identical to that for generalized absorption (equation 2.34). At the free surface, mass flux is equal to zero:

$$r = r_c, \qquad \left(\frac{\partial C_{il}^s}{\partial r}\right) = 0 \tag{2.74}$$

At the outside surface of the coating, diffusional mass transfer rate is equal to the permeation rate through the composite membrane of thickness δ_o

$$r = r_c, \qquad D_{il}\left(\frac{\partial C_{il}^s}{\partial r}\right)r_c = \frac{q_o}{\delta_o}(C_{ig}^{s*}|_{r_c} - \langle C_{ig}^s \rangle)(r_o)_{\ln} \tag{2.75}$$

$$z = 0, \qquad C_{il}^s = C_{il,in}^s \tag{2.76}$$

$$C_{ig}^{s*}|_{r_c} = \frac{C_{il}^s}{H_i} \tag{2.77}$$

$$(r_o)_{\ln} = \frac{r_c - r_i}{\ln\left(\frac{r_c}{r_i}\right)} \tag{2.78}$$

Equation 2.34 can be solved using the boundary conditions 2.74 through 2.76 in a similar way discussed in Section 2.1.5. In order to maintain similarity with the absorption model, equation 2.34 will be solved in nondimensional form. New nondimensional variables are introduced for liquid phase concentrations in the stripper. Other nondimensional variables used here are the same as in equation 2.9:

$$\phi_{ig}^{s} = \frac{C_{ig}^{s}}{C_{il,in}^{s}}, \qquad \phi_{il}^{s} = \frac{C_{il}^{s}}{C_{il,in}^{s}} \tag{2.79}$$

Equation 2.75 can be rearranged in nondimensional form as

$$\xi = \xi_c, \qquad \left(\frac{\partial \phi_{il}^{s}}{\partial \xi}\right)_{\xi_c} = a_s\left(\frac{\phi_{il}^{s}|_{\xi_c}}{H_i} - <\phi_{ig}^{s}>\right) \tag{2.80}$$

$$a_s = \frac{q_o(r_o)_{\ln}}{\delta_o D_{il} \xi_c} \tag{2.81}$$

The solution of shell side concentration profile is similar to equation 2.49 which can be written at $\xi=\xi_c$ as

$$\phi_{il}^{s}|_{\xi_c} = N_s y + \phi_{il,in}^{s} \tag{2.82}$$

$$N_s = -\frac{a_s\left(\frac{\phi_{il}^{s}|_{\xi_c}}{H_i} - <\phi_{ig}^{s}>\right)}{\left(\frac{A\xi_e}{\xi_c} - B\right)} \tag{2.83}$$

From equations 2.82 and 2.83, the following expression for wall concentration is obtained:

$$\phi^s_{il}|_{\xi_c} = \frac{\phi^s_{il,in} + a_s Y \langle \phi^s_{ig} \rangle}{1 + \frac{a_s}{H_i} Y} \tag{2.84}$$

where Y is exactly the same variable described in equation 2.62.

2.2.2.1 Average Liquid Phase Concentration at the Outlet of the First Segment

Average liquid phase concentration at the outlet of the stripper is obtained by equating the convective rate of molar transfer of species i across the segment volume of length Δz with the diffusional rate of mole transfer of the same species across the radial boundaries:

$$\langle V_s \rangle (\phi^s_{il,in} - \langle \phi^s_{il} \rangle) = \frac{2\pi (r_o)_{ln} L_s q_o}{n \delta_o} \left(\frac{\phi^s_{il}|_{\xi_c}}{H_i} - \langle \phi^s_{ig} \rangle \right) \tag{2.85}$$

Substituting equation 2.84 into equation 2.85, the expression for average liquid phase concentration at the exit of the control volume can be obtained as

$$\langle \phi^s_{il} \rangle = \phi^s_{il,in} - \frac{2\pi (r_o)_{ln} L_s q_o}{n \delta_o \langle V_s \rangle} \left(\frac{\phi^s_{il,in} - H_i \langle \phi^s_{ig} \rangle}{H_i + a_s Y} \right) \tag{2.86}$$

Average constant concentration of VOC in the tube side under vacuum can be related to the absolute partial pressure p_i^s as

$$\langle \phi^s_{ig} \rangle = \frac{p_i^s}{RTC^s_{il,in}} \tag{2.87}$$

From equations 2.86 and 2.87, the following condition for effective stripping can be obtained:

$$\phi^s_{il,in} - \frac{H_i p_i^s}{RTC^s_{il,in}} \succ 0 \tag{2.88}$$

The above equation can be used to approximately calculate the minimum pressure needed to be maintained in the vacuum side. For the whole stripper module, $\phi^{s}_{il,in} = 1$. Assuming partial pressure of VOC species i in the vacuum side is nothing but the absolute pressure the following condition can be obtained from equation 2.88 and can be used to calculate approximate vacuum level to be maintained for stripping:

$$p^{s} < \frac{RTC^{s}_{il,in}}{H_i} \tag{2.89}$$

2.2.2.2 Algorithm for Predicting Liquid Phase VOC Concentration at the Stripper Exit Following are the steps employed to calculate the liquid phase VOC concentration at the exit of the stripper module.

1. From the known parametric information of the module, quantities A, B, D, a′,b′,c′,d′,e′ S and a_s for the stripper module were calculated from the relevant equations.
2. For the small segment of length Δz, value of Y was calculated.
3. $<\phi^{s}_{il}>$ was estimated from the known value of $\phi^{s}_{il,in}$.
4. $\phi^{s}_{il,in}$ value was replaced by $<\phi^{s}_{il}>$ for the next segment and step 3 was repeated till the exit of the module was reached.
5. $<\phi^{s}_{il}>$ obtained for the last segment is the outlet concentration of species i at the exit of the stripper module.
6. Actual outlet concentration can be obtained by multiplying $<\phi^{s}_{il}>$ for the last segment with the actual inlet concentration.

2.3 Theoretical Considerations for Estimating Physicochemical Parameters

As discussed in sections 2.1.5.6 and 2.2.2.2, prediction of outlet concentration of VOC requires several inputs. Three different quantities, namely, diffusivities of VOCs in

absorbent liquids, Henry's law constants for different VOC-absorbent systems and permeability of VOCs through the nonporous silicone skin, needed to be determined by independent experiments. A theoretical outline for estimating those quantities are discussed below.

2.3.1 Estimation of VOC Diffusivity in Absorbent Liquid

Knowledge of VOC diffusivities in absorbent liquid and in absorbent liquid-filled membrane pores (case I) is essential along with other physicochemical properties to obtain numerical values from the mathematical model. If one of the two quantities is known, the other can be calculated from equation 2.70.

Diffusivity of a particular species in a liquid phase is generally calculated from the widely used Wilke-Chang equation (Reid et al., 1977). Diffusivities of different VOCs in sunflower oil were estimated using Wilke-Chang equation for calculating mass transfer coefficient (Hutter et al., 1994). Wilke-Chang equation has a few limitations for application to the present system being studied. This equation is valid for aqueous liquid phases and does not give good prediction for organic solvents (Reid et al., 1977). However, there are other equations to predict the diffusivity of organic diffusing species in nonaqueous systems; those have good agreement with experimental data. Different equations available in literature have a common feature namely, the inverse proportionality of liquid phase viscosity with diffusivity of the species (Reid et al., 1977). For higher liquid phase viscosity (higher than that of water), the inverse proportionality between viscosity and diffusivity does not hold good. Both silicone oil and Paratherm oil have higher viscosity (see Table 3.1). Hayduk and Cheng (1971) investigated the effect of solvent viscosity extensively and proposed that for nonaqueous systems $D_{ij} = A\mu^q$. Here the constants A and q are particular for a given solute. Several investigators (Hiss and Cussler, 1973; Davis et al., 1967; Lusis, 1974) have shown that the diffusivity of a solute in a viscous liquid varies inversely with the viscosity of the liquid raised to the power of

some exponent the value of which depends on the solute-solvent system.

Since there is no adequate and reliable information on diffusivity of VOCs in nonaqueous viscous liquids, it was decided to measure diffusion coefficients of various VOCs indirectly from the system under investigation.

The experimental technique for measuring the diffusivity of a VOC in the absorbent liquid is discussed in Section 3.9. The system employs essentially countercurrent permeation of VOC in sweep gas mode through the absorbent liquid immobilized in the pores of the porous wall of the membrane. Comparison of Case I in Section 2.1.5.3 with the present mode of countercurrent sweep gas permeation system reveals that the present system is related to the calculation procedure for the absorption operation of Case I (absorbent liquid inside the pores) which may be employed here with N_2 gas instead of the absorbent liquid passing through the shell side. Keeping this in mind, the equations obtained in the VOC absorption analysis under Case I were modified with appropriate conditions for the sweep gas permeation of VOC through the absorbent filled ILM.

Since in the shell side there is sweep gas (N_2) instead of any liquid, ϕ_{il} used in section 2.1.5 is replaced by ϕ_{isp}. According to Figure 2.7 it is clear that $H_{i1} = H_{i2} = H_i$ (dimensionless Henry's law constant between the absorbent liquid and N_2). There is no coating, so $\xi_o = \xi_c$, and $a = \alpha$. At the boundary, $\xi = \xi_o$, and it is possible to write

$$\phi_{im}|_{\xi_o} = H_i \phi_{isp}|_{\xi_o} \tag{2.90}$$

Hence, the concentration gradient at $\xi = 1$ (equation 2.14) can be modified to

$$\left(\frac{\partial \phi_{ig}}{\partial \xi}\right)_{\xi=1} = PH_i(\phi_{isp}|_{\xi_o} - \phi_{ig}|_{\xi=1}) \tag{2.91}$$

Using equation 2.88 and 2.89 and other conditions mentioned above, one can find out the interfacial concentrations from equations 2.63 and 2.64 as follows:

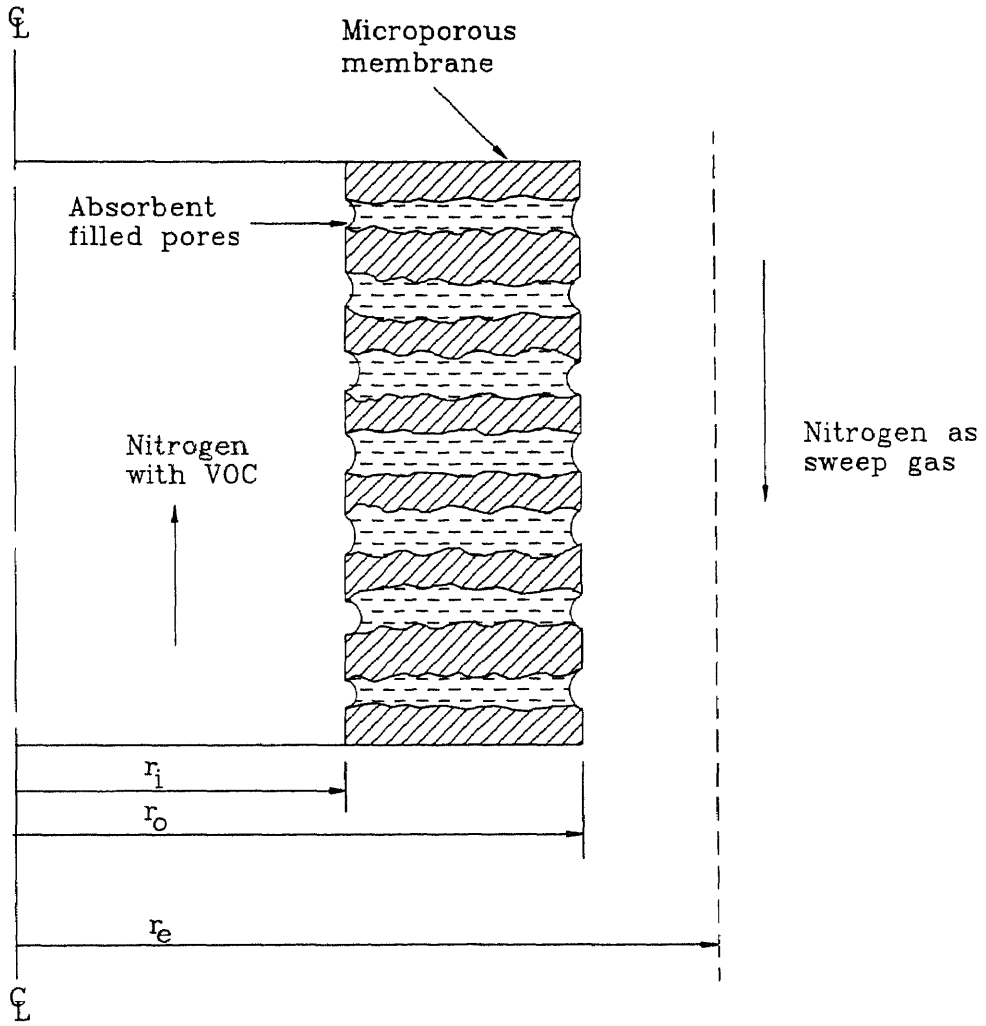

Figure 2.7 Absorbent Liquid is in Immobilized Condition inside the Porous Membrane Wall

$$\phi_{isp}|_{\xi_o} = \frac{\phi_{ig,out} H_i QY + \phi_{isp,in}(1 + 4PXH_i)}{QYH_i + H_i^2(1 + 4PXH_i)} \tag{2.92}$$

$$\phi_{ig}|_{\xi=1} = \frac{\phi_{ig,out}(H_i + QY) + 4PX\phi_{isp,in}}{QY + H_i(1 + 4PXH_i)} \tag{2.93}$$

2.3.1.1 Algorithm For Calculation of D_{il} Following are steps of calculation of D_{il} value.

1. From the geometrical information of the module A, B, D, a′,b′,c′,d′,e′ and S were calculated . $(D_{ig})_{ref}$ was calculated for atmospheric condition. $\langle V_t \rangle_{ref}$ was calculated by dividing measured volumetric gas flow rate by the number of fibers in the absorption module.
2. From the known value of p_{out} , p was calculated at the inlet of the module employing equation 2.73. Outlet and inlet gas phase VOC concentrations in ppmv were then converted into gmol/cc.
3. A value of D_{il} was assumed.
4. $\phi_{ig,out}$ was obtained by dividing $c_{ig,out}$ by $c_{ig,in}$ (step 2). $\phi_{isp,in}$ was also calculated by dividing $c_{isp,in}$ (gmol/ml) by $c_{ig,in}$ (step 2).
5. From known p_{out} and $\langle V_{out} \rangle$, p was calculated at the inlet of the first segment of length Δz (Figure 2.1) from equation 2.73. Arithmetic average of p and p_{out} was then calculated for the segment.
6. The value of $\phi_{ig,out}$ was modified at the average pressure calculated in step 5.
7. D_{ig} was calculated from equation 2.106 (given later) for the segment at average pressure in the tube side. $\langle V_t \rangle$ value was also estimated at the average pressure of the segment. Once the values of D_{ig} and $\langle V_t \rangle$ are known, λ and Δ_{ig} were calculated from equations 2.25 and 2.26 respectively.

8. X and Y are estimated from equations 2.33 and 2.62 respectively .
9. The values of a, P and Q were estimated from known parameters with appropriate conditions as discussed in section 2.3.1 .
10. Nondimensional interfacial concentrations were calculated from equations 2.92 and 2.93 with appropriate conditions as discussed in section 2.31.
11. M and N were calculated for the required case from equations 2.28 and 2.50 respectively (with proper conditions).
12. $<\phi_{ig}>$ and $<\phi_{isp}>$ were estimated for the particular segment from modified equations 2.67 and 2.69 respectively as discussed in section 2.3.1.
13. $\phi_{ig,out}$ and $\phi_{isp,in}$ were replaced by $<\phi_{ig}>$ and $<\phi_{il,sp}>$ respectively for the next segment of equal length Δz.
14. Steps 5 to 13 were repeated till the module entrance was reached.
15. $<\phi_{ig}>$ calculated for the last segment was compared with the known value of $\phi_{ig,in}$. If two values matched within the given tolerance, then step 17 was executed, otherwise step 16 was executed.
16. Steps 3 through 15 were repeated with a different value of D_{il}.
17. Assumed value of D_{il} was the required diffusivity of VOC species i through the liquid absorbent.

2.3.2 Estimation of Henry's Law Constants

Henry's law constant was measured by a static headspace technique described in the next Chapter (section 3.8). The theoretical basis of this technique is discussed here.

Determination of Henry's law constant by static headspace technique is based on the principle of establishing thermal and chemical equilibrium within the enclosed sampling vessel when solute is present at a low concentration. A simple material balance can be written for the equilibrium of a known volume of sample, V_o, having initial concentration of species i, C_{io}, as (Markelov and Biesenberger, 1984):

$$V_o\ C_{io} = V_o C_{il} + V_g C_{ig} \tag{2.94}$$

Here V_g is the headspace volume in the sample vial. C_{il} and C_{ig} are equilibrium concentrations of VOC in the liquid and headspace respectively. It is assumed that there is no evaporation loss of liquid matrix during the establishment of equilibrium. Equilibrium concentration of species i in the gas and liquid phase is related by an equilibrium constant namely, Henry's law constant

$$H_i = \frac{C_{il}}{C_{ig}} \tag{2.95}$$

Considering V_o is equal to V_l , substitution of equation 2.95 into equation 2.94 and rearrangement gives

$$\frac{1}{C_{ig}} = \frac{H_i}{C_{io}} + \frac{1}{C_{io}}\left(\frac{V_g}{V_l}\right) \tag{2.96}$$

Headspace concentration C_{ig} is directly proportional to the GC peak area:

$$C_{ig} = R_f A_p \tag{2.97}$$

where R_f is the response factor. Hence, equation 2.96 can be further written as

$$\frac{1}{A_p} = \frac{H_i R_f}{C_{io}} + \frac{R_f}{C_{io}}\left(\frac{V_g}{V_l}\right) \tag{2.98}$$

Equation 2.98 suggests that a plot of $1/A_p$ versus (V_g/V_l) will give a straight line with a slope, R_f/C_{io} and a y-intercept, $H_i R_f/C_{io}$. If the y-intercept is divided by the slope, a value of H_i can be directly obtained as expressed by equation 2.99:

$$H_i = \frac{y\text{-}intercept}{slope} \tag{2.99}$$

Experimental procedures are discussed in section 3.8. Henry's constant is a strong function of temperature. To minimize the error between simulation and experimental data it is necessary to find out the value of H_i at the temperature of experiments. At a constant pressure, the temperature dependence of Henry's law constant can be expressed by (Robbins et al., 1993; Hutter et al., 1994)

$$H_i = \exp\left(\frac{B_{Hi}}{T} - A_{Hi}\right) \tag{2.100}$$

where T is the temperature in K, A_{Hi} and B_{Hi} are constants depending on the solvent-solute combination and need to be found out from experimental data.

2.3.3 Theoretical Development for Calculation of VOC Permeance through the Composite Membrane

The permeation rate of a species i through the composite membrane can be written as:

$$w_i = \frac{q_o}{\delta_o} A_m \Delta C_i \tag{2.101}$$

Here, q_o/δ_o is the averaged permeance of the species through the composite membrane of thickness δ_o. A_m is the membrane area based on the outside diameter of the porous substrate and ΔC_i is the overall concentration difference between the feed and permeate sides along the whole module. In the above equation, the resistances to mass transfer through the gas films on both sides of the membrane are neglected. Due to lower VOC concentrations being used, it is further assumed that VOC permeance (q_o/δ_o) will be essentially independent of VOC concentration. Average concentration difference ΔC_i is taken as the logarithmic mean concentration difference across the module. For countercurrent permeation this quantity can be written as

$$(\Delta C_i)_{lm} = [(C_{ifi} - C_{ipo}) - (C_{ifo} - C_{ipi})] / \ln\left(\frac{C_{ifi} - C_{ipo}}{C_{ifo} - C_{ipi}}\right) \tag{2.102}$$

Here C_{ifi} and C_{ifo} are the inlet and outlet concentrations of species i in the feed stream while C_{ipi} and C_{ipo} are the corresponding ones in the permeate stream.

The experimental procedure is discussed in section 3.6. In the stand-alone mode of permeation experiment (Guha et al., 1992), one side of the permeate stream corresponding to the concentration C_{ipi} is closed. Hence, three out of four concentrations in equation 2.102 are known. The mole fraction y_{ii} of species i in the permeate at the closed end corresponding to molar concentration C_{ipi} is expressed as a function of the selectivity (α) and the feed outlet mole fraction x_{io} corresponding to the molar concentration C_{ifo} due to the existence of cross flow at that location:

$$\frac{y_{ii}}{1-y_{ii}} = \frac{\alpha\,(x_{io} - \gamma\, y_{ii})}{(1-x_{io}) - \gamma\,(1-y_{ii})} \tag{2.103}$$

For the present system of study, the VOC concentration in the gas stream is extremely low (maximum 0.001 mole fraction). Hence, for all practical purposes $1-x_{io}$ and $1-y_{ii}$ can be replaced by unity. Equation 2.103 can then be simplified to

$$y_{ii} = \frac{\alpha\, x_{io}}{1-\gamma\,(1-\alpha)} \tag{2.104}$$

Here γ is the ratio between the permeate pressure and the feed pressure.

2.3.3.1 Steps to Calculate VOC Permeance through the Composite Membrane

Following are the steps of calculation for VOC permeance through the composite (porous substrate plus nonporous silicone skin).

1. A value of α was assumed.
2. From the experimental information available for the feed side inlet and outlet, w_i was calculated from VOC material balance. N_2 permeation rate was also calculated.

3. From the experimentally known value of x_{io} , y_{ii} was calculated from equation 2.103 or 2.104.
4. C_{ifi}, C_{ifo}, C_{ipi}, C_{ipo} were estimated in gmol/cc from ppmv or mole fraction unit. $(\Delta C_i)_{ln}$ was calculated from equation 2.102.
5. q_o/δ_o i.e. averaged VOC permeance was calculated from equation 2.101 using the value of w_i calculated in step 2.
6. Applying the same method, q_o/δ_o for N_2 was also calculated.
7. Selectivity (α) was calculated by dividing q_o/δ_o for species i by q_o/δ_o for N_2.
8. α value calculated in step 7 was compared with the previous value of α.
9. If two values matched, then q_o/δ_o in step 5 is the required averaged VOC permeance value; otherwise, steps 3 to 8 were repeated with a new value of α.

2.3.3.2 Calculation of VOC Permeance through the Silicone Skin Calculation steps for obtaining VOC permeance through the composite membrane (gas-filled porous substrate plus silicone skin) is discussed in section 2.3.3.1. Once the overall permeance of VOC through the composite membrane is known, the permeance through silicone skin can be calculated from the following relation, obtained from the resistances- in-series model:

$$\frac{\delta_o}{r_o q_o} = \frac{\delta_c}{(r_c)_{ln} q_c} + \frac{\delta_s}{(r_s)_{ln} D_{igp}} \qquad (2.105)$$

Here $(r_e)_{ln}$ is the logarithmic mean radius applicable to the porous substrate.

2.3.4 Estimation of VOC Diffusion Coefficient in Nitrogen

Diffusion coefficient of VOC in a binary gas mixture (VOC-N_2) at low or moderate pressures was calculated from the following equation (Reid et al., 1977)

$$D_{ig} = 27.3051*10^{-3}T^{3/2}\frac{\left[(M_i+M_{N_2})/M_iM_{N_2}\right]^{1/2}}{p\sigma_{iN_2}^2\Omega_D} \qquad (2.106)$$

Here p is the absolute pressure in psi unit. The expressions for σ_{iN_2} and Ω_D are given in the above reference.

2.3.5 Diffusion of Gaseous Species Inside the Pores of Porous Membrane

Transport of gas molecules through the pores (which can be considered as capillary tubes) has been studied extensively by means of kinetic theory of gases. Three types of mechanisms were proposed for gas transport through capillaries: (1) Knudsen flow, (2) slip flow and (3) viscous flow. Depending on the relative magnitude of the pore radius, r_p and the mean free path, λ_m of the gas molecule, the gas molecules passes through the capillary by means of any of the three mechanisms stated above. It has been suggested that (Liepmann, 1961) when $r_p/\lambda_m < 0.05$, Knudsen type of flow is predominant. Slip flow occurs in the range of $0.05 < r_p/\lambda_m < 50$ (Stahl, 1971; Rangarajan et al.,1984) and for $r_p/\lambda_m > 50$, viscous flow occurs (Present, 1958). For the present study in case II (absorption in coated fibers) pores are filled with the gas and information on diffusivity of VOC molecules inside the pores is required to find out the effective diffusivity of VOC in the gas filled porous membrane (D_{im} in equation 2.71). For the system under study, the r_p/λ_m ratio is near about 0.1; according to various flow regimes discussed earlier, slip flow situation is most likely to predominate inside the pores. The expression for diffusivity in the slip flow regime can be obtained from the flow equation given by Rangarajan et al. (1984). After doing necessary unit conversions the following diffusivity expression is obtained for the gaseous species i:

$$D_{igp} = 1.0133*10^{6}\frac{r_pRT}{M_i\bar{c}_i} \qquad (2.107)$$

where $\bar{c}_i$, the mean speed of the molecule, is given by

$$\bar{c}_i = \left(\frac{8.1064 * 10^6 RT}{\pi M_i} \right)^{\frac{1}{2}} \tag{2.108}$$

Here R is the universal gas constant in cc-atm/gmol-k unit.

2.3.6. Densities of Absorbent Liquids

Density values for absorbent liquids are required to estimated the liquid sample volume from known weight of the sample. Densities for both absorbent liquids were expressed as a function of temperature, t, (°C) by a regression procedure employing the data available from the manufacturers (see section 3.1).

For silicone oil 50cs

$$\rho_l = 0.9802 - 8.356 * 10^{-4} t \tag{2.109}$$

For Paratherm™ heat transfer oil

$$\rho_l = 0.8789985 - 4.206 * 10^{-4} t \tag{2.110}$$

2.4 Simulation Steps for Combined Absorption and Stripping

Numerical simulation for combined absorption and stripping can be easily carried out with the help of individual absorption and stripping models discussed in Sections 2.1.5 and 2.2 respectively. The steps are as follows.

1. With an assumed value of $\phi_{il,in}$ (at the arbitrary point O in the recycle line, Figure 2.8), $\phi_{ig,out}$ and $\phi_{il,out}$ were estimated for a given $\phi_{ig,in}$ and $\langle V_r \rangle_{ref}$ from section 2.1.5.6.

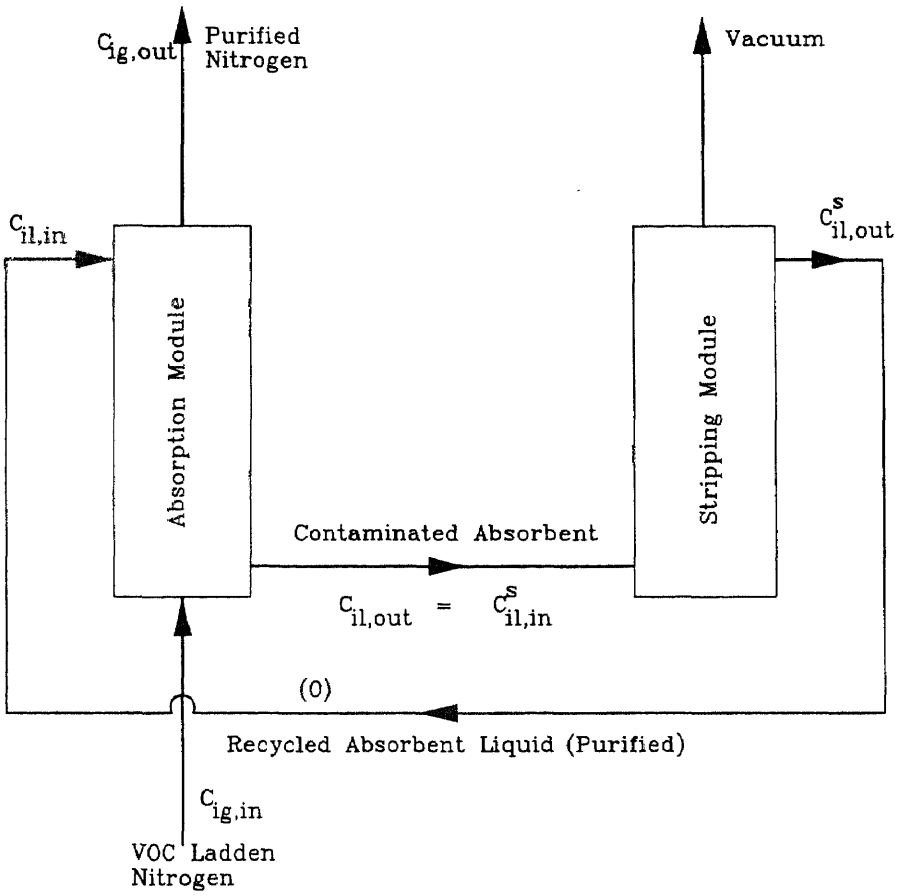

Figure 2.8 Schematic Diagram for Simulation of Simultaneous Absorption-Stripping

2. Equating $\phi_{il,out}$ to $\phi^{s}_{il,in}$, $\phi^{s}_{il,out}$ was calculated from section 2.2.2.2 for given $<V_s>$ (Figure 2.8).

3. Calculated $\phi^{s}_{il,out}$ was compared with the assumed value of $\phi_{il,in}$ at the point O (see Figure 2.8). If the two values matched, then $\phi_{ig,out}$ obtained in step 1 would be the required $\phi_{ig,out}$ for the combined absorption-stripping process.

4. If two values did not match, then steps 1 to 3 were repeated with $\phi_{il,in}=\phi^{s}_{il,out}$

CHAPTER 3

EXPERIMENTAL

3.1 Chemicals

Two absorbents were used in this study:

1. Silicone oil (200 fluid, Dow Corning, Midland, MI) of 50 cs kinematic viscosity and an approximate molecular weight of 300;
2. Paratherm heat transfer fluid (NF™, Paratherm Corporation, Conshohocken, PA) having a viscosity of 30 cp and an approximate molecular weight of 350.

Additional information and other properties of these two absorbents are given in Table 3.1.

3.2 VOC-Nitrogen Gas Mixtures

A number of VOC-N_2 gas mixtures were used ; details are provided in Table 3.2.

3.3 Hollow Fibers and Modules

Two kinds of hollow fibers were used in the experimental studies; the first one was microporous hydrophobic Celgard™ X-10 made of polypropylene. The second one was a micropoprous polypropylene hollow fiber having an ultrathin plasma-polymerized nonporous silicone coating on the outside surface. The detailed properties of these two types of fibers are given in Table 3.3. Three parallel flow shell-and-tube type modules were fabricated using such fibers. The geometrical characteristics of the modules are given in Table 3.4.

3.3.1 Fabrication of Hollow Fiber Modules

Shell-and-tube type parallel flow modules were fabricated using the hollow fibers

Table 3.1 Properties of Absorbents

Properties	Absorbent liquid	
	Silicone oil	Paratherm NF™
Chemical name	Polydimethylsiloxane	-
Molecular weight	300(avg)	350(avg)
Density	0.98 @ 77° F	0.87 gm/cc @ 77° F
Viscosity	50 cs @ 77° F	35 cp @ 77° F
Vapor pressure	< 5 mm Hg @ 77° F	0.001 mm Hg @ 100° F 0.026 mm Hg @ 200° F
Surface tension	-	28 dynes/cm @ 77° F
Flash point	605° F	-
Pour point	-94° F	-45° F
Melt point	-42° F	-
Refractive index	1.402	1.4768
Appearance	Colorless, clear liquid	Colorless, clear liquid
Other properties	Nontoxic, nonbioactive, nonstinging to skin, high oxidation resistance	Nontoxic, FDA/USDA approved for use in food and pharmaceuticals

Table 3.2 Specifications of VOC-N_2 Gas Mixtures

VOC	VOC concentration in feed (ppmv)	Cylinder Pressure (psig)	Type of Analysis	Source
Acetone	993	2000	Primary standard	Matheson Gas Products
Methylene chloride	999	2200	Primary standard	Matheson Gas Products
Methanol	514	1500	Primary standard	Matheson Gas Products
Toluene	236	900	Certified standard	Matheson Gas Products

Table 3.3 Properties of Different Hollow Fibers Used in Experiments.

Type of fibers	Trade name	Fiber ID	Fiber OD	Mean pore diameter	Maximum allowable temperature	Bubble point pressure	Internal burst pressure
Celgard[a] X-10 porous fiber	Celgard X-10[R]	100 μm	150 μm	0.03 μm	75 - 80 °C	150 psi	220 psi
Celgard[b] Coated fiber	Celgard X-10[R]	240 μm	300 μm coating membrane thickness: 1-2Å	0.03 μm	75 -80° C	-	220 psi

a Hoechst Celanese Corporation, Charlotte, NC.
b AMT Inc., Minnetonka, MN.

Table 3.4 Geometrical Characteristics of Different Hollow Fiber Modules Used

Module No.	Type of fiber	Fiber ID (cm)	Fiber OD (cm)	Effective length (cm)	Shell ID (cm)	No. of fibers	Void fraction (%)	Mass transfer area (cm^2)		Mass transfer area per unit volume (cm^2/cm^3)	
								+	++	+	++
1	Celgard* X-10	0.01	0.015	35.7	0.60	600	62.5	1009.40	672.93	100.00	66.67
2	Celgard X-10	0.01	0.015	31.0	0.37	102	83.23	149.00	99.33	44.70	29.80
3	Celgard** with a silicone skin	0.024	0.030	20.5	0.80	300	57.81	579.62	463.7	56.25	45.00

* Hoechst Celanese SPD, Charlotte, NC.
** AMT Inc., Minnetonka, MN.
\+ Based on outside diameter
++ Based on inside diameter

mentioned above. The shell was made from a 1/4" OD stainless steel tube having a male run tee connected at each end. The epoxy used for potting the fibers was Armstrong C-4 epoxy with D activator (Beacon Chemicals, Mt.Vernon, NY) mixed in the ratio of 4:1 of epoxy : activator.

A predetermined number of hollow fibers were counted carefully and then arranged in the form of a bundle on a table. Both ends of the bundle thus made were tied with a thread. This bundle was carefully inserted inside the shell by pulling the thread connected to one end of the fiber bundle through the shell. Insertion of the fiber inside the shell was done by first immersing the shell in water to reduce friction. The fiber length was selected such that about 2 inch (5 cm) length of fibers remained outside the end fittings at both ends of the module. The fibers were then dried by applying vacuum for about 24 hrs.. The ends of the fittings were first sealed with silicone rubber (RTV 118, General Electric, Waterford, N.Y) which was allowed to cure for about two hours. The epoxy and activator were next mixed well in the right proportions and the mixture was degassed by applying vacuum for about 4 to 5 minutes. This mixture was poured through the shell side opening at one end till the lower portion of the male run tee was full. The epoxy was allowed to cure for about 10 hours by keeping the module vertical. The other end of the module was potted in a similar manner. When the epoxy was cured completely, a leak test was performed employing water under 20 psig (239.22 kPa) pressure in the shell side for one hour.

Modules were also prepared with silicone coated Celgard fibers for absorption and stripping experiments. A similar procedure was adopted for fabrication of the module. However, one additional potting layer of silicone rubber, RTV 615 A & B (GE Silicones, Waterford, NY) was essential as epoxy does not make a good enough bonding with the silicone coating of the fiber. This layer was put in between the other two layers of pottings (Figure 3.1). The modules are shown in a photograph (Figure 3.2).

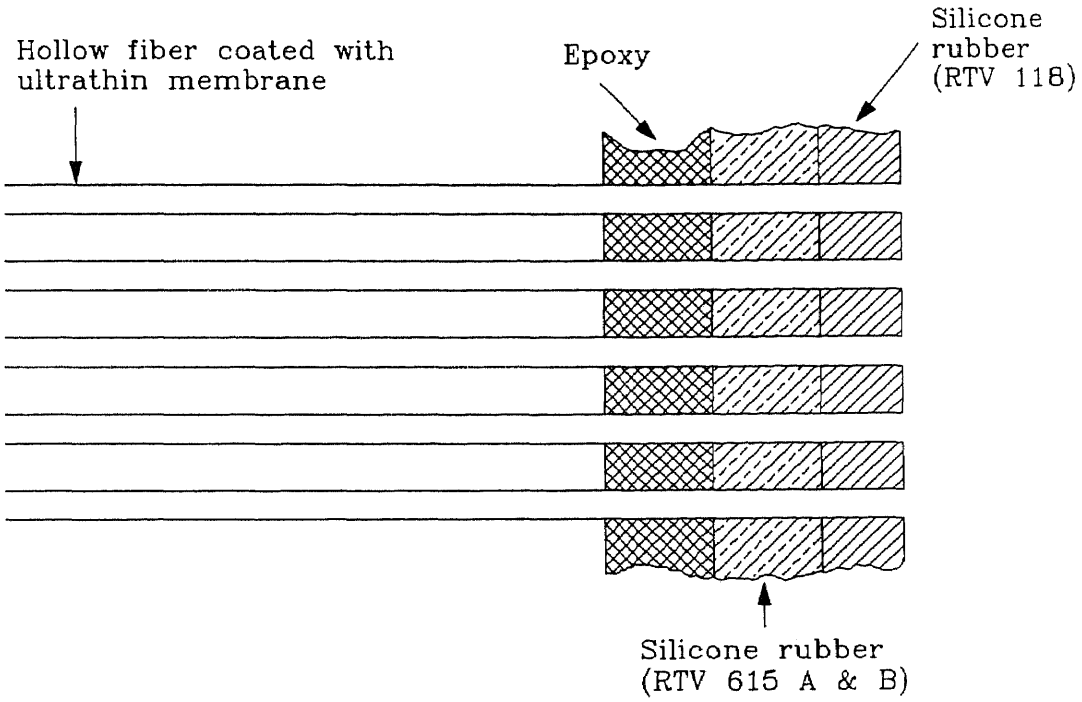

Figure 3.1 Three Layers of Pottings in Silicone-coated Fiber Module

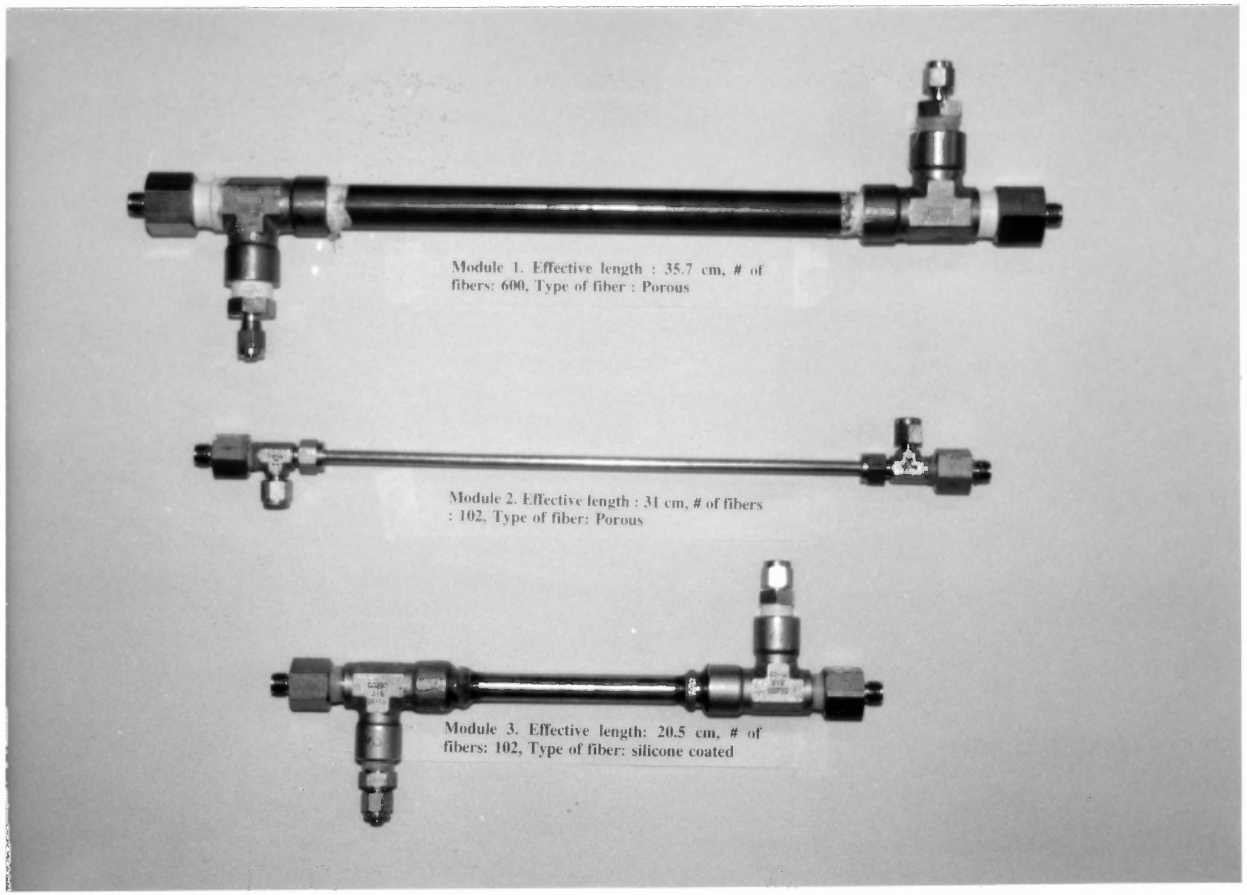

Figure 3.2 Photograph of Different Hollow Fiber Modules Used in Experiments

3.4 Experimental Setup and Procedure for VOC Absorption

The setup for VOC absorption experiments is depicted in Figure 3.3. At the beginning of the experiment, a newly made module employing porous hollow fibers was soaked in the absorbent liquid (silicone oil or Paratherm heat transfer fluid) by pouring the liquid in the shell side to wet the fibers. A specific VOC-containing N_2 gas was passed through the tube side of the module at a predetermined controlled rate. The gas flow rate was controlled and monitored by means of an electronic mass flow transducer (model 8141, Matheson, E. Rutherford, NJ) and a flow controller (model 8209, Matheson, E.Rutherford, NJ). However, the actual gas flow rates were measured manually by means of a bubble flow meter connected to the stream exiting from the process. A pressure of about 3 psig (122.01 kPa) was maintained at the tube side outlet by adjusting the back pressure regulator. Higher pressure in the gas phase than that in the liquid phase was essential for immobilizing the gas-liquid interface at the pore mouth of the inner tube wall.

In the case of a coated fiber-based module, absorption experiments were initiated by pumping the absorbent liquid directly through the shell side of the module. Because of the presence of the ultrathin nonporous silicone skin on the outer surface of the fiber, liquid absorbent in the shell side can not come in direct contact with the gas stream flowing through the fiber bore. Gas side pressure was kept at atmospheric level in order to maintain the condition for nondispersive gas liquid contact.

Experiments were started by pumping the fresh absorbent liquid from a glass container through the shell side of the module by means of an electronic metering pump (10313M, LMI, Milton Roy, Acton, MA). A pulse dampener was used at the discharge side of the pump to eliminate flow pulsations. Liquid flow rates were controlled by adjusting the stroke-length and the stroke-frequency of the pump. Once the liquid flow rate was adjusted, concentration measurement of the exit gas stream from the absorber module was started via the gas chromatograph (GC) (3400 STAR, Varian, Sugarland, TX) having a flame ionization detector. Exit gas from the GC was vented out through a laboratory exhaust hood. A specific experimental run was continued until the gas outlet

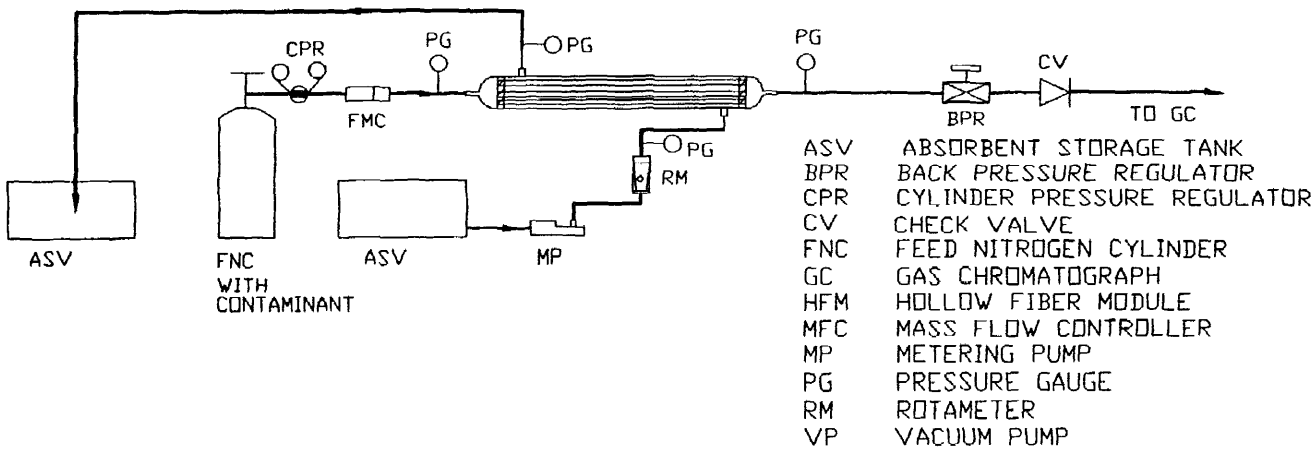

Figure 3.3 Schematic Diagram of Experimental Setup for VOC Absorption

composition was essentially constant as detected by the GC. Most of the measurements were carried out at 23° C ± 2° C.

The effects of three parameters, namely, the gas flow rate, the liquid flow rate and the feed composition on VOC absorption performance were studied. In a set of experiments one of the parameters was varied by maintaining the other two parameters constant.

3.4.1 Complete Regeneration of Absorbent Liquids for Further Use

Regeneration of spent absorbents were essential for subsequent absorption experiments with fresh absorbent liquids. Once a set of absorption run was complete, the spent absorbent liquid was stored in a container. A batch of spent absorbent liquid was then taken in a closed stainless steel vessel leaving sufficient vapor space over the liquid surface. A vacuum connection was provided at the top of the vessel and a slight air was allowed to leak through a crack-open dip-pipe so that the air could bubble through the liquid hold-up under the action of vacuum. The combination of vacuum and air bubbling helped VOC to get stripped out from the liquid. The system was generally run for 20 to 24 hours to ensure complete stripping. To make sure the VOC was completely stripped, a sample of the liquid was analyzed through GC-Headspace arrangement (see Section 3.8). No peak in the GC output ensured the complete regeneration of absorbent liquid. The analyses were also carried out by bubbling nitrogen zero gas at a very low flow rate (2-5 cc/min) through the sample and injecting the gas to GC.

3.5 Apparatus and Procedure for Combined Absorption-Stripping of VOC

The schematic diagram of the experimental setup for combined absorption-stripping is shown in Figure 3.4; a photograph of the actual experimental setup is shown in Figure 3.5. Regenerated absorbent liquid was pumped (MP) from a small glass container (ASV) to the shell side of the absorber module (HFM) for absorbing the VOC from VOC-N_2

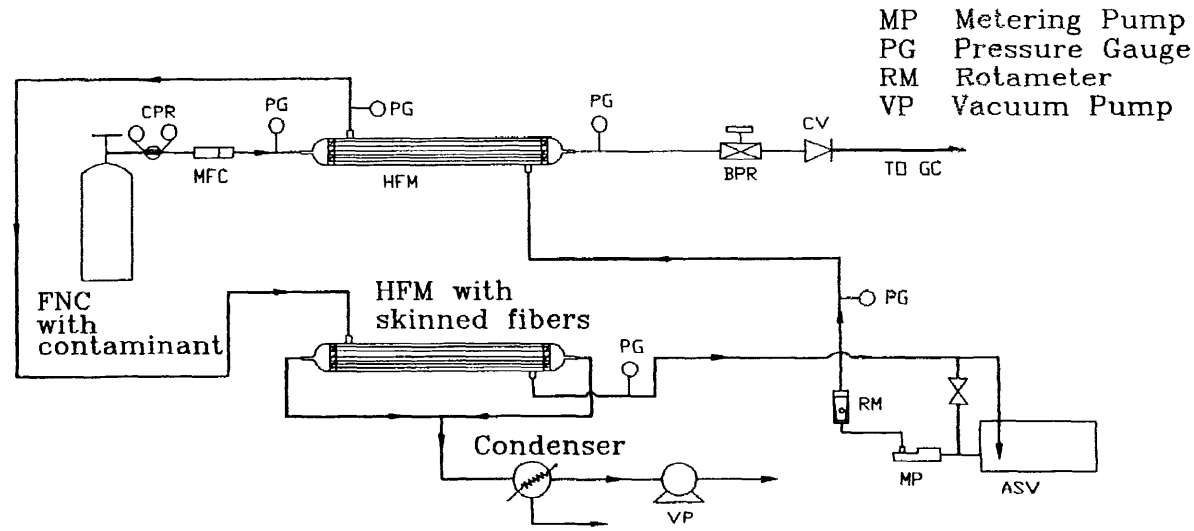

Figure 3.4 Schematic Diagram of Experimental Setup for Combined Absorption and Stripping

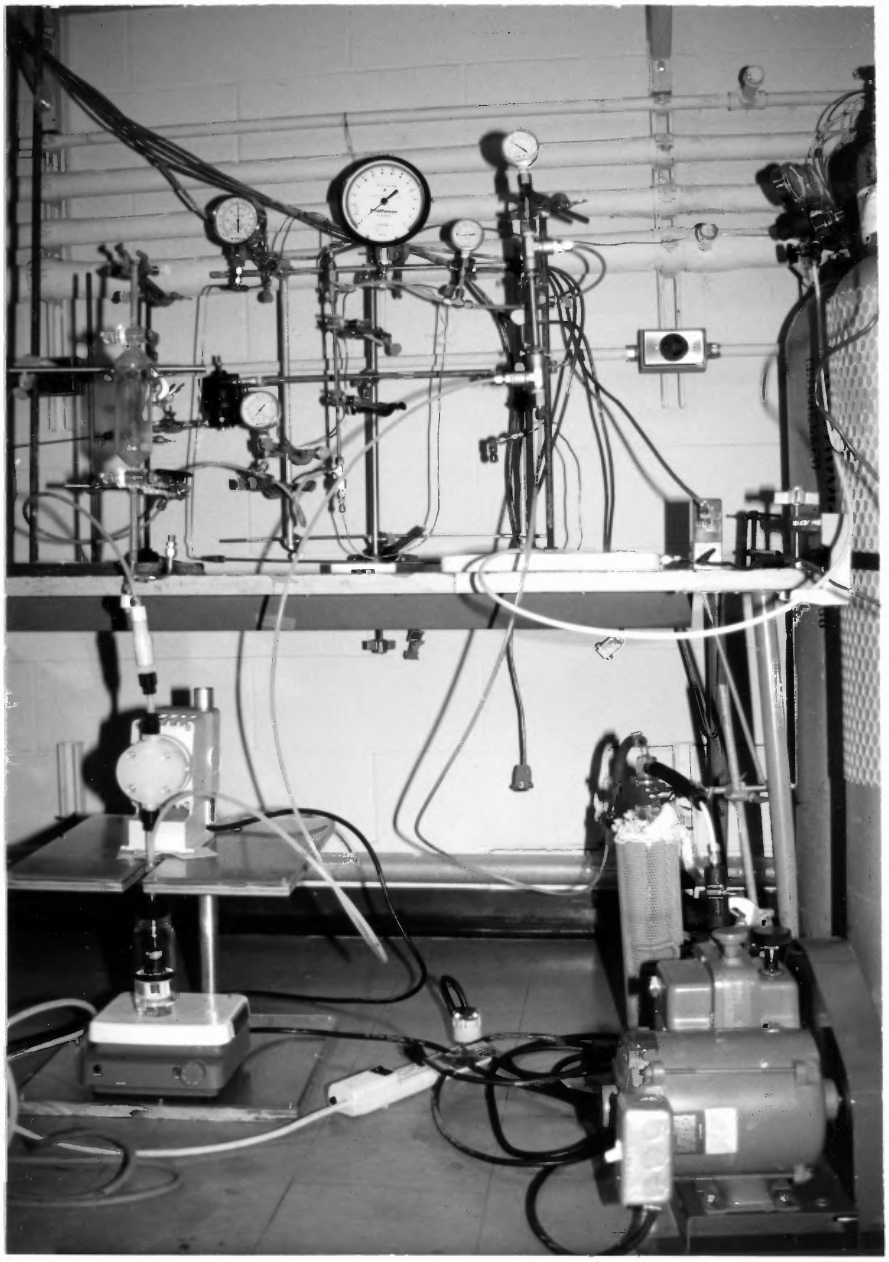

Figure 3.5 Photograph of Experimental Setup for Combined Absorption-stripping of VOCs

feed gas mixture flowing through the tube side of the module countercurrently with respect to the absorbent flow. The absorbent exiting the absorber was connected to the shell side of the stripper hollow fiber module. A vacuum pump (VP) was connected to the tube side of the stripping module via a condenser. The purified absorbent liquid from the stripper was recycled back to the absorbent circulation vessel (ASV). This vessel was closed tightly to avoid any VOC escape from the holdup liquid. The gas outlet from the absorber was connected to the GC via a back pressure regulator. The GC outlet was connected to a bubble flow meter for manual measurement of gas flow rate. Finally the exit gas was vented out through a laboratory fume hood.

Before starting an experiment, the shell side of the absorber module was first filled with the absorbent to wet the membrane in the case of porous membranes without a nonporous coating (for a membrane having a nonporous coating, there is no need to fill the shell side with absorbent liquid before hand). Then the VOC-N_2 gas mixture flow was switched on at a predetermined flow rate through the tube side of the absorber module. The constant gas flow rate was maintained and monitored by means of an electronic mass flow transducer and controller. The tube side gas pressure at the outlet of the absorber was maintained at 3 psig (122.01 kPa) above the liquid phase pressure for porous membranes by adjusting the back pressure regulator. Liquid phase pressure was essentially atmospheric. Absorbent circulation pump was then started. First the liquid flow rate was measured manually by collecting the liquid in a measuring cylinder over a definite period of time from the outlet of the stripper module. Once the liquid flow rate was set, the stripper outlet liquid line was connected to the absorbent circulation vessel. The volume of liquid inside this vessel was in excess over the amount required to fill the pump suction line and the hold-up volume of the setup. The volume of the circulation liquid was kept at the lowest possible level in order to reduce the time required to achieve a steady state. After some time, the absorbent storage vessel may be bypassed. The VOC concentration of exit gas was monitored in the GC every hour. Time taken to attain a

steady state composition of VOC at the absorber outlet was found to be approximately 7 to 8 hrs. The experiments were repeated for different gas flow rates as well as liquid flow rates. After the end of a single run liquid sample was collected from the circulation vessel in a cold trap (sample bottle kept in dry ice) for analysis purposes and was kept in refrigerator. Fresh run was started after making up the absorbent liquid volume in the circulation vessel. Continuous runs as long as 120 hours were carried out without any problem.

3.6 VOC Composition Measurement in the Gas Phase

VOC concentrations in the gas phase were measured in a Varian 3400-STAR gas chromatograph (Varian, Sugarland, TX) using a flame ionization detector (FID). The response from FID was recorded in a built-in integrator in the GC. Certified standard (toluene-N_2) and primary standard (acetone-N_2, methylene-chloride-N_2, and methanol-N_2) gas mixtures from Matheson (E. Rutherford, NJ) were used for calibration. The gas mixture was injected into the GC column through a 6-port gas sampling valve (Valco, Houston, TX). Figure 3.6 shows the positions of the valve in its load and injection mode. Dry air at 80 psig pressure was used to drive the solenoid valve in the actuator of the 6-port valve in the GC. A 6'x 1/8" column (Varian Analytical Instruments, Sunnyvale, CA) having 0.3 % carbowax 20 M on Carbopack c support was used for analysis. Operating parameters used for various VOC-N_2 mixtures are listed in Tables 3.5 and 3.6. Calibration of different VOC composition levels was done by mixing the VOC-N_2 mixture and nitrogen-zero gas (99.99 % pure) in predetermined ratios by means of two electronic mass flow transducers (Figure 3.7). The calibration curves for different VOCs are shown in Figures 3.8 through 3.11. In the calibration gas concentrations used had the units of ppmv (cc of VOC in 10^6 cc of gas at 23 ± 2° C).

3.7 Experimental Setup and Procedure for Determination of VOC Permeance through the Nonporous Silicone Skin of Skinned Hollow Fiber

The experimental setup for determination of permeance of the coating in the coated fiber is illustrated in Figure 3.12. The VOC-N_2 gas mixture was passed through the shell side

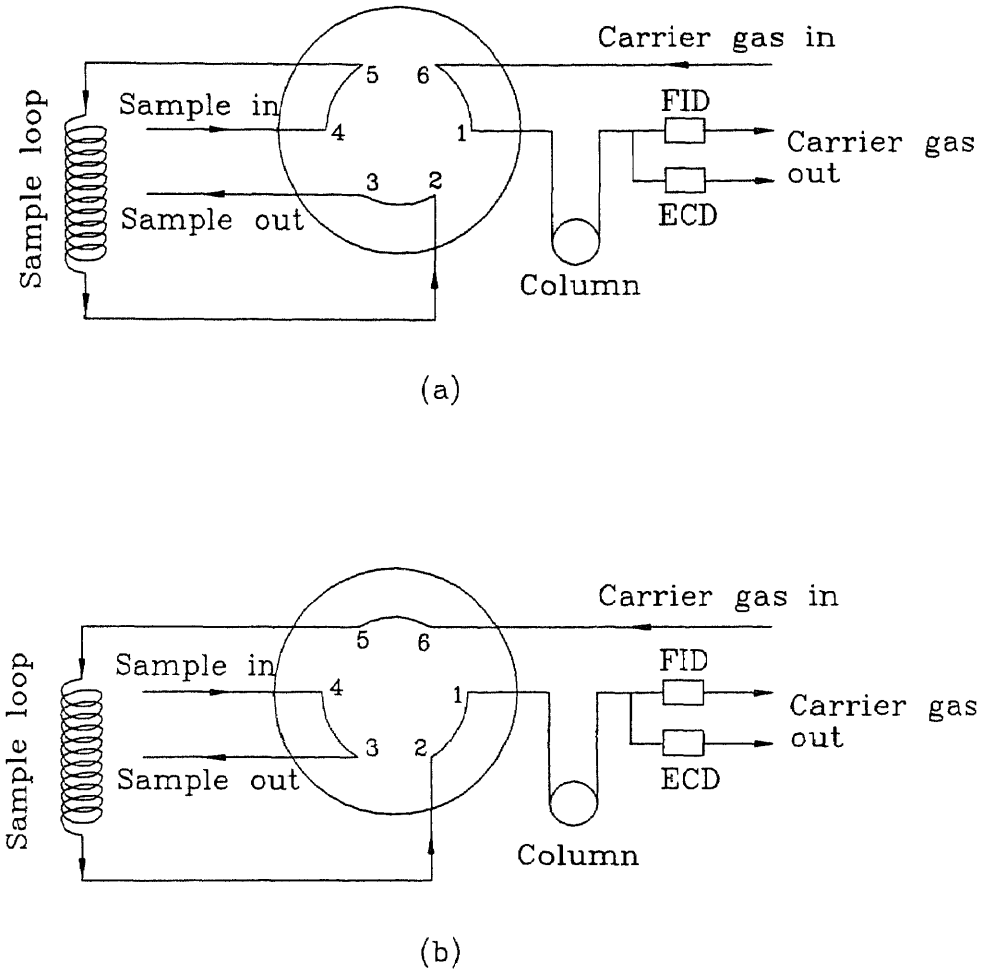

Figure 3.6 Schematic Diagrams of The Six Port Valve in Its (a) Load and (b) Injection Position.

Table 3.5 Operating Parameters of GC for Detecting Various VOCs

VOC	Column Temperature(°C)	Injector Temperature(°C)	Detector Temperature(°C)
Acetone	150	220	250
Methylene chloride	100	150	200
Methanol	150	160	220
Toluene	150	220	250

Table 3.6 Operating Parameters for Analytical Gases Used in GC

	Gas	Flow rate (cc/min)	Pressure (psig)
Gas 1 for FID	Air - zero	300	60
Gas 2 for FID	Hydrogen - zero	30	40
Carrier gas	Nitrogen - zero	30	80

Table 3.7 Operating Parameters of Headspace Autosampler

Parameters	time
Platten equilibration time	0.5 min
Sample equilibration time	35-40 min
Mixing time	0.1 min
Mixing power	1
Stabilization time	0.5 min
Sample vial pressure	3.5 psig
Pressurization time	0.15 min
Pressure equilibrium time	0.15 min
Loop fill time	0.12 min
Loop equlibration time	0.15 min
Injection time	3-6 min

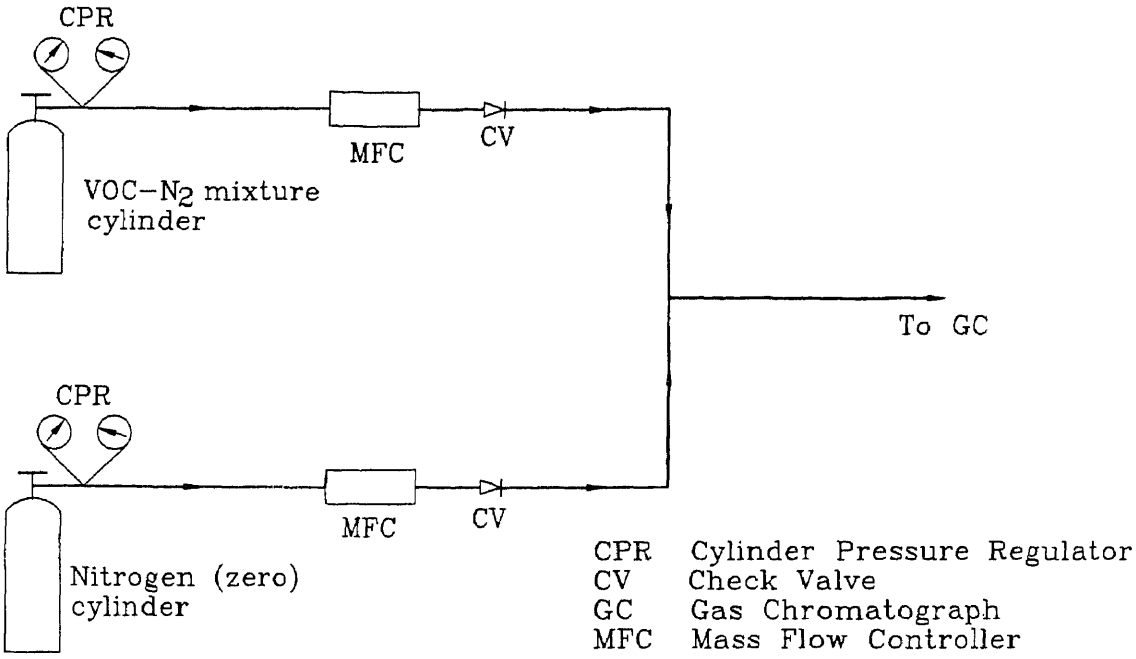

Figure 3.7 Schematic Diagram of Experimental Setup for Calibration

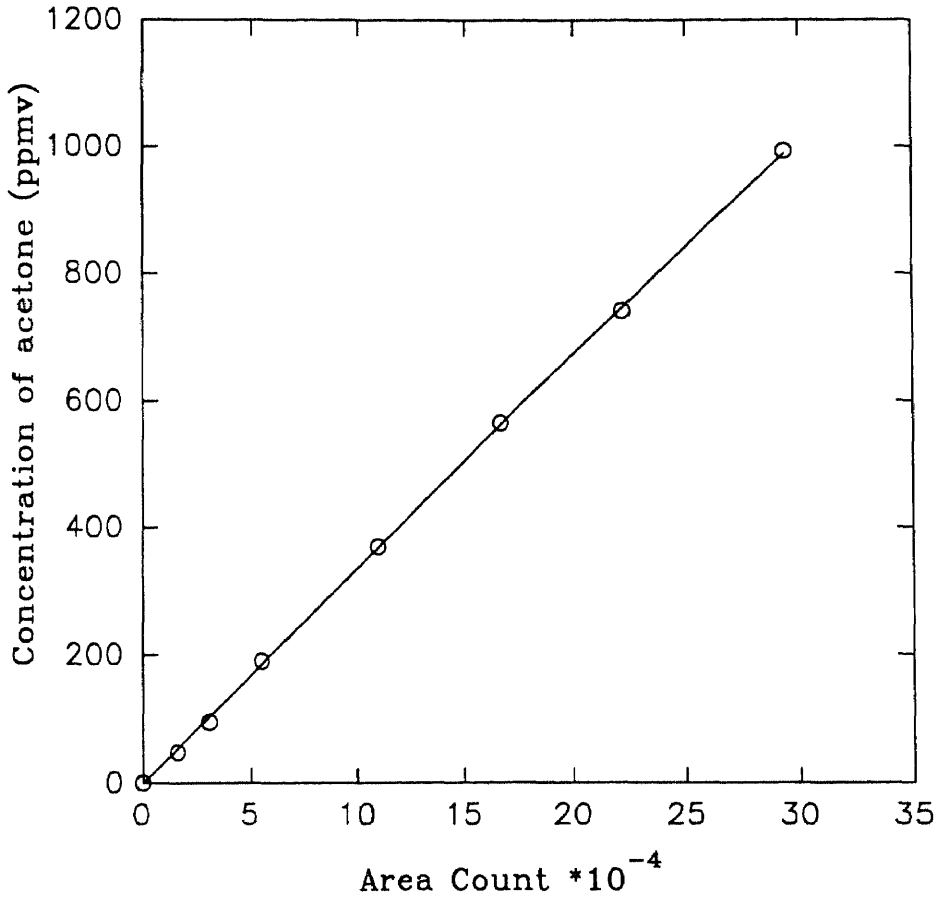

Figure 3.8 Calibration of Acetone-Nitrogen Gas Mixture (Concentration in ppmv vs. GC Peak Area)

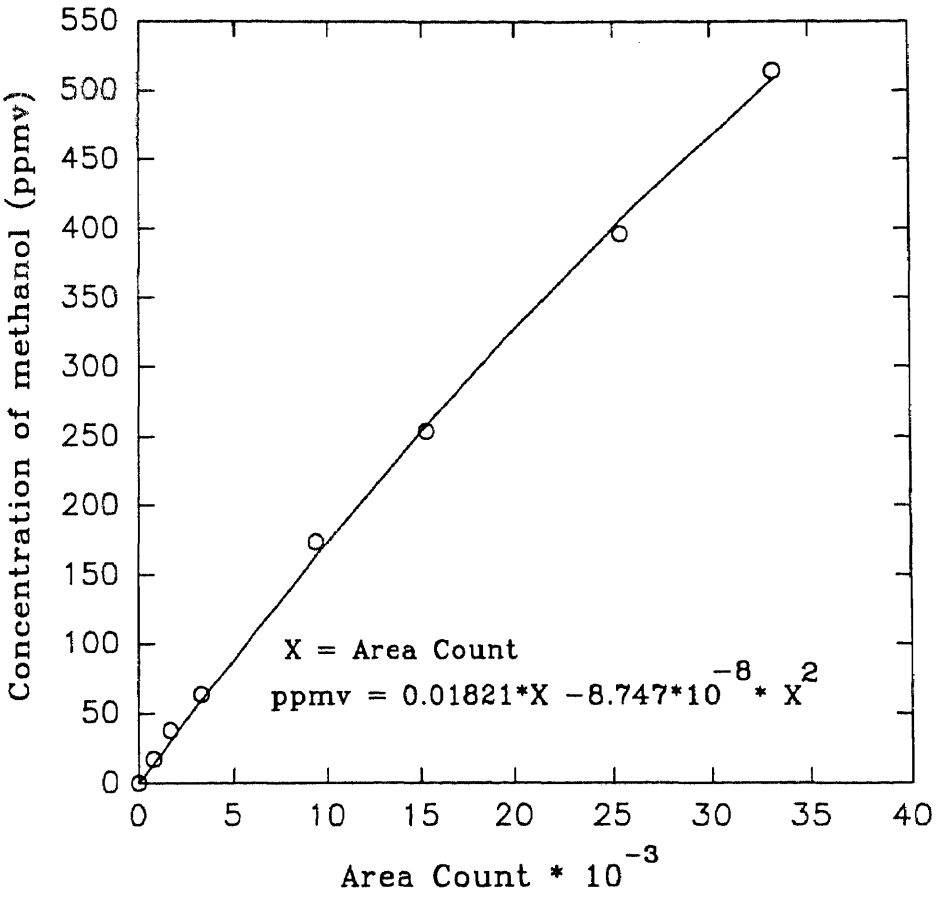

Figure 3.9 Calibration of Methanol-Nitrogen gas Mixture (Concentration in ppmv vs. GC Peak Area)

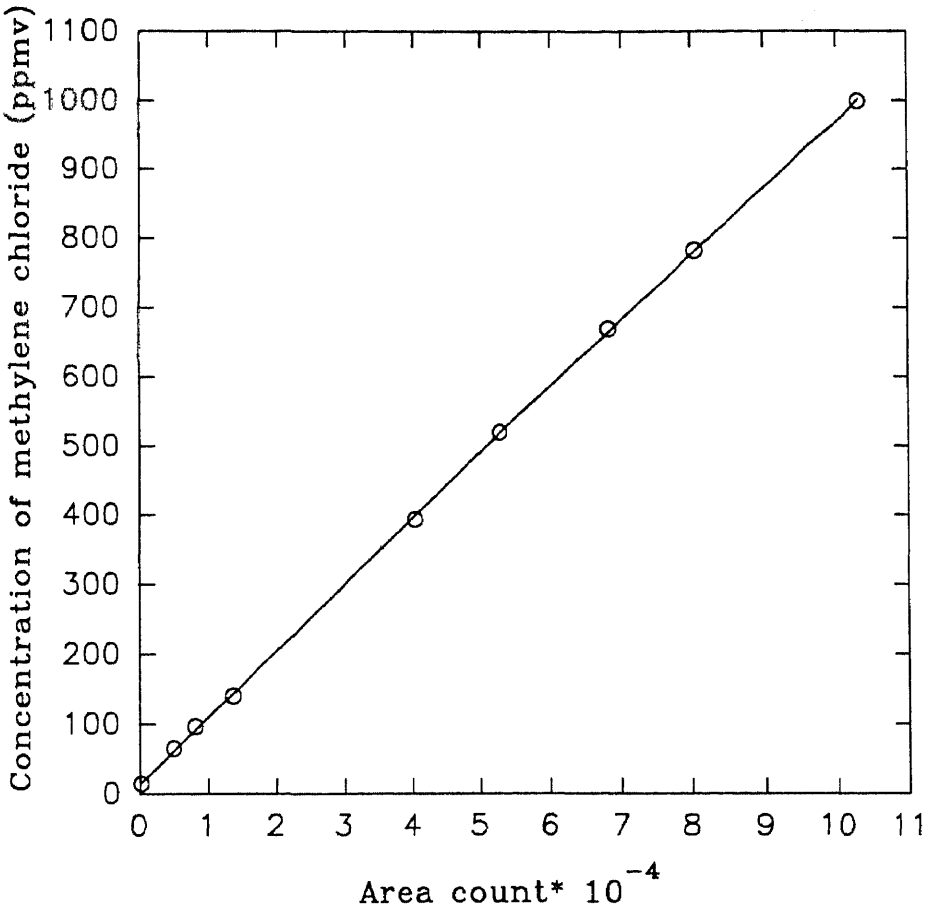

Figure 3.10 Calibration of Methylene Chloride-Nitrogen Gas Mixture (Concentration in ppmv vs. GC Peak Area)

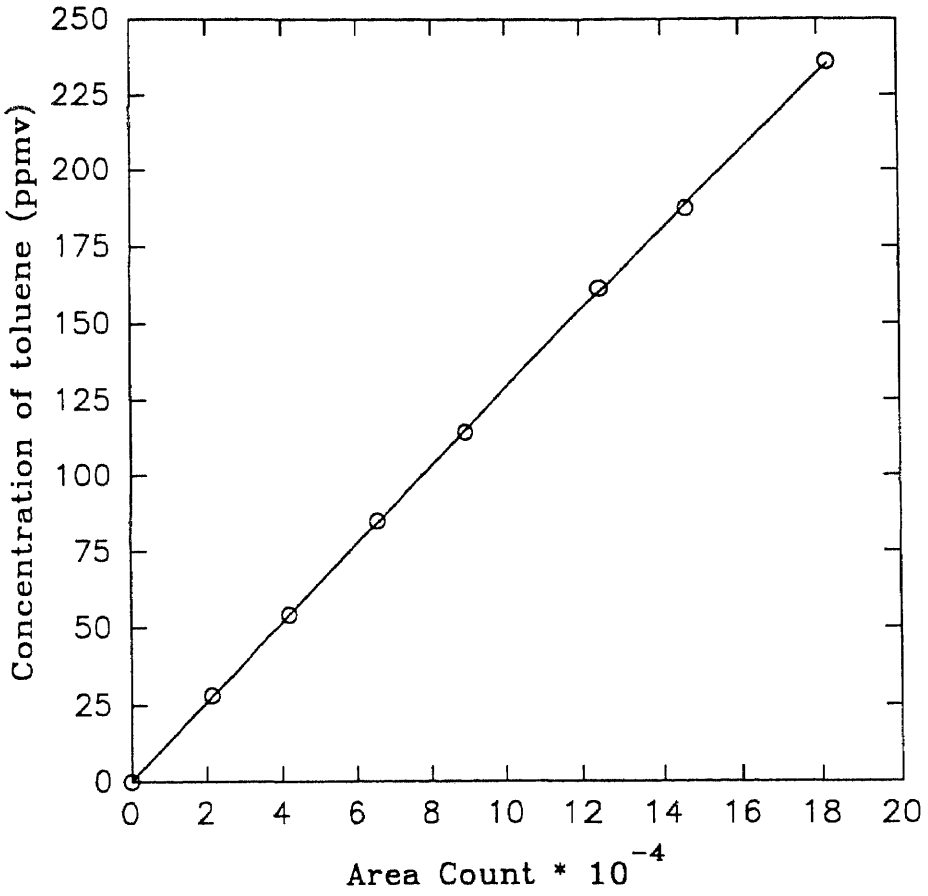

Figure 3.11 Calibration of Toluene-Nitrogen Gas Mixture (Concentration in ppmv vs. GC Peak Area)

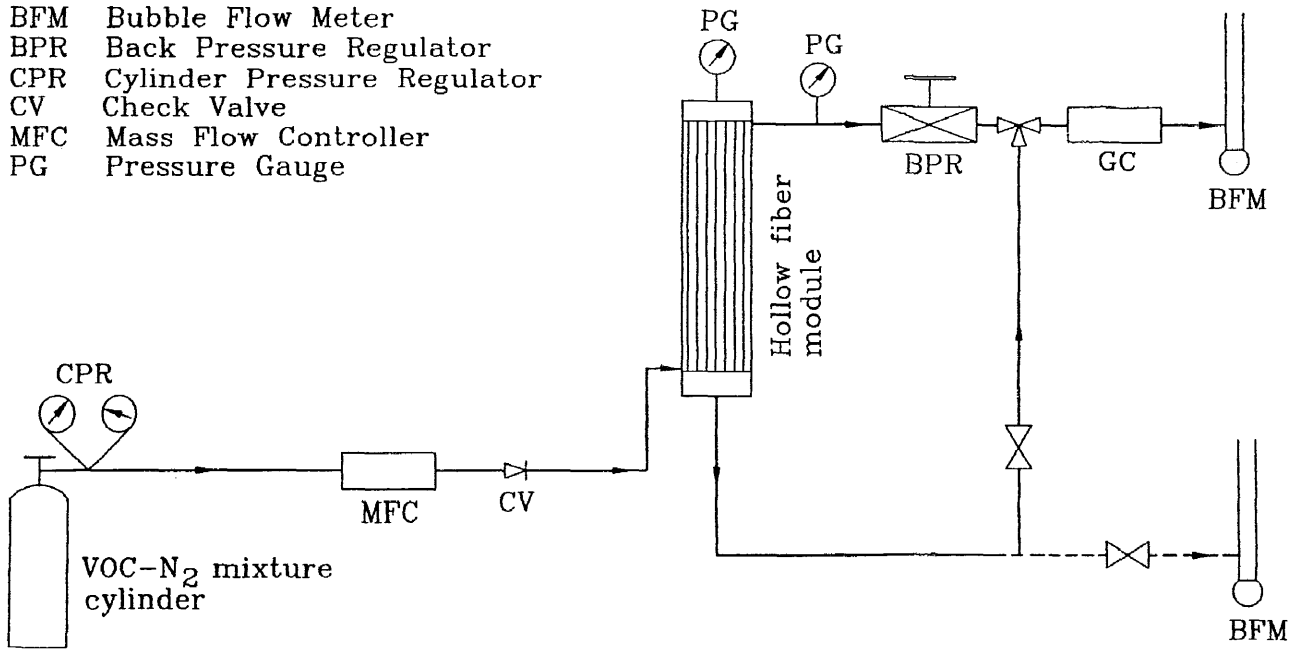

Figure 3.12 Schematic Diagram of Experimental Setup for Determination of Permeability of VOC through the Silicone Skin

of the hollow fiber module from a gas mixture cylinder. The gas flow rate was controlled and monitored by means of a mass flow transducer and a controller (MFC). The gas pressure in the shell side of the module was maintained by a back pressure regulator (BPR) connected to the shell side outlet of the module. The exit gas from the back pressure regulator was injected into the GC. The outlet gas from the GC was vented through the laboratory hood via a bubble flow meter. One end of the tube side of the module was connected to a pressure gauge and the other end was connected to the GC and a bubble flow meter in series before it was vented into the exhaust hood.

For a specific VOC-N_2 gas mixture and a fixed shell side pressure, the feed gas flow rate and the pressure were adjusted such that an appreciable flow of gas was available at both feed outlet and permeate outlet i.e., at the shell side outlet and the tube side outlet respectively. The feed outlet and the permeate flow rates were then measured by means of bubble flow meters connected to the respective gas streams. The permeate VOC-enriched gas composition was measured in the GC at frequent intervals. Once a steady composition of VOC in the permeate gas was monitored in the GC, the feed outlet composition was measured by injecting the feed outlet gas into the GC. Typical time required for obtaining steady state varied between 3 to 4 hrs.

3.8 Determination of Henry's Law Constant

Dimensionless Henry's law constants for acetone, methylene chloride, methanol and toluene were determined independently in two different absorbent liquids (silicone oil and Paratherm™ heat transfer fluid). Various experimental steps are described below.

3.8.1 Stock Solution Preparation

A fixed volume of absorbent liquid was first chilled in a refrigerator. A particular liquid VOC (HPLC grade) was also chilled in a similar way and then a known volume of it was added to the absorbent liquid to make a solution of the VOC of known concentration in

the liquid absorbent. This solution was kept stirred for about 10 minutes. The solution thus prepared was stored in the freezer as a stock solution. All solutions and samples were prepared and handled under low temperature to minimize error from VOC losses through volatilization.

3.8.2 Sample Preparation

Sample vials of 22 ml size (Tekmar, Cincinnati, OH) were used for all experiments needed for determination of Henry's law constant. The exact volume of any vial was measured by obtaining the difference in weight of an empty vial and that of the same vial filled with water and then dividing the weight difference by the density of water. The volumes of the sample vials were found to be essentially constant, 22 ml ± 0.1 ml. A sample vial was prepared in the following way. The stock solution bottle was taken out of the refrigerator and kept inside an open container filled with ice. An empty sample vial was also kept in an open container filled with ice in such a way that most of the surface area of the vial was in contact with ice. A small volume of the stock solution of known concentration was next transferred quickly from the stock solution bottle to the chilled sample vial. The vial was then sealed immediately. The exact volume of the sample transferred was measured by taking the difference in weight of the empty vial and that of the vial along with sample and then dividing the weight difference by the density of the sample. The sealed vial was kept at room temperature for a prolonged period of time so that the sample could eventually attain the room temperature before it was allowed to equilibrate at a relatively higher temperature (w.r.t room temperature) within the headspace autosampler.

3.8.3 Determination of Optimum Equilibration Time

The vapor space available above the liquid in a particular sample vial is referred to as the 'headspace'. The concentration of analytes increases in the headspace with time. In most

cases at a specific temperature after sufficient time the concentration of analytes (here VOCs) reach a steady state condition known as equilibrium. When a sample is in an equilibrium state, analyte concentration within the headspace is at its maximum and does not fluctuate much with heating time. In order to find out the equilibrium time for two different sample matrices (silicone oil and Paratherm) sample vials having the same amount of sample were exposed to different heating times at the same temperature. Figure 3.13a shows a typical time vs. area count plot of acetone in silicone oil and in Paratherm. Similar studies were carried out for other VOCs as well. Plots for toluene and methanol are shown in Figure 3.13b. About 40 to 50 minutes of equilibration time was found to be good enough for analysis with maximum sensitivity and highest precision.

3.8.4 Experimental Technique for Henry's Law Constant Measurement

Various sample vials were prepared (as discussed in Section 3.8.3) by adding different known volumes of samples having a constant concentration of a particular VOC into different vials. The samples were then kept exposed to room temperature for sufficient time so that samples could attain the room temperature. A particular sample vial was then loaded into the headspace autosampler (model 7000, Tekmar, Cincinnati,OH). The headspace autosampler was interfaced with a gas chromatograph (3400-STAR, Varian, Sugarland, TX) by means of an interfacing cable. The operating conditions of the autosampler are listed in Table 3.7.

Operational sequence of the headspace autosampler is shown in Figure 3.14. An incoming supply of carrier gas (N_2) is split into two paths. The upper path provides a constant source of flow-controlled carrier gas (CG1) to the GC column via a six port valve (6PV) in the autosampler. The pressure gauge PG1 reads the column back pressure of GC. The lower path of carrier gas (CG2) provides pressurization gas for the sample vials. This supply is both pressure regulated and flow controlled. In the standby mode (a), the pressurization valve (PV) is open allowing a continuous stream of clean N_2 gas (CG2)

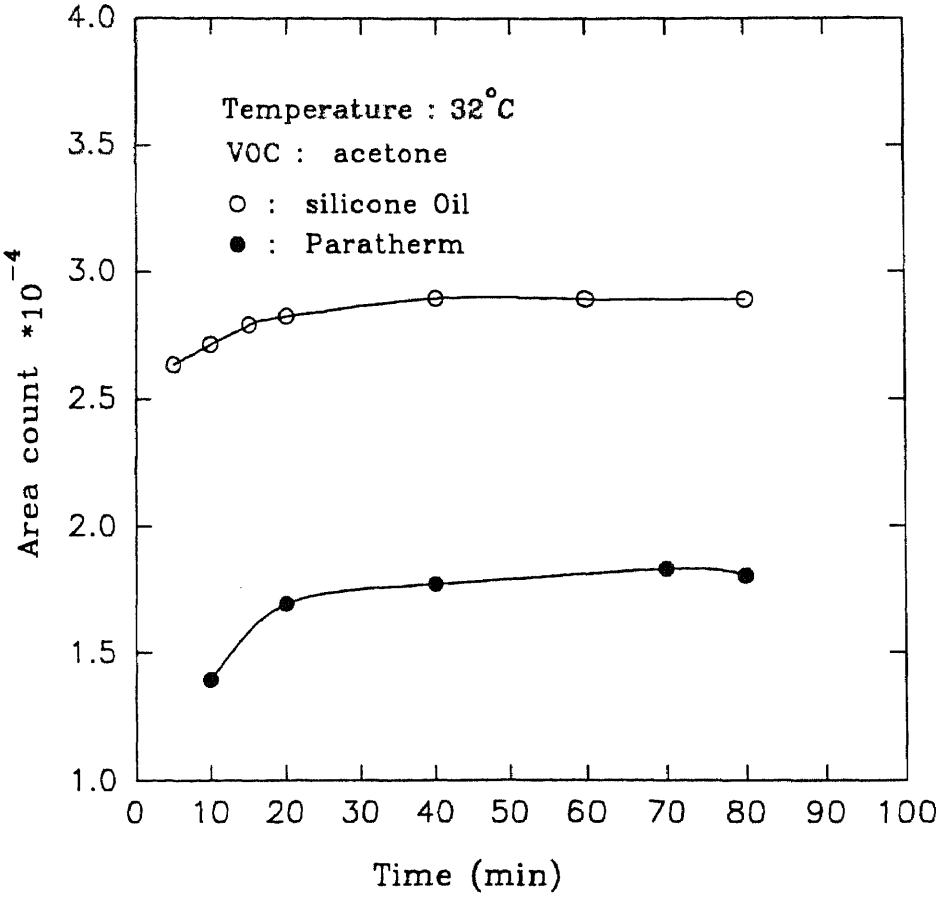

Figure 3.13a Time vs. Headspace VOC Concentration (In Terms of Area Count)

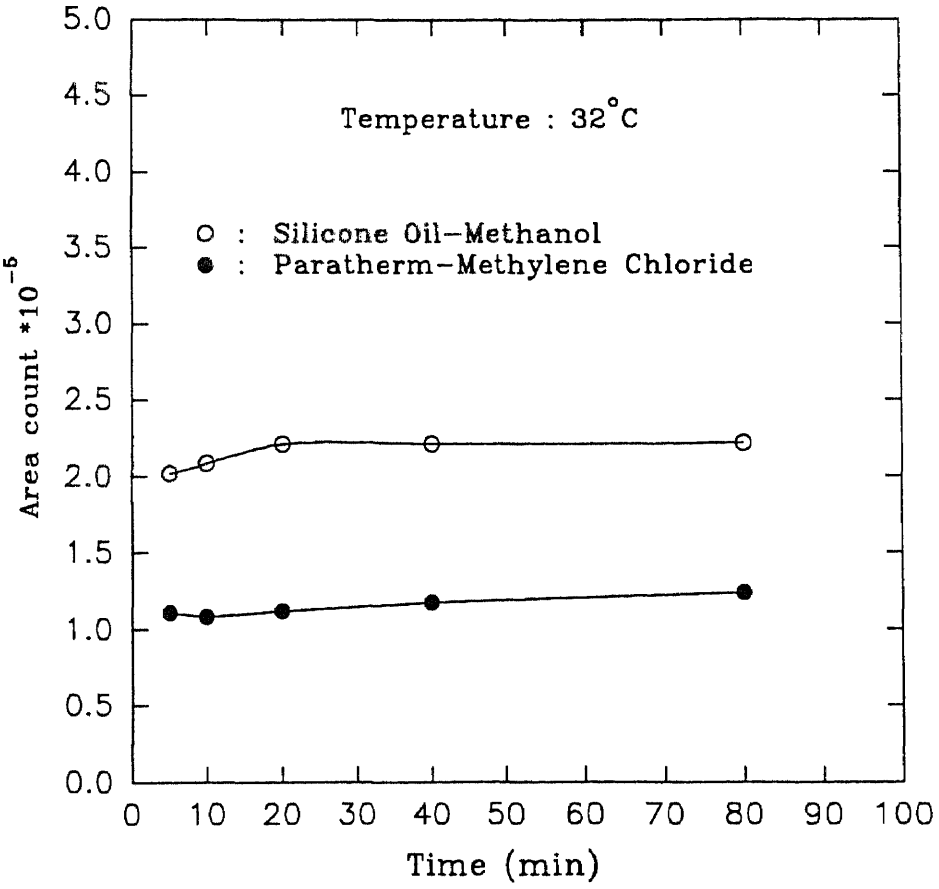

Figure 3.13b Time vs. Headspace VOC Concentration (In Terms of Area Count) for Different VOCs

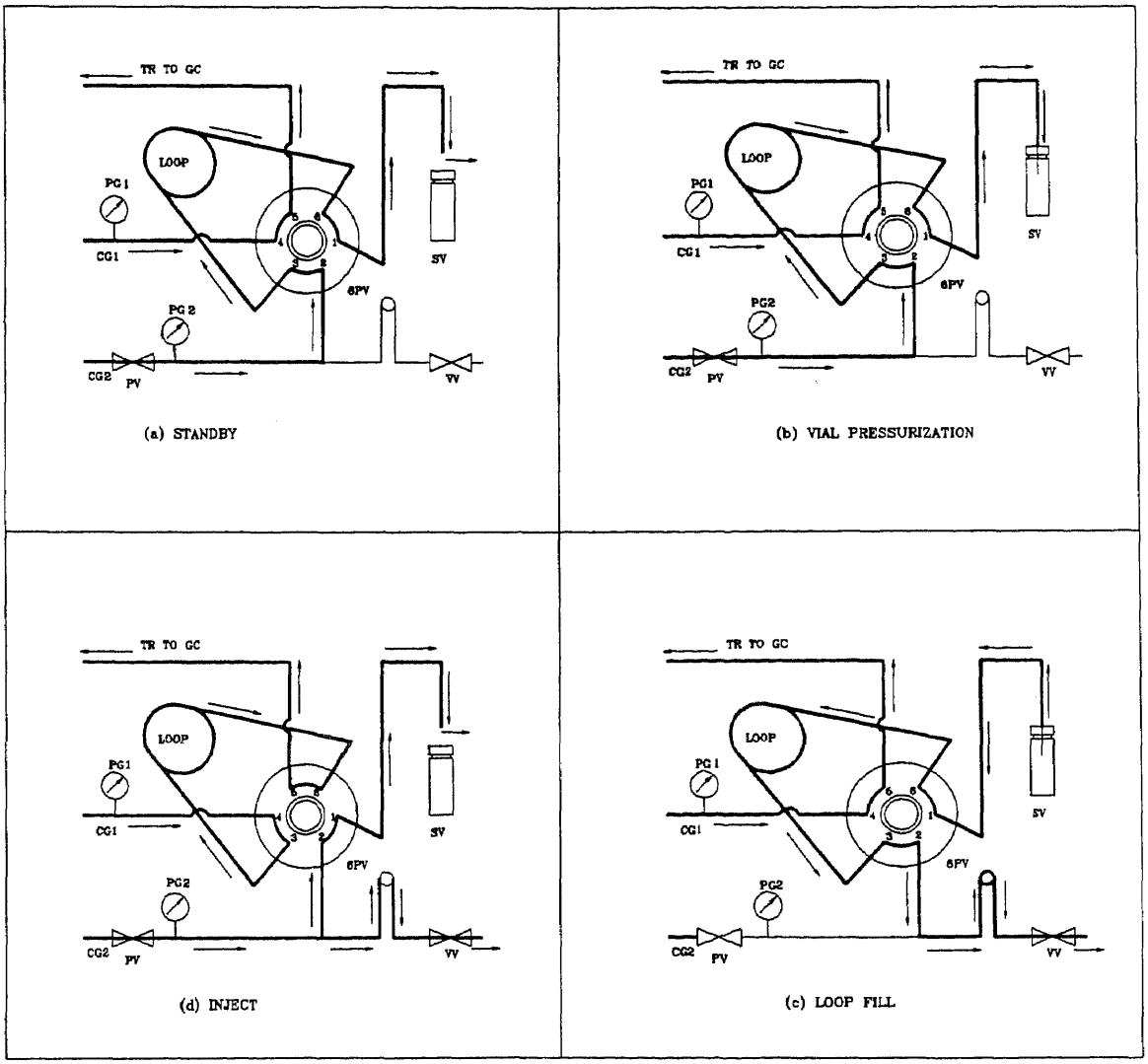

Figure 3.14 Various Operating Sequences of Headspace Autosampler

to sweep the sample loop and exit through the sample needle. This constant flow of N_2 gas prevents any airborne contaminants from entering the system through the needle as well as provides a cleaning flush of the sample loop to minimize carry over. The sample attains equilibrium at the platen temperature in this mode of operation.

In the vial pressurization mode (b) the sample vial is elevated onto the sample needle, piercing the septum top cap. The incoming flow of carrier N_2 gas (CG2) pressurizes the vial to the pressure selected by the regulator (in this case 3.5 psig (125.45 kPa)). This pressure can be read in pressure gauge, PG2. The pressurization is turned off by closing the pressurization valve (PV). In the loop fill mode of the operation (c) the vial is allowed to equilibrate and then the vent valve (VV) is opened. The pressure in the vial vents through the sample loop, filling it with sample vapor. Finally in the injection mode (d) the six port valve is rotated, allowing the carrier gas to backflush the sample out of the loop and goes to the injector of the GC through the insulated transfer line (TR). Built-in integrator of the GC gives the output in terms of area count proportional to the vapor phase concentration in the head space of sample vial. The experiments were repeated for various sample liquid volume at the same temperatures.

Once a set of area count versus gas to liquid volume ratio data were obtained, dimensionless Henry's law constant were calculated by the method as described in the following Section. Experiments were also conducted to determine Henry's law constant at different temperature for a particular VOC-absorbent system.

3.9 Experimental Setup and Procedure for Determination of VOC Diffusivities through the Absorbent Liquids and Absorbent Liquid Filled Membrane

Information of VOC diffusivities through the liquid absorbents is required as an input to the theoretical models for obtaining simulated results. Schematic diagram of experimental setup is shown in Figure 3.15. Experimental setup and procedures were very similar to those for the VOC permeability determination through nonporous silicone skin of skinned

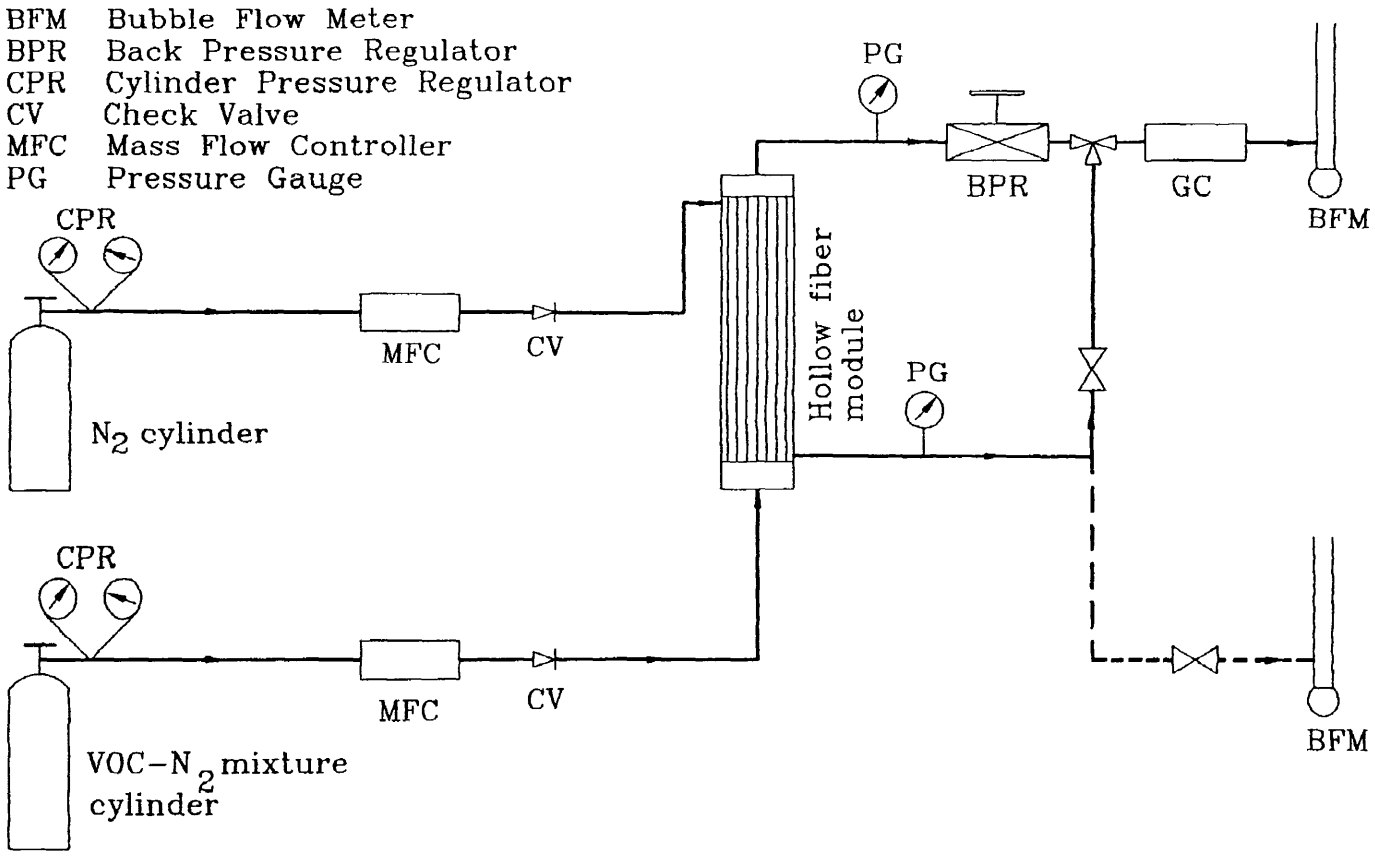

Figure 3.15 Schematic Diagram of Experimental Setup for Determination of Effective VOC Diffusivity through the Absorbent Filled ILM

hollow fiber discussed in Section 3.7. The only major difference was the introduction of pure N_2 as sweep gas through the shell side of the module to facilitate VOC permeation through the immobilized absorbent liquid inside the pores.

Fresh absorbent liquid was poured in the shell side of the module (module # 2) and after 1 to 2 minutes the liquid was drained to the best possible extent. VOC-contaminated N_2 gas mixture was then passed through the tube side at a fixed flow rate. The gas pressure was maintained at 5 psig (135.8 kPa) at the outlet of the gas stream by means of a back pressure regulator (BPR). Pure N_2 was passed at a definite flow rate through the shell side, countercurrently with respect to the tube side gas flow direction. The exact flow rate of the feed gas (VOC-N_2 gas mixture through the tube side) and sweep gas were measured by means of bubble flow meters connected at the exit of the respective gas streams. The outlet VOC composition of the feed gas was monitored continuously in the GC. A particular run was continued till the steady state was reached. For a specific VOC-N_2 gas mixture experiments were done for two different feed gas flow rates with same sweep gas flow rate or vice versa. Experiments were performed for different VOC-N_2 gas mixtures and different absorbent liquids.

CHAPTER 4

RESULTS AND DISCUSSION

For the steady state VOC absorption and VOC absorption-stripping studies conducted, this chapter describes different experimental results, observations and comparison of experimental results with the predictions obtained from mathematical models. Absorption results for four VOCs using two different types of membranes in silicone oil and Paratherm are discussed in detail. Results of estimation of physicochemical parameters e.g. Henry's constant, diffusivity of VOCs in absorbent liquids, and permeabilities of VOCs through the silicone skin are presented first. Absorption results for all or some of the VOCs, e.g., acetone, methanol, methylene chloride, and toluene are provided for both kinds of membranes in terms of exit gas concentration in ppmv of an individual VOC as a function of the feed N_2-VOC gas flow rate. Similar VOC removal results have been shown also as a function of the absorbent flow rate. Estimates of the VOC mass transfer coefficients have been obtained from experimental data as a function of the gas and the liquid flow rates. A comprehensive characterization of the different resistances making up the overall resistance in VOC absorption has been carried out to develop a predictive capability and compare the two kinds of absorbers having two different kinds of membranes.

Results for simultaneous absorption-stripping experiments in terms of the cleaned gas composition as a function of the feed gas flow rate for a given absorbent recirculation rate are provided next. The results of numerical simulations for both absorption as well as absorption-stripping have been compared with the corresponding experimental data. The characteristics of the transport processes are explored in these comparisons to develop a perspective. This will provide a comprehensive basis for adopting such a process for VOC emission control in various large or small processes and operations.

4.1 Estimation of Physicochemical Parameters

Three relevant physicochemical parameters were determined through independent experiments. The experimental procedures are explained in Chapter 3. The results are presented and discussed below.

4.1.1 Henry's Law Constant

Dimensionless Henry's law constants were determined experimentally by the variable volume headspace technique discussed in detail in Section 3.8. Experimental data and calculated results of a particular set of experiments are given in Table 4.1. A sample calculation is shown in Appendix B. In the variable volume technique, dimensionless Henry's constant is determined by dividing the y-intercept by slope of the linear regression of V_g/V_l and the reciprocal of the headspace peak area data. Plots of linear regression of such data for four VOCs in two different absorbents at various temperatures are shown in Figures 4.1 through 4.8. The temperature dependency of Henry's constant is given by equation 2.100. The constants A_H and B_H for each VOC-absorbent combination was determined by linear regression of 1/T and $\ln(H_i)$ data. The plots of 1/T vs. $\ln(H_i)$ for all four VOCs with silicone oil and Paratherm are shown in Figure 4.9 and 4.10 respectively. Data are also given in tabular form in Appendix A. The values of A_H and B_H obtained from such regression are provided in Table 4.2.

The values of Henry's constant for methanol in Paratherm are almost identical at different temperatures (Figure 4.8). For any practical application this can be taken as a constant (independent of temperature). The values of Henry's constant reflect the relative absorption performance of the different VOCs with respect to the specific absorbent. For a given absorbent, toluene shows the maximum Henry's constant value followed by methylene chloride, acetone and methanol; for a particular VOC, silicone oil exhibits higher H_i than Paratherm. These provide a qualitative indication about the likely absorption performance of a VOC in an absorbent in a given module under given flow conditions.

Table 4.1 Experimental Data for Calculation of Henry's Law Constant

VN	WE	WC	WS	V_l	V_g	V_g/V_l	1/PA
163	16.801	17.8034	1.0015	1.04452	20.9555	20.0622	$6.49287*10^{-6}$
164	16.6900	18.6743	1.9843	2.06954	19.9304	9.63035	$5.52346*10^{-6}$
165	16.6608	19.5814	2.9206	3.04607	18.9539	6.22242	$5.28910*10^{-6}$
166	16.8008	20.6994	3.89860	4.06608	17.9339	4.41060	$5.07189*10^{-6}$
167	16.7308	21.5063	4.7755	4.98066	17.0193	3.41709	$4.98298*10^{-6}$

VOC: acetone
Absorbent: silicone oil (50 cs)
Temperature: 25.6° C

VN: Vial number
WE: Weight of the empty vial (gm)
WC: Weight of the vial with sample (gm)
WS: Weight of the sample (gm)
V_l: Volume of the sample (ml)
V_g: Volume of the headspace (cc)
PA: Peak area

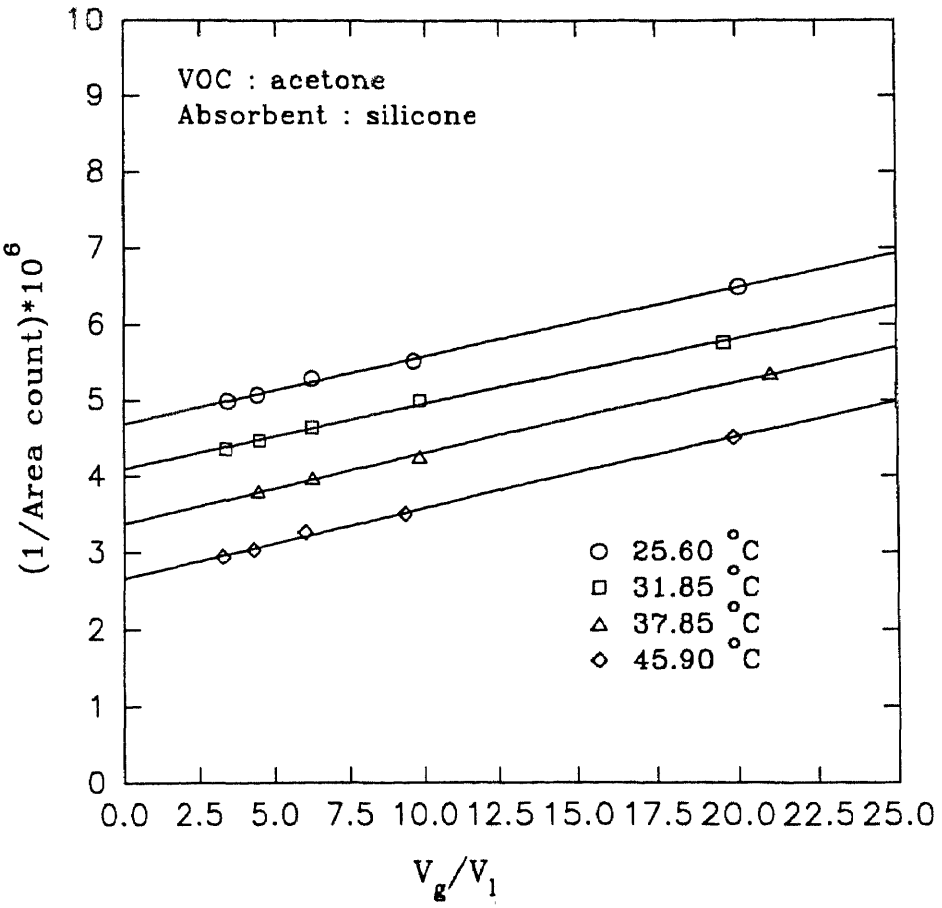

Figure 4.1 Plots of Reciprocal of Peak Area vs. Ratio of Headspace Volume to Liquid Sample Volume for Determination of Henry's Law Constant of Acetone in Silicone Oil at Different Temperatures

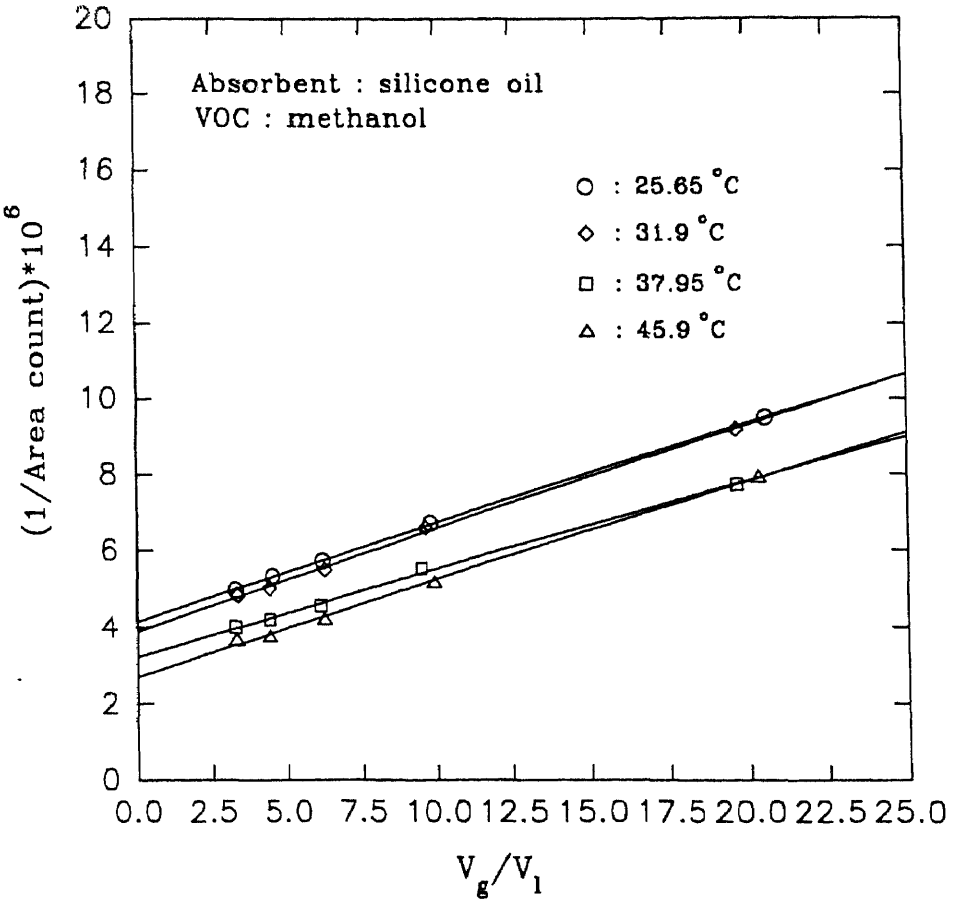

Figure 4.2 Plots of Reciprocal of Peak Area vs. Ratio of Headspace Volume to Liquid Sample Volume for Determination of Henry's Law Constant of Methanol in Silicone Oil at Different Temperatures

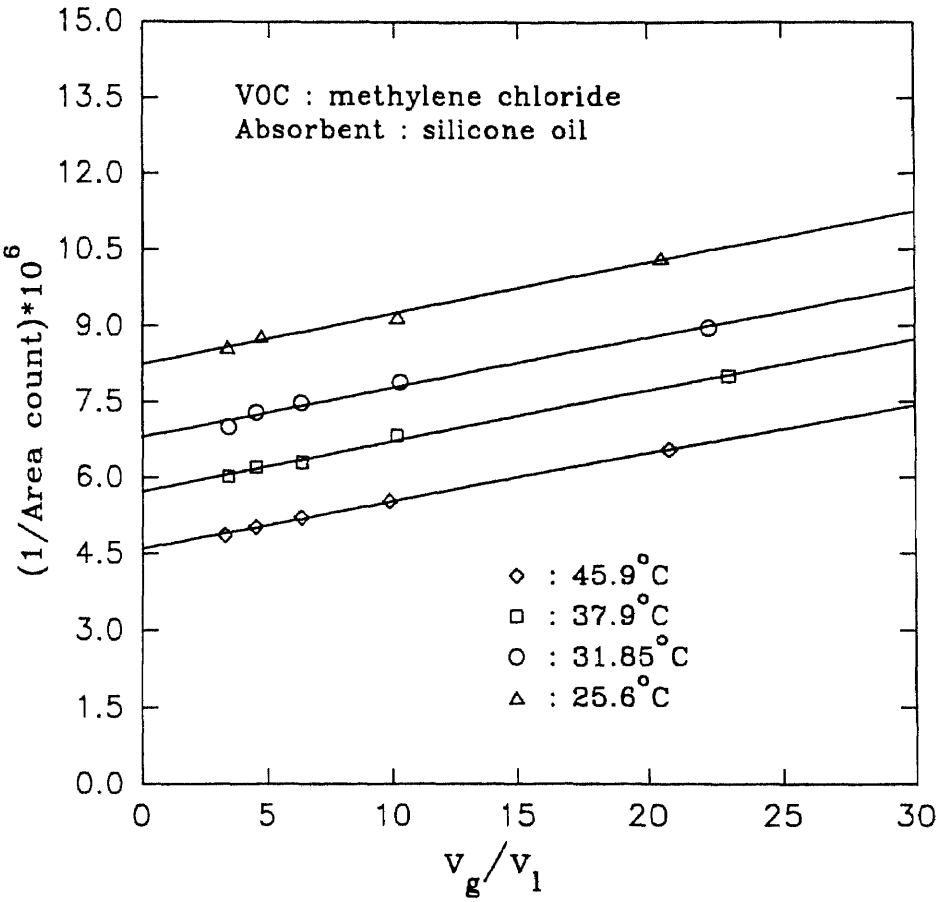

Figure 4.3 Plots of Reciprocal of Peak Area vs. Ratio of Headspace Volume to Liquid Sample Volume for Determination of Henry's Law Constant of Methylene Chloride in Silicone Oil at Different Temperatures

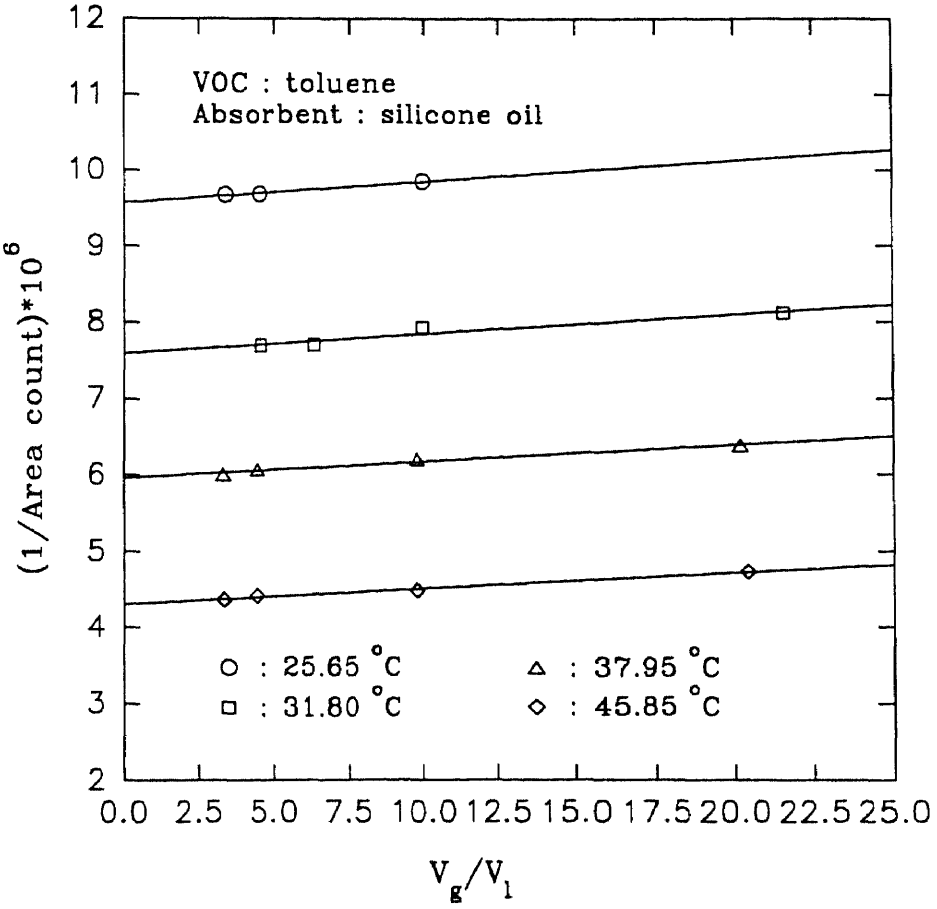

Figure 4.4 Plots of Reciprocal of Peak Area vs. Ratio of Headspace Volume to Liquid Sample Volume for Determination of Henry's Law Constant of Toluene in Silicone Oil at Different Temperatures

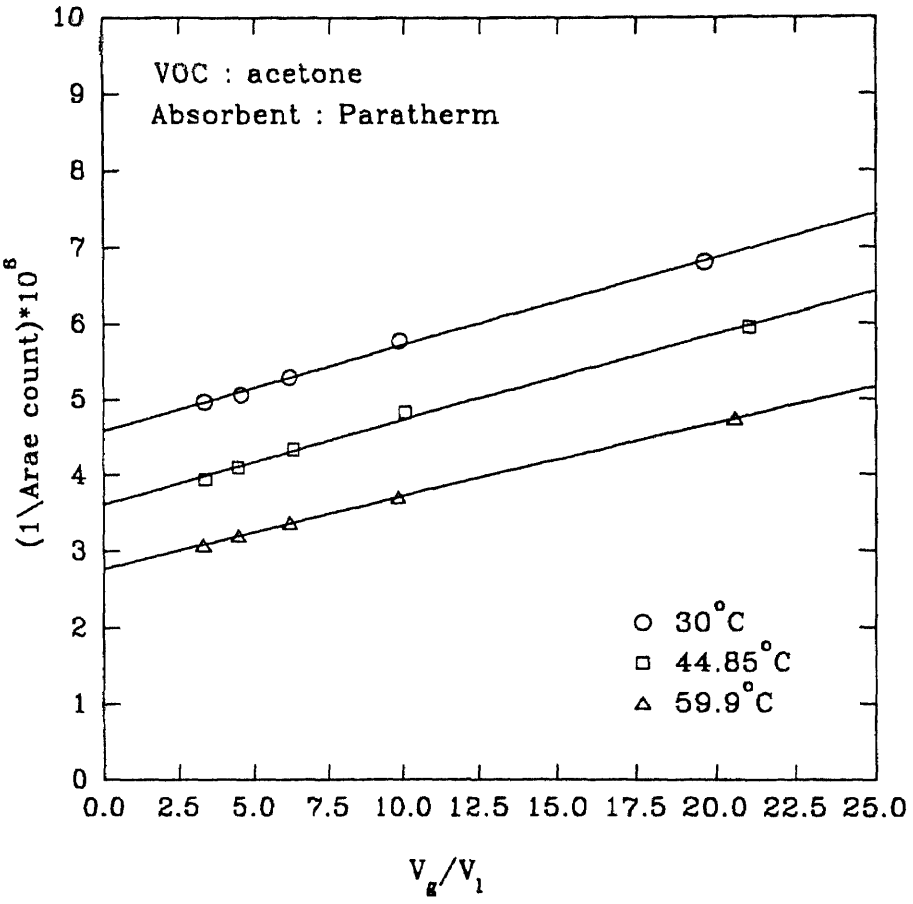

Figure 4.5 Plots of Reciprocal of Peak Area vs. Ratio of Headspace Volume to Liquid Sample Volume for Determination of Henry's Law Constant of Acetone in Paratherm at Different Temperatures

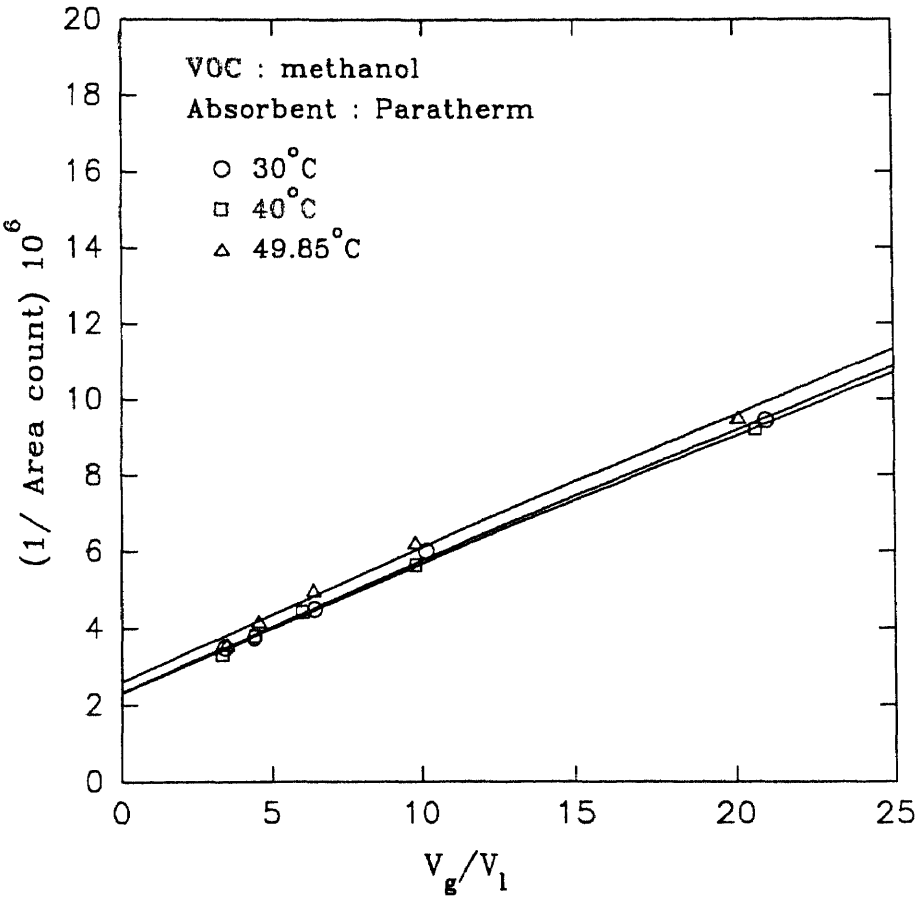

Figure 4.6 Plots of Reciprocal of Peak Area vs. Ratio of Headspace Volume to Liquid Sample Volume for Determination of Henry's Law Constant of Methanol in Paratherm at Different Temperatures

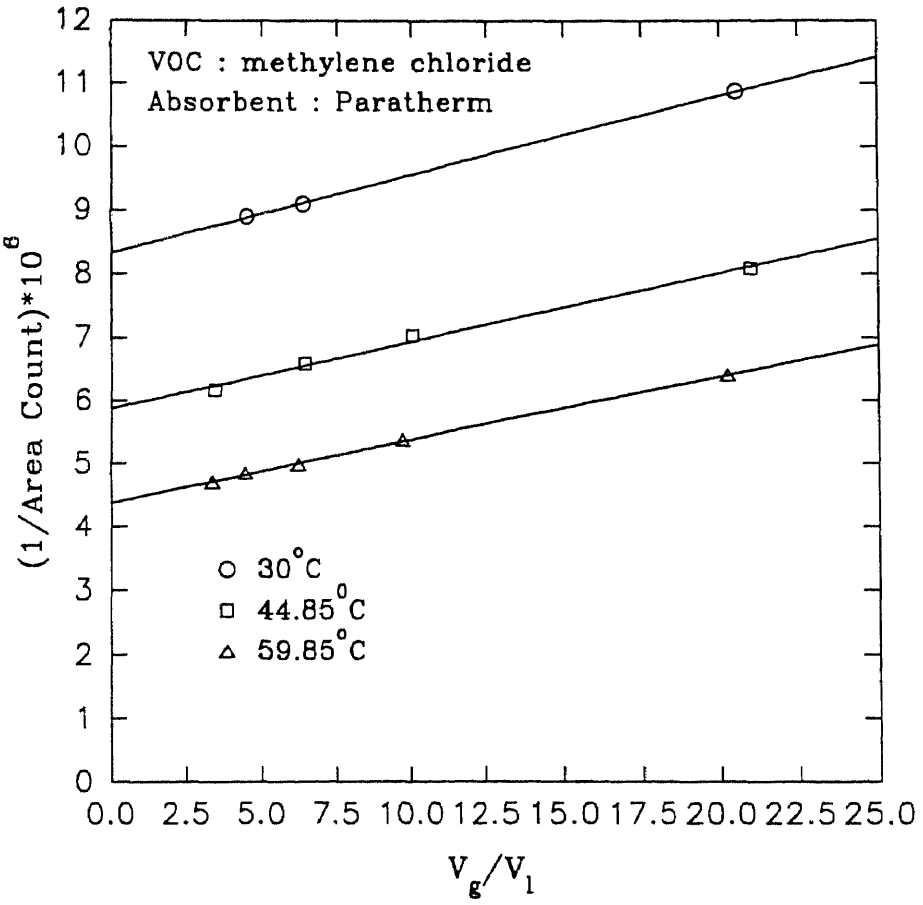

Figure 4.7 Plots of Reciprocal of Peak Area vs. Ratio of Headspace Volume to Liquid Sample Volume for Determination of Henry's Law Constant of Methylene Chloride in Paratherm at Different Temperatures

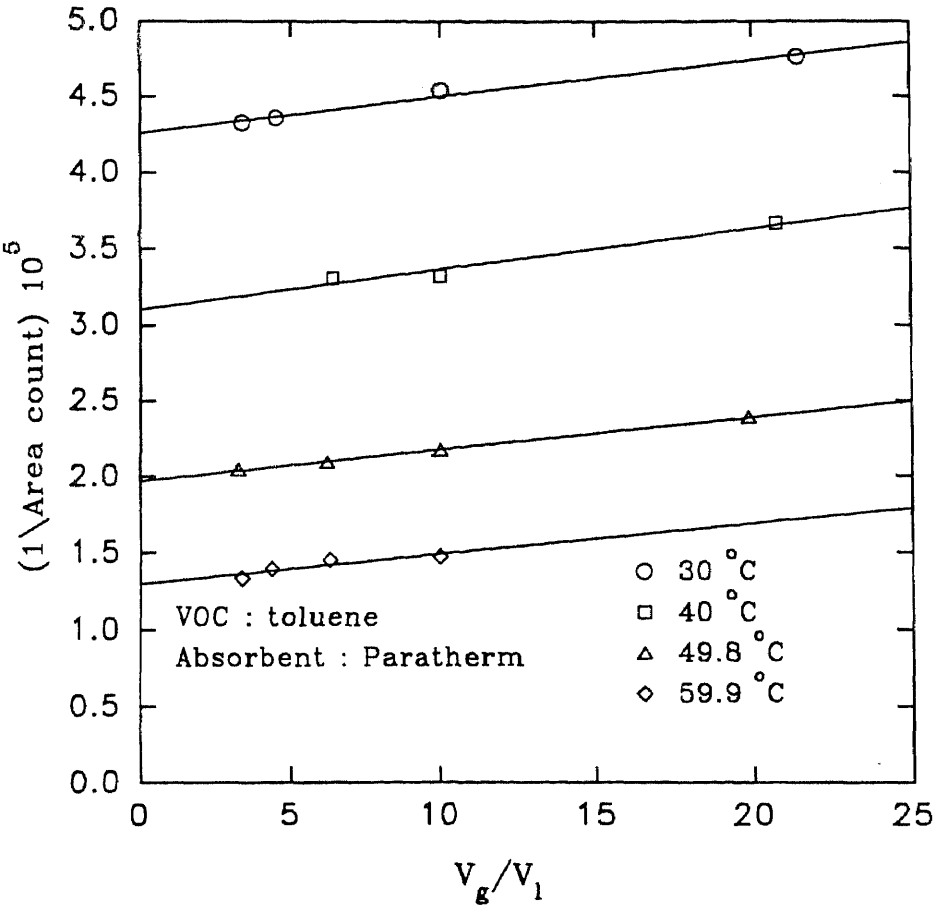

Figure 4.8 Plots of Reciprocal of Peak Area vs. Ratio of Headspace Volume to Liquid Sample Volume for Determination of Henry's Law Constant of Toluene in Paratherm at Different Temperatures

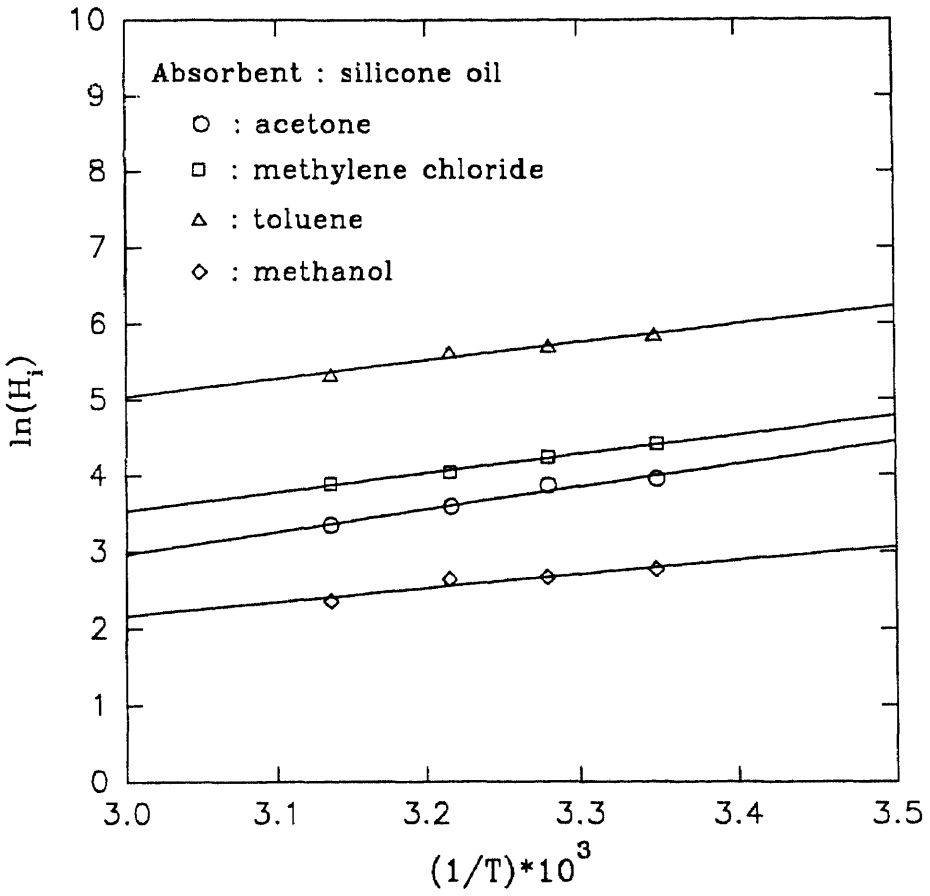

Figure 4.9 Variation of Natural Logarithm of Henry's Law Constant with the Reciprocal of Absolute Temperature for Various VOCs in Silicone Oil

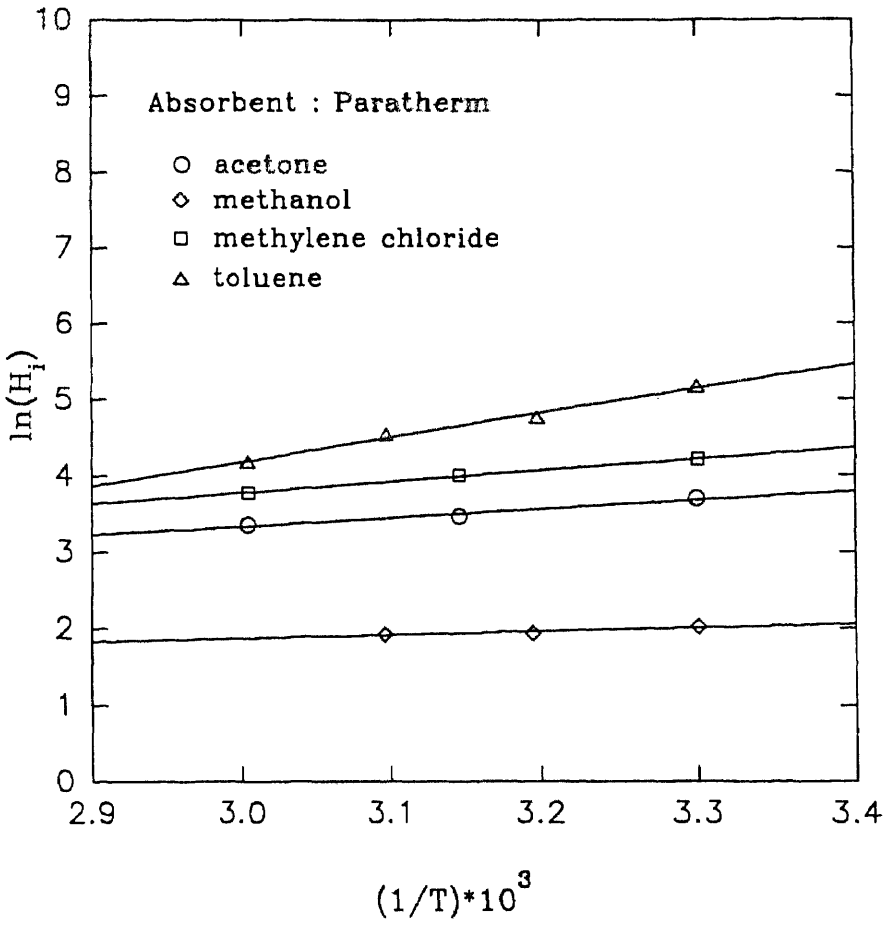

Figure 4.10 Variation of Natural Logarithm of Henry's Law Constant with the Reciprocal of Absolute Temperature for Various VOCs in Paratherm

Table 4.2 Parameters of Temperature Dependent Henry's Law Constant*

VOC	Silicone oil		Paratherm oil	
	A_{Hi}	B_{Hi}	A_{Hi}	B_{Hi}
acetone	5.87853	2948.800	0.016130	1119.434
methanol	3.23630	1802.340	-0.5252	449.6640
methylene chloride	3.98168	2504.381	0.5513	1444.640
toluene	2.08000	2375.005	5.42440	3203.364

* Equation 2.100

4.1.2 Permeance of VOCs through the Silicone Skin

The silicone skin on the outer surface of the hollow fiber acts as a homogeneous membrane. Such a membrane was first characterized via permeation of permanent gases like nitrogen and carbon dioxide. Figures 4.11 and 4.12 show the permeation rates of pure nitrogen and pure carbon dioxide respectively as a function of the pressure differential across the membrane. A selectivity value of 10 - 12 for carbon dioxide over nitrogen was obtained which is comparable to the literature value for silicone rubber (Robb, 1965).

Calculation techniques to determine permeance and hence the permeability values from experimental data are discussed in Section 2.3.3. Permeance through the composite membrane, q_o/δ_o (porous substrate plus the silicone skin) and through the silicone skin, q_c/δ_c, were calculated for all four VOCs and tabulated in Table 4.3. Once the permeance is known, the permeability was calculated by multiplying the former with the proper thickness, δ. Experimental data are given in tabular form in Appendix A. Cha (1994) had observed a very strong dependence of the VOC permeance on its concentration. For the present study, concentrations of VOCs are very low, hence, no attempt was made to investigate the concentration-dependence of permeance. A constant value of permeance

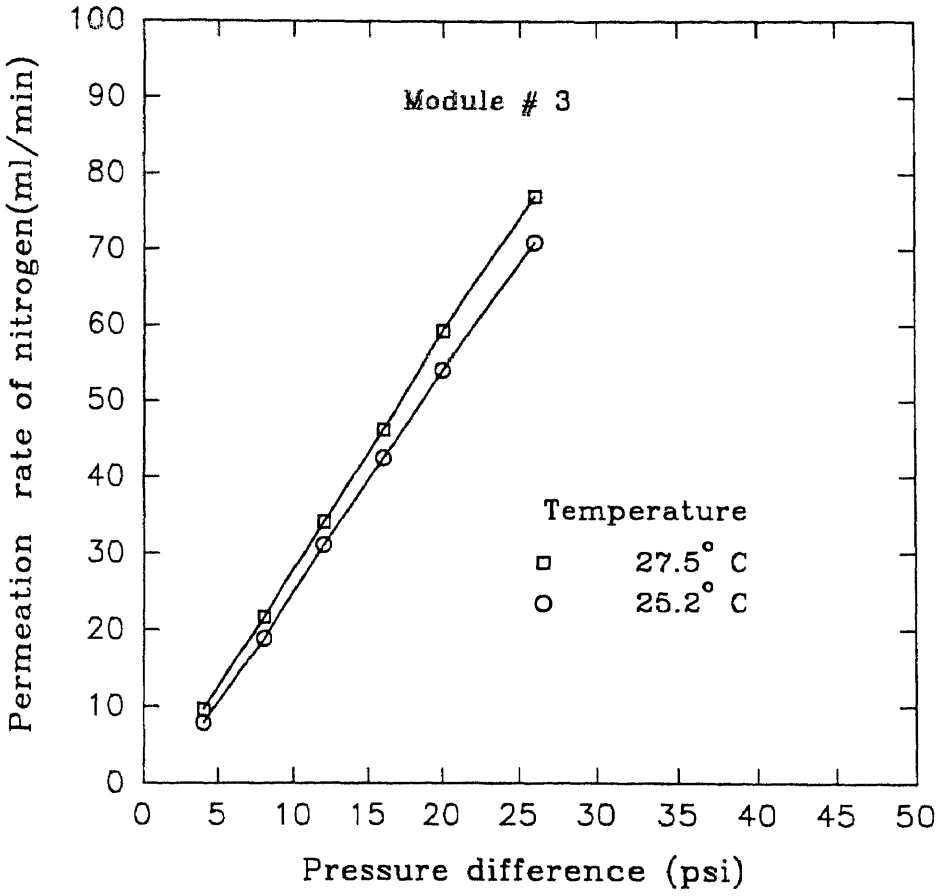

Figure 4.11 Plot of Pure Nitrogen Permeation Rate through the Silicone Coated Fiber as a Function of Pressure Difference Across the Composite Membrane

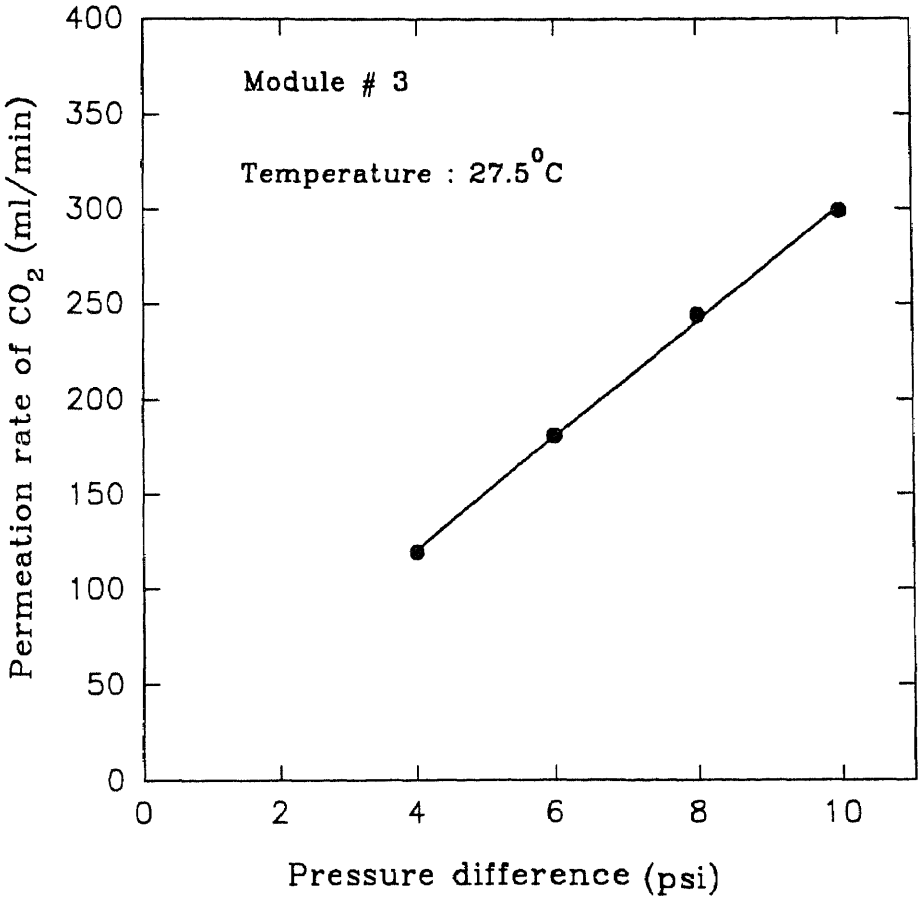

Figure 4.12 Plot of Pure Carbon dioxide Permeation Rate through the Silicone Coated Fiber as a Function of Pressure Difference Across the Composite Membrane

for a particular VOC was used for all calculations. The computer code for calculating the permeance from experimental data is available in Appendix C.

Table 4.3 Diffusivity and Permeance Data for Various VOCs

VOC	Diffusivity (cm^2/sec)		Permeance (cm/sec)	
	silicone oil (50 cs)	Paratherm	Composite membrane (q_o/δ_o)	silicone skin (q_c/δ_c)
acetone	2.806×10^{-6}	3.600×10^{-7}	3.198×10^{-3}	3.22×10^{-3}
methanol	4.709×10^{-6}	1.86×10^{-7}	2.895×10^{-3}	2.911×10^{-3}
methylene chloride	4.300×10^{-6}	8.504×10^{-7}	5.014×10^{-3}	5.065×10^{-3}
toluene	7.625×10^{-6}	4.802×10^{-6}	11.477×10^{-3}	11.754×10^{-3}

4.1.3 Diffusivity of VOCs in the Absorbent Liquid

Diffusivities of VOCs in the absorbent liquids were measured indirectly via VOC permeation experiments through the absorbent-filled porous membranes. Theoretical basis for calculating the diffusivity value from such experiments is discussed in Section 2.3.1. Results obtained are given in Table 4.3 along with the permeance data. The diffusivity values for VOCs in silicone oil are found to be about an order of magnitude larger than those calculated using Wilke-Chang equation, while data obtained for Paratherm are of the same order of magnitude with the diffusivity values obtained from Wilke-Chang equation. However, the comparison is not shown here. A quick comparison of the diffusivity and Henry's constant data for a particular absorbent (Tables 4.3 and 4.2

respectively) reveals that higher solubility does not necessarily mean higher diffusivity. Further, the relative order of diffusivity data for VOCs in silicone oil does not follow that in Paratherm. However, these data need to be checked with data obtained from other experimental measurements or with calculated values from theoretical models, if possible.

4.2 VOC Absorption Results

4.2.1 VOC Absorption Using Porous Hollow Fibers

As discussed earlier on several occasions, all experiments in this study were carried out with gas flowing in the tube side and absorbent oil flowing in the shell side. Figure 4.13-a illustrates how the composition of different VOCs (acetone (feed concentration 993 ppmv), methylene chloride (999 ppmv), and methanol (514 ppmv)) in the treated feed gas mixtures changes as a function of the feed gas flow rate through the fiber bores in module # 2. It can be observed that a feed gas mixture containing 999 ppmv of acetone in N_2 can be reduced to as low as 2 ppmv in the treated gas stream exiting the module at low gas flow rates. Thus, 99.5%+ removal of the polar VOC, acetone, is possible in a microporous hollow fiber gas-liquid contactor using fresh silicone fluid as the organic absorbent flowing countercurrent to the gas.

At the lowest gas flow rates achieving the highest VOC absorption, the gas flow rate per fiber was in the range of 0.1 cc/min/fiber. If the module were longer providing more gas-liquid (and, therefore, membrane) contact area, then higher gas flow rates may be used for equivalent VOC reduction. For lower fractional VOC absorption, say, 90%, a much higher gas flow rate of 0.4 cc/min/fiber can be maintained continuously. These numbers are very convenient for scaling up the VOC scrubber unless the liquid flow pattern on the shell side changes very substantially in a scaled-up module due to bypassing. Figure 4.13b illustrates similar results for toluene (feed concentration 236 ppmv) and methylene chloride (999 ppmv) for a higher gas flow rate range.

It appears that toluene is much more easily removed allowing a much higher gas

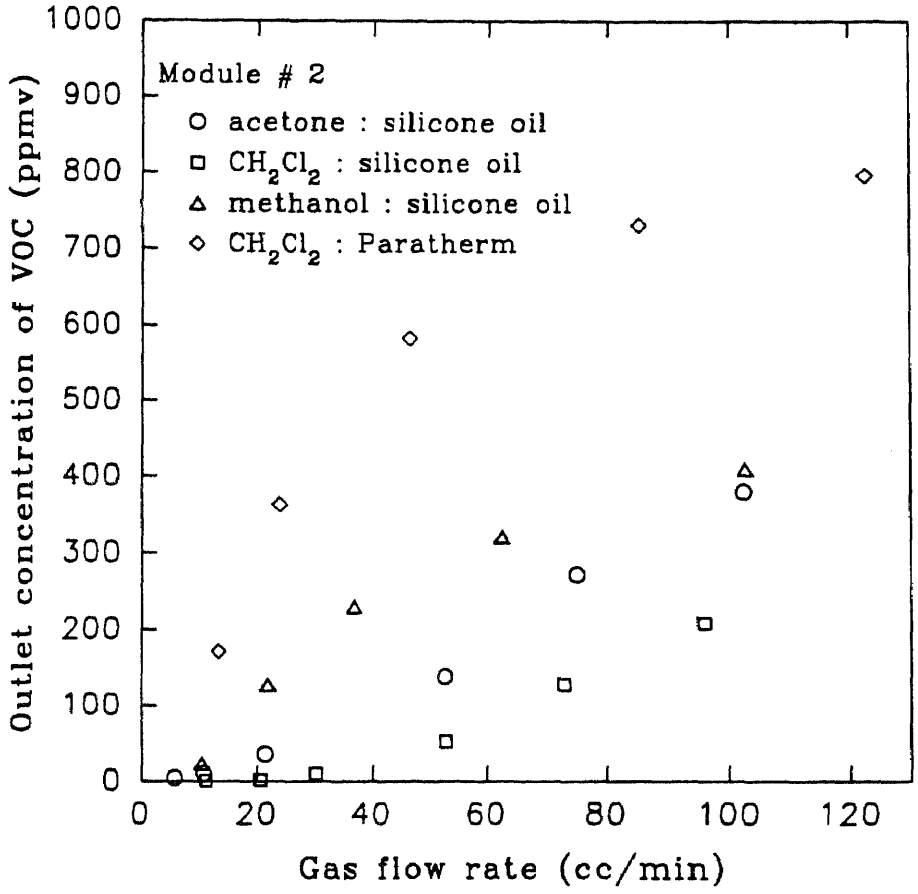

Figure 4.13a Variation of Gas Phase VOC Outlet Concentration with Gas Flow Rate for Absorption of VOCs Using Porous Fibers

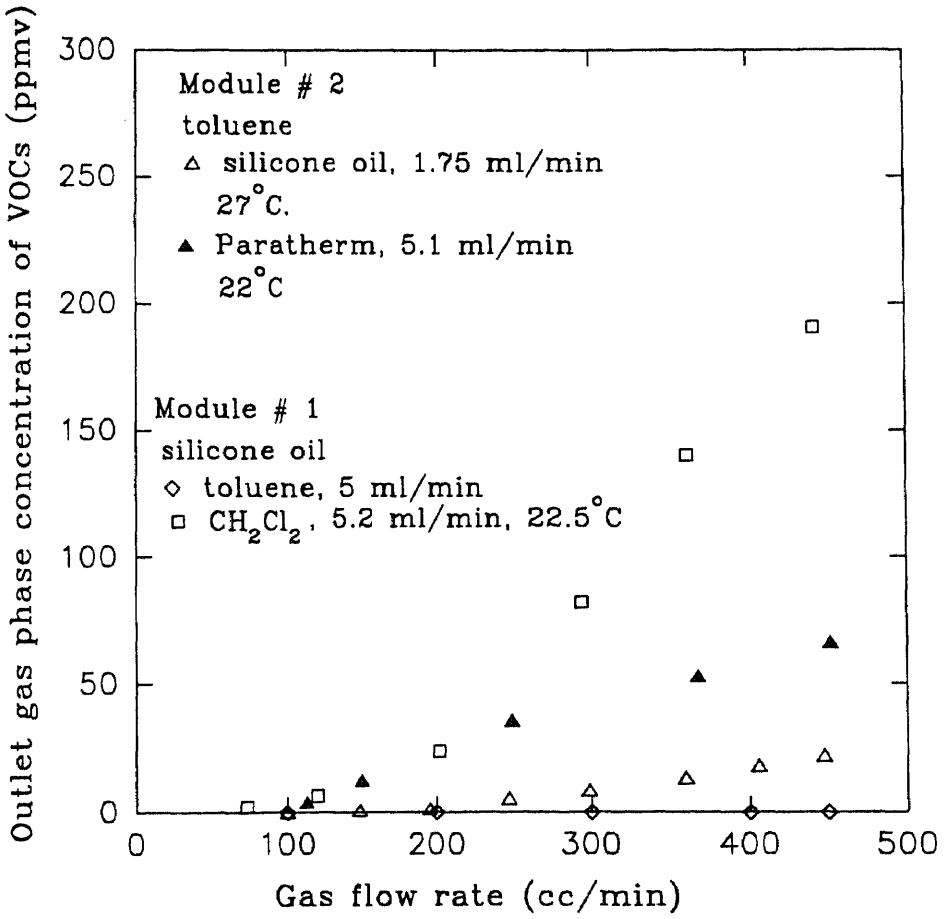

Figure 4.13b Variation of Gas Phase VOC Outlet Concentration with Gas Flow Rate for Absorption of VOCs Using Porous Fibers at Higher Gas Flow Rates

flow rate per fiber in the range of 1 cc/min/fiber for the highest fractional toluene removal. This value of 1cc/min/fiber is reinforced by the results of toluene removal shown in Figure 4.13b where the larger module # 1 was utilized and virtually all of the toluene present in the feed gas was removed for much higher gas flow rates. Figure 4.13 b also shows the results of methylene chloride absorption in module # 1 in the higher range of gas flow rates. The available mass transfer area in module # 1 is about six times larger than that in module # 2. Hence, it required a much higher gas flow rate for a given feed VOC concentration in order to have partial removal from the feed gas stream. Therefore, to avoid excess consumption of limited VOC mixture, very few experiments were carried in module # 1.

Figure 4.14 explores acetone removal in module # 2 as a function of feed gas composition for a given gas flow rate and a given silicone absorbent flow rate. It had been observed that the percent removal of acetone remained independent of the feed composition; however, the outlet concentration of acetone in the treated gas increases with increasing acetone level in the feed gas for the given module and the absorbent liquid flow rate.

The effect of the absorbent flow rate on the exiting VOC composition of the cleaned gas is illustrated by Figures 4.15 and 4.16. As the absorbent liquid flow rate increases, the VOC concentration at the exiting gas stream decreases slowly and essentially becomes independent of the liquid flow rate after approximately 5 ml/min of liquid flow rate.

4.2.2 VOC Absorption Using Fibers Having a Nonporous Skin

The previous experiments employed absorption modules # 1 and # 2 made out of microporous Celgard® X-10 hollow fibers; further, the gas and the liquid contacted directly at each pore mouth on the fiber I.D. under conditions of the gas side having a slightly higher pressure than that of the liquid absorbent to maintain nondispersive

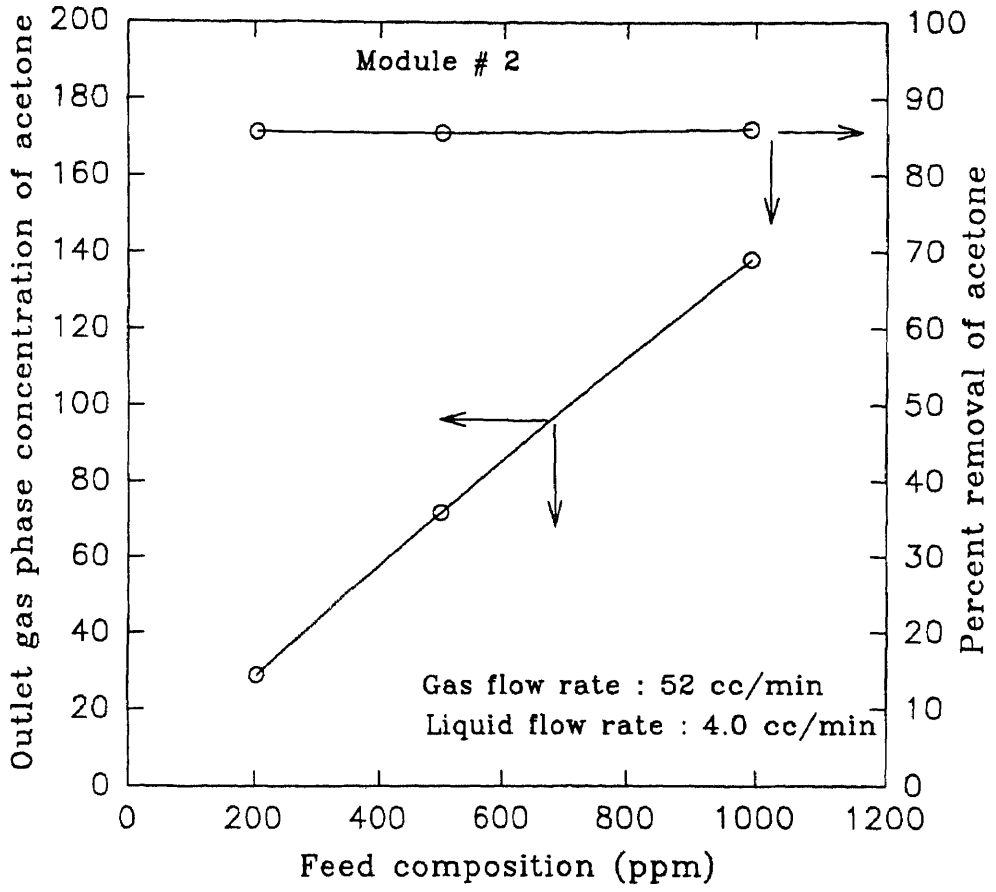

Figure 4.14 Variation of Gas Phase VOC Outlet Concentration with Feed Gas VOC Composition for Acetone Absorption in Silicone Oil

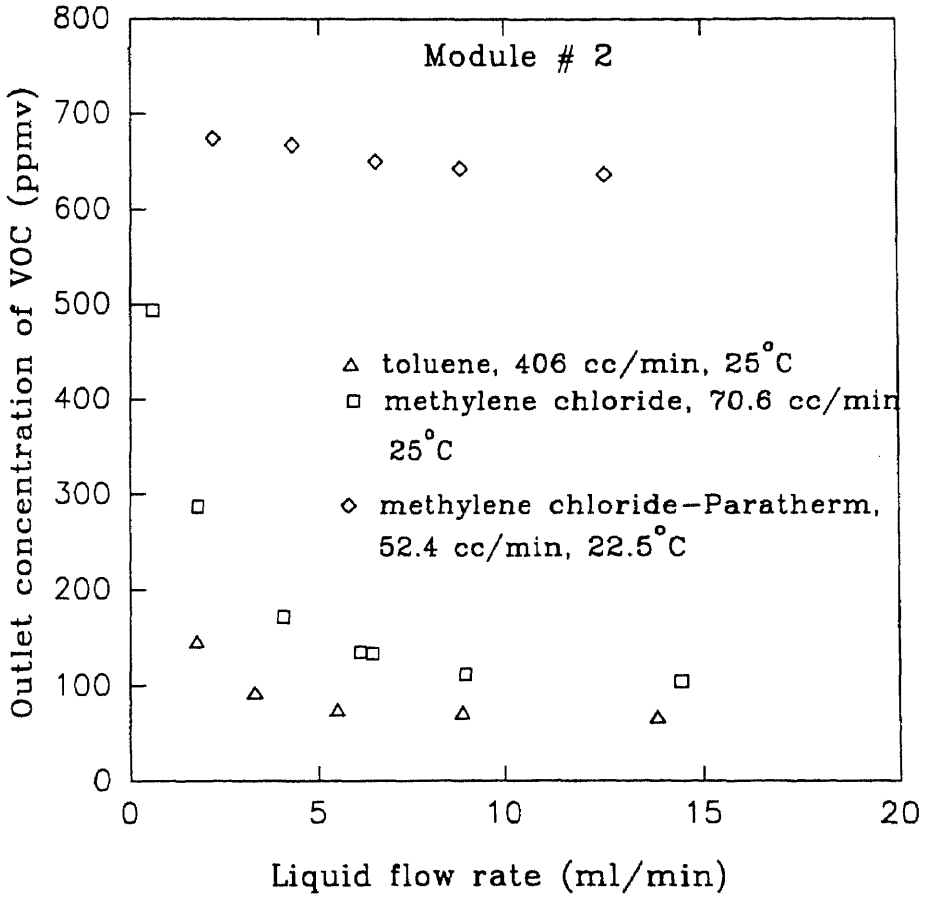

Figure 4.15 Variation of Gas Phase Outlet Concentration of Different VOCs with Absorbent Liquid Flow Rate

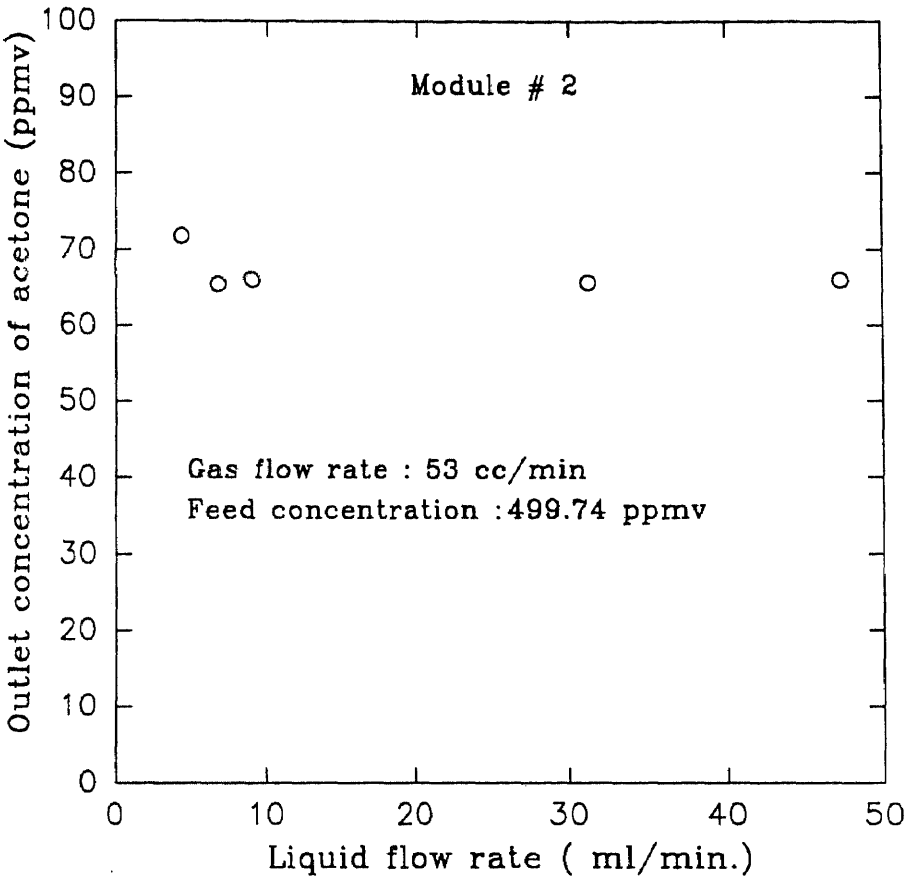

Figure 4.16 Variation of Gas Phase Outlet Concentration of Acetone with Absorbent Liquid Flow Rate

contacting. Absorption experiments were conducted using module # 3 where the microporous polypropylene hollow fibers had an ultrathin plasma polymerized nonporous skin of silicone on the fiber outside diameter which prevented direct gas-liquid contact. There is an explicit criterion of phase pressures in such a case, namely, the gas and liquid pressures should be essentially equal or the liquid pressure should be higher.

Figure 4.17 reports results of methylene chloride and acetone removal by two different absorbents, Paratherm® oil and silicone oil in module # 3 built out of such fibers having a nonporous silicone skin. For both absorbents, the gas flowed on the tube side and the absorbent was on the shell side. One may notice that the outlet concentration of the VOC, methylene chloride, decreased strongly as the gas flow rate was decreased. The behavior shown in this countercurrent membrane absorber is quite similar to those observed earlier in Figures 4.13a and 4.13b. As observed earlier in the case of absorption using a porous fiber (Figure 4.13a), better performance was achieved for methylene chloride compared to that for acetone for a given absorbent (here Paratherm). Removal performance of methylene chloride with two absorbents was very similar, which apparently indicates that the difference in the diffusivities of methylene chloride in two different absorbents has no effect on their absorption performances. This issue will be further discussed later in sections 4.2.3 and 4.5.

As proposed earlier in the introduction chapter, nondispersive gas absorption will not be achieved if the gas pressure is significantly higher than that of the liquid when the fiber has a nonporous skin or coating. Experimental evidence is provided in Figures 4.18a and 4.18b. Experiments were conducted by passing N_2 gas through the tube side and Paratherm through the shell side. Initially both gas and liquid were kept at essentially atmospheric pressure. Under such conditions gas flow rate rates were measured at the inlet and outlet of the module. No measurable difference in flow rates between the inlet and the outlet was observed. The same experiment was repeated at different higher gas pressures by adjusting the back pressure regulator. As shown in Figures 4.18a and 4.18b

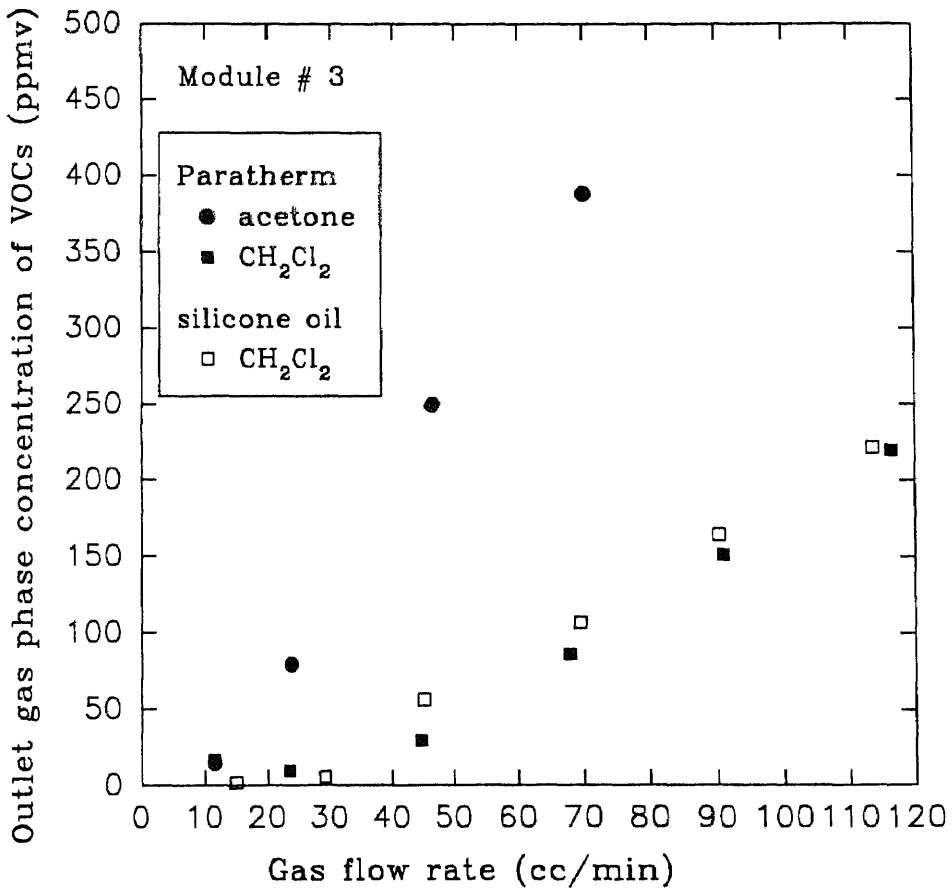

Figure 4.17 Variation of Gas Phase VOC Outlet Concentration with Gas Flow Rate for Absorption of VOCs Using Skinned Fibers

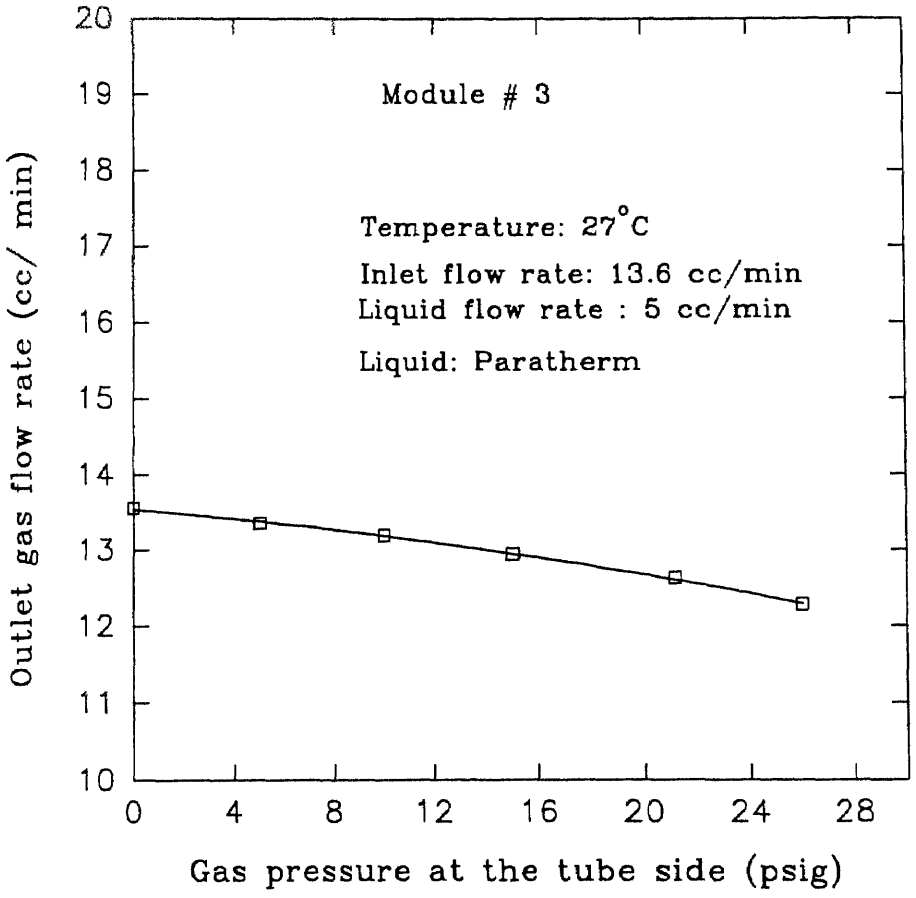

Figure 4.18a Nitrogen Dispersion into Absorbent Liquid Under Adverse Pressure Condition in a Fiber Having Nonporous Silicone Skin at Higher Gas Pressure

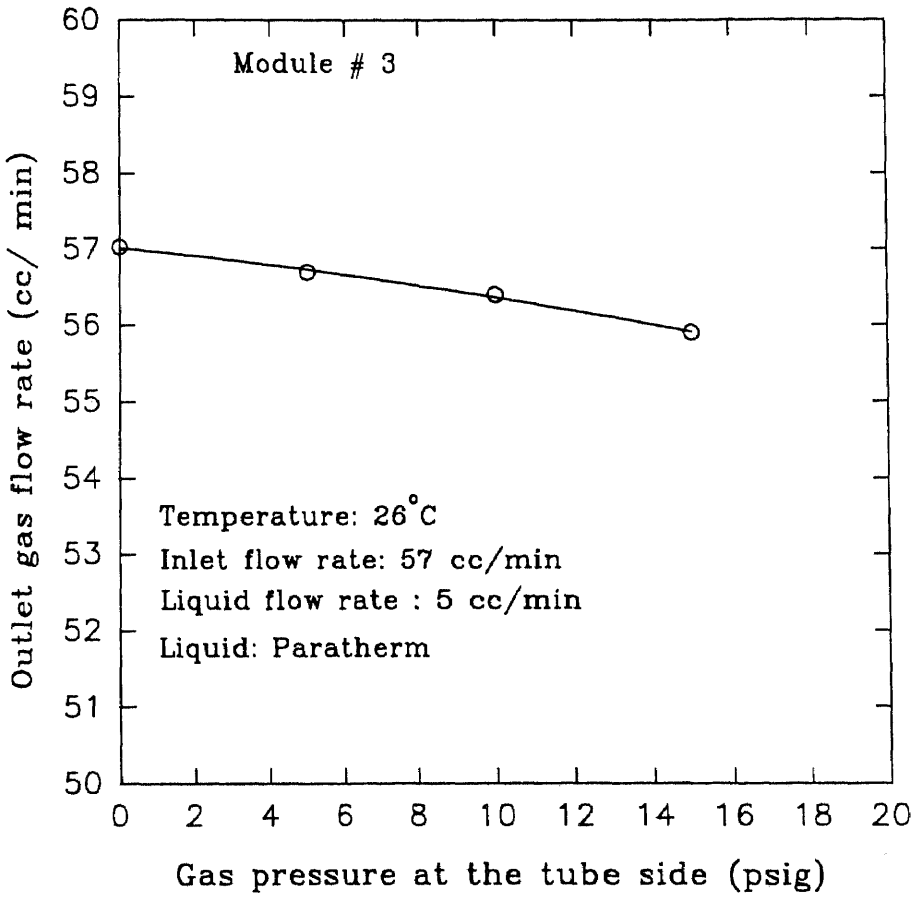

Figure 4.18b Nitrogen Dispersion into Absorbent Liquid Under Adverse Pressure Condition in a Fiber Having Nonporous Silicone Skin at a Higher Gas Flow Rate

outlet gas flow rates decreased as the gas pressure was increased. The difference in gas flow rates (though limited in amount) is the rate at which nitrogen gas essentially permeated through the silicone skin and bubbled through the absorbent in the shell side. The bubbling of N_2 through the translucent absorbent-filled outlet pipe was observed. This phenomenon surely made the process dispersive in nature. On the other hand no bubbling was observed when both gas and liquid were at atmospheric pressure.

N_2 has considerable permeability through the silicone skin (Figure 4.11) but has negligible solubility in absorbent liquids like silicone oil or Paratherm. When both gas and liquid pressures are atmospheric, permeation of N_2 stops soon because of zero driving force for permeation and the absence of excess pressure needed for bubble formation. But, when the gas pressure is higher than the liquid side pressure, the permeation of N_2 will continue because of the persistent driving force. Since N_2 has negligible solubility in Paratherm, it bubbles out through the liquid in the shell side. To stop this bubbling phenomenon, it is essential to elevate the liquid side pressure to the level of gas side pressure or more. One may now wrongly conclude that there may not be any operational advantage to having a nonporous skin or coating since in either case (with or without coating) one of the phases has to be at a higher pressure unless both phases have the same pressure. For many VOC removal applications, the gas (N_2 or air) is at atmospheric pressure. However, the viscous absorbent encounters pressure drop during its flow which suggests that the VOC-containing gas pressure should be raised from atmospheric if a microporous fiber without a nonporous coating or skin is used. This requirement is eliminated when a nonporous skin or coating is employed. This will result in considerable energy saving since the gas pressure does not have to be raised much. The skinned fiber also allows absorption under conditions of arbitrarily high liquid pressure levels for the absorbent (within certain limits so as not to damage the skin or the fibers). This condition is not allowed in a microporous fiber without nonporous skin since breakthrough pressures are usually much lower.

4.2.3 Mass Transfer Characteristics of VOC Absorption in Hollow Fiber Devices

The overall gas-phase based mass transfer coefficient, K_{oG}, for any VOC absorption was calculated from the exit gas phase VOC concentration data by means of following equations:

$$K_{oG} = \frac{(p\ V)_{ref}\ x\ 10^{-9}}{RT\ x\ 14.7\ x\ 60}\ \frac{(ppmv_{in} - ppmv_{out})}{A_m\ (\Delta C)_{lm}}\ \frac{cm}{\text{sec}} \qquad (4.1)$$

where $ppmv_{in}$ is the VOC concentration in gas in ppmv at module inlet

$ppmv_{out}$ in the VOC concentration in gas in ppmv at module outlet

A_m is the membrane surface area at the gas-liquid interface, cm^2

p_{ref} is the pressure of the gas at which the volume of gas is measured (psia)(atmospheric pressure)

V_{ref} is the volumetric flow rate of gas in cm^3/min at atmospheric pressure

R is the universal gas constant, 0.082 liter-atm/gmol-K

T is the absolute temperature, K

and $(\Delta C)_{ln}$ is the logarithmic mean driving force based on gas phase concentration defined by equation (4.2),

$$(\Delta C)_{ln} = \frac{(C_{ig,in} - C^*_{ig,out}) - (C_{ig,out} - C^*_{ig,in})}{\ln \dfrac{(C_{ig,in} - C^*_{ig,out})}{(C_{ig,out} - C^*_{ig,in})}} \qquad (4.2)$$

Here $C_{ig,in}$ is the molar concentration (gmol/cc) of VOC in the gas at module inlet and $C_{ig,out}$ is that at the module outlet; $C^*_{ig,out}$ and $C^*_{ig,in}$ are the hypothetical gas phase concentrations in equilibrium with the absorbent concentrations at the liquid outlet and the liquid inlet respectively. The values of $C^*_{ig,out}$ and $C^*_{ig,in}$ are obtained from the

corresponding liquid phase concentrations of the VOC and the Henry's law constant H_i for the VOC. Liquid phase outlet concentration of VOC can be obtained from material balance

$$C_{ilout} = \frac{(pV)_{ref}(ppmv_{in} - ppmv_{out})\,10^{-9}}{RTV_l} \tag{4.3}$$

Once the liquid phase concentration is known, the corresponding equilibrium gas phase concentration can be calculated from the simple equation:

$$C_{ig}^{*} = \frac{C_{il}}{H_i} \tag{4.4}$$

K_{oG} values obtained from the above equations were plotted against gas flow rate/fiber for individual VOCs for a given liquid flow rate. Figure 4.19 shows the variation of K_{oG} with gas flow rate per fiber for acetone, methanol and methylene chloride absorption using porous fiber modules (module #1 and module # 2). Figure 4.20 shows a similar plot for toluene. Mass transfer coefficients calculated from the experimental data for toluene absorption in silicone oil using porous fibers are given in Table 4.4. At a relatively higher gas flow rate (approximately 0.5 cc/ min/ fiber), K_{oG} became independent of gas flow rate as shown in Figures 4.19 and 4.20. This plateau value is determined by the resistance of VOC diffusion through the stagnant absorbent in the membrane pores and in the flowing absorbent liquid. As expected from Figures 4.13a and 4.13b for VOC concentration in the exiting gas stream, toluene shows the highest K_{oG} values followed by methylene chloride, acetone and methanol. Higher Henry's law constant and higher diffusivity value are responsible for the superior mass transfer characteristics of toluene. Figure 4.21 shows the variation of gas-phase-based overall mass transfer coefficient with absorbent-liquid flow rate for methylene chloride and toluene. K_{oG} values became virtually constant after 5 ml/min of liquid flow rate for both VOCs. No such plot is shown here for acetone;

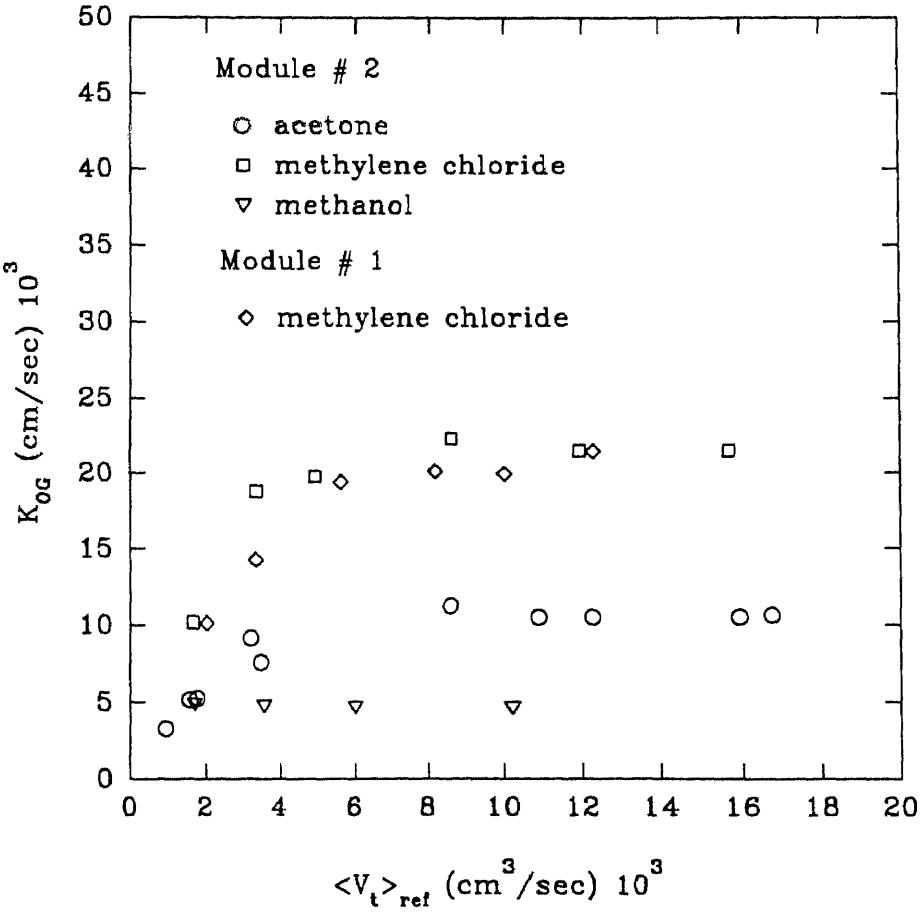

Figure 4.19 Variation of Gas Phase-Based Overall Mass Transfer Coefficient with Gas Flow Rate Per Fiber for Different VOC Absorption in Silicone Oil Using Porous Fibers

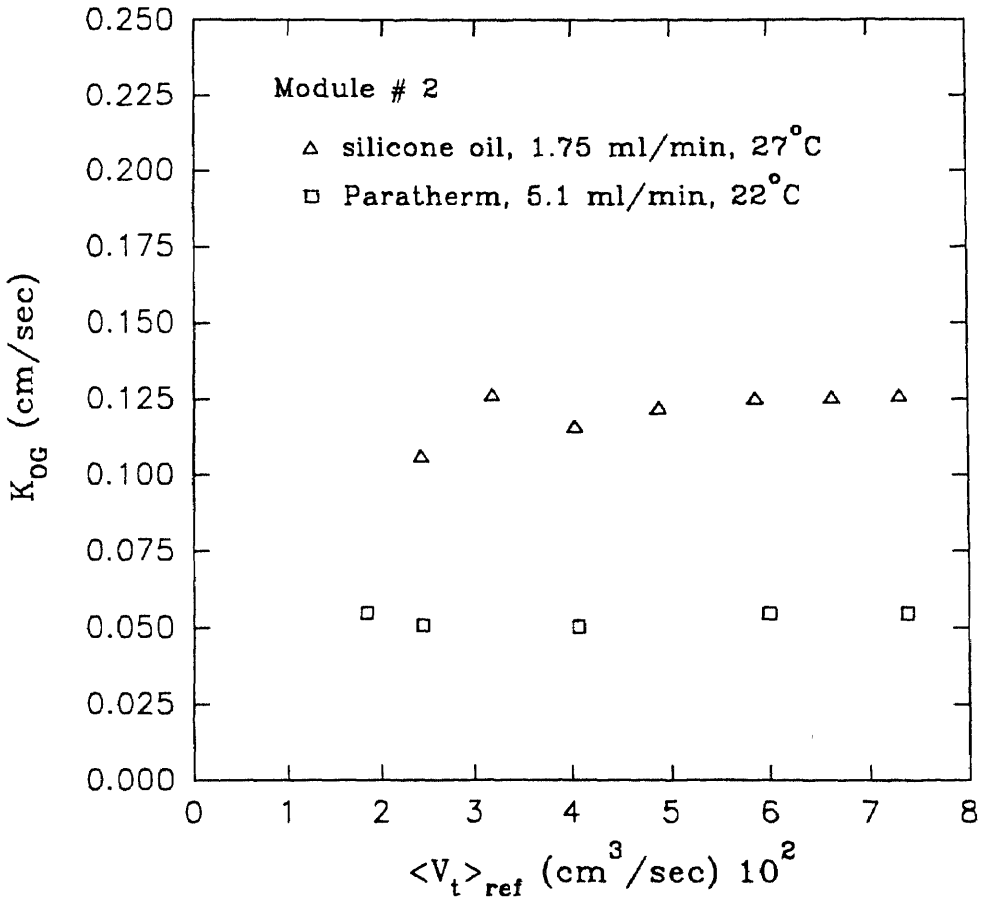

Figure 4.20 Variation of Gas Phase-Based Overall Mass Transfer Coefficient with Gas Flow Rate Per Fiber for Toluene Absorption in Silicone Oil Using Porous Fibers

Table 4.4 Variation of Mass Transfer Coefficient with Gas Flow Rates for Toluene Absorption* in Silicone Oil Using Module #2

p_{inlet} (psia)	p_{outlet} (psia)	V_{ref} (cc/min)	$ppmv_{out}$	K_{oG} (cm/sec)
23.40	17.696	147.93	0.826	0.106
24.93	17.696	195.17	1.335	0.126
26.54	17.696	247.23	5.355	0.116
28.03	17.696	298.51	8.467	0.122
29.69	17.696	359.28	13.43	0.125
30.90	17.696	405.71	18.19	0.125
31.95	17.696	447.46	22.2	0.126

* Liquid absorbent flow rate : 1.75 ml/min, Temperature: 27°C,
Feed gas concentration of toluene : 236 ppmv.

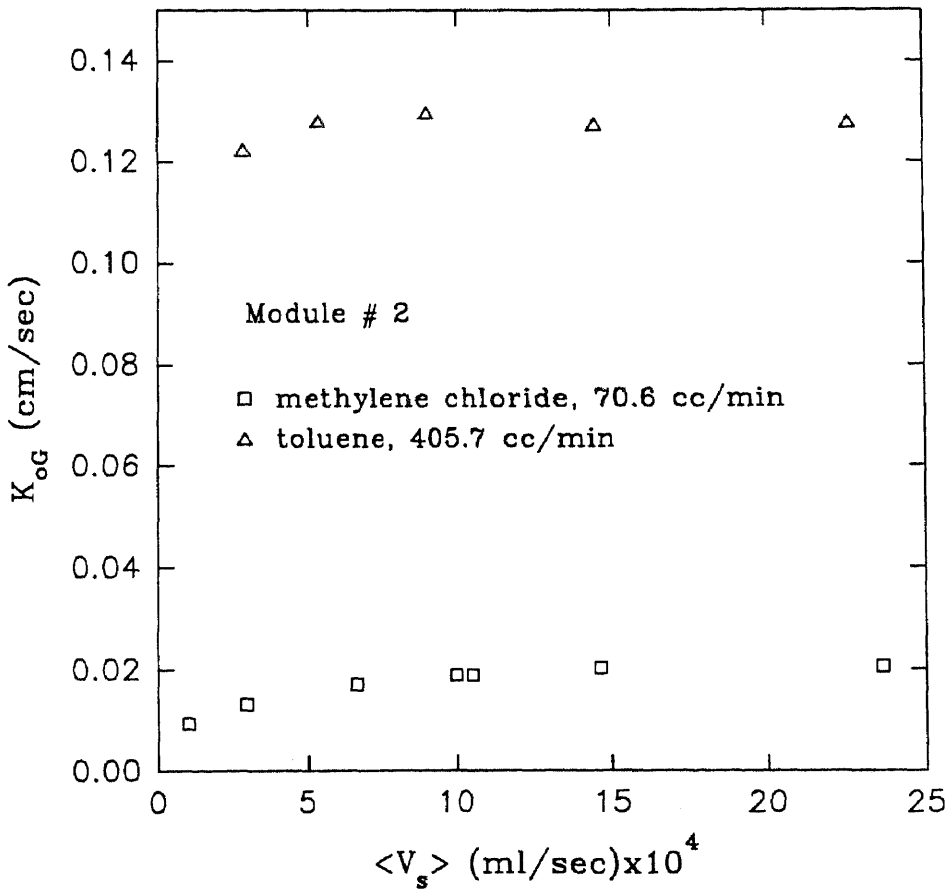

Figure 4.21 Variation of Gas Phase Based Overall Mass Transfer Coefficient with Absorbent Liquid Flow Rate Per Fiber for VOC Absorption in Silicone Oil Using Porous Fibers

however, from Figure 4.16, a similar result can be clearly anticipated.

A comparison of mass transfer characteristics of methylene chloride absorption between two different fibers and two different absorbent liquids is shown in Figure 4.22. Experiments were carried out under essentially identical conditions. In the case of absorption using porous fibers (module #1 and # 2) silicone oil shows a superior mass transfer characteristics than Paratherm oil while there is not much difference in mass transfer characteristics between the two absorbent oils when absorption was carried out in the skinned fiber module (module # 3).

In case of absorption with porous fibers, the pores of the membrane are filled with absorbent oil. Resistance of VOC transfer through this stagnant immobilized absorbent oil was found to control the overall mass transfer coefficient (discussed latter). For a given system membrane mass transfer coefficient is directly proportional to the diffusivity of the VOC through the absorbent liquid inside the pore. Hence, the diffusivity of VOC in the absorbent liquid has significant effect on the overall mass transfer performance. Since methylene chloride has a much lower diffusivity in Paratherm oil than in silicone oil (Table 4.2) the overall mass transfer coefficient of methylene chloride absorption in silicone oil is higher than that in Paratherm. In case of absorption using skinned fiber (module # 3) there is no direct contact between the gas and the absorbent liquid because of the presence of silicone skin on the outer surface of the porous fiber and the pores of the substrate are filled with gas. Mass transfer characteristics of VOC absorption in such type of fibers is generally controlled by the resistance of VOC permeation through the silicone skin. That is why the overall mass transfer coefficient for methylene chloride absorption is apparently independent of nature of absorbent used for a given skinned fiber. However, this can not be generalized for any VOC-absorbent system.

The overall mass transfer coefficient can be related to the individual mass transfer coefficient by the resistances-in-series model.

For the porous fiber

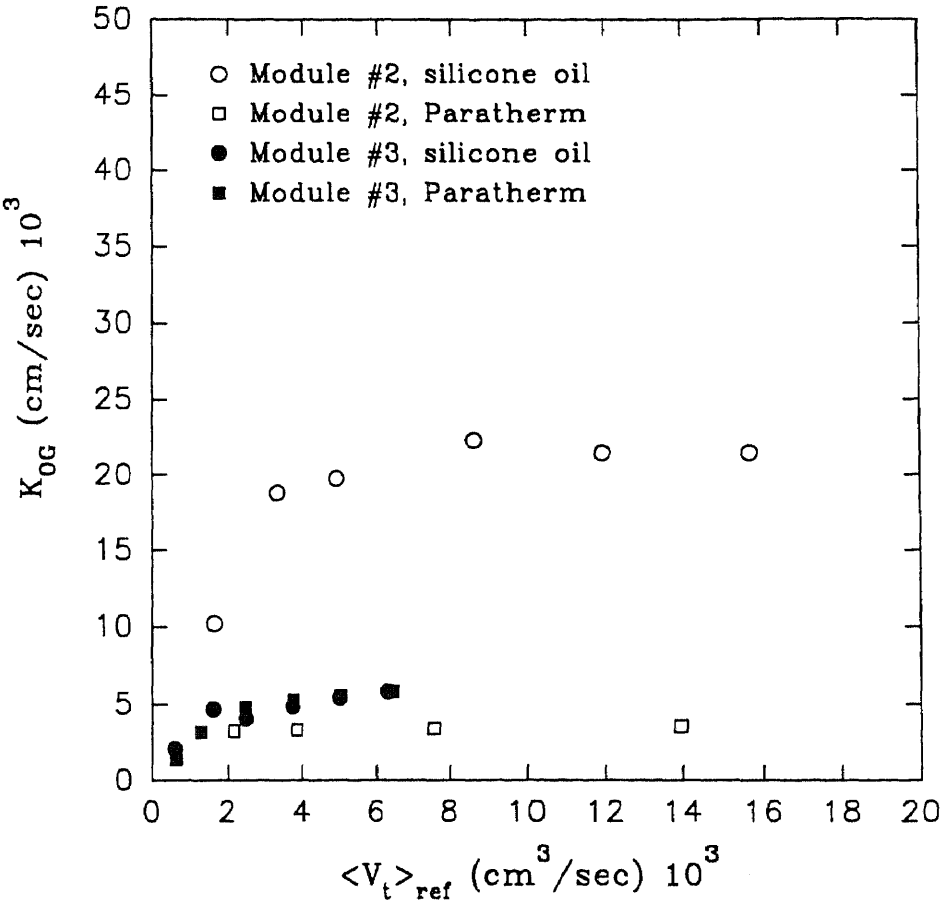

Figure 4.22 Comparison of Mass Transfer Characteristics of Methylene Chloride Absorption between Two Different Absorbents and Two Different Fibers

$$R_{oG} = \frac{1}{K_{oG}} = \frac{1}{k_g} + \frac{1}{H_i \frac{d_{LM}}{d_i} k_m} + \frac{1}{H_i \frac{d_o}{d_i} k_l} \tag{4.5}$$

Here, k_m is the mass transfer coefficient through the absorbent-filled porous membrane which can be expressed as (Prasad and Sirkar, 1988)

$$k_m = \frac{D_{il} \varepsilon}{\tau (r_o - r_i)} \tag{4.6}$$

For the skinned fiber

$$R_{oG} = \frac{1}{K_{oG}} = \frac{1}{k_g \frac{d_i}{d_o}} + \frac{1}{\frac{(d_s)_{ln}}{d_o} k_m} + \frac{1}{\frac{(d_c)_{ln}}{d_o} k_c} + \frac{1}{H_i \frac{d_c}{d_o} k_l} \tag{4.7}$$

Here, k_m is the gas-filled substrate mass transfer coefficient

$$k_m = \frac{D_{igp} \varepsilon}{\tau (r_o - r_i)} \tag{4.8}$$

The mass transfer coefficient through the silicone skin is nothing but the permeance of the VOC through the skin:

$$k_c = \frac{q_c}{\delta_c} \tag{4.9}$$

Here D_{igp} is the diffusivity of gaseous molecules through the porous substrate having straight pores (Section 2.3.5). Each additive term on the right hand side of equations 4.5 and 4.7 is the resistance of the corresponding phase.

Table 4.5 shows the overall mass transfer resistance and the absorbent-filled membrane resistance for different VOC absorptions in silicone oil and Paratherm using the porous fiber module. Total resistance was calculated based on the average maximum values of K_{oG} , obtained as averaged plateau values (from Figures 4.19 and 4.20). It is

Table 4.5 Membrane Resistances for Absorption of Different VOCs Using Porous Fiber

VOC	Absorbent	t (°C)	D_{il} *10^6 (cm^2/sec)	H_i	k_m (cm/sec) 10^4	R_m (sec/cm)	R_{oG} (sec/cm)	R_m/R_{oG}
acetone	silicone oil	22.0	2.806	61.491	1.374	98.050	100.00	0.980
methanol	silicone oil	22.2	6.110	17.623	2.260	203.608	213.74	0.953
methylene chloride	silicone oil	22.0	4.300	90.717	2.064	43.309	47.62	0.910
toluene	silicone oil	27.0	7.625	342.641	3.660	6.466	7.94	0.814
methylene chloride	Paratherm	22.5	0.850	76.5120	0.408	259.773	281.69	0.922
toluene	Paratherm	22.0	4.800	229.178	2.304	15.357	18.52	0.829

very interesting to note that the contribution of the absorbent-filled membrane resistance to the total resistance of mass transfer is quite large. The ratio of membrane resistance to total resistance could be as high as 98% (in case of acetone) to 80% (in case of toluene). Similar results for skinned fiber are shown in Table 4.6. Only two VOCs (acetone and methylene chloride) were investigated using the skinned-fiber module. The resistance of the silicone skin is inversely proportional to the VOC permeance through the skin. Despite having a lower diffusion coefficient, Paratherm appears to provide a slightly higher mass transfer coefficient than that does silicone oil for methylene chloride absorption because of higher Paratherm flow rate (silicone oil flow rate was 4.0 ml/min as against Paratherm flow rate 5.4 ml/min). It was observed that the mass transfer coefficient attained the plateau at a liquid flow rate 5 ml/min or higher in module # 2.

It is clear from Figure 4.22 that the skin resistance controlled the mass transfer characteristics for methylene chloride absorption i.e. skin resistance to overall resistance would be very high (close to unity) However, From Table 4.6, ratios slightly higher than unity was observed. This is apparently contrary to reality. Skin resistance for a particular VOC was calculated based on the permeance value obtained from experiments using dry skinned hollow fiber. In the absorption experiments, organic liquid (silicone oil or Paratherm) was flowing through shell side which caused a possible swelling of the silicone skin and thus decreased the skin resistance for mass transfer. Data for methylene chloride in Table 4.6 can be explained by this swelling phenomenon of the silicone skin. Contribution of skin resistance is much less in the case of acetone absorption, only 0.64. This clearly indicates that skin resistance controlling phenomenon can not be taken as granted for any VOC-absorbent combination using skinned fiber.This will highly depend on the relative performance of the permeation phenomena through the skin and diffusional phenomena in the liquid absorbent in the shell side for a given VOC-absorbent system.

Comparison of VOC absorption characteristics between porous and skinned fibers reveals that, for methylene chloride-silicone oil system, porous fiber offers much lower

Table 4.6 Skin Resistances for Absorption of VOCs Using Skinned Hollow Fiber

VOC	Absorbent	k_c (cm/sec)	R_c (sec/cm)	K_{oG} (cm/sec)	R_{oG} (sec/cm)	R_c/R_{oG}
acetone	Paratherm	0.00322	309.53	$2.07x10^{-3}$	482.59	0.6414
methylene chloride	Silicone oil	0.00506	196.97	$5.40x10^{-3}$	185.94	1.058
methylene chloride	Paratherm	0.00506	196.97	$5.58x10^{-3}$	179.20	1.098

resistance than does skinned fiber (Tables 4.5 and 4.6). However, the reverse is true for methylene chloride-Paratherm system. The contribution of VOC diffusional resistance in the pore absorbent liquid to the overall resistance is more pronounced in the case of porous fiber than that in the case of skinned fiber (there is no such absorbent-filled membrane). Because of the lower diffusivities of VOCs in Paratherm than that in silicone oil, porous fiber exhibits higher resistance than does skinned fiber for Paratherm. Correspondingly, porous fiber exhibits lower resistance than skinned fiber for silicone oil. Hence, porous fiber will have better mass transfer characteristics than skinned fiber with absorbents having high diffusion coefficient for VOC; whereas, reverse will be true with absorbents having low diffusion coefficient for VOC.

The information obtained from the above analysis will be quite important for porous hollow fiber module design for VOC absorption in organic absorbent liquids which wet the fiber. From the results given in Table 4.5 it is possible to conclude conservatively that about 80% of the total resistance to mass transfer for VOC absorption in porous fiber module is due to the membrane. These figures are obtained at gas and liquid flow rates where the overall mass transfer coefficient becomes almost independent of the gas and liquid flow rates. Therefore in order to develop a preliminary design for a module for

VOC absorption from gas phase there is no need to have highly reliable gas phase (tube side) or liquid phase (shell side) mass transfer coefficient correlations. The membrane resistance/mass transfer coefficient can readily be calculated from equation 4.8 using known parameters. For all practical purposes, this resistance can be assumed as approximately 80% (a conservative value) of the total resistance to calculate the area required for a given VOC absorption system design. The gas flow rate should be more than 0.5 cc/min/fiber and a liquid rate of 0.05 ml/min/fiber or more is recommended with appropriate allowance for membrane length. Note, however, these values are highly VOC-dependent especially the gas flow rate for VOCs having higher H_i , e.g. toluene.

However, the above approach cannot be a generalized one for all hollow fiber based gas absorption design. In case of gas absorption in aqueous medium using non-wetted hydrophobic membranes (for example, SO_2 absorption in water) the overall mass transfer characteristics would be controlled either by the gas or the liquid resistance; the resistance of gas- filled porous membrane will no longer control the mass transfer. In such cases it is very necessary to have reliable gas film and liquid film mass transfer coefficient correlations.

4.2.4 Simultaneous Removal of Multiple VOCs

Absorption experiments have been carried out to a limited extent where the N_2 gas stream contained multiple VOCs. Table 4.7 shows the Paratherm®-based absorption data for two flow rates of a N_2 stream containing acetone (226 ppmv), methylene chloride (201 ppmv), toluene (204 ppmv) and methanol (163 ppmv). These experiments were carried out in module # 3. High rates of removal of all VOCs except the highly polar methanol was observed. The removal performance of a particular VOC from a mixture appears to be somewhat inferior to that from a single VOC -N_2 mixture.

Table 4.7 Absorption Data* for a Mixed VOC-N_2 Gas Mixture

VOC composition in inlet N_2 gas stream (ppmv)		Gas flow rate (cc/min)			
		11.65		34.08	
		Outlet composition (ppmv)	Removal (%)	Outlet composition (ppmv)	Removal (%)
acetone	226	13.42	94.06	86.97	61.52
methylene chloride	201	9.17	95.43	17.35	91.34
toluene	204	0.00	100.00	0.00	100.00
methanol	163	77.23	52.62	128.35	21.26
Total	794	99.82	87.43	232.67	70.70

* module # 3
absorbent : Paratherm NF™
liquid flow rate : 5.6 ml/min
temperature: 22° C

4.3 Simultaneous Absorption-Stripping of VOCs

A continuous process for VOC absorption from N_2/air into an absorbent via either of two different kinds of hollow fibers requires simultaneous regeneration of the spent absorbent in a VOC stripper. In this work, membrane module # 2 containing microporous hydrophobic hollow fibers was used as the VOC absorber where the gas flowed at a pressure slightly higher than that of the absorbent along with the membrane module # 3 as the VOC stripper (and, therefore, an absorbent regenerator).

The results for simultaneous VOC absorption and stripping using silicone oil are shown in Figure 4.23. Full vacuum was applied to the bore of the fibers in module # 3 to remove the VOC from the absorbent flowing on the shell side of module # 3 on a continuous basis. The actual level of pressure could not be monitored due to the sensitivity limitations of the vacuum gauge. In module # 2, the absorber, the flow arrangement was similar to simple absorption experiments, namely, gas through the fiber bore and the absorbent on the shell side (and in the pores) flowing countercurrent to the gas flow direction. It was observed that the feed gas containing 999 ppmv of methylene chloride was brought down to around 20 ppmv on a continuous basis when the feed gas flow rate was low. Results of simultaneous absorption / stripping experiments for different VOCs (methylene chloride, methanol and acetone) in terms of the outlet gas phase concentration as a function of gas flow rate are shown in Figure 4.23. Results of methylene chloride removal by Paratherm oil are also shown in this figure. The relative removal performance of different VOCs are similar to that observed in simple absorption experiments. Figure 4.24 shows the variation of the gas phase outlet concentration with the absorbent liquid flow rate for acetone removal by simultaneous absorption-stripping for a fixed gas flow rate. At a slightly higher liquid circulation rate the exit gas phase concentration of VOC is virtually independent of liquid circulation rate. A comparison of the removal performance of methylene chloride and methanol between only absorption and closed loop absorption-stripping experiments are shown in Figures 4.25a and 4.25b.

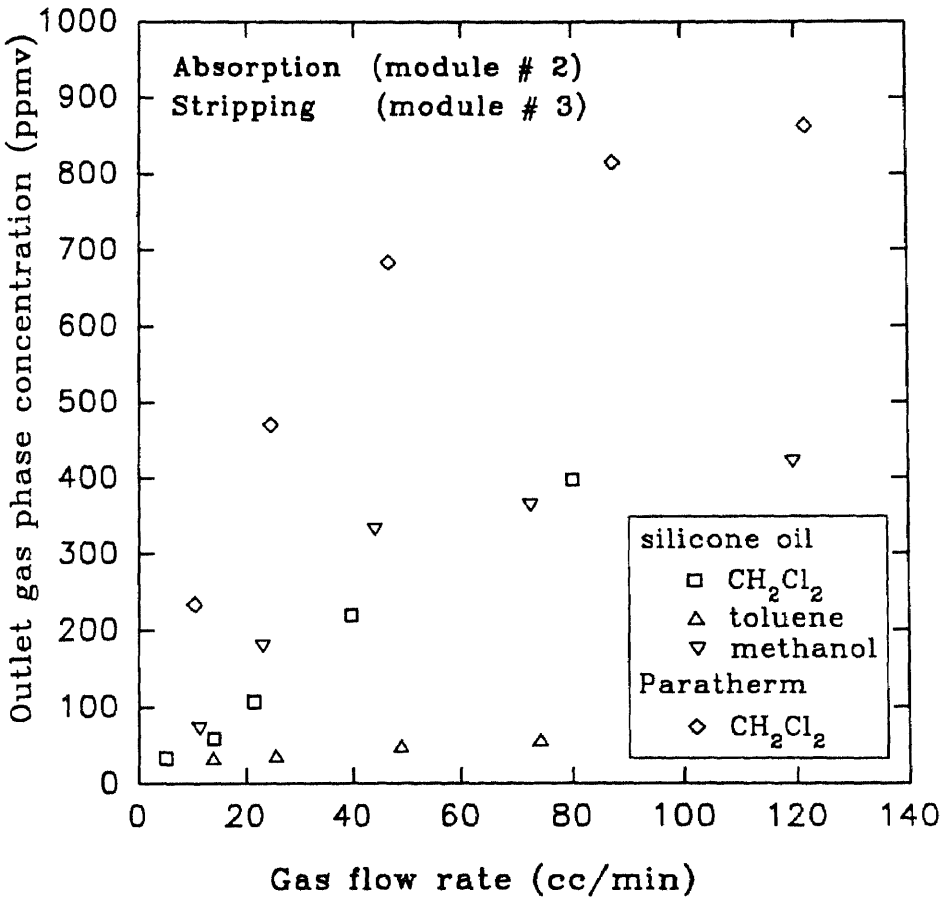

Figure 4.23 Steady State Outlet Concentration vs. Gas Flow Rate for Simultaneous Absorption and Stripping of Different VOCs

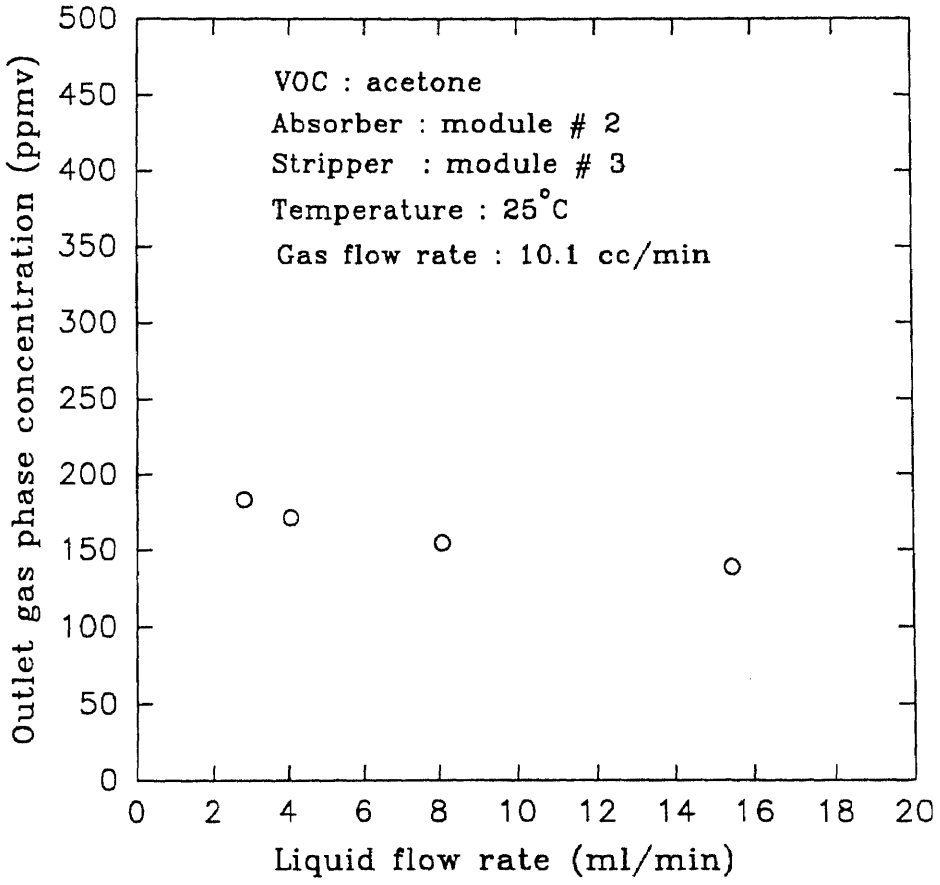

Figure 4.24 Steady State Outlet Concentration vs. Liquid Flow Rate for Simultaneous Absorption and Stripping of Acetone

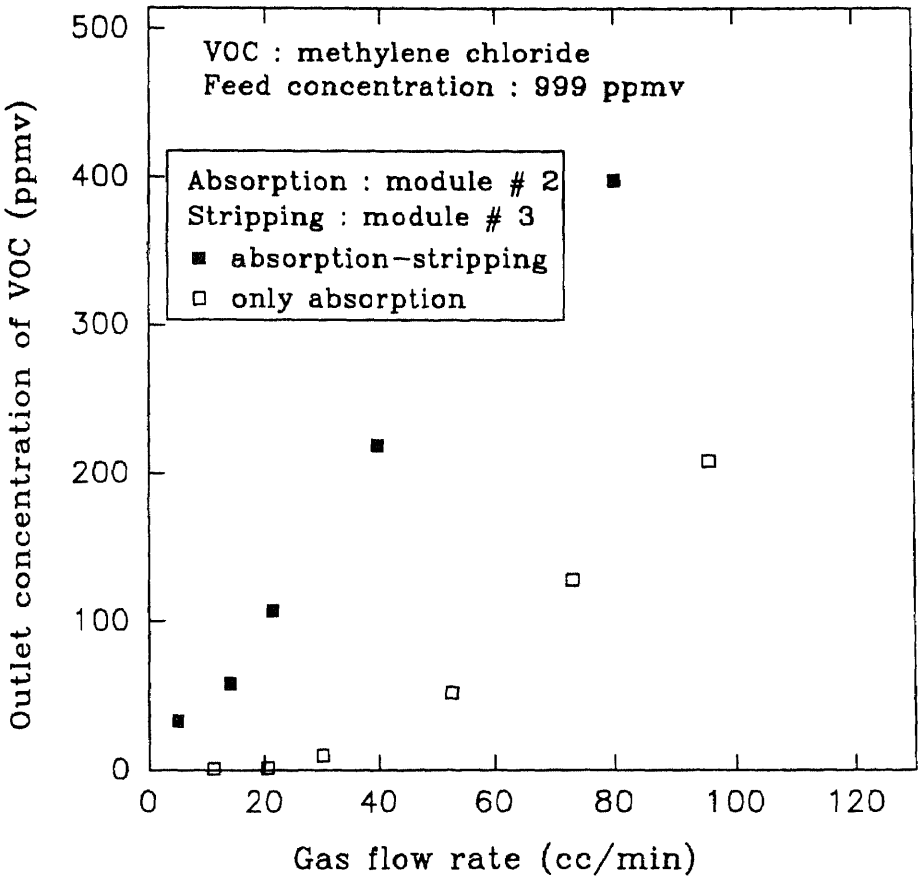

Figure 4.25a Comparison of Methylene Chloride Removal Results by Only Absorption and Combined Absorption-Stripping

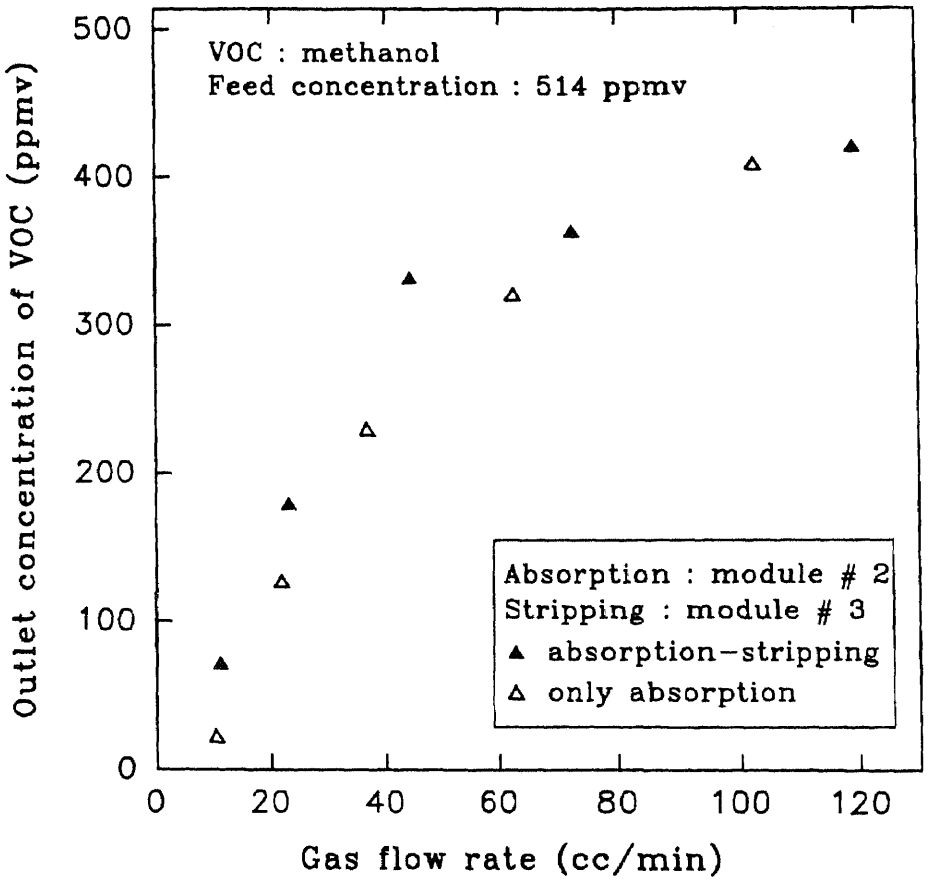

Figure 4.25b Comparison of Methanol Removal Results by Only Absorption and Combined Absorption-Stripping

For methylene chloride simultaneous absorption-stripping experiments exhibits poorer performance than absorption alone (Figure 25a). This discrepancy is due to a lack of perfect regeneration of the circulating absorbent in the stripper. On the other hand, in case of methanol, the performances in terms of outlet gas phase concentration in the two processes are almost identical (Figure 25b). It was easy to strip methanol from the absorbent oil because of the much lower H value. This indicates that the higher the H value of a VOC-absorbent system, the higher will be the difference between results in absorption and combined absorption-stripping process under similar process conditions.

4.4 Additional Results and Considerations

During various experiments with Paratherm® or silicone oil, no peaks of the vapors of these absorbents in the GC were observed. This indicated that their very low vapor pressures at ambient temperatures and the silicone skin barrier on the membrane in the case of coated fibers have reduced their partial pressure (if any) in the gas stream to be scrubbed to sub-ppmv level.

Paratherm® absorbent is known to be stable over long lengths of time. Silicone oil, having a higher vapor pressure (reported), however, slowly starts deteriorating after about one and a half year. Such a degraded silicone oil was used and small peaks were observed in GC from such a deteriorated silicone oil flowing as an absorbent in the microporous hollow fiber.

4.5 Comparison of Experimental Results and Model Simulations

In the model development for absorption (section 2.1) a quantity appears in the denominator in the dimensionless expression of average VOC concentration as $\left(<V_t>/D_{ig}L\right)_{ref}$. This quantity is a dimensionless number, known as Graetz number and is generally expressed as (Perry and Green, 1984)

$$N_{GZ} = \frac{\pi r}{2L}(N_{Re}N_{Sc})_{ref} = \left(\frac{<V_t>}{D_{ig}L}\right)_{ref} \qquad (4.10)$$

For a particular run, $(N_{GZ})_{ref}$ remains constant and varies only with gas flow rates for different runs. As described in Section 2.1.5, the dimensionless gas phase VOC concentration at the module exit (Φ) was calculated for different gas flow rates from the simulation. From the independent variable, gas flow rate per fiber ($<V_t>_{ref}$), $(N_{GZ})_{ref}$ was then calculated using the calculated value of $(D_{ig})_{ref}$. $(D_{ig})_{ref}$ was calculated from equation 2.106 using thermodynamic parameters given in Appendix (Table A1). The corresponding Φ was calculated from experimental data. A tortuosity value of 2.5 (Prasad and Sirkar, 1990; Karoor and Sirkar, 1993) and surface porosity 0.3 (Karoor and Sirkar, 1993) were used for simulation.

Figure 4.26 shows plots of Φ as a function of the inverse of Graetz number comparing model simulations and experimental data for acetone, methanol, and methylene chloride absorption in silicone oil using module # 1 and 2. For methylene chloride, experimental results from module # 1 at higher gas flow rates as well from module # 2 at lower gas flow rates show very good agreement with model simulations. One may notice that the simulation results for module # 1 and module # 2 differs slightly. This is because of the fact that Graetz number is not a completely module independent parameter; even for identical fibers two module could be having two different packing factors (37.5% and 16.75% for module #1 and #2 respectively). For acetone, experimental results for two different feed concentrations follow the predictions of the model. Figure 4.27 shows similar plots for toluene absorption in silicone oil as well as in Paratherm using module # 2. Both plots show very good agreement with the model simulation.

Variation of Φ as a function of absorbent liquid flow rate has also been predicted by the mathematical model. Comparison of such variation between model simulations and experimental results are shown in Figure 4.28. Experimental results follow the predictions from model quite well.

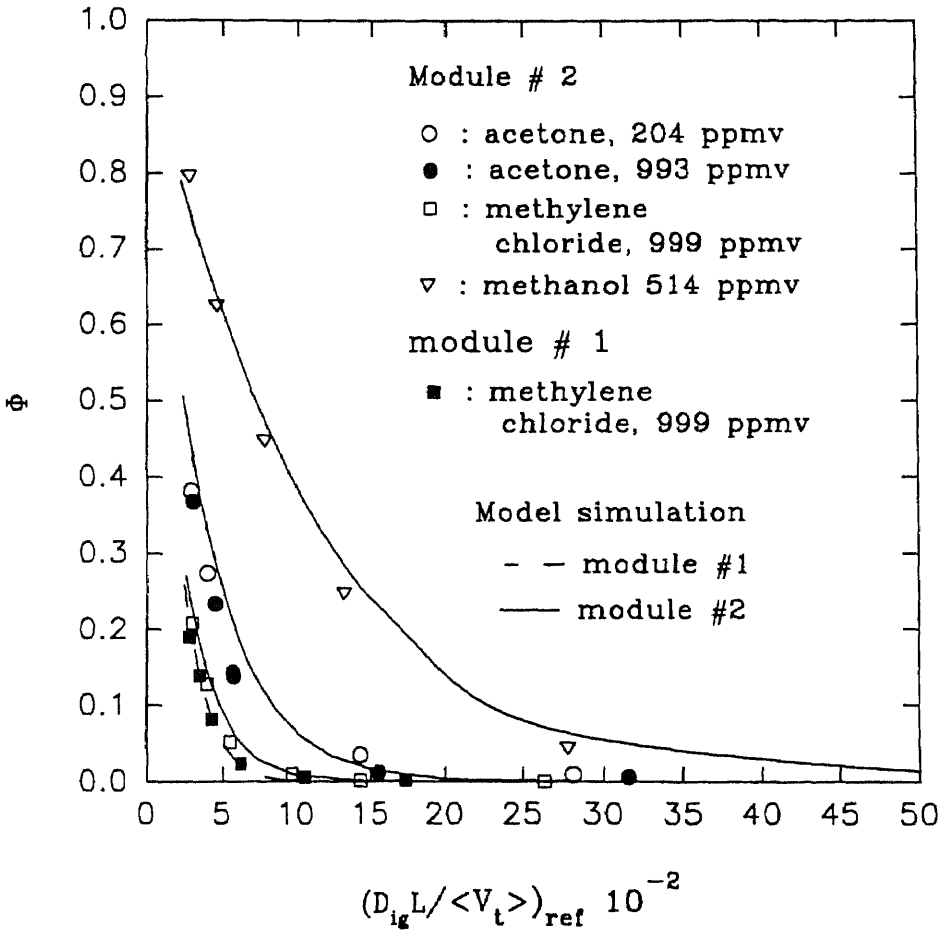

Figure 4.26 Ratio of Outlet to Inlet Gas Phase Concentration of Different VOCs as a Function of Inverse of Graetz Number

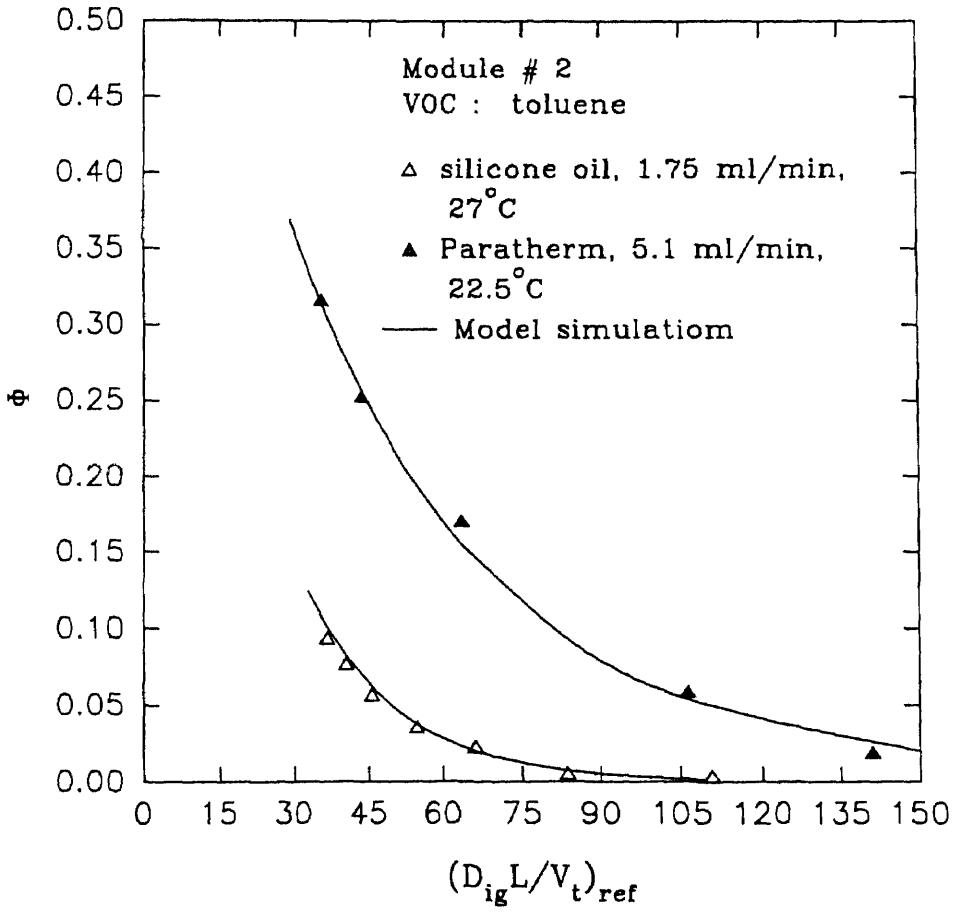

Figure 4.27 Ratio of Outlet to Inlet Gas Phase Concentration of Toluene as a Function of Inverse of Graetz Number

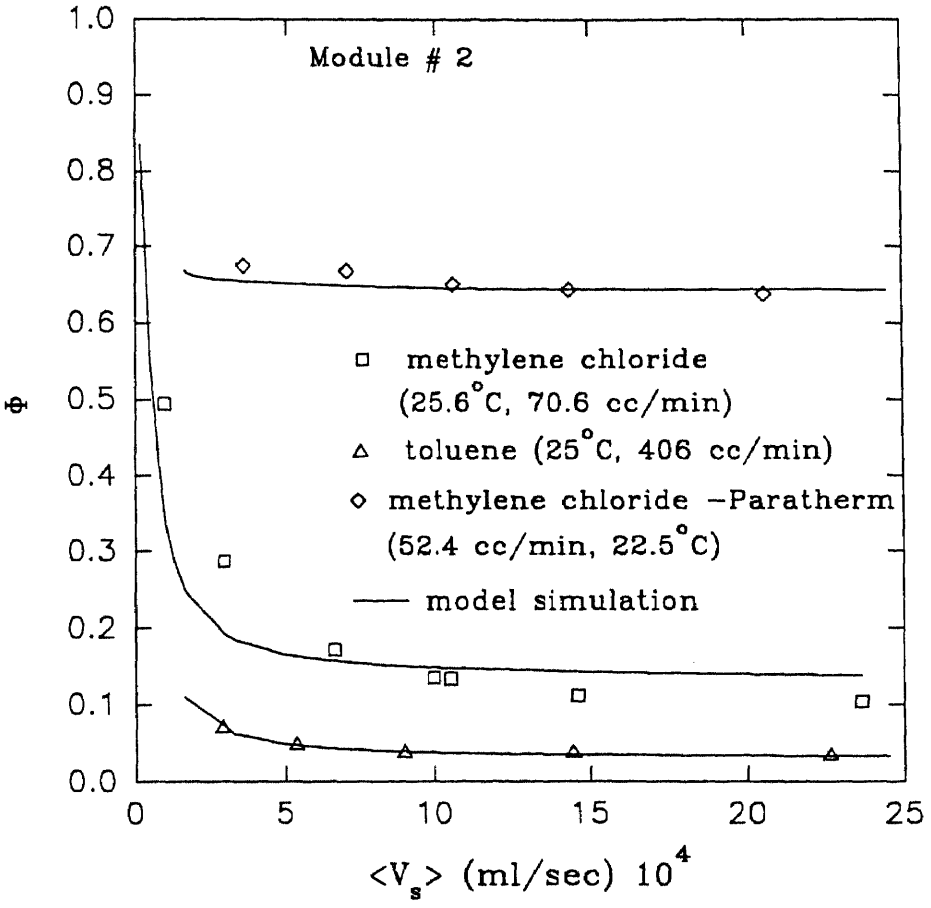

Figure 4.28 Ratio of Outlet to Inlet Gas Phase Concentration of VOCs as a Function of Liquid Flow Rate

Figure 4.29 illustrates the variation of Φ vs. inverse of Graetz numbers from model simulations and experimental data for methylene chloride absorption in silicone oil and Paratherm using skinned fiber module (module # 3). Both model simulations and experimental data show almost identical performance between absorption in Paratherm and silicone oil. This indicates that the difference in the diffusivities in the two absorbents does not control the absorption performance of methylene chloride. It is the skin resistance which controls the performance. However, this cannot be generalized for any VOC absorption using skinned fiber module. Simulation plots of Φ vs. inverse of Graetz numbers for acetone absorption using skinned fibers show that there is an effect of characteristics of absorbent flowing through the shell side (Figure 4.29).

Figure 4.30 shows the simulation plots for absorption of methylene chloride in two different absorbents using porous fibers. The effects of absorbent diffusivity and Henry's law constant on the performance of absorption are well predicted by the mathematical model.

Almost all plots for various absorption experiments show good agreements with model simulation results. At higher gas flow rates, maximum deviation of 10 to 15 % was observed between experimental and simulation results for Φ. However, the deviation between the two results are much more when the gas flow rates were very low (0.1 cc/min/fiber or less). Deviations as high as 50 to 60 % were obtained at such lower gas rates. Experimental as well as simulated gas phase VOC concentrations are very low at lower gas flow rates hence, their deviations are not clear in the plots. However, their relative magnitude is high. One should look at such deviations from a different perspective. It is necessary to compare the total amount or percent of VOC removed from feed gas at low gas flow rates. For example, if a feed VOC mixture of 999 ppmv is brought down to 6 ppmv and the model predicts 2 ppmv, the theory is quite successful, yet direct comparison of Φ will indicate strong deviation. Further, operation of VOC absorption at lower gas flow rate per fiber will not be economical any way because

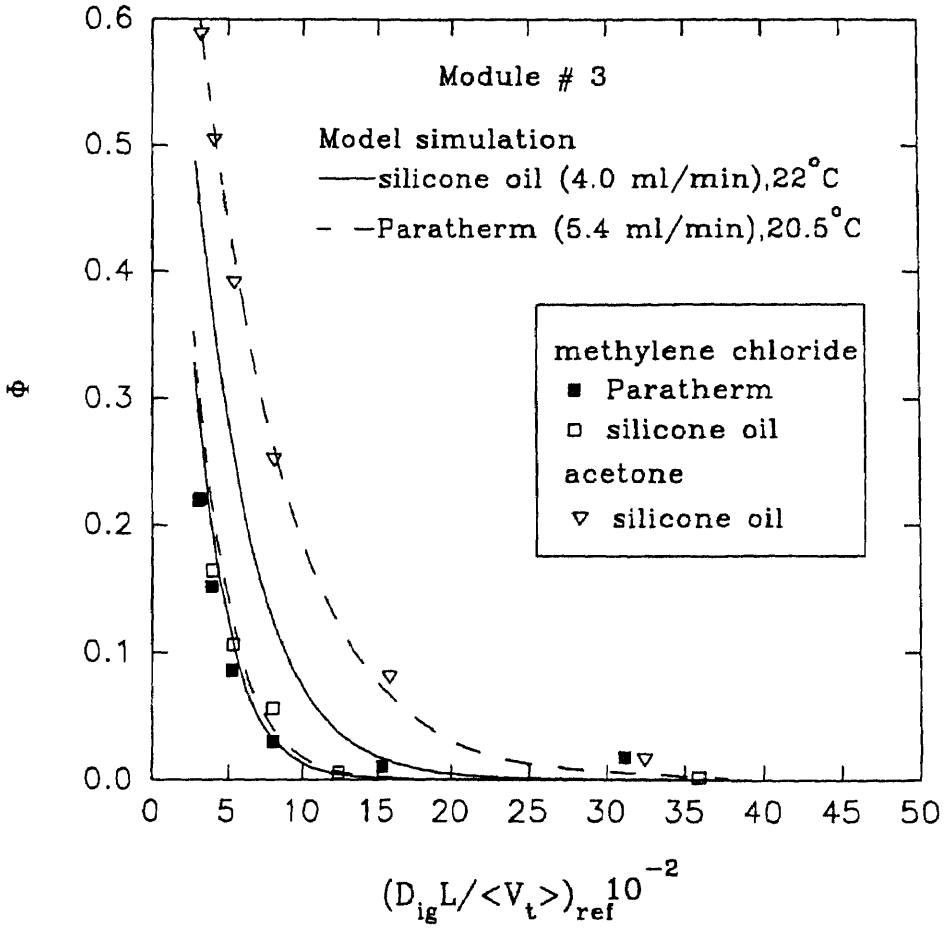

Figure 4.29 Ratio of Outlet to Inlet Gas Phase Concentration of Methylene Chloride and Acetone as a Function of Inverse of Graetz Number for Absorption Using Skinned Fiber with Two Different Absorbents

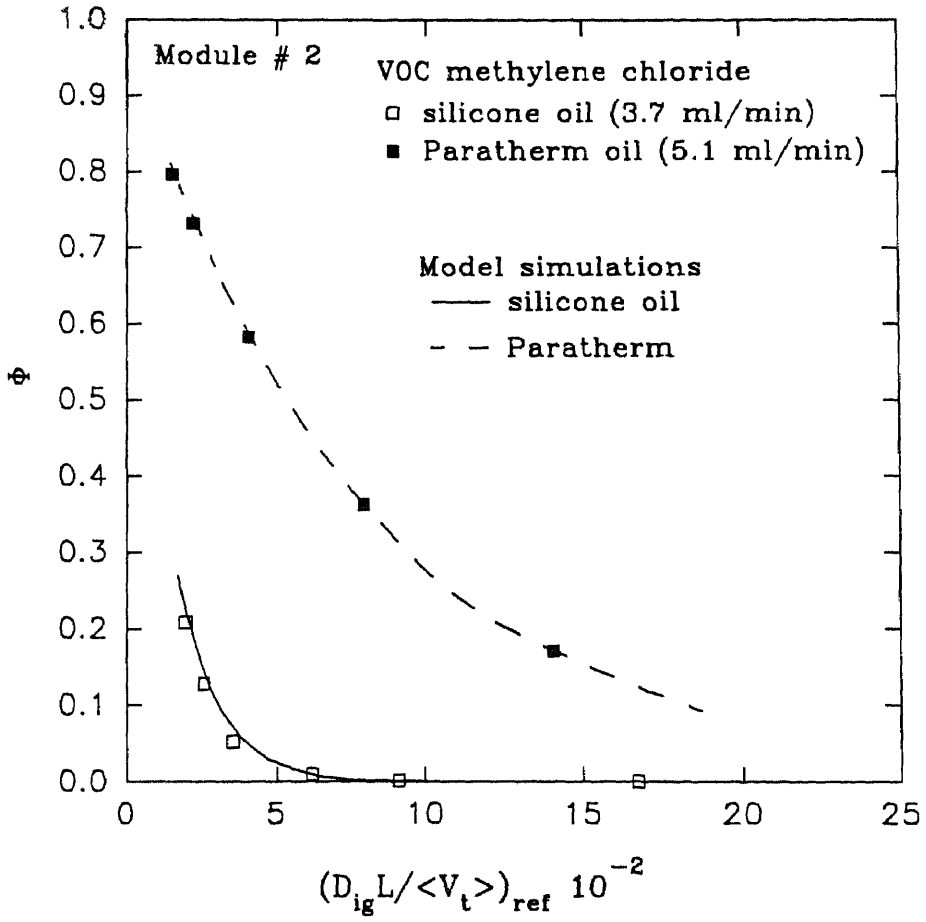

Figure 4.30 Ratio of Outlet to Inlet Gas Phase Concentration of Methylene Chloride as a Function of Inverse of Graetz Number for Absorption Using Porous Fiber with Two Different Absorbents

overall mass transfer coefficient will be lower. It would be economical to design the absorber module at higher gas flow rate per fiber to take advantage of higher value of mass transfer coefficients. At higher gas flow rates, concentration of VOC can be brought to a low level by increasing the effective length of the module.

Simulation results were also obtained for VOC removal by combined absorption-stripping process. The steps for such simulations are discussed in Section 2.4. Dimensionless gas phase VOC concentrations at the absorber outlet (Φ) were plotted as a function of inverse of gas phase Graetz numbers for different VOC removals (Figure 4.31) by the absorption-stripping process. Experimental results were compared with simulation results; all VOCs except methanol show a very good fit between the two results.

Finally the effects of stripping temperature and stripper area performance on the overall absorption-stripping process were also simulated. Figure 4.32 shows the plots of Φ vs. stripping temperatures at different Graetz numbers (gas flow rates). At a lower gas flow rate (0.25 cc/min/fiber), the drop in outlet VOC concentration is about 46.7 % for a rise in stripping temperature from 20°C to 60°C. For a higher gas flow rate (1 cc/min/fiber), the corresponding drop is 22.7%. Figure 4.33 shows the plots of Φ vs. stripper area at different gas phase Graetz numbers. A 78.5% drop in outlet VOC concentration was observed for a 5 fold increase in stripper area, at a gas flow rate of 0.25 cc/min/fiber.

4.6 Comparison of Overall Volumetric Mass Transfer Coefficient for VOC Absorption between Hollow Fiber Contactor and Packed Tower

Overall gas phase based mass transfer coefficient (K_{oG}) and the volumetric mass transfer coefficient ($K_{oG}a$) were calculated (Treybal, 1980) for methylene chloride absorption with silicone oil in a conventional packed bed. Results of calculations for different liquid to gas flow rate ratios are shown in Table 4.8. Higher $K_{oG}a$ values were obtained for higher liquid to gas flow rate ratios. For high levels of purification, it is not possible to design

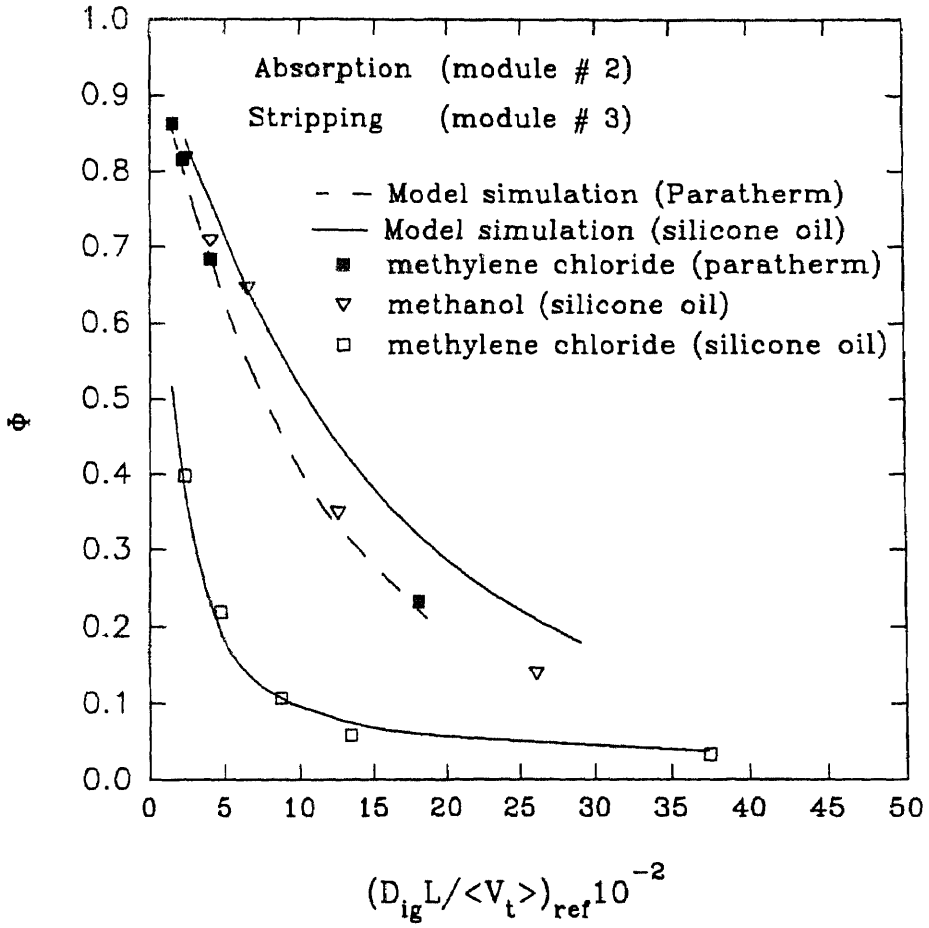

Figure 4.31 Ratio of Steady State Outlet to Inlet Gas Phase Concentration of VOCs as a Function of Inverse of Graetz Number for Continuous Absorption-Stripping Process

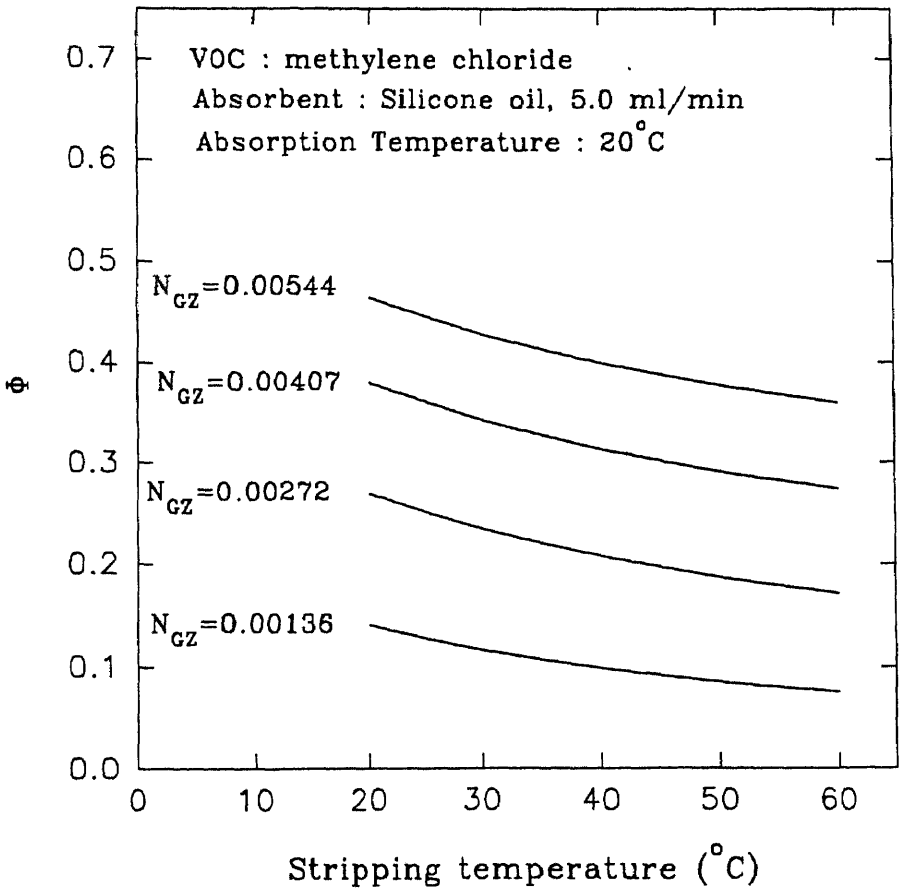

Figure 4.32 Simulation Plots of Dimensionless Outlet Gas Phase Concentration vs. Stripping Temperature at Different Graetz Numbers

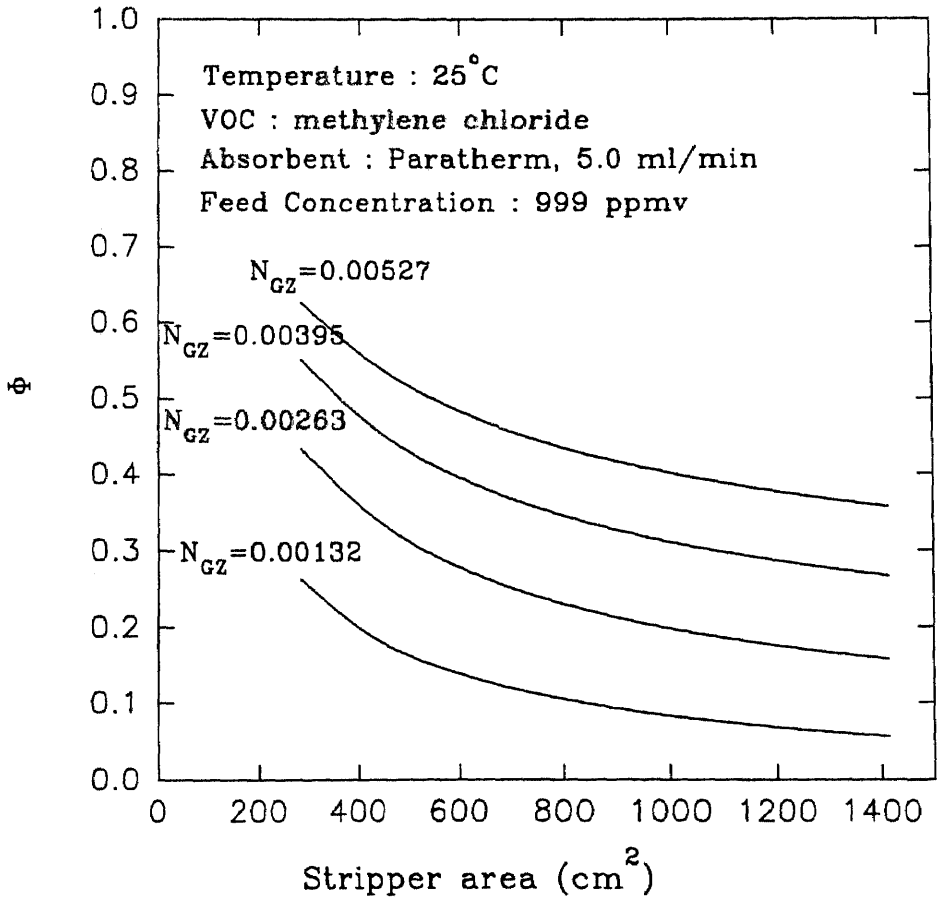

Figure 4.33 Simulation Plots of Dimensionless Outlet Gas Phase Concentration vs. Stripper Area at Different Graetz Numbers

a packed tower with a very high liquid to gas flow rate ratio due to the flooding problem. There are no correlations in literature for higher liquid to gas flow rate ratios. This problem does not arise in the case of hollow fiber module design. One may note that even for the low packing density (a = 29.8 cm^2/cm^3) in module # 2, ratios for $K_{oG}a$ values between module # 2 and the packed tower are quite large. Further improvement of the membrane module performance is possible by having transverse liquid flow with baffles in the shell side and by introducing fibers having higher porosity (e.g. Celgard X-20), lower tortuosity and thinner membrane wall .

Table 4.8 Comparisons of Volumetric Mass Transfer Coefficients between Hollow Fiber Modules and Packed Bed for Methylene Chloride Absorption in Silicone Oil

G	L/G	D_T	k_g	k_l*10^3	$(K_{oG})_{PT}$	$(a)_{PT}$	$(K_{oG}a)_{PT}$	$(K_{oG}a)_{HFM}/(K_{oG}a)_{PT}$	
								1	2
32.94	5	30	1.20	3.93	0.257	0.53	0.137	10.5	4.8
65.88	10	42	1.30	5.49	0.338	0.68	0.231	6.3	2.8
16.47	20	27	1.42	5.98	0.368	0.71	0.262	5.6	2.5

Temperature : 25°C, H_i: 83.3, Packing : 13 mm Berl saddles, Pressure drop : 400 N/m^2
PT : Packed tower, HFM : Hollow fiber module
1: module #1; a = 66.67 cm^2/cm^3
2: module #2; a = 29.8 cm^2/cm^3

CHAPTER 5

CONCLUSIONS AND RECOMMENDATIONS

5.1 Conclusions

The present work was initiated to explore VOC removal from exhaust air by novel absorption/stripping technology employing efficient and compact hollow fiber devices made out of different types of hollow fiber membranes. The absorbents used are inert, essentially nonvolatile and high-boiling liquids such as silicone oil and Paratherm. In the separation scheme studied, contaminated air flows inside (tube side) the hollow fiber and the absorbent liquid is pumped countercurrently through the shell side. VOCs were efficiently removed from the nitrogen stream to a potentially very low level. Spent absorbent liquid was regenerated in a separate hollow fiber stripper by applying vacuum through the tube side and recycled back to the absorber. Mathematical models were also developed to simulate the absorption process for two different types of fibers and the combined absorption-stripping process. The following brief concluding remarks can be made from the results of this study.

- Hollow fiber contactor based removal of VOCs from nitrogen by absorption in a nonvolatile nontoxic absorbent liquid like silicone oil or Paratherm is a very effective process.
- For a given absorbent and process conditions, absorption efficiency varies with different VOCs. In this present study, toluene showed the best result among all four VOCs, followed by methylene chloride, acetone and methanol in that order.
- For a given VOC and process conditions, silicone oil showed better removal efficiency than Paratherm. This is because of the higher VOC diffusivity and Henry's constant values in the silicone oil. However, Paratherm appeared to be better from stability and vapor pressure point of view.

• For absorption using porous hydrophobic hollow fibers, a stable gas-liquid interface can be created at the pore mouth on the gas-side of the fiber by maintaining gas-side pressure higher than the liquid-side pressure.

• For absorption using skinned fibers, it is essential to maintain the liquid-side pressure equal to or higher than the gas side pressure.

• It was observed that the absorbent-filled porous membrane wall contributed about 80-95 % of the total resistance to mass transfer at relatively higher gas and liquid flow rates.

• For absorption using skinned fibers, mass transfer characteristics appeared to be controlled by the silicone skin resistance and the resistance of the absorbent liquid film outside the fiber.

• Comparison of VOC absorption characteristics between porous and skinned fiber reveals that the relative performance of the two types of fiber for a given VOC absorption depends on the diffusivity of the VOC in the absorbent liquid used.

• For a given VOC, combined absorption-stripping yielded results slightly inferior to that for absorption only because of the partial regeneration of the absorbent liquid in the stripper. The deviation between the absorption only results and combined absorption-stripping results is significant for toluene and negligible for methanol.

• Experimental results plotted as dimensionless concentration against the inverse of Graetz number demonstrated a good agreement with predictions from the mathematical model.

• Simulation results for combined absorption-stripping process show that higher stripping temperature and larger stripper area improves the VOC removal results significantly.

5.2 Recommendations for Future Work

The performance of a VOC absorption process in a given contacting unit primarily depends on the absorbent selected. Two key factors found to be important in this respect are Henry's constant and diffusivity. An absorbent which is very good for one VOC may not be good for another VOC. It would be quite useful to develop a data base for various

absorbent-VOC systems by carrying out experiments systematically. Determination of Henry's constant and diffusivity would involve time and complexities. Another way of selecting a good absorbent for given VOCs would be to search for them by carrying out absorption experiments with various VOC-absorbent systems under identical experimental conditions.

It has been discussed earlier that the performance of the membrane-based overall absorption-stripping process is ultimately controlled by the limitations of the stripping process. Efficient regeneration of a good absorbent liquid for a given VOC will always be a difficult task unless considerable amount of energy is spent. To increase stripping efficiency it is required to operate the stripper at a higher temperature (within the tolerance of the materials of construction). Simulation results of combined absorption-stripping process with higher stripping temperatures do show an appreciable improvement in overall performance. However, necessary experiments should be carried out with a heating and cooling arrangement of absorbent liquid in a closed loop. A schematic diagram of this process is shown in Figure 5.1

Another effective way to strip VOCs from the absorbent oil would be to use low temperature steam stripping in a silicone skinned fiber module. This could be achieved by generating steam at low temperatures (maximum 60°C) under moderate vacuum. The process will generate water mixed with VOCs in the condenser; it has to be separated first by gravity separator if possible, and then the water should be sent to a treatment plant.

It has been demonstrated earlier that absorption of a VOC in a good absorbent in hollow fiber devices is extremely efficient. In order to take full advantage of the absorption process alone, the following two alternatives for stripping could be thought of.

1. Stripping could be performed effectively in a conventional way by simple distillation technique instead of vacuum stripping in a skinned hollow fiber module.

2. Low concentration of VOCs in the emission streams can be treated by absorption in fuel oil using a hollow fiber device. The fuel oil will be ultimately burnt

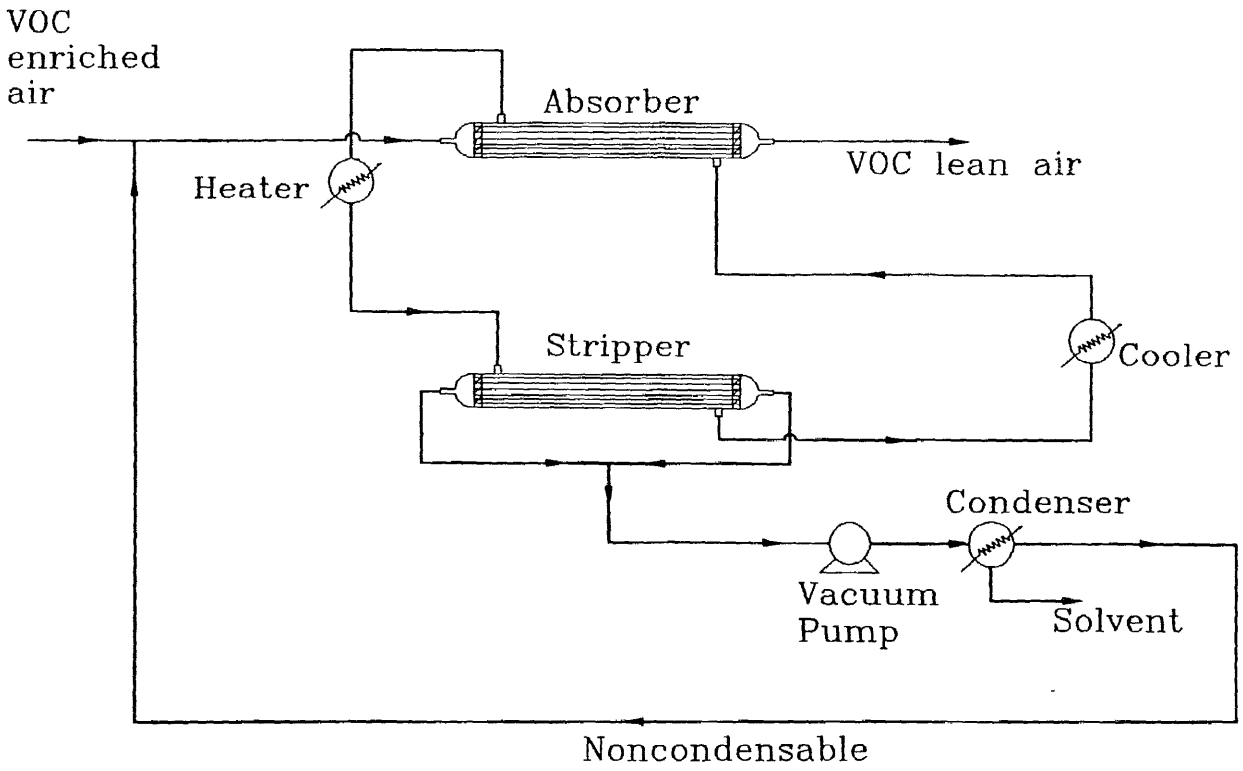

Figure 5.1 Schematic Diagram of VOC Removal by Hollow Fiber-Based Absorption-stripping with Cooling and Heating Arrangement of Circulating Absorbent Liquid

any way in the furnace or in the boiler. This will provide complete destruction of VOCs without any additional expense of energy or material. Of course the unit should have the facilities and requirements for fuel oil firing. Absorption experiments with VOCs and fuel oil could be conducted to check its technical feasibility. The two key issues here are the fuel oil vapor pressure and the possibility of other contaminants being produced in the combustion process and any subsequent scrubbing requirement.

Information about the behavior of unsteady state absorption would be useful for developing an absorption-stripping scheme for VOC cleanup in a cyclic fashion. A preliminary absorption experiment was carried out in a transient fashion to demonstrate the nature of the breakthrough curve. Initially the experiment was started with pure N_2 flowing through the tube side and absorbent oil (Paratherm) stationary on the shell side. When the gas flow rate was stabilized, VOC-N_2 gas mixture flow was switched on through the tube side while pure N_2 flow was switched off at the same time. This switching of two gas streams was done instantaneously at the same time by means of a three way valve connected at the gas inlet lines. At this moment, the exiting gas from the module was injected into the GC and the concentration of VOC was monitored at frequent time intervals. Initially no peak of VOC was observed in the GC-output; but, as time passed, the VOC showed up in the exiting gas stream and its concentration started increasing. The result of this transient absorption experiment is shown in Figure 5.2. This experiment allows the possibility of using the absorption oil like an activated carbon bed.

Sometimes it is difficult to meet the conditions and requirements imposed on the design of VOC control system by a single process. Combination of two or more technologies discussed earlier in the Introduction chapter may result in a much better level of VOC emission control than what the individual technology may offer, yet it would be quite cost effective. Such processes are commonly known as hybrid processes (API Publication, 1993). Though addition of two or more technologies for a single application may appear complicated and costly, some of these technologies may complement each

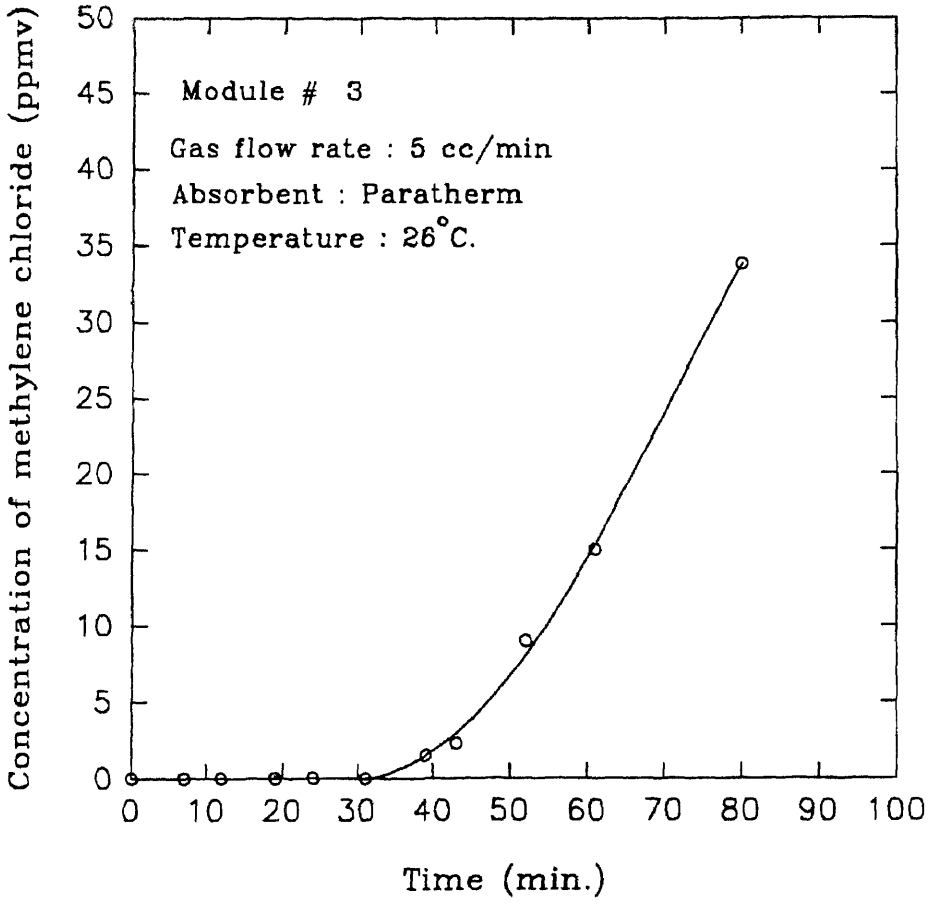

Figure 5.2 Breakthrough Curve for Unsteady State Absorption of Methylene Chloride from Nitrogen in Paratherm Using Skinned Hollow Fibers

other and the combination may be more economical than a single process.

A hybrid experiment was conducted by combining membrane permeation (vapor permeation) and absorption-stripping experiment for cleaning up the VOC from nitrogen. The process is depicted in the schematic diagram, Figure 5.3. VOC-contaminated N_2 stream was fed to a membrane permeation unit at an optimum flow rate to get maximum removal and selectivity. The exiting stream from the permeation unit was then fed to the closed-loop absorption-stripping process for further reduction of VOC concentration. As shown in Figure 5.3, the same vacuum pump and condensation facility could be used for membrane permeation as well as the absorption-stripping process.

A few experiments were conducted in a hybrid system as described above using a N_2 stream containing 6000 ppmv methylene chloride as feed gas. Gas was passed through the permeation unit at a definite flow rate and the concentration of methylene chloride in the exiting gas stream was monitored by the GC. When a steady state concentration was achieved, the exiting gas was directed to the absorption-stripping setup. The same vacuum pump was used for the permeation and the stripping unit. Full vacuum (measurement of actual pressure was limited by the sensitivity of the vacuum gauge) was applied to both units. Results of this experiment are shown in Table 5.1. Using this combined system it was possible to reduce the methylene chloride concentration from 6000 ppmv to as low as 2 ppmv at the low gas flow rate of about 60 cc/min. Results are also shown in Figure 5.4.

The same result could be obtained in the permeation process itself by increasing the membrane area for a given gas flow rate. But, higher membrane area will enhance N_2 permeation resulting in a decrease in selectivity. This excess permeating N_2 will increase the load in the condenser and vacuum pump. On the other hand, in order to achieve the VOC reduction in a absorption stripping unit at the same level as that of the hybrid process, large absorber and stripper area would be required for a given gas flow rate, which certainly would not be economical. To develop a perspective compare this result

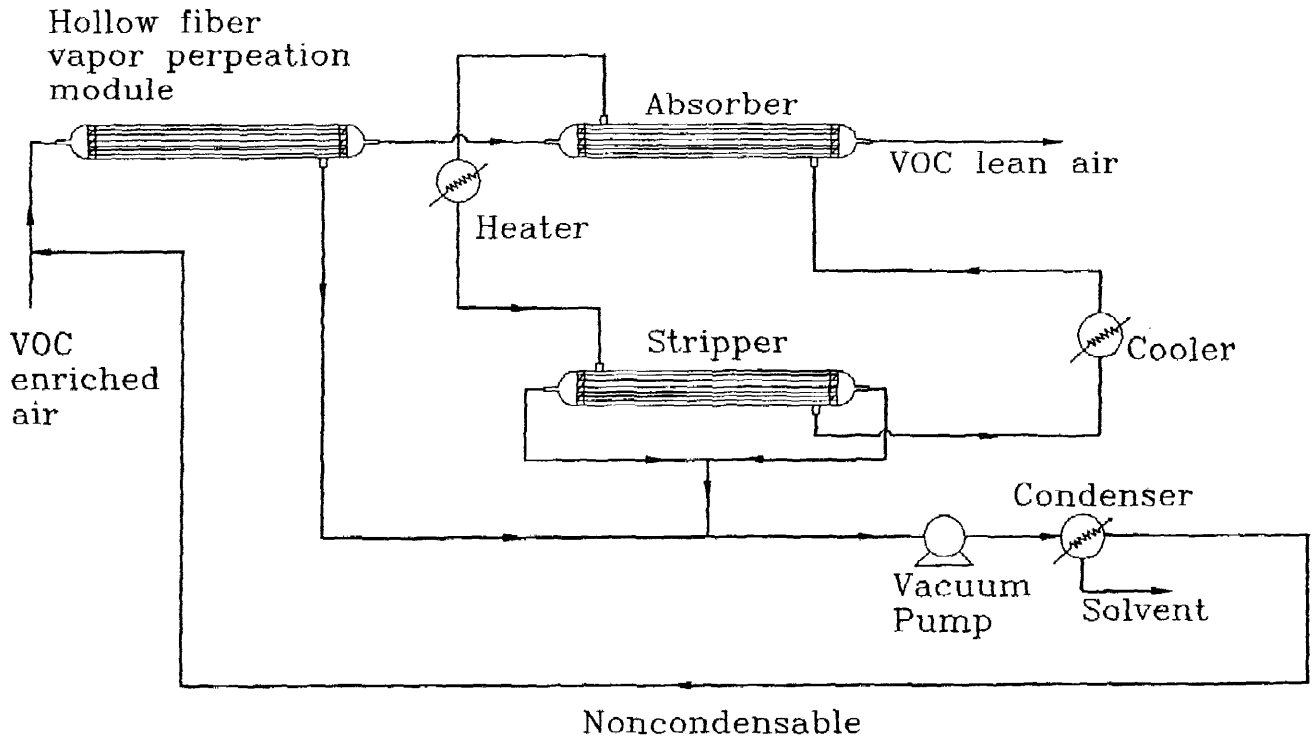

Figure 5.3 Schematic Diagram of VOC Removal by a Hybrid Process of Vapor Permeation and Membrane Based Absorption-stripping

Table 5.1 Experimental Results of VOC Removal by a Hybrid Process of Vapor Permeation and Hollow Fiber-Based Absorption-stripping

Gas flow rate (cc/min)	Exit conc. after Permeator (ppmv)	Removal (%)	Exit conc. after absorption-stripping (ppmv)	Removal (%)	Overall removal (%)
58.8	63	98.95	2	96.82	99.97
78.0	275	95.42	28	89.82	99.53
100.4	374	93.76	88	76.47	98.53

* Feed concentration : 6000 ppmv; absorbent : Paratherm; absorbent circulation rate : 5.2 ml/min;
Temperature: 22.5°C
Permeator specification:
Type of fiber : skinned, # of fiber =50, effective length =25 cm, fiber ID =240 μm, fiber OD =300 μm

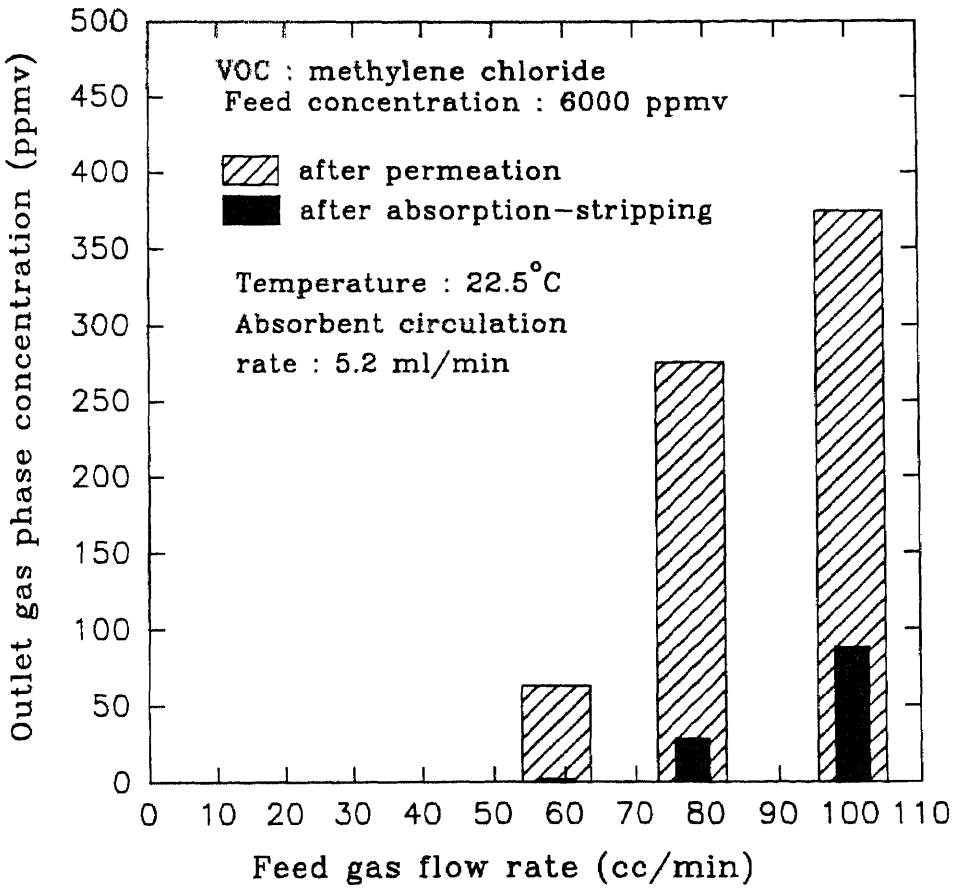

Figure 5.4 Results of Methylene Chloride Removal by a Hybrid Process of Vapor Permeation and Membrane-Based Absorption-stripping

with that for simple membrane absorption-stripping (Figure 4.13a) where 2 ppmv level of methylene chloride absorption could be achieved only for a gas flow rate 0.05 cc/min/fiber or less for a feed concentration of 999 ppmv. Yet the additional membrane area required in the permeator is only 40% of that of the absorber. More experiments, preferably at pilot scale should be carried out to ascertain the technical and economic feasibility of this hybrid process. The final aim would be the optimal design of the permeation unit by trading off between exit VOC concentration and selectivity. A good piece of simulation / design work would be possible by combining the individual models for permeation and absorption-stripping together.

In the models developed for VOC absorption, it was assumed that the molar flow rate of the VOC-N_2 gas mixture remains constant throughout the module length. This assumption is reasonably correct for low concentrations of the VOC stream (in this case maximum of 1000 ppmv). However, for higher feed-VOC concentrations, this assumption will lead to an erroneous prediction. Variable molar flow rate along the length of the module can be incorporated easily in the algorithm of the numerical simulation. The basic analytical solutions applicable to each small segment will remain unchanged because it is necessary to assume that, in the small segment the molar flow rate is constant in order to solve the governing mass balance differential equations without inviting further complications. The molar flow rate in a particular segment should be calculated by subtracting the molar transfer rate of VOC through the area of the previous segment. In this fashion, the volumetric gas flow rate will be reduced along the length of the module because of two factors: pressure drop and the reduction of total number of moles of gas flowing through the fiber per unit time.

There are a number of other aspects that need to be explored. Studies where the vacuum level is not as high as used here are necessary to simulate what can be achieved industrially. Using silicone skin thickness that are much smaller will increase the mass transfer performance of the skinned absorption unit as well as the membrane stripper

significantly. Correspondingly, transverse flow of the liquid on the shell side with or without baffles will substantially increase the liquid phase mass transfer coefficient. Similarly, for the porous fibers, transverse flow will reduce the liquid film resistance. Additionally, it will be helpful to have fibers having higher porosity with lowered tortuosity and thickness.

The absorption scheme and the operational conditions vis-a-vis the different phase pressures are equally useful and applicable to general gas scrubbing and regeneration of absorbents. The gas species to be selectively removed could be CO_2, H_2S, SO_2, O_2, etc. The absorbents may be aqueous solutions of alkanolamines, hindered amines and pure polar hydrocarbons like n-methylpyrollidone, dimethylsulfoxide, sulfolane, etc.

This thesis has explored hollow fibers having an ultrathin nonporous skin of plasma polymerized silicone (poly (diemtheylsiloxane)) on the hollow fiber outer surface. This skin material must be highly permeable to the gas species or VOCs to be absorbed. Other materials of considerable use for VOC removal are copolymers of silicone-polycarbonate, neoprene and different rubbers, poly (1-trimethyl silyl-1-propyne) etc.

Microporous hollow fibers that are hydrophobic were used in this study. It is equally useful to use microporous hollow fibers that are hydrophilic. However, when used in that contacting mode without a nonporous skin, it is important to have the nonpolar organic absorbent in the pore and not water since that would increase the resistance to VOC mass transfer considerably. One can also employ a hollow fiber membrane whose wall is essentially a gel membrane. It is preferable that the gel is due to the organic absorbent being used; otherwise, the resistance to VOC transfer will be significantly increased.

APPENDIX A

EXPERIMENTAL RESULTS

Table A1. Thermodynamic Properties of Nitrogen and VOCs

VOC/N_2	Mol. Wt	BP(K)	FP(K)	T_C (K)	P_C (atm)	V_C (cc/mole)	ε/K (K)	σ(Å)	δ_m(Debyes)
Acetone	58.08	329.4	178.2	509.1	47.0	211.0	560.2	4.600	2.9
Methanol	32.042	337.8	175.5	512.6	79.9	118.0	481.8	3.626	1.7
Methylene Chloride	84.922	313.0	178.1	510.0	60.0	193.0	356.3	4.898	1.8
Toluene	92.141	383.8	178.0	592.0	41.6	316.0	452.91	5.375	0.4
Nitrogen	28.013	77.4	63.3	126.2	33.5	90.1	71.4	3.798	0.0

For toluene, σ and ε/k values are calculated from the following equations (Reid et al., 1977).

$$\frac{\varepsilon}{k} = 1.18(1+1.3\delta^2)T_b$$

$$\sigma = \left(\frac{1.585V_b}{1+1.3\delta^2}\right)^{\frac{1}{3}}$$

$$\delta = \frac{1.94x10^{3}\delta_m^2}{V_bT_b}$$

$$V_b = 0.285V_C^{1.048}$$

Table A2. Henry's Law Constant As a Function of Temperature ; Acetone-Silicone Oil

Experiment #	t (°C)	1/T $(K)^{-1}$	H	ln(H)
1	25.60	0.0033489	52.1125	3.95341
2	31.85	0.0032803	47.7197	3.86534
3	37.85	0.0032169	36.4201	3.59512
4	45.90	0.0031357	28.5920	3.35300

Table A3. Henry's Law Constant As a Function of Temperature ; Methanol-Silicone Oil

Experiment #	t (°C)	1/T $(K)^{-1}$	H	ln(H)
1	25.65	0.0033484	15.9470	2.76927
2	31.90	0.0032797	14.4590	2.67132
3	37.95	0.0032159	14.0707	2.64409
4	45.90	0.0031357	10.6329	2.36395

Table A4. Henry's Law Constant As a Function of Temperature; Methylene Chloride-Silicone Oil

Experiment #	t (°C)	1/T $(K)^{-1}$	H	ln(H)
1	25.65	0.0033489	15.9470	4.41345
2	31.90	0.0032803	14.4590	4.23804
3	37.95	0.0032164	14.0707	4.04343
4	45.90	0.0031357	10.6329	3.88844

Table A5. Henry's Law Constant As a Function of Temperature; Toluene-Silicone Oil

Experiment #	t (°C)	1/T $(K)^{-1}$	H	ln(H)
1	25.7	0.0033478	349.7600	5.85725
2	31.80	0.0032808	300.5476	5.70560
3	37.95	0.0032159	277.788	5.62686
4	45.85	0.00313627	207.2364	5.33386

Table A6. Henry's Law Constant As a Function of Temperature ; Acetone-Paratherm

Experiment #	t (°C)	1/T $(K)^{-1}$	H	ln(H)
1	30.05	0.0032998	40.2153	3.69425
2	44.85	0.0031461	32.1766	3.47124
3	-	-	-	-
4	59.90	0.0030039	28.91756	3.36445

Table A7. Henry's Law Constant As a Function of Temperature ; Methanol-Paratherm

Experiment #	t (°C)	1/T $(K)^{-1}$	H	ln(H)
1	30.00	0.0033033	7.5504	2.02160
2	40.00	0.0031948	6.9339	1.936435
3	-	-	-	-
4	49.85	0.0030974	6.8931	1.930526

Table A8. Henry's Law Constant As a Function of Temperature; Methylene Chloride-Paratherm

Experiment #	t (°C)	1/T $(K)^{-1}$	H	ln(H)
1	30.00	0.0033003	67.3367	4.20971
2	44.85	0.00314614	55.0151	4.00761
3	-	-	-	-
4	59.85	0.003004356	43.8821	3.78151

Table A9. Henry's Law Constant As a Function of Temperature; Toluene-Paratherm

Experiment #	t (°C)	1/T $(K)^{-1}$	H	ln(H)
1	30.00	0.0033003	176.1786	5.17149
2	40.00	0.0031948	117.1236	4.76323
3	49.80??	0.0032159	94.02971	4.54361
4	59.90	0.0030039	65.7447	4.18578

Table A10. Experimental Results for Estimation of VOC Permeance through the Silicone Skin

Expt. #	VOC	t °C	F_{in} cc/min	F_{out} cc/min	$F_{ppm,in}$ ppmv	$F_{ppm,out}$ ppmv	P cc/min	$(q_o/\delta_o)10^3$ cm/sec	Av.$(q_o/\delta_o)10^3$ cm/sec
1	acetone	20.4	42.39	30.43	993	866.2	11.96	3.198	3.198
2		-	-	-	-	-	-	-	
3	methanol	19.5	24.27	12.49	514	427.0	11.78	2.895	2.895
4		-		-	-	-	-	-	
5	methylene chloride	22.4	24.78	12.40	999	791.4	12.38	4.124	5.014
6		22.4	43.74	30.91	999	893.6	12.83	5.905	
7	toluene	21.0	22.0	9.86	205	145.0	12.14	11.353	11.477
8		21.0	44.62	32.39	205	186.0	12.23	11.601	

F_{in} : Feed gas inlet flow rate

F_{out} : Feed gas outlet flow rate

$F_{ppm,in}$: VOC concentration in feed gas inlet

$F_{ppm,out}$: VOC concentration in feed gas outlet

P : Permeate gas flow rate

q_o/δ_o : VOC permeance through the composite membrane

t : Temperature

Av. : Arithmetic average

Table A11. Experimental Results for Estimation of Diffusivity of VOCs in Silicone Oil

Expt. #	VOC	F_{in} cc/min	F_{out} cc/min	S cc/min	$F_{ppm,in}$ ppmv	$F_{ppm,out}$ ppmv	t °C	H_i	D_{il} 10^6 cm^2/sec	Av. D_{il} 10^6 cm^2/sec
1	acetone	17.5	17.5	76.15	993	21.0	24	57.40	2.796	2.806
2		28.8	28.8	76.15	993	102.75	24	57.40	2.817	
3	methanol	18.02	18.02	34.6	514	102.05	26	16.31	4.696	4.709
4		33.5	33.5	34.6	514	219.43	26	16.31	4.722	
5	CH_2Cl_2	38.0	38.0	39.1	999	89.83	25	83.28	4.293	4.300
6		38.0	38.0	18.2	999	348.09	25	83.28	4.308	
7	toluene	34.4	34.4	24.9	210	4.93	26	351.83	7.58	7.625
8		34.4	34.4	14.6	210	92.85	26	351.83	7.67	

F_{in} : Feed gas inlet flow rate

F_{out} : Feed gas outlet flow rate

$F_{ppm,in}$: VOC concentration in feed gas inlet

$F_{ppm,out}$: VOC concentration in feed gas outlet

H_i : Henry's law constant

S : Sweep gas flow rate

t : Temperature

Av. : Arithmetic average

Table A12. Experimental Results for Acetone Absorption in Silicone Oil; Gas Flow Rate Variation

Experiment #	Gas flow rate (cc/min)	Outlet gas conc. (ppmv)	Φ	Percent removal
1	5.800	4.44	0.0045	99.52
2	10.77	9.65	0.0097	99.03
3	21.26	34.75	0.0350	96.50
4	52.71	138.03	0.1390	86.10
5	75.04	271.85	0.2738	72.62
6	102.45	379.19	0.3819	61.81

Module # 2, Liquid flow rate: 4.4 ml/min, Feed concentration: 993 ppmv, Temperature: 22.0°C, Outlet pressure: 9.00 psig

Table A13. Experimental Results for Methanol Absorption in Silicone Oil; Gas Flow Rate Variation

Experiment #	Gas flow rate (cc/min)	Outlet gas conc. (ppmv)	Φ	Percent removal
1	10.31	22.47	0.0437	95.63
2	21.78	126.91	0.2469	75.31
3	36.77	229.87	0.4472	55.28
4	62.53	321.02	0.6245	37.55
5	102.74	408.83	0.7953	20.47

Module # 2, Liquid flow rate: 3.73 ml/min, Feed concentration: 514 ppmv, Temperature: 22.2°C, Outlet pressure: 3.00 psig

Table A14. Experimental Results for Methylene Chloride Absorption in Silicone Oil; Gas Flow Rate Variation.

Experiment #	Gas flow rate (cc/min)	Outlet gas conc. (ppmv)	Φ	Percent removal
1	11.10	0.75	0.00075	99.92
2	20.47	1.51	0.0015	99.85
3	30.11	9.88	0.0099	99.01
4	52.76	52.23	0.0523	94.77
5	72.99	128.06	0.1282	87.18
6	95.97	208.22	0.2084	79.16
7	246.71	544.33	0.5449	45.51

Module # 2, Liquid flow rate 3.71 ml/min, Temperature 22°C, Outlet pressure 3.00 psig, Feed concentration 999 ppmv

Table A15. Experimental Results for Toluene Absorption in Silicone Oil; Gas flow rate Variation

Experiment #	Gas flow rate (cc/min)	Outlet gas concn. (ppmv)	Φ	Percent removal
1	100.00	00.00	0.00	100.00
2	147.93	0.826	0.0035	0.9965
3	195.17	1.335	0.0057	0.9943
4	247.23	5.355	0.0227	0.9923
5	298.51	8.467	0.0358	0.9642
6	359.28	13.433	0.0569	0.9431
7	405.71	18.194	0.0771	0.9229
8	447.46	22.196	0.0940	0.9059

Module # 2, Liquid flow rate: 1.75 ml/min, Feed concentration: 236 ppmv, Temperature: 27°C , Outlet pressure of the gas stream: 3.00 psig

Table A16. Experimental Results for Acetone Absorption in Silicone Oil-Gas at Lower Feed Concentration; Flow Rate Variation

Experiment #	Gas flow rate (cc/min)	Outlet gas conc. (ppmv)	Φ	Percent removal
1	9.6	1.2	0.006	99.4
2	19.6	2.4	0.012	98.8
3	52.8	29.0	0.142	85.8
4	66.6	47.35	0.232	76.8
5	97.5	75.2	0.368	63.2
6	-	-	-	-

Module # 2, Liquid flow rate: 4.4 ml/min, Feed concentration: 204 ppmv, Temperature: 22.0°C, Outlet pressure: 9.00 psig

Table A17. Experimental Results for Acetone Absorption in Silicone Oil; Liquid Flow Rate Variation

Experiment #	Liquid flow rate (cc/min)	Outlet gas conc. (ppmv)	Φ	Percent removal
1	6.8	65.5	0.1311	86.89
2	9.8	66.1	0.1323	86.77
3	31.2	65.7	0.1315	86.85
4	47.3	65.9	0.1318	86.82
5	-	-	-	-

Module # 2, Gas flow rate: 53.0 cc/min, Feed concentration: 499.7 ppmv, Temperature: 25°C, Outlet gas pressure: 3.00 psig

Table A18. Experimental Results for Methylene Chloride Absorption in Silicone Oil; Liquid Flow Rate Variation

Experiment #	Liquid flow rate (ml/min)	Outlet gas conc. (ppmv)	Φ	Percent removal
1	0.6	493.88	0.4980	50.20
2	1.8	287.24	0.2870	71.30
3	4.1	171.96	0.1720	82.80
4	6.1	135.00	0.1351	86.49
5	8.9	111.68	0.1118	88.82
6	14.5	104.22	0.1043	89.57

Module # 2, Gas flow rate: 70.6 cc/min, Feed concentration: 999 ppmv, Temperature: 25.6°C, Outlet pressure: 3.00 psig

Table A19. Experimental Results for Toluene Absorption in Silicone Oil; Liquid Flow Rate Variation

Experiment #	Liquid flow rate (ml/min)	Outlet gas conc. (ppmv)	Φ	Percent removal
1	1.68	18.43	0.0781	92.19
2	3.28	11.69	0.0495	95.05
3	5.50	9.41	0.0398	96.02
4	8.85	9.23	0.0391	96.09
5	13.85	8.45	0.0358	96.42

Module # 2, Gas flow rate: 405.7 cc/min, Feed concentration: 236 ppmv, Temperature: 25°C, Outlet pressure: 3.00 psig

Table A20. Experimental Results for Methylene Chloride Absorption in Paratherm; Gas Flow Rate Variation .

Experiment #	Gas flow rate (cc/min)	Outlet gas conc. (ppmv)	Φ	Percent removal
1	13.30	171.3	0.171	82.90
2	23.30	363.1	0.363	63.70
3	46.28	582.7	0.583	41.70
4	85.40	731.7	0.732	26.80
5	122.74	796.0	0.797	20.30
6	-	-	-	-

Module # 2, Absorbent flow rate 5.1 ml/min, Feed concentration 999 ppmv, Temperature 23°C, Outlet pressure 3.00 psig.

Table A21. Experimental Results for Toluene Absorption in Paratherm; Gas Flow Rate Variation.

Experiment #	Gas flow rate (cc/min)	Outlet gas conc. (ppmv)	Φ	Percent removal
1	112.72	4.1	0.0195	98.05
2	149.50	12.5	0.0595	94.05
3	249.50	35.9	0.1710	82.90
4	366.90	53.1	0.2530	74.70
5	451.80	66.5	0.03170	68.30

Module # 2, Absorbent flow rate: 5.1 ml/min, Feed concentration: 210 ppmv, Temperature: 22°C, Outlet pressure: 3.00 psig.

Table A22 Experimental Results for Methylene Chloride Absorption in Silicone Oil Using Skinned Fiber; Gas Flow Rate Variation .

Experiment #	Gas flow rate (cc/min)	Outlet gas conc. (ppmv)	Φ	Percent removal
1	15.00	1.8	0.00184	99.82
2	29.15	5.4	0.00540	99.46
3	45.10	56.1	0.05615	94.38
4	69.50	106.3	0.10640	89.36
5	90.30	164.1	0.1643	83.57
6	113.57	220.8	0.2210	77.90

Module # 3, Absorbent flow rate: 4.0 ml/min, Feed concentration: 999 ppmv, Temperature: 22°C, Outlet pressure: 0.00 psig.

Table A23. Experimental Results for Methylene Chloride Absorption in Paratherm Using Skinned Fiber; Gas Flow Rate Variation

Experiment #	Gas flow rate (cc/min)	Outlet gas conc. (ppmv)	Φ	Percent removal
1	11.52	17.7	0.0177	98.23
2	23.42	10.6	0.0106	98.94
3	44.61	30.6	0.0306	96.94
4	67.84	86.7	0.0868	91.32
5	90.85	151.7	0.1518	84.82
6	116.37	219.5	0.2197	78.03

Module # 3, Gas flow rate: 5.4 ml/min, Feed concentration: 999 ppmv, Temperature: 20.5°C, Outlet pressure: 0.00 psig.

Table A24. Experimental Results for Acetone Absorption in Paratherm Using Skinned Fiber; Gas Flow rate Variation

Experiment #	Gas flow rate (cc/min)	Outlet gas conc. (ppmv)	Φ	Percent removal
1	11.60	15.5	0.0156	98.44
2	23.75	80.1	0.081	91.90
3	46.51	249.9	0.2517	74.83
4	70.07	388.5	0.3912	60.88
5	92.09	500.6	0.5041	49.59
6	116.35	583.9	0.5880	41.20

Module # 3, Absorbent flow rate: 5.4 ml/min, Feed concentration 993 ppmv, Temperature 23°C, Outlet pressure: 0.00 psig.

Table A25. Experimental Results for Methylene Chloride Absorption in Silicone Oil at Higher Gas Flow Rate; Gas Flow Rate Variation .

Experiment #	Gas flow rate (cc/min)	Outlet gas conc. (ppmv)	Φ	Percent removal
1	72.97	2.0	0.0020	99.8
2	119.81	6.4	0.0064	99.36
3	201.92	23.8	0.0238	97.62
4	294.25	82.2	0.0823	91.77
5	360.8	140.0	0.140	86.00
6	441.89	190.4	0.190	81.00

Module # 1, Absorbent flow rate: 5.2 ml/min, Feed concentration: 999 ppmv, Temperature: 22.5°C, Outlet pressure: 3.00 psig.

Table A26. Experimental Results for Acetone Removal by Combined Absorption-Stripping; Liquid Flow Rate Variation

Experiment #	Liquid flow rate (ml/min)	Outlet gas conc. (ppmv)	Φ	Percent removal
1	2.80	183.6	0.1850	81.50
2	4.00	171.1	0.1723	82.27
3	8.10	154.7	0.1558	84.42
4	15.50	139.1	0.1400	86.00
5	-	-	-	-
6	-	-	-	-

Module # 1, Gas flow rate: 13.7 cc/min, Feed concentration: 993 ppmv, Temperature: 24.5°C, Outlet pressure: 3.00 psig.

Table A27. Experimental Results for Methanol Removal by Combined Absorption-Stripping; Gas Flow Rate Variation

Experiment #	Gas flow rate (cc/min)	Outlet gas conc. (ppmv)	Φ	Percent removal
1	11.12	71.7	0.1395	86.05
2	23.00	179.4	0.3840	61.60
3	44.24	332.2	0.6463	35.37
4	72.64	363.8	0.7078	29.22
5	119.5	420.3	0.8177	18.23

Module # 2 & 3, Absorbent: silicone oil, Absorbent circulation rate: 4.5 ml/min, Feed concentration: 514 ppmv, Temperature: 25°C, Outlet pressure: 3.00 psig

Table A28. Experimental Results for Methylene Chloride Removal by Combined Absorption-Stripping; Gas Flow Rate Variation

Experiment #	Gas flow rate (cc/min)	Outlet gas conc. (ppmv)	Φ	Percent removal
1	5.00	33.0	0.0330	96.70
2	13.90	58.5	0.0585	94.15
3	21.40	107.3	0.1074	89.26
4	39.60	219.2	0.2194	78.06
5	80.15	379.8	0.3802	61.98
6	-	-	-	-

Module # 1, Absorbent: Silicone Oil, Absorbent circulation Rate: 5.2 ml/min, Feed concentration: 999 ppmv, Temperature: 22.5°C, Outlet pressure: 3.00 psig,

Table A29. Experimental Results for Methylene Chloride Removal by Combined Absorption-Stripping; Gas Flow Rate Variation

Experiment #	Gas flow rate (cc/min)	Outlet gas conc. (ppmv)	Φ	Percent removal
1	10.31	232.9	0.2331	76.69
2		470.2	0.4707	52.93
3	46.70	683.35	0.6840	31.60
4	84.50	815.1	0.8160	18.40
5	12.95	862.4	0.8632	13.68

Module # 2 & 3, Absorbent: Paratherm, Absorbent circulation rate: 5.7 ml/min, Feed concentration: 999 ppmv, Temperature: 23°C, Outlet pressure : 3.00 psig

Table A30. Experimental Results for Toluene Removal by Combined Absorption-stripping ; Gas Flow Rate Variation

Experiment #	Gas flow rate (cc/min)	Outlet gas conc. (ppmv)	Φ	Percent removal
1	13.75	33.0	0.1570	84.30
2	25.50	35.8	0.1705	82.95
3	49.15	48.4	0.2305	76.95
4	74.26	57.8	0.2750	72.50
5	-	-	-	-

Module # 2 & 3, Absorbent: silicone oil, Absorbent circulation rate: 2.8 ml/min, Feed concentration: 210 ppmv, Temperature: 25°C, Outlet pressure: 3.00 psig

APPENDIX B

SAMPLE CALCULATIONS

B1 Calculation of Dimensionless Henry's Law Constant

From the set of experimental data shown in Table 4.1, data corresponding to vial number, 164, were taken for the following sample calculation:

WE = 16.6900 gm.

WC = 18.6743 gm.

V_t = 22.0 ml

t = 25.6 °C

WS = WC - WE = 18.6743 - 16.6900 = 1.9843 gm

Density of silicone oil at 25.6 °C is calculated from equation 2.109:

$\rho_l = 0.9802 - 8.356*10^{-4}*25.6 = 0.9588$ gm/ml

V_l = 1.9843/0.9588 = 2.0695 ml

V_g = 22.0 - 2.0695 = 19.9305 ml

V_g/V_l = 9.96303

From the plot of 1/PA vs. V_g/V_l (Figure 4.1) the following slope and intercept are obtained.

Intercept = $4.68546*10^{-6}$

Slope = $0.08991*10^{-6}$

Hence, H_i = 4.68546/0.08991 = 52.113

B2 Calculation of Overall Mass Transfer Coefficient

The following sample calculation of mass transfer coefficient is for toluene absorption with silicone oil carried out in module # 2.

Reference : Second row of Table 4.4

Temperature, T = 27+273 =300 K

Liquid flow rate = 1.75 ml/min

Henry's law constant, H = exp(2375.005/300 - 2.08)= 342.641 (Ref: Table 4.2)

Fiber inside diameter = 0.01 cm

Fiber outside diameter = 0.015 cm

Effective length = 31 cm

Mass transfer area, $A_m = \pi*0.01*31*102 = 99.34$ cm^2

From equation 4.3 liquid phase outlet concentration $C_{il,out}$ can be calculated as

$C_{il,out} = 1*195.17*(236-1.33)*10^{-9} /0.08206*300*1.75 = 1.063*10^{-6}$ gmol/ml

The corresponding gas phase equilibrium concentration, $C^*_{ig,out} = C_{il,out} / H$

$= 1.063*10^{-6}/342.641$

$= 3.1024*10^{-9}$ gmol/cc

Gas phase inlet concentration, $C_{ig,in} = 236*10^{-6}*24.9/14.696*82.06*300$

$= 16.243*10^{-9}$ gmol/cc

Gas phase outlet concentration, $C_{ig,out} = 1.33*10^{-6}*17.696/14.696*82.06*300$

$= 6.5054*10^{-11}$ gmol/cc

For fresh absorbent liquid, inlet liquid phase concentration, $C_{il,in} = 0.0$

Hence, the corresponding gas phase equilibrium concentration, $C^*_{ig,in} = 0.0$

Substituting the values of $C_{ig,in}$, $C_{ig,out}$, $C^*_{ig,in}$ and $C^*_{ig,out}$ into equation 4.2

$(\Delta C)_{ln} = 2.463*10^{-9}$ gmol/cc

The overall mass transfer coefficient from equation 4.1 then

$K_{oG} = (236-1.33)*1*195.17*10^{-6}/(82.06*300*60*99.34*2.463*10^{-9})$

$= 0.1265$ cm/sec

APPENDIX C

COMPUTER PROGRAMS

Computer codes for the following simulations and calculations are provided here

1. Simulation for VOC absorption using porous fiber
2. Simulation for VOC absorption using skinned fiber
3. Simulation for VOC removal by combined absorption-stripping
4. Calculation of diffusivity of VOC via permeation through absorbent ILM
5. Calculation of VOC permeance through the silicone skin
6. Calculation of gas-phase-based overall mass transfer coefficient
7. Calculation of Henry's law constant from experimental data

```
C ---------------------------------------------------------------------
C  SIMULATION FOR ABSORPTION IN COUNTER CURRENT HOLLOW FIBER CONTACTOR
C  CASE I:  POROUS FIBER
C ---------------------------------------------------------------------
C  ALF          :       EFFECTIVE LENGTH OF FIBER (cm)
C  AS           :       AREA OF ANNULUS ASSOCIATED WITH A SINGLE FIBER (cm2 )
C  CILIN        :       VOC CONCENTRATION IN INLET LIQUID STREAM  (mole/ml)
C  CIGIN        :       VOC CONCENTRATION IN INLET GAS STREAM (mole/cc)
C  CIGOT        :       VOC CONCENTRATION IN OUTLET  GAS STREAM (GUESSED) (mole/cc)
C  CGO          :       VOC CONCENTRATION IN OUTLET GAS STREAM (CALCULATED) (mole/cc)
C  CLO          :       VOC CONCENTRATION IN OUTLET LIQUID STREAM (CALCULATED)
                        (mole/ml)
C  CIGAV        :       AVERAGE CONCENTRATION IN GAS PHASE (mole/cc)
C  CILAV        :       AVERAGE CONCENTRATION IN LIQUID PHASE (mole/cc)
C  DELZ         :       DIFFERENTIAL LENGTH (cm)
C  DIL          :       DIFFUSIVITY OF VOC IN LIQUID (cm2/sec)
C  DIG          :       DIFFUSIVITY OF VOC IN NITROGEN (cm2/sec)
C  H            :       HENRY'S CONSTANT
C  NF           :       NUMBER OF FIBERS
C  N            :       NUMBER OF INCREMENT IN Z DIRECTION
C  MUG          :       VISCOSITY OF GAS (cp)
C  MUL          :       VISCOSITY OF LIQUID (cp)
C  MWI          :       MOLECULAR WEIGHT OF VOC (gm mwt)
C  MWL          :       MOLECULAR WEIGHT OF LIQUID (gm mwt)
C  PIC          :       CRITICAL PRESSURE OF VOC
C  POT          :       GAUGE PRESSURE AT OUTLET OF THE FIBER (psig)
C  POUT         :       ABSOLUTE PRESSURE AT THE FIBER OUTLET (psia)
C  PPMIT        :       VOC CONCENTRATION AT INLET GAS STREAM (ppmv)
C  PPMOT        :       VOC CONCENTRATION AT OUTLET GAS STREAM (ppmv)
C  RI           :       INSIDE RADIUS OF FIBER (cm)
C  RO           :       OUTSIDE RADIUS OF FIBER (cm)
C  RE           :       INSIDE RADIUS OF ANNULAR SPACE ASSOCIATED   WITH EACH FIBER (cm)
C  RS           :       INSIDE RADIUS OF SHELL (cm)
C  TEMP         :       TEMPERATURE (° C)
C  VAT          :       AVERAGE VELOCITY OF GAS STREAM  THROUGH FIBER (cm/sec)
C  VMT          :       MAXIMUM VELOCITY OF GAS THROUGH FIBER (cm/sec)
C  VAS          :       AVERAGE LIQUID VELOCITY THROUGH SHELL (cm/sec)
C  VOLG         :       MEASURED VOLUMETRIC GAS FLOW RATE AT ATMS.(cc/min)
C  VOLL         :       MEASURED VOLUMETRIC LIQUID FLOW RATE (cc/min)
C ======================================================================
      IMPLICIT REAL*8(A-H,M-Z)
      DIMENSION CIGOT(3),CIGOUT(3),PPMOT(3),GI1(3),CILRO(3),CIGRI(3),AM(3)
     1,AN(3),CIGAV(3),CILAV(3),FUN(3),PPMAV(3),AINC(3),AINC1(3),AINCL(3)
     1,AINCL1(3),aincl2(3),DIFF(3),CIGAV1(3),GA(5),SUM(6),CN(5),den(5)
     1,PI(3),PP(3),PPI(3),PPP(3),PFN(3)
      OPEN(10,FILE='ABS.DAT',STATUS='OLD')
      OPEN(20,FILE='ABS.OUT',STATUS='NEW')
      READ(10,*)RI,RO,NF,ALF,RS,POR,TOR
      READ(10,*)CILIN,POT,PPMIT,VOLL
      READ(10,*)MUG,MUL,TEMP,MWL,MWI,MN
      READ(10,*)PIC,VIC,TIC
      READ(10,*)SIGN,SIGI,EPSN,EPSI,PHI
      READ(10,*)AH,BH,DIL,N,SV,INC,NV
      A1=1.06036
      B1=0.15610
      C1=0.19300
      D1=0.47635
      E1=1.03587
      F1=1.52996
      G1=1.76474
      H1=3.89411
      R=0.08206
      TEMP=TEMP+273.0
      H=EXP((BH/TEMP)-AH)
      DI=2.0*RI
      DELZ=ALF/N
```

```
      RE=RS/(NF**0.5)
      A=((RE/4.0)-(((RO/RE)**2.0)*(RE/2))+(RE*DLOG(RO/RE))+(RE/2.0))
      B=((RO/2.0)-((RO**3.0)/(4.0*(RE**2.0))))
      D=1.0+DLOG(RO)-(((RO/RE)**2.0)/2.0)
      AS=(3.14159*(RE**2.0))-(3.14159*(RO**2.0))
      VAS=VOLL/(AS*NF*60.0)
      AK11=2.0*VAS*(1.0-((RO/RE)**2.0))
      AK22=(3.0+((RO/RE)**4.0))-(4.0*((RO/RE)**2.0))+(4.0*DLOG(RO/RE))
      AK1=AK11/AK22
C     ****************************************************************
      AA1=((RE**8.0)-(RO**8.0))/(8.0*16.0*(RE**4.0))
      AA21=((DLOG(RO)/(48.0*(RE**2.0)))-((RO**2.0)/(96.0*(RE**4.0))))
      AA2=AA21*((RE**6.0)-(RO**6.0))
      AA3=((RE**6.0)*(DLOG(RE)-(1.0/6.0)))/6.0
      AA4=((RO**6.0)*(DLOG(RO)-(1.0/6.0)))/6.0
      AA5=(AA3-AA4)/(8.0*(RE**2.0))
      AA=(AA1+AA2-AA5)
C     ****************************************************************
      BB1=((RE**6.0)-(RO**6.0))/(12.0*(RE**2.0))
      BB2=((DLOG(RO)/4.0)-((RO/RE)**2.0)/8.0)*((RE**4.0)-(RO**4.0))
      BB3=((RE**4.0)*(DLOG(RE)-(1.0/4.0)))/4.0
      BB4=((RO**4.0)*(DLOG(RO)-(1.0/4.0)))/4.0
      BB5=(BB3-BB4)
      BB=(BB1+BB2-BB5)*D
C     ****************************************************************
      CC11=((RO**6.0)*(DLOG(RO)-(1.0/6.0)))/6.0
      CC22=((RE**6.0)*(DLOG(RE)-(1.0/6.0)))/6.0
      CC1=(CC11-CC22)/(2*(RE**2))
      CC2=(((RO/RE)**2.0)/2.0)-DLOG(RO)-0.5
      CC3=((RE**4.0)*(DLOG(RE)-(1.0/4.0)))/4.0
      CC4=((RO**4.0)*(DLOG(RO)-(1.0/4.0)))/4.0
      CC5=CC2*(CC3-CC4)
      CC6=((DLOG(RE))**2.0)*((RE**4.0)/4.0)-((DLOG(RO))**2.0)*((RO**4)/4.0)
      CC=(CC1+CC5+CC6)
C     ****************************************************************
      DD1=((RE**4.0)*(DLOG(RE)-(1.0/4.0)))/4.0
      DD2=((RO**4.0)*(DLOG(RO)-(1.0/4.0)))/4.0
      DD3=(DD1-DD2)*(-A/RE)
      DD4=((A*(RO**2.0))/RE)-(2.0*A*RE*DLOG(RO))-(2.0*A*RE)
      DD5=((RE**2.0)*(DLOG(RE)-(1.0/2.0)))/2.0
      DD6=((RO**2.0)*(DLOG(RO)-(1.0/2.0)))/2.0
      DD7=DD4*(DD5-DD6)
      DD8=A*RE*((RE**2.0)*((DLOG(RE))**2.0)-(RO**2.0)*((DLOG(RO))**2.0))
      DD=(DD3+DD7+DD8)
C     ****************************************************************
      E=((3.0/4.0)*(RE**2.0))+((RO**4.0)/(4.0*(RE**2.0)))-
     1 (RO**2.0)+(RE**2.0)*(DLOG(RO/RE))
      T=E
C     ****************************************************************
      S=(AA+BB+CC+DD)
C     ****************************************************************
      VIB=0.285*(VIC**1.048)
      SIGIN=(SIGI+SIGN)/2.0
      EPSIN=(EPSI*EPSN)**0.5
      TSTAR=TEMP/EPSIN
      OMEGA1=(A1/(TSTAR**B1))+(C1/(EXP(D1*TSTAR)))+(E1/(EXP(F1*TSTAR)))
      OMEGA=OMEGA1+(G1/(EXP(H1*TSTAR)))
      MAV=((MWI+MN)/(MWI*MN))**0.5
      DIM=(DIL*POR)/TOR
C     ****************************************************************
      WRITE(20,11)
11    FORMAT(1X,75('=')/1X,'GAS FLOWRATE',5X,'GAS OUTLET CONC.',5X,'
     1 LIQ. OUTLET CONC.',5X,'GZREF',5X,'PHI'/
     1 5X,'(cc/min)',5x,'(ppmv)',18x,'(gmole/ml)'/1x,75('='))
      M=1
      VOLG=SV
```

```
      DO WHILE ( M .LE.NV)
      VOLG=VOLG+INC
      PPMOT(1)=0.0
      PPMOT(2)=PPMIT
  100 PPMOT(3)=(PPMOT(1)+PPMOT(2))/2.0
      DO 400 L=1,3
      POUT=POT+14.696
      CIGOT(L)=(PPMOT(L)*POUT)/(R*TEMP*1000000.0*1000.0*14.696)
      I=1
      CILIN1=CILIN
      CIGOUT(L)=CIGOT(L)
      ALC=0.0
  200 ALC=ALC+DELZ
      VOLGA=(VOLG*14.696)/POUT
      VOLGOT= VOLGA
      DELP1=(8.0*32.0*MUG*DELZ*VOLGOT*POUT*(2.54**2.0))
      DELP=DELP1/(NF*3.14159*6000*(DI**4)*981*453.6)
      PIN=((DELP+(POUT**2.0))**0.5)
      PAV=(PIN+POUT)/2.0
      IF(I.EQ.1) THEN
      CIGOUT(L)=(CIGOUT(L)*PAV)/POUT
      ELSE
      CIGOUT(L)=CIGOUT(L)*PAV
      ENDIF
      VOLGAV=(VOLGOT*POUT)/PAV
      VOLGIN=(VOLGOT*POUT)/PIN
      VAT=VOLGAV/(3.14159*NF*60*(RI**2.0))
      VMT=2.0*VAT
      VREF=(VOLG)/(NF*60)
C     ************************************************************************
C     CALCULATION OF DIFFUSIVITY IN NITROGEN
C     ************************************************************************
      DIG1=(1.858*(10.0**(-3.0))*(TEMP**1.5)*MAV)/(POUT*(SIGIN**2.0))
      DIG=(DIG1*14.696)/OMEGA
      DIGRE=(1.858*(10.0**(-3.0))*(TEMP**1.5)*MAV)/(14.696)
      DIGREF=(DIGRE*14.696)/((SIGIN**2.0)*OMEGA)
      P=(DIM/DIG)*(1/(RI*DLOG(RO/RI)))
      Q=(DIM/DIL)*(1/(RO*DLOG(RO/RI)))
      X=((11.0*RI)/96.0)-((DIG*DELZ)/(VMT*RI))
      YY1=((RO**4.0)/(16.0*(RE**2.0)))+(((RO**2.0)*D)/2.0)
      YY2=(((RO**2.0)*DLOG(RO))/2.0)
      YY3=A*RE*DLOG(RO)
      YY4=(S/T)
      YY5=((DIL*DELZ)/AK1)
      YY=YY1-YY2-YY3-YY4+YY5
C     ************************************************************************
      FF=(A*(RE/RO))-B
      Y=(YY/FF)
C     ************************************************************************
C     INTERFACIAL CONCENTRATIONS
C     ************************************************************************
      GI1(L)=(CIGOUT(L))/(1.0+(4.0*P*X*H))
      GI2=(4.0*P*X)/(1.0+(4.0*P*X*H))
      GI3=(1.0+(Q*Y))/(Q*Y*H)
      GI4=CILIN1/(Q*Y*H)
      CILRO(L)=((GI1(L)+GI4)/(GI3-GI2))
      CIGRI(L)=GI1(L)+(GI2*CILRO(L))
      DIFF(L)=CILRO(L)-(H*CIGRI(L))
C     ************************************************************************
C     CALCULATION OF AVARAGE CONCENTRATIONS
C     ************************************************************************
      AM(L)=0.0-(4*P*(CILRO(L)-(H*CIGRI(L))))/RI
      AN(L)=0.0-(Q*(CILRO(L)-(H*CIGRI(L))))/((A*(RE/RO))-B)
      AINC1(L)=(2.0*3.14159*(RI**2.0)*DELZ*DIG*AM(L))/(4*VOLGAV)
      AINC(L)=AINC1(L)*60*NF
      CIGAV(L)=AINC(L)+CIGOUT(L)
```

```
      CIGAV1(L)=AINC(L)+CIGOUT(L)
      AINCL1(L)=((2.0*3.14159*DELZ*DIL*AN(L)*E*60*NF)/VOLL)
      CILAV(L)=AINCL1(L)+CILIN1
      IF(I.GE.N)THEN
      GO TO 300
      ELSE
      I=I+1
      CIGOUT(L)=CIGAV(L)/PAV
      CILIN1=CILAV(L)
      POUT=PIN
      GO TO 200
  300 END IF
      PPMAV(L)=(CIGAV(L)*R*TEMP*1000.0*1000000.0*14.696)/PAV
      CIGIN=(PPMIT*PIN)/(R*TEMP*1000000.0*1000.0*14.696)
      FUN(L)=(PPMIT-PPMAV(L))
  400 CONTINUE
      IF(ABS(FUN(3)).LE.0.001)GO TO 600
      AKP=FUN(1)*FUN(3)
      IF(AKP.GT.0.0)GO TO 500
      PPMOT(2)=PPMOT(3)
      GO TO 100
  500 PPMOT(1)=PPMOT(3)
      GO TO 100
  600 PPMIO=PPMOT(3)
      CLO=CILAV(3)
      PHIO=PPMIO/PPMIT
      GZREF=(DIGREF*ALF)/VREF
      WRITE(20,33)VOLG,PPMIO,CLO,GZREF,PHIO
   33  FORMAT(5X,F8.3,5X,F8.3,15X,F12.10,8X,F7.2,2X,F6.4)
      M=M+1
      END DO
      WRITE(*,*)DIGREF
      WRITE(20,55)
   55  FORMAT(1X,75('='))
      STOP
      END
```

```
C     ------------------------------------------------------------------
C     SIMULATION FOR ABSORPTION IN COUNTER CURRENT HOLLOW FIBER CONTACTOR
C     CASE II SKINNED FIBER
C     ------------------------------------------------------------------
C
C     ALF    :    EFFECTIVE LENGTH OF FIBER (cm)
C     AS     :    AREA OF ANNULUS ASSOCIATED WITH A SINGLE FIBER (cm²)
C     CILIN  :    VOC CONCENTRATION AT INLET LIQUID STREAM (mole/ml)
C     CIGIN  :    VOC CONCENTRATION AT INLET GAS STREAM (mole/cc)
C     CIGOT  :    VOC CONCENTRATION AT OUTLET GAS STREAM (GUESSED) (mole/cc)
C     CGO    :    VOC CONCENTRATION IN OUTLET GAS STREAM (mole/cc)
C     CLO    :    VOC CONCENTRATION IN OUTLET LIQUID STREAM (CALCULATED)
                  (mole/ml)
C     CIGAV  :    AVERAGE CONCENTRATION IN GAS PHASE (mole/cc)
C     CILAV  :    AVERAGE CONCENTRATION IN LIQUID PHASE (mole/cc)
C     DELZ   :    DIFFERENTIAL LENGTH (cm)
C     DIL    :    DIFFUSIVITY OF VOC IN LIQUID (cm²/sec)
C     DIG    :    DIFFUSIVITY OF VOC IN NITROGEN (cm²/sec)
C     H      :    HENRY'S CONSTANT
C     NF     :    NUMBER OF FIBERS
C     N      :    NUMBER OF INCREMENT IN Z DIRECTION
C     MUG    :    VISCOSITY OF GAS  (cp)
C     MUL    :    VISCOSITY OF LIQUID (cp)
C     MWI    :    MOLECULAR WEIGHT OF VOC (gm mwt)
C     MWL    :    MOLECULAR WEIGHT OF LIQUID (gm mwt)
C     PIC    :    CRITICAL PRESSURE OF VOC
C     POT    :    GAUGE PRESSURE AT OUTLET OF THE FIBER (psig)
C     POUT   :    ABSOLUTE PRESSURE AT THE FIBER OUTLET (psia)
C     PPMIT  :    VOC CONC. AT INLET GAS STREAM  (ppmv)
C     PPMOT  :    VOC CONC. AT OUTLET GAS STREAM  (ppmv)
C     RI     :    INSIDE RADIUS OF FIBER (cm)
C     RO     :    OUTSIDE RADIUS OF FIBER (cm)
C     RE     :    INSIDE RADIUS OF ANNULAR SPACE ASSOCIATED WITH EACH FIBER (cm)
C     RS     :    INSIDE RADIUS OF SHELL (cm)
C     TEMP   :    TEMPERATURE (° C)
C     VAT    :    AVERAGE VELOCITY OF GAS STREAM THROUGH FIBER (cm/sec)
C     VMT    :    MAXIMUM VELOCITY OF GAS THROUGH FIBER (cm/sec)
C     VAS    :    AVERAGE LIQUID VELOCITY THROUGH SHELL (cm/sec)
C     VOLG   :    MEASURED VOLUMETRIC GAS FLOW RATE AT ATMS. (cc/min)
C     VOLL   :    MEASURED VOLUMETRIC LIQUID FLOW RATE (cc/min)
C     ==================================================================
      IMPLICIT REAL*8(A-H,M-Z)
      DIMENSION CIGOT(3),CIGOUT(3),PPMOT(3),GI1(3),CIMZO(3),CIGZI(3),AM(3)
     1,AN(3),CIGAV(3),CILAV(3),FUN(3),PPMAV(3),AINC(3),,AINC1(3),AINCL(3)
     1,AINCL1(3),aincl2(3),DIFF(3)
      OPEN(99,FILE='ABSC.DAT',STATUS='OLD')
      OPEN(20,FILE='ABS.OUT',STATUS='NEW')
      READ(99,*)RI,RO,RC,NF,ALF,RS,POR,TOR,RP
      READ(99,*)CILIN,POT,PPMIT,VOLL
      READ(99,*)MUG,MUL,TEMP,MWL,MWI,MN
      READ(99,*)PIC,VIC,TIC
      READ(99,*)ANTA,ANTB,ANTC
      READ(99,*)SIGN,SIGI,EPSN,EPSI,PHI
      READ(99,*)AH,BH,DIL,QC
      READ(99,*)N,SV,INC,NV
      A1=1.06036
      B1=0.15610
      C1=0.19300
      D1=0.47635
      E1=1.03587
      F1=1.52996
      G1=1.76474
      H1=3.89411
      R=0.08206
      TEMP=TEMP+273.0
      H=EXP((BH/TEMP)-AH)
```

```
      DI=2.0*RI
      DELZ=ALF/N
      RE=RS/(NF**0.5)
      ZO=RO/RI
      ZE=RE/RI
      ZC=RC/RI
      A=((ZE/4.0)-(((ZC/ZE)**2.0)*(ZE/2))+(ZE*DLOG(ZC/ZE))+(ZE/2.0))
      B=((ZC/2.0)-((ZC**3.0)/(4.0*(ZE**2.0))))
      D=1.0+DLOG(ZC)-(((ZC/ZE)**2.0)/2.0)
      AS=(3.14159*(RE**2.0))-(3.14159*(RC**2.0))
      VAS=VOLL/(AS*NF*60.0)
      AK11=2.0*VAS*(1.0-((RC/RE)**2.0))
      AK22=(3.0+((RC/RE)**4.0))-(4.0*((RC/RE)**2.0))+(4.0*DLOG(RC/RE))
      AK1=AK11/AK22
C     ****************************************************************
      AA1=((ZE**8.0)-(ZC**8.0))/(8.0*16.0*(ZE**4.0))
      AA21=((DLOG(ZC)/(48.0*(ZE**2.0)))-((ZC**2.0)/(96.0*(ZE**4.0))))
      AA2=AA21*((ZE**6.0)-(ZC**6.0))
      AA3=((ZE**6.0)*(DLOG(ZE)-(1.0/6.0)))/6.0
      AA4=((ZC**6.0)*(DLOG(ZC)-(1.0/6.0)))/6.0
      AA5=(AA3-AA4)/(8.0*(ZE**2.0))
      AA=(AA1+AA2-AA5)
C     ****************************************************************
      BB1=((ZE**6.0)-(ZC**6.0))/(12.0*(ZE**2.0))
      BB2=((DLOG(ZC)/4.0)-((ZC/ZE)**2.0)/8.0)*((ZE**4.0)-(ZC**4.0))
      BB3=((ZE**4.0)*(DLOG(ZE)-(1.0/4.0)))/4.0
      BB4=((ZC**4.0)*(DLOG(ZC)-(1.0/4.0)))/4.0
      BB5=(BB3-BB4)
      BB=(BB1+BB2-BB5)*D
C     ****************************************************************
      CC11=((ZC**6.0)*(DLOG(ZC)-(1.0/6.0)))/6.0
      CC22=((ZE**6.0)*(DLOG(ZE)-(1.0/6.0)))/6.0
      CC1=(CC11-CC22)/(2*(ZE**2))
      CC2=(((ZC/ZE)**2.0)/2.0)-DLOG(ZC)-0.5
      CC3=((ZE**4.0)*(DLOG(ZE)-(1.0/4.0)))/4.0
      CC4=((ZC**4.0)*(DLOG(ZC)-(1.0/4.0)))/4.0
      CC5=CC2*(CC3-CC4)
      CC6=((DLOG(ZE))**2.0)*((ZE**4.0)/4.0)-((DLOG(ZC))**2.0)*((ZC**4)/4.0)
      CC=(CC1+CC5+CC6)
C     ****************************************************************
      DD1=((ZE**4.0)*(DLOG(ZE)-(1.0/4.0)))/4.0
      DD2=((ZC**4.0)*(DLOG(ZC)-(1.0/4.0)))/4.0
      DD3=(DD1-DD2)*(-A/ZE)
      DD4=((A*(ZC**2.0))/ZE)-(2.0*A*ZE*DLOG(ZC))-(2.0*A*ZE)
      DD5=((ZE**2.0)*(DLOG(ZE)-(1.0/2.0)))/2.0
      DD6=((ZC**2.0)*(DLOG(ZC)-(1.0/2.0)))/2.0
      DD7=DD4*(DD5-DD6)
      DD8=A*ZE*((ZE**2.0)*((DLOG(ZE))**2.0)-(ZC**2.0)*((DLOG(ZC))**2.0))
      DD=(DD3+DD7+DD8)
C     ****************************************************************
      E=((3.0/4.0)*(ZE**2.0))+((ZC**4.0)/(4.0*(ZE**2.0)))-
     1 (ZC**2.0)+(ZE**2.0)*(DLOG(ZC/ZE))
      T=E
C     ****************************************************************
      S=(AA+BB+CC+DD)
C     ****************************************************************
      VIB=0.285*(VIC**1.048)
      SIGIN=(SIGI+SIGN)/2.0
      EPSIN=(EPSI*EPSN)**0.5
      TSTAR=TEMP/EPSIN
      OMEGA1=(A1/(TSTAR**B1))+(C1/(EXP(D1*TSTAR)))+(E1/(EXP(F1*TSTAR)))
      OMEGA=OMEGA1+(G1/(EXP(H1*TSTAR)))
      MAV=((MWI+MN)/(MWI*MN))**0.5
C     ****************************************************************

11    FORMAT(1X,60('=')/1X,'GAS FLOWRATE',5X,'GAS OUTLET CONC.',5X,'
```

```
      1 LIQ. OUTLET CONC.'/
      1 5X,'(cc/min)',5x,'(ppmv)',18x,'(gmole/ml)'/1x,60('=')
      M=1
      VOLG=SV
      DO WHILE ( M .LE.NV)
      VOLG=VOLG+INC
      PPMOT(1)=0.000
      PPMOT(2)=PPMIT
100   PPMOT(3)=(PPMOT(1)+PPMOT(2))/2.0
      VOLGO=(VOLG*14.696)/(POT+14.696)
      POUT=POT+14.696
      DELP1=(8.0*32.0*MUG*ALF*VOLGO*POUT*(2.54**2.0))
      DELP=DELP1/(NF*3.14159*6000*(DI**4)*981*453.6)
      PINLET=((DELP+(POUT**2.0))**0.5)
      DO 400 L=1,3
      POUT=POT+14.696
      CIGOT(L)=(PPMOT(L)*POUT)/(PPMIT*PINLET)
      I=1
      CILIN1=CILIN
      CIGOUT(L)=CIGOT(L)
      ALC=0.0
200   ALC=ALC+DELZ
      VOLGA=(VOLG*14.696)/POUT
      VOLGOT=VOLGA
      DELP1=(8.0*32.0*MUG*DELZ*VOLGOT*POUT*(2.54**2.0))
      DELP=DELP1/(NF*3.14159*6000*(DI**4)*981*453.6)
      PIN=((DELP+(POUT**2.0))**0.5)
      PAV=(PIN+POUT)/2.0
      IF(I.EQ.1)THEN
      CIGOUT(L)=(CIGOUT(L)*PAV)/POUT
      ELSE
      CIGOUT(L)=CIGOUT(L)*PAV
      END IF
      VOLGAV=(VOLGOT*POUT)/PAV
      VAT=VOLGAV/(3.14159*NF*60.0*(RI**2.0))
      VMT=2.0*VAT
      VREF=VOLG/(NF*60)
      NUE=VOLGAV/(NF*60*VREF)
C     ************************************************************************
C     CALCULATION OF DIFFUSIVITY IN NITROGEN
C     ************************************************************************
      DIG1=(1.858*(10.0**(-3.0))*(TEMP**1.5)*MAV)/(PAV*(SIGIN**2.0))
      DIG=(DIG1*14.696)/OMEGA
      DIGRE=(1.858*(10.0**(-3.0))*(TEMP**1.5)*MAV)/((0.0+14.696))
      DIGREF=(DIGRE*14.696)/((SIGIN**2.0)*OMEGA)
      DELIG=DIG/DIGREF
C     ************************************************************************
C     REYNOLDS NUMBER AT REFERENCE CONDITION
      GZREF=VREF/(DIGREF*ALF)
C     ************************************************************************
      CBAR=((8.1064*(10.0**6.0)*82.06*TEMP)/(3.14159*MWI))**0.5
      DIGP=(1.0133*(10.0**6.0)*RP*82.06*TEMP)/(CBAR*MWI)
      DIM=(DIGP*POR)/TOR
      P=(DIM/DIG)*(1/(DLOG(ZO)))
      Q=(DIM/DIL)*(1/(ZC*DLOG(ZO)))
      DELTA=RC-RO
      RCLN=(RC-RO)/(DLOG(RC/RO))
      AC=(QC*RCLN)/(DELTA*DIG)
      X=((11.0)/96.0)-((3.14159*DELIG)/(2*N*NUE*GZREF))
      YY1=((ZC**4.0)/(16.0*(ZE**2.0)))+(((ZC**2.0)*D)/2.0)
      YY2=(((ZC**2.0)*DLOG(ZC))/2.0)
      YY3=A*ZE*DLOG(ZC)
      YY4=(S/T)
      YY5=((DIL*DELZ)/(AK1*(RI**2.0)))
      YY=YY1-YY2-YY3-YY4+YY5
C     ************************************************************************
```

```
      FF=(A*(ZE/ZC))-B
      Y=YY/FF
C     ****************************************************************
C     INTERFACIAL CONCENTRATIONS
C     ****************************************************************
      GI1(L)=CIGOUT(L)/(1.0+(4.0*P*X))
      GI2=(4.0*P*X)/(1.0+(4.0*P*X))
      GI3=(((1.0+(P/AC))*H)+(Q*Y))/((Q*Y)+((H*P)/AC))
      GI4=CILIN1/((Q*Y)+((H*P)/AC))
      CIMZO(L)=((GI1(L)+GI4)/(GI3-GI2))
      CIGZI(L)=GI1(L)+(GI2*CIMZO(L))
      DIFF(L)=CIMZO(L)-(H*CIGZI(L))
C     ****************************************************************
C     CALCULATION OF AVARAGE CONCENTRATIONS
C     ****************************************************************
      AM(L)=0.0-(4.0*P*(CIMZO(L)-CIGZI(L)))
      AN(L)=0.0-(Q*(CIMZO(L)-CIGZI(L)))/((A*(ZE/ZC))-B)
      AINC1(L)=(3.14159*DELIG*AM(L))/(2.0*N*NUE*GZREF)
      AINC(L)=AINC1(L)
      CIGAV(L)=AINC(L)+CIGOUT(L)
      AINCL(L)=(((CIGAV(L)-CIGOUT(L))*VOLGA)/VOLL)
      AINCL1(L)=((2.0*3.14159*DELZ*DIL*AN(L)*E*60*NF)/VOLL)
      CILAV(L)=AINCL1(L)+CILIN1
      IF(I.GE.N)THEN
      GO TO 300
      ELSE
      I=I+1
      CIGOUT(L)=CIGAV(L)/PAV
      CILIN1=CILAV(L)
      POUT=PIN
      GO TO 200
300   END IF
      CIGIN=1.00
      FUN(L)=(CIGIN-CIGAV(L))
400   CONTINUE
22    FORMAT(1X,'PPMAV(3)=',F8.2,1X,'CILAV(3)=',F20.10,1X,
      1 'FUN(3)=',F20.10)
      IF(ABS(FUN(3)).LE.0.001)GO TO 600
      AKP=FUN(1)*FUN(3)
      IF(AKP.GT.0.0)GO TO 500
      PPMOT(2)=PPMOT(3)
      GO TO 100
500   PPMOT(1)=PPMOT(3)
      GO TO 100
600   PPMIO=PPMOT(3)
      CLO=CILAV(3)
      WRITE(*,*)DIGREF
      GZREF=(DIGREF*ALF)/VREF
      WRITE(20,33)VOLG,PPMIO,CLO,GZREF,PPMIO/PPMIT
33    FORMAT(5X,F8.3,5X,F8.3,15X,F12.10)
      M=M+1
      END DO
55    FORMAT(1X,60('='))
      STOP
      END
```

```
C-------------------------------------------------------------------------
C       ESTIMATION OF VOC DIFFUSIVITY IN ABSORBENT VIA SWEEP GAS PERMEATION THROUGH THE
C       ABSORBENT LIQUID ILM
C-------------------------------------------------------------------------
C       ALF     :       EFFECTIVE LENGTH OF FIBER (cm)
C       AS      :       AREA OF ANNULUS ASSOCIATED WITH A SINGLE FIBER (cm2)
C       CILIN   :       VOC CONCENTRATION AT LIQUID STREAM INLET (mole/ml)
C       CIGIN   :       VOC CONCENTRATION AT GAS STREAM INLET (mole/cc)
C       CIGOT   :       VOC CONCENTRATION AT GAS STREAM OUTLET(GUESSED) (mole/cc)
C       CGO     :       VOC CONCENTRATION AT GAS STREAM OUTLET (CALCULATED) (mole/cc)
C       CLO     :       VOC CONCENTRATION AT LIQUID STREAM OUTLET (mole/ml)
C       CIGAV   :       AVERAGE CONCENTRATION IN GAS PHASE (mole/cc)
C       CILAV   :       AVERAGE CONCENTRATION IN LIQUID PHASE (mole/cc)
C       DELZ    :       DIFFERENTIAL LENGTH (cm)
C       DIL     :       DIFFUSIVITY OF VOC IN LIQUID (cm2/sec)
C       DIG     :       DIFFUSIVITY OF VOC IN NITROGEN (cm2/sec)
C       H       :       HENRY'S CONSTANT
C       NF      :       NUMBER OF FIBERS
C       N       :       NUMBER OF INCREMENT IN Z DIRECTION
C       MUG     :       VISCOSITY OF GAS (cp)
C       MUL     :       VISCOSITY OF LIQUID (cp)
C       MWI     :       MOLECULAR WEIGHT OF VOC (gm mwt)
C       MWL     :       MOLECULAR WEIGHT OF LIQUID (gm mwt)
C       PIC     :       CRITICAL PRESSURE OF VOC
C       POT     :       GAUGE PRESSURE AT OUTLET OF THE FIBER (psig)
C       POUT    :       ABSOLUTE PRESSURE AT THE FIBER OUTLET (psia)
C       PPMIT   :       VOC CONC. AT INLET GAS STREAM (ppmv)
C       PPMOT   :       VOC CONC. AT OUTLET GAS STREAM (ppmv)
C       RI      :       INSIDE RADIUS OF FIBER (cm)
C       RO      :       OUTSIDE RADIUS OF FIBER (cm)
C       RE      :       INSIDE RADIUS OF ANNULAR SPACE WITH EACH FIBER ASSOCIATED (cm)
C       RS      :       INSIDE RADIUS OF SHELL (cm)
C       TEMP    :       TEMPERATURE (°C)
C       VAT     :       AVERAGE VELOCITY OF GAS STREM THROUGH FIBER (cm/sec)
C       VMT     :       MAXIMUM VELOCITY OF GAS THROUGH FIBER (cm/sec)
C       VAS     :       AVERAGE LIQUID VELOCITY THROUGH SHELL (cm/sec)
C       VOLG    :       MEASURED VOLUMETRIC GAS FLOW RATE AT ATMS. (cc/min)
C       VOLL    :       MEASURED VOLUMETRIC LIQUID FLOW RATE (cc/min)
C       ========================================================================
        IMPLICIT REAL*8(A-H,M-Z)
        DIMENSION GI1(3),CILRO(3),CIGRI(3),AM(3),DIL(3),DIM(3)
        1,AN(3),CIGAV(3),CILAV(3),FUN(3),PPMAV(3),AINC(3),AINC1(3),AINCL(3)
        1,AINCL1(3),aincl2(3),DIFF(3),P(3),Q(3),GI2(3),GI3(3),GI4(3)
        OPEN(44,FILE='ILM.DAT',STATUS='OLD')
        OPEN(55,FILE='ILM.OUT',STATUS='NEW')
        READ(44,*)RI,RO,NF,ALF,RS,POR,TOR
        READ(44,*)CILIN,POT,PPMIT,PPMOT,VOLG,VOLL
        READ(44,*)MUG,MUL,TEMP,MWL,MWI,MN
        READ(44,*)PIC,VIC,TIC
        READ(44,*)SIGN,SIGI,EPSN,EPSI,PHI
        READ(44,*)N,AH,BH
        A1=1.06036
        B1=0.15610
        C1=0.19300
        D1=0.47635
        E1=1.03587
        F1=1.52996
        G1=1.76474
        H1=3.89411
        R=0.08206
        TEMP=TEMP+273.0
        H=EXP((BH/TEMP)-AH)
        DI=2.0*RI
        DELZ=ALF/N
        RE=RS/(NF**0.5)
        A=((RE/4.0)-(((RO/RE)**2.0)*(RE/2))+(RE*DLOG(RO/RE))+(RE/2.0))
```

```
      B=((RO/2.0)-((RO**3.0)/(4.0*(RE**2.0))))
      D=1.0+DLOG(RO)-(((RO/RE)**2.0)/2.0)
      AS=(3.14159*(RE**2.0))-(3.14159*(RO**2.0))
      VAS=VOLL/(AS*NF*60.0)
      AK11=2.0*VAS*(1.0-((RO/RE)**2.0))
      AK22=(3.0+((RO/RE)**4.0))-(4.0*((RO/RE)**2.0))+(4.0*DLOG(RO/RE))
      AK1=AK11/AK22
C     ****************************************************************
      AA1=((RE**8.0)-(RO**8.0))/(8.0*16.0*(RE**4.0))
      AA21=((DLOG(RO)/(48.0*(RE**2.0)))-((RO**2.0)/(96.0*(RE**4.0))))
      AA2=AA21*((RE**6.0)-(RO**6.0))
      AA3=((RE**6.0)*(DLOG(RE)-(1.0/6.0)))/6.0
      AA4=((RO**6.0)*(DLOG(RO)-(1.0/6.0)))/6.0
      AA5=(AA3-AA4)/(8.0*(RE**2.0))
      AA=(AA1+AA2-AA5)
C     ****************************************************************
      BB1=((RE**6.0)-(RO**6.0))/(12.0*(RE**2.0))
      BB2=((DLOG(RO)/4.0)-((RO/RE)**2.0)/8.0)*((RE**4.0)-(RO**4.0))
      BB3=((RE**4.0)*(DLOG(RE)-(1.0/4.0)))/4.0
      BB4=((RO**4.0)*(DLOG(RO)-(1.0/4.0)))/4.0
      BB5=(BB3-BB4)
      BB=(BB1+BB2-BB5)*D
C     ****************************************************************
      CC11=((RO**6.0)*(DLOG(RO)-(1.0/6.0)))/6.0
      CC22=((RE**6.0)*(DLOG(RE)-(1.0/6.0)))/6.0
      CC1=(CC11-CC22)/(2*(RE**2))
      CC2=(((RO/RE)**2.0)/2.0)-DLOG(RO)-0.5
      CC3=((RE**4.0)*(DLOG(RE)-(1.0/4.0)))/4.0
      CC4=((RO**4.0)*(DLOG(RO)-(1.0/4.0)))/4.0
      CC5=CC2*(CC3-CC4)
      CC6=((DLOG(RE))**2.0)*((RE**4.0)/4.0)-((DLOG(RO))**2.0)*((RO**4)/4.0)
      CC=(CC1+CC5+CC6)
C     ****************************************************************
      DD1=((RE**4.0)*(DLOG(RE)-(1.0/4.0)))/4.0
      DD2=((RO**4.0)*(DLOG(RO)-(1.0/4.0)))/4.0
      DD3=(DD1-DD2)*(-A/RE)
      DD4=((A*(RO**2.0))/RE)-(2.0*A*RE*DLOG(RO))-(2.0*A*RE)
      DD5=((RE**2.0)*(DLOG(RE)-(1.0/2.0)))/2.0
      DD6=((RO**2.0)*(DLOG(RO)-(1.0/2.0)))/2.0
      DD7=DD4*(DD5-DD6)
      DD8=A*RE*((RE**2.0)*((DLOG(RE))**2.0)-(RO**2.0)*((DLOG(RO))**2.0))
      DD=(DD3+DD7+DD8)
C     ****************************************************************
      E=((3.0/4.0)*(RE**2.0))+((RO**4.0)/(4.0*(RE**2.0)))-
     1 (RO**2.0)+(RE**2.0)*(DLOG(RO/RE))
      T=E
C     ****************************************************************
      S=(AA+BB+CC+DD)
C     ****************************************************************
C     CALCULATION OF DIFFUSIVITY IN LIQUID ABSORBENT PHASE
C     ****************************************************************
      VIB=0.285*(VIC**1.048)
      SIGIN=(SIGI+SIGN)/2.0
      EPSIN=(EPSI*EPSN)**0.5
      TSTAR=TEMP/EPSIN
      OMEGA1=(A1/(TSTAR**B1))+(C1/(EXP(D1*TSTAR)))+(E1/(EXP(F1*TSTAR)))
      OMEGA=OMEGA1+(G1/(EXP(H1*TSTAR)))
      MAV=((MWI+MN)/(MWI*MN))**0.5
C     ****************************************************************
      DIL(1)=0.0000001
      DIL(2)=0.00001
100   DIL(3)=(DIL(1)+DIL(2))/2.0
      DO 400 L=1,3
      POUT=POT+14.696
      CIGOT=(PPMOT*POUT)/(R*TEMP*1000000.0*1000.0*14.696)
      I=1
```

```
      CILIN1=CILIN
      CIGOUT=CIGOT
      ALC=0.0
200   ALC=ALC+DELZ
      VOLGA=(VOLG*14.696)/POUT
      VOLGOT=VOLGA
      VAT=VOLGA/(3.14159*(RI**2.0)*NF*60.0)
      DELP1=(8.0*32.0*MUG*DELZ*VOLGOT*POUT*(2.54**2.0))
      DELP=DELP1/(NF*3.14159*6000*(DI**4)*981*453.6)
      PIN=(DELP+(POUT**2.0))**0.5
      PAV=(PIN+POUT)/2.0
      IF(I.EQ.1) THEN
      CIGOUT=(CIGOUT*PAV)/POUT
      ELSE
      CIGOUT=CIGOUT*PAV
      ENDIF
      VOLGAV=(VOLGA*POUT)/PAV
      VOLGIN=(VOLGA*POUT)/PIN
      VAT=VOLGAV/(3.14159*(RI**2.0)*NF*60.0)
      VMT=2.0*VAT
      VREF=(VOLG)/(NF*60)
C     ************************************************************************
C     CALCULATION OF DIFFUSIVITY IN NITROGEN
C     ************************************************************************
      DIG1=(1.858*(10.0**(-3.0))*(TEMP**1.5)*MAV)/(PAV*(SIGIN**2.0))
      DIG=(DIG1*14.696)/OMEGA
      DIGRE=(1.858*(10.0**(-3.0))*(TEMP*1.5)*MAV)/(14.696)
      DIGREF=(DIGRE*14.696)/((SIGIN**2.0)*OMEGA)
C     ************************************************************************
      DIM(L)=(DIL(L)*POR)/TOR
      P(L)=(DIM(L)/DIG)*(1/(RI*DLOG(RO/RI)))
      Q(L)=(DIM(L)/DIGREF)*(1/(RO*DLOG(RO/RI)))
      X=((11.0*RI)/96.0)-((DIG*DELZ)/(VMT*RI))
      YY1=((RO**4.0)/(16.0*(RE**2.0)))+(((RO**2.0)*D)/2.0)
      YY2=(((RO**2.0)*DLOG(RO))/2.0)
      YY3=A*RE*DLOG(RO)
      YY4=(S/T)
      YY5=((DIGREF*DELZ)/AK1)
      YY=YY1-YY2-YY3-YY4+YY5
C     ************************************************************************
      FF=(A*(RE/RO))-B
      Y=YY/FF
C     ************************************************************************
C     INTERFACIAL CONCENTRATIONS
C     ************************************************************************
      GI1(L)=CIGOUT/(1.0+(4.0*P(L)*X*H))
      GI2(L)=(4.0*P(L)*X*H)/(1.0+(4.0*P(L)*X*H))
      GI3(L)=(1.0+(Q(L)*Y*H))/(H*Q(L)*Y)
      GI4(L)=CILIN1/(H*Q(L)*Y)
      CILRO(L)=((GI1(L)+GI4(L))/(GI3(L)-GI2(L)))
      CIGRI(L)=GI1(L)+(GI2(L)*CILRO(L))
      DIFF(L)=(CILRO(L)-CIGRI(L))*H
C     ************************************************************************
C     CALCULATION OF AVARAGE CONCENTRATIONS
C     ************************************************************************
      AM(L)=0.0-(4.0*P(L)*((CILRO(L)-CIGRI(L))*H))/RI
      AN(L)=0.0-(Q(L)*((CILRO(L)-CIGRI(L))*H))/((A*(RE/RO))-B)
      AINC1(L)=(2.0*3.14159*(RI**2.0)*DELZ*DIG*AM(L))/(4.0*VOLGAV)
      AINC(L)=AINC1(L)*60*NF
      CIGAV(L)=AINC(L)+CIGOUT
      AINCL(L)=(((CIGAV(L)-CIGOUT)*VOLGA)/VOLL)
      AINCL1(L)=((2.0*3.14159*DELZ*DIGREF*AN(L)*E*60*NF)/VOLL)
      CILAV(L)=AINCL1(L)+CILIN1
      IF(I.GE.N)THEN
      GO TO 300
      ELSE
```

```
      I=I+1
      CIGOUT=CIGAV(L)/PAV
      CILIN1=CILAV(L)
      POUT=PIN
      GO TO 200
300   END IF
      PPMAV(L)=(CIGAV(L)*R*TEMP*1000.0*1000000.0*14.696)/PAV
      CIGIN=(PPMIT*PIN)/(R*TEMP*1000000.0*1000.0*14.696)
      FUN(L)=(PPMIT-PPMAV(L))
400   CONTINUE
22    FORMAT(1X,'PPMAV(3)=',F8.2,1X,'CILAV(3)=',F20.10,1X,
     1 'FUN(3)=',F20.10)
      IF(ABS(FUN(3)).LE.0.01)GO TO 600
      AKP=FUN(1)*FUN(3)
      IF(AKP.GT.0.0)GO TO 500
      DIL(2)=DIL(3)
      GO TO 100
500   DIL(1)=DIL(3)
      GO TO 100
600   DEM=DIL(3)
      CLO=CILAV(3)
      WRITE(*,*)DEM,CLO,H
      STOP
      END
```

```
C     ------------------------------------------------------------------
C     SIMULATION FOR COMBINED ABSORPTION  AND STRIPPING IN HOLLOW FIBER
C     CONTACTORS TO REMOVE VOC (VERY LOW CONCENTRATION) FROM EXHAUST AIR
C     BY : TARUN K. PODDAR
C     ------------------------------------------------------------------
C     VARIABLES FOR ABSORBER SIMULATION
C     ---------------------------------------------------------------
C     ALF    :    EFFECTIVE LENGTH OF FIBER (cm)
C     AS     :    AREA OF ANNULUS ASSOCIATED WITH A SINGLE FIBER (cm2)
C     CILIN  :    VOC CONCENTRATION AT LIQUID INLET STREAM (mole/ml)
C     CIGIN  :    VOC CONCENTRATION AT GAS INLET STREAM (mole/cc)
C     CIGOT  :    VOC CONCENTRATION AT OUTLET GAS STREAM (GUESSED) (mole/cc)
C     CGO    :    VOC CONCENTRATION AT GAS OUTLET STREAM (mole/cc)
C     CLO    :    VOC CONCENTRATION AT LIQUID OUTLET STREAM (CALCULATED) (mole/ml)
C     CIGAV  :    AVERAGE CONCENTRATION IN GAS PHASE (mole/cc)
C     CILAV  :    AVERAGE CONCENTRATION IN LIQUID PHASE (mole/cc)
C     DELZ   :    DIFFERENTIAL LENGTH (cm)
C     DIL    :    DIFFUSIVITY OF VOC IN LIQUID (cm2/sec)
C     DIG    :    DIFFUSIVITY OF VOC IN NITROGEN (cm2/sec)
C     H      :    HENRY'S LAW CONSTANT
C     NF     :    NUMBER OF FIBERS
C     N      :    NUMBER OF INCREMENT IN Z DIRECTION
C     MUG    :    VISCOSITY OF GAS (cp)
C     MUL    :    VISCOSITY OF LIQUID (cp)
C     MWI    :    MOLECULAR WEIGHT OF VOC (gm mwt)
C     MWL    :    MOLECULAR WEIGHT OF LIQUID (gm mwt)
C     PIC    :    CRITICAL PRESSURE OF VOC
C     POT    :    GAUGE PRESSURE AT OUTLET OF THE FIBER (psig)
C     POUT   :    ABSOLUTE PRESSURE AT THE FIBER OUTLET (psia)
C     PPMIT  :    VOC CONC. AT INLET GAS STREAM  (ppmv)
C     PPMOT  :    VOC CONC. AT OUTLET GAS STREAM  (ppmv)
C     RI     :    INSIDE RADIUS OF FIBER (cm)
C     RO     :    OUTSIDE RADIUS OF FIBER (cm)
C     RE     :    INSIDE RADIUS OF ANNULAR SPACE ASSOCIATED WITH EACH FIBER (cm)
C     RS     :    INSIDE RADIUS OF SHELL (cm)
C     TEMP   :    TEMPERATURE (°C)
C     VAT    :    AVERAGE VELOCITY OF GAS STREM THROUGH FIBER  (cm/sec)
C     VMT    :    MAXIMUM VELOCITY OF GAS THROUGH FIBER (cm/sec)
C     VAS    :    AVERAGE LIQUID VELOCITY THROUGH SHELL (cm/sec)
C     VOLG   :    MEASURED VOLUMETRIC GAS FLOW RATE AT ATMS. (cc/min)
C     VOLL   :    MEASURED VOLUMETRIC LIQUID FLOW RATE (cc/min)
C     ---------------------------------------------------------------
C     VARIABLES FOR STRIPPER SIMULATION
C     ---------------------------------------------------------------
C     ALS    :    EFFECTIVE LENGTH OF THE FIBER (cm)
C     AST    :    SHELL SIDE CROSS SECTION (cm2)
C     RIS    :    INSIDE RADIUS OF FIBER (cm)
C     ROS    :    OUTSIDE RADIUS OF FIBER (cm)
C     RCS    :    OUTSIDE RADIUS OF COATING (cm)
C     RSS    :    INSIDE DIAMETER OF SHELL (cm)
C     ===================================================================
      IMPLICIT REAL*8(A-H,M-Z)
      DIMENSION CIGOT(3),CIGOUT(3),PPMOT(3),GI1(3),CILRO(3),CIGRI(3),AM(3)
     1,AN(3),CIGAV(3),CILAV(3),FUN(3),PPMAV(3),AINC(3),AINC1(3),AINCL(3)
     1,AINCL1(3),aincl2(3),DIFF(3),CIGAV1(3),GA(5),SUM(6),CN(5),den(5)
     1,PI(3),PP(3),PPI(3),PPP(3),PFN(3)
      OPEN(25,FILE='ABST.DAT',STATUS='OLD')
      OPEN(26,FILE='ABST.OUT',STATUS='NEW')
      READ(25,*)RI,RO,NF,ALF,RS,POR,TOR
      READ(25,*)RIS,ROS,RCS,NFS,ALS,RSS,PS,PERO
      READ(25,*)CILIN,POT,PPMIT,VOLL
      READ(25,*)MUG,MUL,TEMPA,TEMPS,MWL,MWI,MN
      READ(25,*)SIGN,SIGI,EPSN,EPSI,PHI
      READ(25,*)AH,BH,DIL,DILS
      READ(25,*)N,SV,ANC,NV
      A1=1.06036
```

```
      B1=0.15610
      C1=0.19300
      D1=0.47635
      E1=1.03587
      F1=1.52996
      G1=1.76474
      H1=3.89411
      R=0.08206
      TEMPA=TEMPA+273.0
      TEMPS=TEMPS+273.0
      HA=EXP((BH/TEMPA)-AH)
      HS=EXP((BH/TEMPS)-AH)
      WRITE(*,*)HA,HS
      DI=2.0*RI
      DELZ=ALF/N
      RE=RS/(NF**0.5)
      A=((RE/4.0)-(((RO/RE)**2.0)*(RE/2))+(RE*DLOG(RO/RE))+(RE/2.0))
      B=((RO/2.0)-((RO**3.0)/(4.0*(RE**2.0))))
      D=1.0+DLOG(RO)-(((RO/RE)**2.0)/2.0)
      AS=(3.14159*(RE**2.0))-(3.14159*(RO**2.0))
      VAS=VOLL/(AS*NF*60.0)
      AK11=2.0*VAS*(1.0-((RO/RE)**2.0))
      AK22=(3.0+((RO/RE)**4.0))-(4.0*((RO/RE)**2.0))+(4.0*DLOG(RO/RE))
      AK1=AK11/AK22
C     ****************************************************************
      AA1=((RE**8.0)-(RO**8.0))/(8.0*16.0*(RE**4.0))
      AA21=((DLOG(RO)/(48.0*(RE**2.0)))-((RO**2.0)/(96.0*(RE**4.0))))
      AA2=AA21*((RE**6.0)-(RO**6.0))
      AA3=((RE**6.0)*(DLOG(RE)-(1.0/6.0)))/6.0
      AA4=((RO**6.0)*(DLOG(RO)-(1.0/6.0)))/6.0
      AA5=(AA3-AA4)/(8.0*(RE**2.0))
      AA=(AA1+AA2-AA5)
C     ****************************************************************
      BB1=((RE**6.0)-(RO**6.0))/(12.0*(RE**2.0))
      BB2=((DLOG(RO)/4.0)-((RO/RE)**2.0)/8.0)*((RE**4.0)-(RO**4.0))
      BB3=((RE**4.0)*(DLOG(RE)-(1.0/4.0)))/4.0
      BB4=((RO**4.0)*(DLOG(RO)-(1.0/4.0)))/4.0
      BB5=(BB3-BB4)
      BB=(BB1+BB2-BB5)*D
C     ****************************************************************
      CC11=((RO**6.0)*(DLOG(RO)-(1.0/6.0)))/6.0
      CC22=((RE**6.0)*(DLOG(RE)-(1.0/6.0)))/6.0
      CC1=(CC11-CC22)/(2*(RE**2))
      CC2=(((RO/RE)**2.0)/2.0)-DLOG(RO)-0.5
      CC3=((RE**4.0)*(DLOG(RE)-(1.0/4.0)))/4.0
      CC4=((RO**4.0)*(DLOG(RO)-(1.0/4.0)))/4.0
      CC5=CC2*(CC3-CC4)
      CC6=((DLOG(RE))**2.0)*((RE**4.0)/4.0)-((DLOG(RO))**2.0)*((RO**4)/4.0)
      CC=(CC1+CC5+CC6)
C     ****************************************************************
      DD1=((RE**4.0)*(DLOG(RE)-(1.0/4.0)))/4.0
      DD2=((RO**4.0)*(DLOG(RO)-(1.0/4.0)))/4.0
      DD3=(DD1-DD2)*(-A/RE)
      DD4=((A*(RO**2.0))/RE)-(2.0*A*RE*DLOG(RO))-(2.0*A*RE)
      DD5=((RE**2.0)*(DLOG(RE)-(1.0/2.0)))/2.0
      DD6=((RO**2.0)*(DLOG(RO)-(1.0/2.0)))/2.0
      DD7=DD4*(DD5-DD6)
      DD8=A*RE*((RE**2.0)*((DLOG(RE))**2.0)-(RO**2.0)*((DLOG(RO))**2.0))
      DD=(DD3+DD7+DD8)
C     ****************************************************************
      E=((3.0/4.0)*(RE**2.0))+((RO**4.0)/(4.0*(RE**2.0)))-
     1 (RO**2.0)+(RE**2.0)*(DLOG(RO/RE))
      T=E
C     ****************************************************************
      S=(AA+BB+CC+DD)
C     ****************************************************************
```

```
C       CALCULATION OF DIFFUSIVITY IN LIQUID ABSORBENT PHASE
C       ********************************************************************
        SIGIN=(SIGI+SIGN)/2.0
        EPSIN=(EPSI*EPSN)**0.5
        TSTAR=TEMPA/EPSIN
        OMEGA1=(A1/(TSTAR**B1))+(C1/(EXP(D1*TSTAR)))+(E1/(EXP(F1*TSTAR)))
        OMEGA=OMEGA1+(G1/(EXP(H1*TSTAR)))
        MAV=((MWI+MN)/(MWI*MN))**0.5
C       ********************************************************************
c       WRITE(20,11)
11      FORMAT(1X,60('=')/1X,'GAS FLOWRATE',5X,'GAS OUTLET CONC.',5X,'
   1 LIQ. OUTLET CONC.'/
   1 5X,'(cc/min)',5x,'(ppmv)',18x,'(gmole/ml)'/1x,60('='))
        M=1
        VOLG=SV
        DO WHILE ( M .LE.NV)
        CILIN=0.0
        VOLG=VOLG+ANC
75      PPMOT(1)=0.0
        PPMOT(2)=PPMIT
100     PPMOT(3)=(PPMOT(1)+PPMOT(2))/2.0
        DO 400 L=1,3
        POUT=POT+14.696
        CIGOT(L)=(PPMOT(L)*POUT)/(R*TEMPA*1000000.0*1000.0*14.696)
        I=1
        CILIN1=CILIN
        CIGOUT(L)=CIGOT(L)
        ALC=0.0
200     ALC=ALC+DELZ
        VOLGA=(VOLG*14.696)/POUT
        VOLGOT= VOLGA
        DELP1=(8.0*32.0*MUG*DELZ*VOLGOT*POUT*(2.54**2.0))
        DELP=DELP1/(NF*3.14159*6000*(DI**4)*981*453.6)
        PIN=((DELP+(POUT**2.0))**0.5)
        PAV=(PIN+POUT)/2.0
        IF(I.EQ.1) THEN
        CIGOUT(L)=(CIGOUT(L)*PAV)/POUT
        ELSE
        CIGOUT(L)=CIGOUT(L)*PAV
        ENDIF
        VOLGAV=(VOLGOT*POUT)/PAV
        VOLGIN=(VOLGOT*POUT)/PIN
        VAT=VOLGAV/(3.14159*NF*60*(RI**2.0))
        VMT=2.0*VAT
        vatin=volgin/(3.14159*nf*60*(ri**2))
        vatot=volgot/(3.14159*nf*60*(ri**2))
        VREF=(VOLG)/(NF*60)
C       ********************************************************************
C       CALCULATION OF DIFFUSIVITY IN NITROGEN
C       ********************************************************************
        DIG1=(1.858*(10.0**(-3.0))*(TEMPA**1.5)*MAV)/(POUT*(SIGIN**2.0))
        DIG=(DIG1*14.696)/OMEGA
        DIGRE=(1.858*(10.0**(-3.0))*(TEMPA**1.5)*MAV)/(14.696)
        DIGREF=(DIGRE*14.696)/((SIGIN**2.0)*OMEGA)
C       ********************************************************************
        DIM=(DIL*POR)/TOR
        P=(DIM/DIG)*(1/(RI*DLOG(RO/RI)))
        Q=(DIM/DIL)*(1/(RO*DLOG(RO/RI)))
        X=((11.0*RI)/96.0)+((DIG*DELZ)/(VMT*RI))
        YY1=((RO**4.0)/(16.0*(RE**2.0)))+(((RO**2.0)*D)/2.0)
        YY2=(((RO**2.0)*DLOG(RO))/2.0)
        YY3=A*RE*DLOG(RO)
        YY4=(S/T)
        YY5=((DIL*DELZ)/AK1)
        YY=YY1-YY2-YY3-YY4+YY5
C       ********************************************************************
```

```
      FF=(A*(RE/RO))-B
      Y=(YY/FF)
C     ****************************************************************
C     INTERFACIAL CONCENTRATIONS
C     ****************************************************************
      GI1(L)=(CIGOUT(L))/(1.0+(4.0*P*X*HA))
      GI2=(4.0*P*X)/(1.0+(4.0*P*X*HA))
      GI3=(1.0+(Q*Y))/(Q*Y*HA)
      GI4=CILIN1/(Q*Y*HA)
      CILRO(L)=((GI1(L)+GI4)/(GI3-GI2))
      CIGRI(L)=GI1(L)+(GI2*CILRO(L))
      DIFF(L)=CILRO(L)-(HA*CIGRI(L))
C     ****************************************************************
C     CALCULATION OF AVARAGE CONCENTRATIONS
C     ****************************************************************
      AM(L)=0.0-(4*P*(CILRO(L)-(HA*CIGRI(L))))/RI
      AN(L)=0.0-(Q*(CILRO(L)-(HA*CIGRI(L))))/((A*(RE/RO))-B)
      AINC1(L)=(2.0*3.14159*(RI**2.0)*DELZ*DIG*AM(L))/(4*VOLGAV)
      AINC(L)=AINC1(L)*60*NF
      CIGAV(L)=AINC(L)+CIGOUT(L)
      AINCL1(L)=((2.0*3.14159*DELZ*DIL*AN(L)*E*60*NF)/VOLL)
      CILAV(L)=AINCL1(L)+CILIN1
      IF(I.GE.N)THEN
      GO TO 300
      ELSE
      I=I+1
      CIGOUT(L)=CIGAV(L)/PAV
      CILIN1=CILAV(L)
      POUT=PIN
      GO TO 200
300   END IF
      PPMAV(L)=(CIGAV(L)*R*TEMPA*1000.0*1000000.0*14.696)/PAV
      CIGIN=(PPMIT*PIN)/(R*TEMPA*1000000.0*1000.0*14.696)
      IF(ABS(PPMAV(L)).NE.0.0) THEN
      FUN(L)=(PPMIT-PPMAV(L))/ABS(PPMAV(L))
      ELSE
      FUN(L)=(PPMIT-PPMAV(L))
      ENDIF
400   CONTINUE
      IF(PPMOT(3).LE.1.00E-8)THEN
      GO TO 600
      ELSE
      ENDIF
      IF(ABS(FUN(3)).LE.0.001)GO TO 600
      AKP=FUN(1)*FUN(3)
      IF(AKP.GT.0.0)GO TO 500
      PPMOT(2)=PPMOT(3)
      GO TO 100
500   PPMOT(1)=PPMOT(3)
      GO TO 100
600   PPMIO=PPMOT(3)
      CLO=CILAV(3)
33    FORMAT(5X,F8.3,5X,F8.3,15X,F12.10)
      PHIO=PPMIO/PPMIT
      GZREF=(DIGREF*ALF)/(VREF)
C     WRITE(20,*)GZREF/100.0,PHIO
c     WRITE(20,55)
55    FORMAT(1X,60('='))
C     WRITE(*,*)CLO
      DIS=2.0*RIS
      DELZS=ALS
      RES=RSS/(NFS**0.5)
      AS=((RES/4.0)-(((RCS/RES)**2.0)*(RES/2))+
     1 (RES*DLOG(RCS/RES))+(RES/2.0))
      BS=((RCS/2.0)-((RCS**3.0)/(4.0*(RES**2.0))))
      DS=1.0+DLOG(RCS)-(((RCS/RES)**2.0)/2.0)
```

```
      AST=(3.14159*(RES**2.0))-(3.14159*(RCS**2.0))
      VAST=VOLL/(AST*NFS*60.0)
      AKS11=2.0*VAST*(1.0-((RCS/RES)**2.0))
      AKS22=(3.0+((RCS/RES)**4.0))-(4.0*((RCS/RES)**2.0))+
     1 (4.0*DLOG(RCS/RES))
      AKS1=AKS11/AKS22
C     ****************************************************************
      AAS1=((RES**8.0)-(RCS**8.0))/(8.0*16.0*(RES**4.0))
      AAS21=((DLOG(RCS)/(48.0*(RES**2.0)))-((RCS**2.0)/
     1 (96.0*(RES**4.0))))
      AAS2=AAS21*((RES**6.0)-(RCS**6.0))
      AAS3=((RES**6.0)*(DLOG(RES)-(1.0/6.0)))/6.0
      AAS4=((RCS**6.0)*(DLOG(RCS)-(1.0/6.0)))/6.0
      AAS5=(AAS3-AAS4)/(8.0*(RES**2.0))
      AAS=(AAS1+AAS2-AAS5)
C     ****************************************************************
      BBS1=((RES**6.0)-(RCS**6.0))/(12.0*(RES**2.0))
      BBS2=((DLOG(RCS)/4.0)-((RCS/RES)**2.0)/8.0)*((RES**4.0)-
     1 (RCS**4.0))
      BBS3=((RES**4.0)*(DLOG(RES)-(1.0/4.0)))/4.0
      BBS4=((RCS**4.0)*(DLOG(RCS)-(1.0/4.0)))/4.0
      BBS5=(BBS3-BBS4)
      BBS=(BBS1+BBS2-BBS5)*DS
C     ****************************************************************
      CCS11=((RCS**6.0)*(DLOG(RCS)-(1.0/6.0)))/6.0
      CCS22=((RES**6.0)*(DLOG(RES)-(1.0/6.0)))/6.0
      CCS1=(CCS11-CCS22)/(2*(RES**2))
      CCS2=(((RCS/RES)**2.0)/2.0)-DLOG(RCS)-0.5
      CCS3=((RES**4.0)*(DLOG(RES)-(1.0/4.0)))/4.0
      CCS4=((RCS**4.0)*(DLOG(RCS)-(1.0/4.0)))/4.0
      CCS5=CCS2*(CCS3-CCS4)
      CCS6=((DLOG(RES))**2.0)*((RES**4.0)/4.0)-((DLOG(RCS))**2.0)*
     1 ((RCS**4)/4.0)
      CCS=(CCS1+CCS5+CCS6)
C     ****************************************************************
      DDS1=((RES**4.0)*(DLOG(RES)-(1.0/4.0)))/4.0
      DDS2=((RCS**4.0)*(DLOG(RCS)-(1.0/4.0)))/4.0
      DDS3=(DDS1-DDS2)*(-AS/RES)
      DDS4=((AS*(RCS**2.0))/RES)-(2.0*AS*RES*DLOG(RCS))-(2.0*AS*RES)
      DDS5=((RES**2.0)*(DLOG(RES)-(1.0/2.0)))/2.0
      DDS6=((RCS**2.0)*(DLOG(RCS)-(1.0/2.0)))/2.0
      DDS7=DDS4*(DDS5-DDS6)
      DDS8=AS*RES*((RES**2.0)*((DLOG(RES))**2.0)-(RCS**2.0)*((DLOG(RCS))
     1 **2.0))
      DDS=(DDS3+DDS7+DDS8)
C     ****************************************************************
      ES=((3.0/4.0)*(RES**2.0))+((RCS**4.0)/(4.0*(RES**2.0)))-
     1 (RCS**2.0)+(RES**2.0)*(DLOG(RCS/RES))
      TS=ES
C     ****************************************************************
      ST=(AAS+BBS+CCS+DDS)
C     ****************************************************************
      DELTA=RCS-RIS
      ROLN=(RCS-RIS)/(DLOG(RCS/RIS))
      ACCS=(PERO*ROLN)/(DILS*RCS)
      YYS1=((RCS**4.0)/(16.0*(RES**2.0)))+(((RCS**2.0)*D)/2.0)
      YYS2=(((RCS**2.0)*DLOG(RCS))/2.0)
      YYS3=AS*RES*DLOG(RCS)
      YYS4=(ST/TS)
      YYS5=((DILS*ALS)/(AKS1*N))
      YYS=YYS1-YYS2-YYS3-YYS4+YYS5
C     ****************************************************************
      FFS=(AS*(RES/RCS))-BS
      YS=YYS/FFS
C     ****************************************************************
C     CALCULATION FOR STRIPPER OUTLET CONCENTRATION
```

```
C     ********************************************************************
      CIGBAR=(PS)/(R*TEMPS*1000.0*760.00)
      J=1
650   CONDIF=(CLO-(HS*CIGBAR))/(HS+(ACCS*YS))
      MT=((2*3.14159*ACCS*DILS*ALS*RCS*CONDIF*60*NFS)/(VOLL*N))
      CILINN=CLO-MT
      IF(J.GE.N) THEN
      GO TO 700
      ELSE
      CLO=CILINN
      J=J+1
      GO TO 650
      END IF
700   ERROR=(CILINN-CILIN)/CILINN
      IF(ABS(ERROR).LE.0.001) THEN
      GO TO 800
      ELSE
      CILIN=CILINN
      GO TO 75
      END IF
800   CLINA=CILIN
      CLOA=CLO
      CLINS=CLO
      CLOS=CILIN
      WRITE(*,*)VOLG,PPMIO
      WRITE(26,*)GZREF/100,PHIO
      M=M+1
      END DO
      WRITE(*,*)DIGREF
      STOP
      END
```

```
C     ------------------------------------------------------------------------
C     THIS PROGRAM CALCULATES THE PERMEABILITY AND PERMEANCE OF A COMPOSITE MEMBRANE (POROUS
C     SUBSTRATE AND HOMOGENEOUS SKIN) AS WELL AS OF THE SKIN, APPLICABLE TO BINARY SYSTEM. IT
C     ALSO PROVIDES SELECTIVITY
C     ------------------------------------------------------------------------
C     INPUT PARAMETERS
C     ********************
C     ALF    :    EFFECTIVE LENGTH OF THE MODULE (cm)
C     ALFA   :    GUESSED VALUE OF SELECTIVITY OF VOC OVER NITROGEN
C     MI     :    MOLECULAR WEIGHT OF PERMEATING SPECIES (gmol wt)
C     NF     :    NUMBER OF FIBERS INSIDE A MODULE
C     PF     :    FEED GAS PRESSURE (psig)
C     PP     :    PERMEATE GAS PRESSURE (psig)
C     PPFIN  :    FEED INLET CONCENTRATION (ppmv)
C     PPFOUT :    FEED OUTLET CONCENTRATION (ppmv)
C     POR    :    POROSITY OF SUBSTRATE
C     RI     :    INSIDE RADIUS OF FIBER (cm)
C     RC     :    OUTSIDE RADIUS OF THE COATING (cm)
C     RO     :    OUTSIDE RADIUS OF FIBER (cm)
C     RP     :    MEAN PORE RADIUS (cm)
C     T      :    TEMPERATURE (°C)
C     TOR    :    TORTUOSITY OF THE POROUS SUBSTRATE
C     VFIN   :    VOLUMETRIC FLOW RATE OF FEED GAS AT INLET (cc/min)
C     VFOUT  :    VOLUMETRIC FLOW RATE OF FEED GAS AT OUTLET (cc/min)
C     ************************************************************************
C
      IMPLICIT REAL*8(A-H,M-Z)
      DIMENSION Y(3),A(3),B(3),FUN(3)
      OPEN(1, FILE='Q.DAT', STATUS='OLD')
      READ(1,*)RI,RO,RC,VFIN,VFOUT,PF,PP,POR,TOR,RP
      READ(1,*)ALF,NF,PPFIN,PPFOUT,T,ALFA,MI
      TEMP=T+273.0
      R=82.06
      CBAR=((8.0*8.039*(10.0**7.0)*TEMP)/(3.14159*MI))**0.5
      DISSLP=(1.0133*(10.0**6)*POR*RP*R*TEMP)/(MI*CBAR*TOR)
      WRITE(*,*)DISSLP
      PF=(PF+14.696)/14.696
      PP=(PP+14.696)/14.696
      ROLN=(RC-RI)/(DLOG(RC/RI))
      AREA=2*3.14159*RC*ALF*NF
      MFIN=(VFIN)/(82.06*TEMP*60)
      MFOUT=(VFOUT)/(82.06*TEMP*60)
      XFOUT=PPFOUT*(10.0**-6.0)
      XFIN=PPFIN*(10.0**-6.0)
      MVT=((MFIN*XFIN)-(MFOUT*XFOUT))
      XPOUT=MVT/(MFIN-MFOUT)
      XNFIN=1-XFIN
      XNFOUT=1-XFOUT
      XNPOUT=1-XPOUT
      GAMA=PP/PF
C     ------------------------------------------------------------------
C     CALCULATION OF PERMEATE COMPOSITION AT THE CLOSED END
C     ------------------------------------------------------------------
100   Y(1)=0.0
      Y(2)=0.9
10    Y(3)=(Y(1)+Y(2))/2.0
      DO 20 L=1,3
      A(L)=Y(L)/(1.0-Y(L))
      B(L)=(ALFA*(XFOUT-(GAMA*Y(L))))/((1.0-XFOUT)-GAMA*(1.0-Y(L)))
      FUN(L)=(A(L)-B(L))
20    CONTINUE
      IF(ABS(FUN(3)/B(3)).LE.0.0001)GO TO 50
      AKP=FUN(1)*FUN(3)
      IF(AKP.GT.0.0)GO TO 30
      Y(2)=Y(3)
```

```
      GO TO 10
30    Y(1)=Y(3)
      GO TO 10
50    XPIN=Y(3)
      XNPIN=1-XPIN
      CFIN=(XFIN*PF)/(82.06*TEMP)
      CFOUT=(XFOUT*PF)/(82.06*TEMP)
      CPIN=(XPIN*PP)/(82.06*TEMP)
      CPOUT=(XPOUT*PP)/(82.06*TEMP)
      CNFIN=(XNFIN*PF)/(82.06*TEMP)
      CNFOUT=(XNFOUT*PF)/(82.06*TEMP)
      CNPIN=(XNPIN*PP)/(82.06*TEMP)
      CNPOUT=(XNPOUT*PP)/(82.06*TEMP)
      DELCFP=((CFIN-CPOUT)-(CFOUT-CPIN))/
     1 DLOG((CFIN-CPOUT)/(CFOUT-CPIN))
      DELCN=((CNFIN-CNPOUT)-(CNFOUT-CNPIN))/
     1 DLOG((CNFIN-CNPOUT)/(CNFOUT-CNPIN))
      PERV=MVT/(DELCFP*AREA)
      MNT=(MFIN*(1-XFIN))-(MFOUT*(1-XFOUT))
      PERN=MNT/(DELCN*AREA)
      ALFANW=PERV/PERN
      ERR=(ALFA-ALFANW)/ALFA
      IF(ABS(ERR).LE.0.001)THEN
      GO TO 200
      ELSE
      ALFA=ALFANW
      GO TO 100
      END IF
200   WRITE(*,*)PERN, PERV
      QVO=PERV*(RC-RI)
      DELTAO=RC-RI
      DELTAS=RO-RI
      DELTAC=RC-RO
      RSLN=(RO-RI)/DLOG(RO/RI)
      RCLN=(RC-RO)/DLOG(RC/RO)
      RESSUB=1.0/((DISSLP*RSLN)/(DELTAS*RC))
      RESOVR=1.0/((QVO)/DELTAO)
      RESCOT=RESOVR-RESSUB
C     WRITE(*,*)RESOVR,RESSUB,RESCOT
      QVC=(DELTAC*RC)/(RESCOT*RCLN)
      PERVC=QVC/DELTAC
      WRITE(*,*)QVO,QVC,PERV,PERVC,ALFA
      STOP
      END
```

```
C     ------------------------------------------------------------------
C     CALCULATION OF GAS PHASE BASED-OVERALL MASS TRANSFER COEFFICIENT FOR VOC ABSORPTION
C     ------------------------------------------------------------------
C     INPUT PARAMETERS
C     ********************
C     AH      :       CONSTANT OF TEMPERATURE DEPENDENT HENRY'S LAW CONSTANT EQN.
C     BH      :       CONSTANT OF TEMPERATURE DEPENDENT HENRY'S LAW CONSTANT EQN.
C     DI      :       INSIDE DIAMETER OF THE FIBER (cm)
C     DO      :       OUTSIDE DIAMETER OF THE FIBER (cm)
C     LM      :       EFFECTIVE LENGTH OF THE MODULE (cm)
C     MUG     :       VISCOSITY OF GAS (cp)
C     NF      :       NUMBER OF FIBERS INSIDE THE MODULE
C     PI      :       INLET GAS PRESSURE (psig)
C     FT      :       = 0 FOR POROUS FIBER; = NON0 FOR COATED FIBER
C     PPMIN   :       VOC CONCENTRATION AT INLET GAS STREAM (ppmv)
C     PPMOUT  :       VOC CONCENTRATION AT OUTLET GAS STREAM (ppmv)
C     TEMP    :       TEMPERATURE (°C)
C     VG      :       VOLUMETRIC GAS FLOW RATE AT AMTS. PRESSURE (cc/min)
C     VL      :       VOLUMETRIC LIQUID FLOW RATE (ml/min)
C     Y1      :       VOC CONCENTRATION OF LIQUID INLET STREAM (gmol/ml)
C     ********************************************************************************
      REAL K1,L,LM,KGO,MUG,MG,MGV
      OPEN(10,FILE='MASS.DAT',STATUS='OLD')
      READ(10,*)PI,VG,VL,Y1,PPMIN,PPMOUT,NF,DO,DI,TEMP,MUG,LM
      READ(10,*)AH,BH,FT
      T=TEMP+273
      H=EXP((BH/T)-AH)
      K1=1/H
      ROL=0.9802-(0.0008356*TEMP)
      PI=PI+14.7
      R=0.08206
      L=0.1
      PIN=PI
10    VAC=(VG*14.7)/PIN
      DELP=(8*16*MUG*0.1*VAC*(2.54**2))/(NF*3.14159*6000*(DI**4)*981*453.6)
      POUT=PIN-DELP
      IF(L.GT.LM)THEN
      GO TO 20
      ELSE
      PIN=POUT
      L=L+0.1
      GO TO 10
      ENDIF
20    WRITE(*,*)PI,POUT
      IF(FT.EQ.0)THEN
      D=DI
      ELSE
      D=DO
      END IF
      A=3.14159*D*LM*NF
      C1=(PPMIN*PI)/(R*T*14.7*1000000*1000)
      C2=(PPMOUT*POUT)/(R*T*14.7*1000000*1000)
      VAC1=(VG*1*14.7)/PI
      VAC2=(VG*1*14.7)/POUT
      X2=(((VAC1*C1)-(C2*VAC2)))/(VL)
      Y2=K1*X2
      DELC=((C1-Y2)-(C2-Y1))/ALOG((C1-Y2)/(C2-Y1))
      KGO=(VG*(ppmin-ppmout)*1)/(A*(DELC)*60*R*T*1000000*1000)
      ROG=(14.7*28)/(R*T*14.7*1000)
      MG=VG*ROG
      MGV=(MG*4)/(3.14159*(DI**2)*NF)
      REG=(MGV*DI)/MUG
      WRITE(*,*)VG,KGO
      STOP
      END
```

```
C     ------------------------------------------------------------------
C     THIS  PROGRAM CALCULATES THE VOLUME RATIO AND INVERSE OF HEADSPACE PEAK AREA FROM THE
C     EXPERIMENTAL DATA OF VIAL WEIGHTS AND HEADSPACE PEAK AREA FOR CALCULATION OF HENRY'S
C     LAW CONSTANT BY VARIABLE VOLUME HEADSPACE TECHNIQUE.
C     ------------------------------------------------------------------
C     INPUT PARAMETERS
C     ******************
C     AREA    :       AREA COUNT OF GC OUTPUT
C     N       :       NUMBER OF DATA
C     N1      :       VIAL SERIAL NUMBERS
C     T       :       TEMPERATURE (°C)
C     VG      :       VOLUME OF HEADSPACE IN THE SAMPLE VIAL (cc)
C     VL      :       VOLUME OF LIQUID SAMPLE IN THE SAMPLE VIAL (ml)
C     VT      :       TOTAL VOLUME OF SAMPLE VIAL (ml)
C     WVIC    :       WEIGHT OF THE VIAL WITH LIQUID SAMPLE (gm)
C     WVIE    :       WEIGHT OF THE EMPTY VIAL (gm)
C     ************************************************
      DIMENSION WVIE(10),WVIC(10),AREA(10),WL(10),VL(10),VG(10),X(10)
     1 ,Y(10),VGPRM(10),NO(10)
      OPEN(5,FILE='HENRY.DAT',STATUS='OLD')
      READ (5,*)N,PEQ,N1
      READ(5,*)(WVIE(I),I=1,N)
      READ(5,*)(WVIC(I),I=1,N)
      READ(5,*)(AREA(I),I=1,N)
      READ(5,*)T,VT
      WRITE (*,*) T
      DIF=0.0004206*T
      WRITE(*,*)DIF
      ROL=0.8789985-DIF
C     ROL=0.99793-(8.9*(10**(-4.0))*T)
      WRITE(*,*)ROL
      DO 10 I=1,N
      NO(I)=N1-1+I
      WL(I)=WVIC(I)-WVIE(I)
      VL(I)=WL(I)/ROL
      VG(I)=VT-VL(I)
      X(I)=VG(I)/VL(I)
      Y(I)=1/AREA(I)
      WRITE(*,*)NO(I),WL(I),VL(I),VG(I),X(I),Y(I)
10    CONTINUE
      STOP
      END
```

REFERENCES

API Publication 2557, "Vapor Collection and Control Options for Storage and Transfer Operations in the Petroleum Industry", 1st Ed., (March, 1993).

Armand, B. L., H. B. Uddholm and P. T. Vikstrom, "Absorption Method to Clean Solvent-Contaminated Process Air", *Ind. Eng. Chem. Res.*, **19**, 436 (1990).

Baker, R. W., C. M. Bell and H. Wijmans, "On Membrane Vapor Separation versus Carbon Absorption", paper 174d presented at the AIChE Annual Meeting, at San Francisco, CA (1989).

Bhave, R. R., and K. K. Sirkar, "Gas Permeation and Separation by Aqueous Membranes Immobilized Across the Whole Thickness or in a Thin Section of Hydrophobic Microporous Celgard Films", *J. Mem. Sci.*, **27**, 41 (1986).

Bhave, R. R., and K. K. Sirkar, "Gas Permeation and Separation by Aqueous Membranes Immobilized in Microporous Hydrophobic Hollow Fibers. In Liquid Membranes Theory and Applications, Noble, R.D. and J.D. Way (Eds.)", *ACS Symp. Ser.*, **347**, 138 (1987).

Bird, R. B., W. E. Stewart, and E. N. Lightfoot, *Transport Phenomena*, John Wiley & Sons, Inc., New York, Wiley International Edition, 296 (1960).

Cha, J., "Removal of Vapors for Air by Selective Membrane Processes", PhD. Diss., New Jersey Institute of Technology, Newark, NJ (1994).

Davis, G. A., A. B. Ponter and K. Craine, "The Diffusion of Carbon Dioxide in Organic Liquids", *Can. J. Chem. Eng.*, **45**, 372 (1967).

Esato, K. and B. Eiseman, "Experimental Evaluation of Gore-Tex Membrane Oxygenator", *J. Thorac. Cardiovascular Surg.*, **69**, 690 (1975).

Gill, W. N., and B. Bansal, "Hollow Fiber Reverse Osmosis Systems Analysis and Design", *AIChE J.*, **19**(4), 823 (1973).

Guha, A. K., S. Majumdar, and K. K. Sirkar,"Gas Separation Modes in a Hollow Fiber Contained Liquid Membrane Permeator", *I & EC Research*, **31**, 593 (1992).

Happel, J., "Viscous Flow Relative to Arrays of Cylinders", *AIChE J.*, **5**(2), 174 (1959).

Hayduk, W., and S. C. Cheng, "Review of Relation between Diffusivity and Solvent Viscosity in Dilute Liquid Solutions", *Chem. Eng. Sci.*, **26**, 635 (1971).

REFERENCES
(Continued)

Hiss, T. G., and E. L. Cussler, "Diffusion in High Viscosity Liquids", *AIChE J.*, **19**, 698 (1973).

Hutter, J. C., G. F. Vandegrift, L. N. Nunez, and D. H. Redfield, "Removal of VOCs from Groundwater Using Membrane-Assisted Solvent Extraction", *AIChE J.*, **40**(1), 166 (1994).

Jansen, A. E., P. H. M. Feron, J. J. Akkerhuis, and B. P. T. Meulen, "Vapor Recovery from Air with Selective Membrane Absorption", paper presented at ICOM, 93, Heidelberg, Germany, (Sept., 1993).

Karoor, S., and K. K. Sirkar, "Gas Absorption Studies in Microporous Hollow Fiber Membrane Modules", *Ind. Eng. Chem. Res.*, **32**, 674 (1993).

Keller, H. K., and T. R. Stein, "A Two Dimensional Analysis of Porous Membrane Transport", *Mathematical Biosciences*, **1**, 421 (1967).

Kohl, A. L., and F. C. Riesenfeld, *Gas Purification*, Gulf Publishing Company, Houston, 3rd Ed., (1979).

Kreulen, H., C. A. Smolders, G. F. Versteeg, and W. P. M. van Swaaij, "Microporous Hollow Fiber Membrane Module as Gas-Liquid Contactors. Part 1. Physical Mass Transfer Processes. A Specific Application: Mass Transfer in Highly Viscous Liquids", *J. Mem. Sci.*, **78**, 197 (1993).

Kvaerner Engineering, Sanderfjord, Norway, Letter to Prof. Sirkar, November 15 (1993).

Liepmann, H. W., "Gaskinetics and Gasdynamics of Orifice Flow", *J. Fluid Mech.*, **10**, 65 (1961).

Lusis, M.A., Letter to the editor, *AIChE J.*, **20**, 207 (1974).

Markelov, M., and J. Biesenberger (Ed.), *Devolatilization of Polymers*, Hanser Publisher, 1984, Chap. 4.

Moretti, E. C., and N. Mukhopadhyay, "VOC Control: Current Practices and Future Trends", *Chem. Eng. Prog.*, 20 (July, 1993).

REFERENCES
(Continued)

Mukhopadhyay, N. and E. C. Moretti, "Current and Potential Future Industrial Practices for Reducing and Controlling Volatile Organic Compounds", *A Publication by Center for Waste Reduction Technologies: AIChE* (1993).

Ogundiran, O. S., S. E. LeBlanc, and S. Varanasi, "Membrane Contactors for SO_2 Removal from Flue Gases", paper presented at the Pittsburgh Coal Conference, Pittsburgh, (Sept., 1989).

Peinemann, K. V., J. M. Mohr, and R. W. Baker, "The Separation of Organic Vapors from Air", *AIChE. Symp. Series*, **82**(250), 19 (1986).

Perry, R. H., and D. W. Green, *Perry's Chemical Engineers Handbook*, 6th ed., (1984).

Prasad, R., and K. K. Sirkar, "Dispersion-Free Solvent Extraction with Microporous Hollow Fiber Modules", *AIChE J.* , **34**(2), 177(1988).

Present, R.D., *Kinetic Theory of Gases*, McGraw-Hill, New York, 61 (1958).

Rangarajan, R., M. A. Mazid, T. Matsuura, and S. Sourirajan, "Permeation of Pure Gases under Pressure through Asymmetric Porous Membranes. Membrane Characterization and Prediction of Performance", *Ind. Eng. Chem. Process Des. Dev.*, **23**, 79 (1984).

Reid, R. C., J. M. Prausnitz, and T. K. Sherwood, *The Properties of Gases and Liquids*, McGraw-Hill Book Company, New York, 3rd Ed., (1977).

Robb, W. L, "The Silicone Membrane -Their Permeation Properties and Some Applications", General Electric Co. Research and Development Center, Report No: 65-C-301, (Oct., 1965).

Robbins, G. A., S. Wang and J. D. Stuart, "Using the Static Headspace Method To Determine Henry's Law Constants", *Anal. Chem.*, **65**, 3113 (1993).

Ruddy, E. N., and L. A. Carroll, "Select the Best VOC Control Strategy", *Chem. Eng.Prog.*, 28 (July, 1993).

Sellars, J. R., M. Tribus, and J. S. Klein, "Heat Transfer to Laminar Flow in a Round Tube or Flat Conduit-The Graetz Problem Extended", *Transaction of the ASME*, 441 (Feb., 1956).

REFERENCES
(Continued)

Semmens, M. J., R. Qin, and A. Zander, "Using a Microporous Hollow Fiber Membrane to Separate VOCs from Water", *Journal AWWA*, 162 (Aril, 1989).

Shah J. J. and H. B. Singh, "Distribution of Volatile Organic Chemicals in Outdoor and Indoor Air: A National VOC Data Base", *Environmental Science and Technology*, **22**(12), (1988).

Schmid, J., "Longitudinal Laminar Flow in an Array of Cylinders", *Int. J. Heat Mass Transfer*, **9**, 925 (1966).

Skelland, A. H. P., *Diffusional Mass Transfer*, John Wiley, New York, (1973).

Sparrow, E. M., A. L. Loeffler and H. A. Hubbard, "Heat Transfer to Longitudinal Laminar Flow between Cylinders", *ASME J. of Heat Transfer*, 415 (1961).

Stahl, D. E., PhD. Diss., Chemical Engineering Department, The University of Iowa, Iowa City, IA (1971).

Tsuji, T., K. Suma, K. Tanishita, Z. Fukazawa, M. Kanno, H. Hasegawa, and A. Takahashi, " Development of Clinical Evaluation of Hollow Fiber Membrane Oxygenator", *Trans. Am. Soc. Arti. Intern. Organs. XXVII*, 280 (1981).

Yang, M. C., and E. L. Cussler, "Designing Hollow-fiber Contactors", *AIChE J.*, **32**, 1910 (1986).

Zhang, Q., and E. L. Cussler, "Microporous Hollow Fibers for Gas absorption. I. Mass Transfer in the Liquid", *J. Mem. Sci.*, **23**, 321 (1985a).

Zhang, Q., and E. L. Cussler, "Microporous Hollow Fibers for Gas absorption. II. Mass Transfer across the Membrane", *J. Mem. Sci.*, **23**, 333 (1985b).